Spring 5-23-2020

Development of a Pharmaceutical Tablet Authentication system using Spectroscopic Techniques in combination with Multivariate Chemometric Methods

Md Nayeem Hossain

DEVELOPMENT OF A PHARMACEUTICAL TABLET AUTHENTICATION SYSTEM USING SPECTROSCOPIC TECHNIQUES IN COMBINATION WITH MULTIVARIATE CHEMOMETRIC METHODS

A Dissertation

Submitted to the Graduate School of Pharmaceutical Sciences

Duquesne University

In partial fulfillment of the requirements for

the degree of Doctor of Philosophy

By

Md Nayeem Hossain

May 2020

DEVELOPMENT OF A PHARMACEUTICAL TABLET AUTHENTICATION SYSTEM

USING SPECTROSCOPIC TECHNIQUES IN COMBINATION

WITH MULTIVARIATE CHEMOMETRIC METHODS

By

Md Nayeem Hossain

Approved November 14, 2019

_____

James K. Drennen, III, Ph.D., Associate Dean
Associate Professor of Pharmaceutics
Graduate School of Pharmaceutical Sciences
Duquesne University, Pittsburgh, PA
(Committee Chair)

_____

Carl Anderson, Ph.D.
Associate Professor of Pharmaceutics
Graduate School of Pharmaceutical Sciences
Duquesne University, Pittsburgh, PA
(Committee Member)

_____

Wilson Meng, Ph.D.
Professor of Pharmaceutics
Graduate School of Pharmaceutical Sciences
Duquesne University, Pittsburgh, PA
(Committee Member)

_____

Dr. Frederick Fochtman
Scholar and Resident
Bayer School of Natural &
Environmental Sciences
Duquesne University, Pittsburgh, PA
(Committee Member)

_____

David J. Wargo, Ph.D.
Head OSD Tech Services
Mylan Inc.
(Committee Member)

_____

Lauren O'Donnell, Ph.D.
Associate Professor of Pharmacology
Graduate School of Pharmaceutical Sciences
Duquesne University, Pittsburgh, PA

_____

J. Douglas Bricker, Ph.D., Dean
School of Pharmacy and Graduate School of
Pharmaceutical Sciences
Duquesne University, Pittsburgh, PA

ABSTRACT

DEVELOPMENT OF A PHARMACEUTICAL TABLET AUTHENTICATION SYSTEM USING SPECTROSCOPIC TECHNIQUES IN COMBINATION WITH MULTIVARIATE CHEMOMETRIC METHODS

By

Md Nayeem Hossain

May 2020

Dissertation supervised by James K. Drennen, III, Ph.D.

The spread of falsified drugs is increasing worldwide. Currently, 10%-30% of drugs in the world are falsified. Unfortunately, the supply chain system of developing countries (from manufacturers to customers) is not well monitored and suffers the highest rates of fraudulent activities. Also, the rise of product procurement from the internet increases the chance of American consumers' exposure to poor quality drugs. To combat this horrendous activity, surveillance of pharmaceutical materials is required in the supply chain system. Spectroscopic techniques (e.g., Near-Infrared and Raman spectroscopies) can be a potential solution to authenticate samples in different locations; they are non-destructive, safe, rapid, portable, and affordable. However, before deploying these techniques in the field, rigorous method development is required with the help of chemometrics. The chemometric tools to be used should declare the test sample as either target class (authentic samples) or non-

target class (alternate class or falsified samples). One challenge of method development is the sensitivity of spectrometers toward unwanted variabilities including moisture, batch to batch variabilities, raw material variabilities, etc. Initial research for this dissertation observed that the traditional chemometric methods, which are based on distribution assumptions, provided a high number of false negatives due to violation of distribution assumptions in the presence of unwanted variations. It was demonstrated that adding samples from different seasons in the calibration set created binominal or multimodal distributions due to moisture variations - which violated the assumptions of the principal component analysis based soft independent modeling of class analogy (SIMCA) method. Hence, the support vector data description (SVDD) method—which has no distribution assumption—is proposed for use as a class modeling approach for authentication purposes. Implementing the SVDD algorithm improved model performance by reducing false negatives relative to the traditional multivariate class modeling approach (i.e., SIMCA). In addition, while developing the SVDD method, this dissertation suggested using different non-target class samples produced by competitor manufacturers or synthetic samples generated in the laboratory using design of experiment (DOE) as test or validation set to decrease false positives. This work also evaluated several commercially available products in two local pharmacies using portable spectrometers to validate the practical usefulness of the proposed methods. To summarize, the research performed for this dissertation has demonstrated the value of critical prior knowledge regarding pharmaceutical products, pharmaceutical manufacturing/processing, analytical methodology, and advanced chemometric techniques in a unique way to develop a successful spectroscopic authentication system.

DEDICATION

This thesis is dedicated to my parents, for making me who I am today,

And to my wife, for always believing in me.

ACKNOWLEDGEMENT

First and foremost, I would like to thank my amazing advisor, Dr. James K Drennen III. His contribution to my Ph.D., and to the process of my growing up as scholar in general, cannot be expressed in words. Though our lab did not focus on the detection of the falsified product before my dissertation project, the urgent requirement of this study was supported by Dr. Drennen without any hesitation. I am always grateful for all the discussions we had during my grad school about leadership and philosophy of life.

I would like to give a very special thanks to Dr. Carl Anderson who always encouraged me to jump into new ideas. Dr. Anderson pushed me to do a project about implementing spectroscopic tools to help developing countries using portable spectrometer and helped to build my solid background on chemometrics, instrumental analysis, and pharmaceutics through his teaching and advice during the group meetings.

I would like to give my special appreciation to my committee members Dr. Wilson Meng, Dr. Frederick Fochtman, and Dr. Dave Wargo. Dr. Meng is one of my favorite professors in Duquesne. From day one, Dr. Meng was supportive of my work. I would like to thank Dr. Fochtman for serving on my committee and shared his experience. I also offer my heartfelt thanks to Dr. Wargo for supporting my work. His insight into the industry helped me to reshape my ideas in many ways and focus on current unmet needs.

I would like to thank Dr. Peter Wildfong, Dr. Ira Buckner, Dr. Jelena Janjic and Dr. Robert Guttendorf for their contributions and helping me to become a better pharmaceutical scientist

I am also thankful to my incredibly supportive colleagues and lab mates at Duquesne. My friendship with Shikhar did not only contribute to my intellectual growth but also helped me survive some difficult episodes of my Duquesne life. I also learned a lot from my everyday conversations with my very talented lab mates– Yuxiang, Suyang, Natasha, Maddie, Jacob, Adam, Sam and Eric. I also want to emphasize the value of my friendship with long-time friend Anik; my journey to study pharmacy started with him in Bangladesh and continued in the USA, providing so many good memories which are difficult to forget. I offer special thanks to my previous colleagues Hanzhou, Yi, Sameer, Ryan, Bob and Benoit. I am also thankful to undergraduate students who worked with me on different projects. They include Jake Wargo, Chloe Drennen, and Beatrice Aristei. A

special thanks to my friend Kevin with whom I have so many memories while working for AAPS. I also wish to thank all my dearest friends who lifted me up during my difficult days- Tanvir, Suchi, Junayed, Tasdique, Maria, Annie, Fahima, Mahmud, Michele, Pradip, Ashwini, Mustafa, Wanzhu, Kandarp, Eric, Sherlock, Anwar, Zobaer, Zahir, Saeed, Tomal and Faria. A special thanks to Jordan for her friendship and for helping in editing this document.

I would like to thank my family for their sacrifice and constant support during my life in the USA. My mother, Parvin Akter, always inspired me to become a kind-hearted person and help people. Her words kept me focused during the hardest times of my graduate school. My father, Md Mosharrof Hossain, always told me that I could overcome any challenge with my honesty, hard work, and faith in god, and I tried to follow his words which was necessary for me to undertake the new challenges in my project. My wife, Nabila Farhin Jahan, sacrificed a lot for the successful completion of my study in Pittsburgh. She always provided me with the emotional support that I needed to survive and overcome the challenges. Her own work in Clinical Psychology also inspired me to become an empathetic person and I tried to adopt this philosophy beyond my personal life which led me to do this project. My brother, Nahid, sister, Nusrat, and her child, Nameer, and brother-in-law, Nasim, remained as a source of joy and happiness throughout my academic life. I want to give a special thanks to my father-in-law, Dr. Sarwar Jahan and my mother-in-law, Syeda Anwari Jahan for their benevolent supports and prayer during my graduate school. A very special thanks to Shama, Wasif and Hasan to cheer me up always whenever I fell behind.

I want to thank Duquesne University for giving me this opportunity. I am thankful to the faculty and staff for their support and cooperation.

Finally, Thanks to Allah for everything.

TABLE OF CONTENTS

Chapter 2: Evaluation of SVDD and SIMCA methods as Class-Modeling Techniques using Near-Infrared Calibration Sets of Pharmaceutical Tablets Containing Moisture Variation

Chapter 3: Application of Class-Modeling Techniques using Raman spectroscopy in the Presence of Moisture Variation

Chapter 5: Application of Experimental Design to Generate Synthetic Non-Target Class Samples and the Effect of Raw Material Variability of the Target Class on the Class- Model Performance

Chapter 6: Onsite Implementation of Portable Spectrometers to Analyze Commercially Available Pharmaceutical Products

LIST OF TABLES

LIST OF FIGURES

LIST OF ABBREVIATIONS

ACT	Artemisinin-based combination therapy
APAP	Acetaminophen
CA	Cluster analysis
CE	Capillary electrophoresis
CLS	Classical least squares
CV	Cross validation
DCPT	Duquesne University Center for Pharmaceutical Technology
DEG	Diethylene glycol
DOE	Design of experiment
FN	False negative
FP	False positive
GA	Genetic algorithm
HCA	Hierarchical cluster analysis
HPLC-DAD	High-performance liquid chromatography with diode-array detection
K-NN	k-nearest neighbors
KP	Kilo pond
LBC	Linear baseline correction
LC-MS/MS	Liquid chromatography- mass spectroscopy
LDA	Linear discriminant analysis
LOOV	Leave one out of validation
LWL_NIR	Low wavelength Near Infrared
MG	Milligram
MSC	Multiplicative scatter correction
Ncal	Number of calibration sample
Ncounter	Number of counterfeit
NM	Nano meter
NIRS	Near-Infrared spectroscopy
NIR-CI	Near Infrared chemical imaging
OC-SVM	One class support vector machine

OD	Orthogonal distance
PCA	Principal component analysis
PCR	principal component regression
PLS	Partial least squares regression
PLS-DA	Partial least squares discriminant analysis
PP	Preprocessing
PXRD	Powder X-Ray diffraction
ROC	Receiver operating characteristic
Savgol	Savitzky–Golay
SC	Spectral correlation
S	Second
SD	Score distance
SIMCA,	Soft independent modelling by class analogy
SIMCA-DD	Soft independent modelling by class analogy data description
SM	Spectral matching
SPA	successive projections algorithm
SVDD	Support vector data description
SVM	Support vector machine
SV	Support vector
SWL-NIR	Short wavelength Near Infrared
TLC	Thin layer chromatography
TN	True negative
TP	True positive
UPLS-DA	Unfolded partial least squares with discriminant analysis
USP	United Sates of Pharmacopeia
WHO	World Health Organization
WS	Wavelength selection

Chapter 1: Introduction

1.1 Background, Statement of Problem

A sound authentication process is vital to protect pharmaceutical materials from falsification or any fraudulent activities. According to the World Health Organization (WHO), the term “falsified medicines” can be defined as “Medical products that deliberately/fraudulently misrepresent their identity, composition or source. Such deliberate/fraudulent misrepresentation refers to any substitution, adulteration, or reproduction of an authorized medical product or the manufacture of a medical product that is not an authorized product” [1]. Specifically, composition refers to the raw material or final dosage form in accordance with applicable specifications authorized/recognized by national or regional regulatory bodies. In May 2017, the WHO published this definition of falsified products to bring harmony among the member countries and replaced the word “counterfeit medicine” which was widely used [1].

Protection of pharmaceutical materials from fraudulent activities is becoming increasingly critical as falsified products are more widely distributed. Currently, 10%-30% of drugs in the world are falsified [2]. Unfortunately, the supply chain system of developing countries (from manufacturers to customers) is not well monitored, and suffers the highest rates of fraudulent activities [3, 4]. Also, the rise of product procurement from the internet increases the chance of American consumers' exposure to poor quality drugs [2].

A variety of techniques have developed to eliminate such fraudulent activities. Among these, visual inspections or image analysis have been used as the very first step of the identification

process. However, many counterfeiters and producers of falsified products can evade sophisticated visual tests [5]. Therefore, a variety of analytical tools have been used to reveal the different chemical compositions of falsified products from authentic samples. Among these analytical methods, several rapid screening tools provide an effective way to increase the number of products that can be subjected to chemical testing before reaching patients or consumers [6]. Handheld and portable instrument platforms provide an opportunity to implement the screening process in more locations (e.g., in different locations of the supply chain including rural hospitals, clinics, drugstores, etc.). Spectroscopic techniques offer a number of advantages for screening pharmaceutical products, including rapidity, portability, etc. In particular, Near-Infrared (NIR) and Raman spectroscopies have been demonstrated to be valuable tools [7]. These spectroscopic techniques are fast and easily deployable to different inspection sites, facilitating detection of falsified drug products in developing countries to reduce the life-threatening prevalence of this scourge [8-10]. Also, these spectroscopic techniques can be applied in the developed world to advance internet-of-things (IoT) based smart applications.

However, the use of such spectroscopic techniques is not straightforward due to the multivariate nature of the data and the significant variety of potential factors influencing the analytical measurements. Therefore, rigorous method development is required, usually involving advanced chemometric methods, before deploying such analytical techniques in the field. These analytical systems should declare the test sample as either target class (authentic samples) or non-target class (an alternate class, or falsified samples). All practical methods should offer good performance in terms of limiting both false negatives (identification of samples as false samples

when, in fact, they are authentic samples), and false positives (identification of samples as belonging to the target class when they are actually false samples).

Two types of chemometric techniques have been well described in the literature for authentication methods, including spectral matching (SM) and class modeling (CM) techniques [11]. Most of the current portable spectrometers come with some variety of SM algorithm. These algorithms facilitate the comparison of two spectra, including a reference spectrum collected from a genuine or authentic material and a spectrum of the unknown material under study [12, 13]. These two spectra are used to calculate spectral correlation or spectral distance. If these correlation or distance values match with a target threshold value, the unknown samples are declared as genuine or authentic samples. Research showed that the SM method was successful when samples included chemical differences, providing sufficient spectral uniqueness to allow detection [14, 15]. For example, the SM method was used to identify placebo samples and samples containing the wrong API. However, this method struggled to differentiate samples containing identical APIs and similar excipient compositions, resulting in high false positives [16].

A variety of class-modeling techniques can also be applied for authentication. Multivariate methods such as SIMCA and its extended version, data driven SIMCA, etc. have been used for spectroscopic identification of pharmaceutical samples. The primary premise of these methods is to develop a target class using representative samples from an authentic source. A calibration model is developed from the target class, which is comprised of spectral data containing API and excipient information. Class-modeling (CM) estimates a decision boundary which is formed around the data at a specific significance level. This boundary is developed based on certain

assumptions regarding the data (e.g., normal distribution, χ^2 distribution, etc.) [17-19]. The pharmaceutical literature reveals several studies proposing that CM techniques are more powerful than the SM method in separating samples containing similar compositions using portable spectrometers [15, 20]. Critical considerations for the analytical method developer include identifying an appropriate sample of target class product, adequately defining boundary conditions for the target class, and selecting suitable non-target samples. CM methods will not be successful without suitable training samples.

To achieve desirable performance, CM methods must account for the anticipated chemical and physical variations to be encountered in the target class of product; NIR and Raman spectroscopies are sensitive to different physical and chemical factors such as moisture variation, tablet hardness, component particle size, instrument drift, etc. This is particularly important for the implementation of spectroscopic methods in the field, as samples will be collected in various locations. Therefore, models must include this variability at the outset, or must be updated with new authentic samples over time to include new sources of variation. To limit the demands of calibration updates that might be required due to such new target class variability, different spectral preprocessing techniques are applied to remove or limit the spectral effect of this variability. While different data processing techniques reduce the unwanted effect of these variabilities, adding new samples over time to update the model by including such target class variability is sometimes considered the most effective approach.

Defining appropriate boundary conditions for the target class is a critical aspect of defining a suitable set of "good" product samples for model development. A test sample is assigned to the

target group if the computed distances of tested samples to model is shorter than a predefined threshold value based on a mathematical boundary. However, several challenges arise during this boundary formation. As analysts may be required to update the model by adding samples containing recently evolved variations into the calibration sample set, these newly added samples are often considered as extreme objects or outliers. Moreover, this may violate the assumptions of the model by forming clusters or binomial distribution in the model space. Therefore, the caveat of defining boundary condition is—without prior knowledge of the shape of the underlying distribution of samples, satisfactory boundary formations may not be achieved.

A CM method can also be developed without relying on distribution assumptions. Unlike the traditional CM methods used for the authentication, forming a decision boundary based on boundary samples of the calibration set includes all of the samples produced during the model update or after the risk-assessment. Support vector machine (SVM) based methods are a viable approach for establishing a boundary through the identification of boundary samples. Here, an algorithm developed by Tax et al. is proposed as a method for development of a spectroscopic authentication system for pharmaceutical products [21]. This method is often identified as a support vector data description (SVDD), which has shown similar performance to the one-class support vector machine (OC-SVM) developed by Schölkopf et al [22]. The proposed SVDD method has been applied for detection of machine faults, outlier detection, etc., but has not yet been evaluated for analyzing pharmaceutical samples using spectroscopic data, particularly for the authentication purpose.

After developing a calibration model using an appropriate decision boundary, an analyst should use a complex sample set to test or validate the model performance. Particularly, to validate the model's capability of rejecting falsified samples, it is critical to evaluate samples from alternate classes. These samples are used to test the specificity of the method, which is the portion of alternate class samples that are correctly identified as negative or outlier samples with respect to the target class. In practice, alternate class samples may be very similar to the target class; therefore, alternate class test samples must include samples that are 'highly similar' to the target class. Usually, these 'highly similar' samples are those which contain the same API and similar excipient composition and are manufactured using similar techniques. Therefore, the choice of the alternate class test samples is essential for assessing false positives (FP). Legitimate generic versions of the target class drugs that are manufactured by various producers can be used to test the FPs as such drugs should contain identical API and may contain similar excipient compositions. These non-target class samples should be used to optimize the boundary condition of the proposed SVDD model. This avoids the unnecessary acceptance of non-target class samples during boundary optimization and decreases FPs.

Because the analyst will not always have access to the competitors' products during method development, selecting an alternative strategy such as preparing samples using statistical design of experiment (DOE) may be a suitable approach to overcoming the limitations associated with inaccessible samples. Various challenging samples can be generated by altering the chemical composition of target class samples using DOE. Moreover, depending on the analytical technique to be used, the chemical compositions of non-target class samples may be unique based on the inherent sensitivity to the chemical compositions. Utilizing both NIR and Raman spectroscopic

techniques could prove the value of using different non-target class samples for different techniques.

1.2 Hypothesis and Specific Aims

The proposed hypothesis is:

Development of a support vector machine based algorithm with pertinent calibration and validation sets enables a multivariate spectroscopic authentication method that provides a superior system for both NIR and Raman spectroscopy compared to traditional multivariate methods of classification (e.g., SIMCA).

Given the central hypothesis, the objectives of this dissertation are to:

1. Demonstrate the development of a robust authentication system using NIRS and a SVM based algorithm in the presence of moisture variations.
2. Demonstrate the use of Raman spectroscopy and the SVDD algorithm for authentication in the presence of moisture variations.
3. Demonstrate model development for the detection of 'highly similar' non-target class samples collected from different developing countries (produced by various manufacturers).
4. Demonstrate the application of DOE concepts to generate 'highly similar' samples for testing of NIR and Raman spectroscopic systems.
5. Demonstrate portable NIR spectrometers as an onsite screening tool for rapid testing of pharmaceutical samples.

In summary, the objectives of this dissertation were achieved by obtaining two figures of merit as described in Figure 1-1:

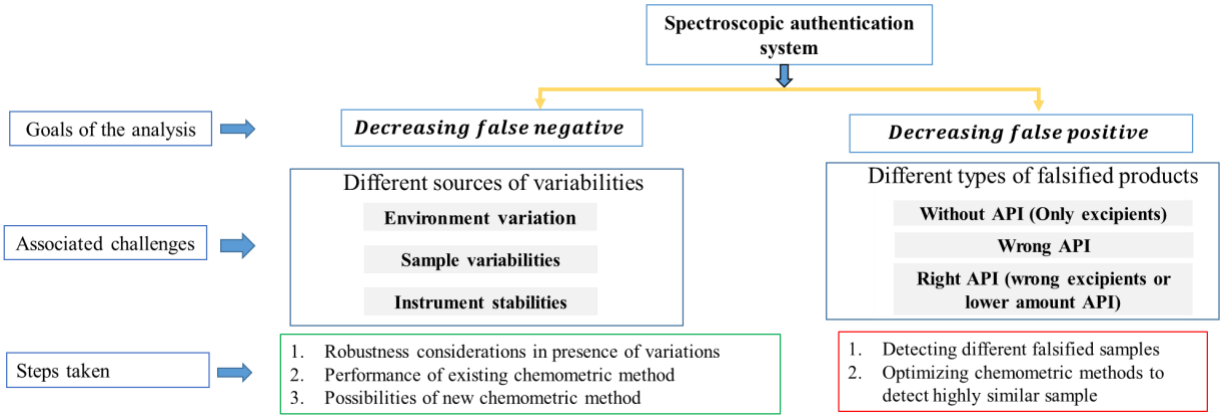

Figure 1-1: Two primary goals of an authentication method, associated challenges of each goal and steps taken to address the challenges.

The first two objectives addressed opportunities to improve the sensitivity of models (decreasing false negatives) used for pharmaceutical authentication by addressing the critical quality attributes and material attributes relevant to a robust authentication of pharmaceutical samples. These parameters are crucial for both NIR and Raman techniques. In Chapters 2 and 3, respectively, the work defines how a machine learning based algorithm can be used to improve model performance of NIR and Raman spectroscopy and compared with an existing multivariate method.

The next two chapters, Chapters 4 and 5, asses the model's ability to reject non-target class samples by decreasing false positives (objectives 3 and 4). In Chapter 4, the document discusses the analysis of a variety of highly similar samples, collected from across the globe and manufactured by different companies. These were used to assess the performance of spectrometers and models for pharmaceutical tablet authentication. Because a competitor's product may not

always be available, the work of Chapter 5 demonstrated the use of laboratory generated tablets as non-target class samples. Since the spectral response of different analytical techniques is unique for any composition, unique non-target class samples are likely to be required in model development for each different analytical technique. Finally, Chapter 6 describes the use of portable spectrometers for sample analysis in the field. Two spectrometers were used to scan pharmaceutical samples in local pharmacies.

The novelty of the work should be apparent due to 1) the requirement of applying critical prior knowledge regarding pharmaceutical products, pharmaceutical manufacturing methods, analytical methodology, and chemometric techniques, and 2) the application of a specific modern approach to calibration development for a new application.

1.3 Literature Review of Falsified Drug Detection

Different chemometric methods have been used for the qualitative and quantitative analyses of NIR and Raman spectral data to detect various types of falsified products. This literature review compiles the details of such previously described work. Critical evaluation of these chemometric methods is provided to define the inherent limitations. Finally, directions are provided to develop an accurate and robust spectroscopic method for the authentication of pharmaceutical products.

1.3.1 Analytical Method Development to Detect Falsified Drugs

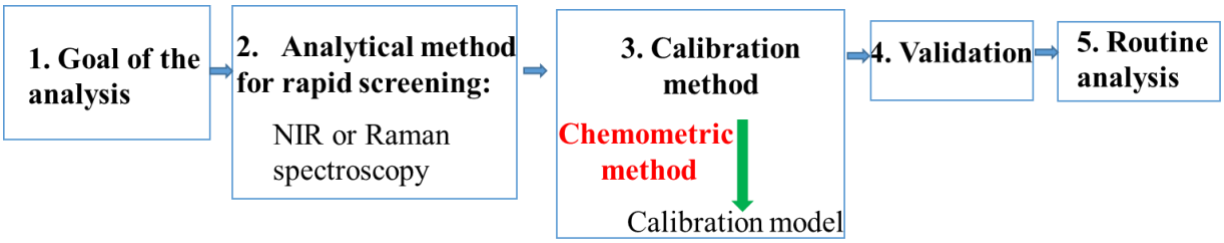

Figure 1-2: Method development strategies for a pharmaceutical product authentication system

Analyical method development starts with setting the goals of the analysis. This guides the subsequent method development steps (see Figure 1-2). In this case, to protect pharmaceutical products from any falsification activities, the analytical system should have the capabilities to separate genuine products from falsified products. This target will be effectively achieved if analysts are aware of the many potential falsified products. The pharmaceutical literature has reported many approaches to falsifying both pure components and finished dosage forms [2]. Such falsification frequently involves different counterfeit product composition. This includes, but is

not limited to, intentional adulteration of pharmaceutical ingredients, tablets prepared without active pharmaceutical ingredient (API) (e.g., using only excipients), tablets manufactured using the wrong API, and tablets generated with the correct API, but different compositions of excipients (see Figure 1-3). Different types of falsified products are also compiled in Table 1-1.

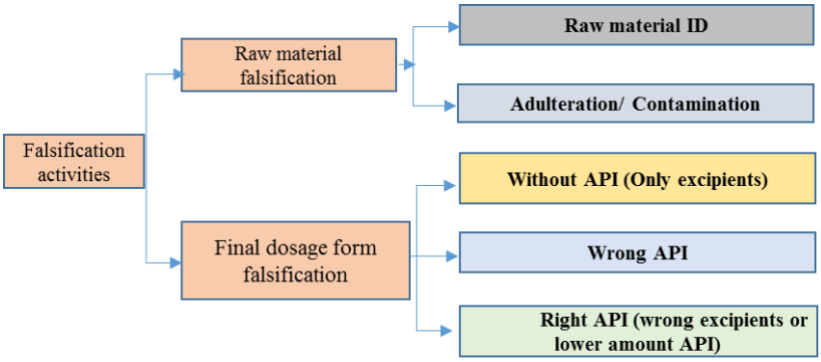

Figure 1-3: Types of falsified products

NIR or Raman spectroscopy have been used successfully to detect different approaches to falsification; examples of these counterfeiting activities are discussed in Section 1.3.2 (Step 2 in Figure 1-2). Selection of analytical techniques to detect such falsification activities also depend on the fundamental capability of the analytical techniques itself, which is further discussed in this section [23, 24]. Both NIR and Raman spectroscopy will typically require multivariate modeling approaches for the development of a suitable calibration model, discussed in Section 1.3.3 (Steps 3-4 in Figure 1-2). Development of a robust model will reduce the need to update a calibration over time (discussed in Section 1.3.4**)**. Finally, the chemometric approaches proposed in this dissertation are provided in Section 1.3.5

Table 1-1: Overview of representative pharmaceutical authentication studies using NIR and Raman spectroscopy, including model development details regarding preprocessing, number of samples, cross-validation, robustness studies.

Category of falsified products*	**Analyzed medicine, brand name in parenthesis.**	**Analytical techniques and types (L- Lab based, P- Portable)**	**Product origin(s)/ Source**	**Reported chemometric approaches and relevant comments - preprocessing, internal validation (type, split ratio), external validation, model validation, robustness testing, performance & validation parameter.**	**Ref.**
Pure material	309 different USP materials	Raman L	USP material	peak match, correlation, and PP: first derivative	[25]
Adulterants in the raw material	DEG in glycerin, melamine in lactose	Raman P	Lab based experiment	Spectral correlation method, PLS. PP: Savgol 1st Derv, SNV, MNCN, CV: LOOCV, Sensitivity, Specificity, RMSEP	[11]
Adulterant detection in Tablet	glibenclamide	NIR-L, solid-phase fluorescence spectrometry	Brazil	SIMCA, PLS-DA, UPLS-DA; WS:GA, SPA; Type I, Type II error.	[26]
Tablet without API.	chloroquine, ciprofloxacin HCl, hydroxychloroquine, levofloxacin, metronidazole, quinine sulfate	Raman P	Commercially purchased sample, simulated counterfeit	Spectral correlation, PP: SavGol (first derivative, 2nd order, W-31-point), wavelength selection to the API specific regions	[27]
Tablet without API.	artesunate	-	South-East Asia	PLSDA, Ncal=112, Ncounter=55, CV, PP: mean-centering.	[28]

Category of falsified products*	Analyzed medicine, brand name in parenthesis.	Analytical techniques and types (L- Lab based, P- Portable)	Product origin(s)/ Source	Reported chemometric approaches and relevant comments - preprocessing, internal validation (type, split ratio), external validation, model validation, robustness testing, performance & validation parameter.	Ref.
Capsule without API	miltefosine	NIR-L, LC-MS/MS	Bangladesh	Spectral investigation	[29]
Tablet without API, Tablet with wrong API	artesunate	Raman L.	Vietnam, Laos PDR, Burma, China, Ghana, Thailand-Burma border	Spectral peak identification- assigned to the corresponding functional groups, PCA, K-mean clustering, Ncal- 50. PP: SavGol, SNV (to remove fluorescence). Robustness issue: API has strong fluorescence background.	[30]
Tablet with wrong API	atorvastatin	NIR L and Raman L, LC-MS	Dutch Health Care Inspectorate	PCA, PLS-DA, Robustness issue: Effect of storage condition was tested	[31]
Tablet with wrong API	acyclovir, amoxicillin, cephalexin, ciprofloxacin, doxycycline, levofloxacin	Raman-P	Commercially purchased, counterfeit product was lab based (simulated).	Raman barcode, PP: SavGol to remove fluorescence.	[32]
Tablet without API, Tablet with right API but different excipient compositions	sibutramine	NIR L, Raman L, LC-MS	Internet, Korea, Egypt, Libya, Turkey, Syria, Philippines, Thailand	Spectral analysis, PCA analysis.	[33]
Tablet without API, Tablet with right API but different excipient compositions	aspirin, ampicillin, KCL, ampicillin, enalapril, (wide variety of falsified drug)	NIR L	Brazil	PCA/SIMCA, N=50, CV: LOOV, PP: SavGol (5 w, 2nd polynomial). Robustness: effect of humidity alteration, sample position and sample face (for tablets) on model performance was tested.	[34]
Tablet without API, Tablet with right API but different excipient compositions	sildenafil citrate (Viagra)	NIR L, TLC, UV, HPLC-DAD, HPLC-DAD-MS	Netherlands	SavGol (2nd derivative) SC, PCA.	[35]

Category of falsified products*	Analyzed medicine, brand name in parenthesis.	Analytical techniques and types (L- Lab based, P- Portable)	Product origin(s)/ Source	Reported chemometric approaches and relevant comments - preprocessing, internal validation (type, split ratio), external validation, model validation, robustness testing, performance & validation parameter.	Ref.
Tablet without API, Tablet with right API but different excipient compositions	sildenafil (Cialis)	Raman L, HPLC	Medsafe, intercepted at New Zealand's International Mail Centre	SIMCA, PLS-DA, SVM. PP= LBC, MSC. N=250. Split: Cal-67%. Test-33%. CV, Quantitative modeling: PCR, PLS	[36]
Tablet without API, Tablet with right API but different excipient compositions	sildenafil	Raman L	China, Mexico.	PCA-HCA, PP: SavGol (13W), NCal=19, NTest=9, Robustness: Baseline-corrected before presentation, to eliminate the influence of broad fluorescence background	[37]
Tablet with right API but different excipients composition	sildenafil	Raman L	Federal Agency for Medicines and Health Products in Belgium (AFMPS/FAG)	PCA (different wavelength range), LDA, K-NN, SIMCA. CV: LOOCV. Ncal= 26, Ntest= 12.	[38]
Tablet with right API but different excipient composition	not specified	NIR P	Not specified	SC, PCA, PP: SNV, SavGol (2nd, W-5, 2nd order), unit vector normalization. Robustness: lamp change, lot-to-lot variabilities	[13]
Tablet with right API but different excipient composition	atorvastatin calcium	Raman P, PXRD, X-Ray tomography	India, Thailand, Pakistan, Germany	Characteristic peaks around 1600 cm^{-1} was used to determine whether Atorvastatin was present or not.	[39]
Tablet with right API but different excipient composition	trimethoprim, metronidazole	NIR	Not specified	PCA, SIMCA	[40]
Tablet with right API but different excipient composition	antimicrobial, antispasmodic-coated, film coated, crushed - wide varieties of counterfeit product	NIR L, NIR Imaging	Not specified	PCA/SIMCA, PP: MSC, N=10	[41]

Category of falsified products*	Analyzed medicine, brand name in parenthesis.	Analytical techniques and types (L- Lab based, P- Portable)	Product origin(s)/ Source	Reported chemometric approaches and relevant comments - preprocessing, internal validation (type, split ratio), external validation, model validation, robustness testing, performance & validation parameter.	Ref.
Tablet with right API but different excipients compositions	calcium channel blocker	NIR P	Not specified	Correlation coefficient, SIMCA	[15]
Liquid ampoule with right API different compositions	dexamethasone	NIR-L, HPLC-DAD-MS, CE-UV	Not specified	SNV, SIMCA, PP: SNV, N=30	[42]
Injectable	doxofylline, Levofloxacin, HPLC	Raman P	China	SC, CLS models., N(Dox)= 60, N(Lev)=60.	[43]
Expired tablets	paracetamol	Raman P	China	Spectral Correlation; PP: max–min normalization (MN), SavGol (1st and 2nd deriv), N=120, CV: 7-round cross-validation, SIMCA, PLS-DA, SVM, k-NN. (SVM proved robust compared other methods.)	[44]
Seized products	Not specified	NIR L, Raman L	Not specified	PCA, HCA, k-NN, PLSD-DA, SVM, ANN, CV: venetian blinds, 9 splits.	[45]

Note: USP: United Sates of Pharmacopeia; DEG: Diethylene glycol; PP: Preprocessing; Savgol: Savitzky–Golay; Ncal: Number of calibration sample; SIMCA: Soft independent modelling by class analogy; PLS-DA: Partial Least Squares Discriminant Analysis; UPLS-DA: Unfolded Partial Least Squares with Discriminant Analysis; WS: Wavelength selection; GA: Genetic algorithm; SPA: successive projections algorithm; Ncounter: Number of counterfeit samples; CV:Cross validation; LC-MS/MS: Liquid chromatography-mass spectroscopy; LOOV: Leave one out of validation; TLC: Thin layer chromatography; HPLC-DAD: High-performance liquid chromatography with diode-array detection; SC: Spectral correlation; SVM: Support vector machine; LBC: linear baseline correction; MSC: multiplicative scatter correction; PCR: principal component regression; PLS: Partial least squares; regression; HCA: hierarchical cluster analysis; LDA: Linear discriminant analysis; K-NN: k-nearest neighbors; PXRD: Powder X-Ray Diffraction; CE: Capillary electrophoresis; CLS: Classical Least Squares.* The mentioned category of falsified products are an approximation to give readers an idea of the types of products.

1.3.2 Analytical Tools

1.3.2.1 Near Infrared Spectroscopy

Near-infrared spectroscopy (NIRS) is based on the absorption of electromagnetic radiation in the range of 700 nm to 2500 nm, which includes overtone and combination bands of the fundamental vibrations observed in the mid-infrared region [46]. NIRS is a useful analytical tool due to its non-destructive nature and flexible sample interface. These properties provide extensive opportunities for qualitative and quantitative prediction of critical components of pharmaceutical products, managing critical process parameters and for assuring that products meet real-time release criteria [47].

Detecting falsified pharmaceutical materials is one of the potential applications of NIRS. Typically, this application is based on the comparison of the presence or absence of spectral features of genuine products. A significant number of studies have been undertaken by NIRS for the authentication of medicines. Significantly, medicines which are critical for treating diseases prevalent in low and middle income countries, including antimalarial, antimicrobial, and antispasmodic [28, 41] medicines, were successfully authenticated using NIRS [48]. While NIR applications for detecting falsified drugs began in the laboratory, successful results led regulatory bodies to use NIRS directly in the field. Initiatives using mobile van laboratories in rural areas of China and India have set examples for other regions [49]. Advances in instrumentation technology has led to dramatic reductions in the size of NIR spectrometers, with handheld devices now available [50]. These spectrometers are light-weight and do not need any dedicated vehicle to mount them onto. Typically, these spectrometers are available with sizes 20x10x5 cm (~8x4x2 in.)

or smaller, and weights of just 1 kg (~2 lbs) or less. A good review of different hand-held spectrometers will be found in Crocombe et al. [51]

In addition to the single point NIR spectrometer, another important spectral collection mode of NIRS is hyperspectral chemical imaging (NIR-CI). This enables the collection of additional information from pharmaceutical products such as the surface distribution of APIs, excipients, powders and granules [52]. NIR-CI was shown to be superior to single-point NIRS in some cases because it combines the capability of spectroscopy with the potential of visualization of API and excipients in the falsified products [52]. Furthermore, NIR-CI can be useful to measure both potency and the quality of the formulation, even without knowing the exact composition of the drug, which is critical when falsified products are collected without prior information [53].

1.3.2.2 Raman Spectroscopy

Raman spectroscopy, a molecular spectroscopy, generates a polarization in the molecule resulting in in-elastically scattered photons [54]. The spectrum observed from a Raman spectrometer is a measure of the amount of energy a photon has lost (Stokes Raman scattering) or gained (anti-Stokes Raman scattering) which is frequently expressed as wavenumber shift. Stokes Raman scattering is most commonly measured because this is of higher intensity than anti-Stokes scattering (due to the lower probability of the molecule being in an excited vibrational state).

Raman spectroscopy has demonstrated value as a method in the array of techniques for pharmaceutical analysis [47, 55]. The advent of several configuration of Raman spectrometers (backscattering, transmission, surface enhanced Raman (SER), and imaging systems) have opened opportunities for the evaluation of different types of falsified samples [30, 31, 37, 56-58]. A

primary advantage of Raman spectroscopy is the significant selectivity, which allows identification of different APIs, excipients and impurities present in the pharmaceutical materials [25, 59]. Packaging materials, including dyes, markers, etc., can also be authenticated with Raman spectroscopy, adding to the list of advantages for this method in the fraud detection process [60, 61]. However, there are other possible ways to authenticate pharmaceutical packaging materials, which are out of the scope of this review.

Like NIRS, application of Raman spectroscopy has also spread from benchtop to field-based use at the point of sample collection [62, 63]. Although the portable Raman spectrometer is relatively new, it shows promise for detecting falsified and unapproved drugs [64]. Moreover, similar to NIRS, the imaging configuration of Raman spectroscopy was also successfully used to gain an understanding of the spatial distribution of formulation components of tablets [38, 65, 66].

Although both Raman and NIR spectroscopy have been proven effective for the detection of falsified medicine, they are not without limitations. NIRS suffers from a lack of specificity issue due to the absence of sharp peak features (due to broad overtones and combination bands) which necessitates the careful use of multivariate chemometric methods. On the other hand, Raman spectroscopy for chemical analysis suffers from relatively low sensitivity and interference from fluorescence [59]. In spite of their relative advantages and limitations, both techniques have been used successfully to detect falsified products (Table 1-1). Understanding these the potential of each method facilitates selection of the appropriate analytical tool for development of suitable product authentication systems.

Table 1-2: Some features and shortcomings of NIR and Raman spectroscopy. Italics indicate disadvantages

NIR	Raman
Advantages • Noninvasive • Sensitive to the Physical factors including particle size and compression force • Pharmaceutical excipients have strong NIR signal • Penetration is higher for NIR light ***Disadvantages*** • *Wide bandwidth* • *Weak fingerprints of API and excipients*	**Advantages** • Noninvasive • Sharper peak features • Less sensitive to the physical factors • Typically, API has strong Raman signal. ***Disadvantages*** • *Fluorescence interferences* • *Pharmaceutical excipients exhibit less Raman signal relative to the API Penetration depth is lower (and often insignificant for coated dosage forms)*

1.3.3 Chemometric Techniques for Model Development and Relevant Applications

Numerous chemometric techniques have been used to extract the relevant chemical and physical information from the collected NIR and Raman spectra of falsified samples. These chemometric techniques can be divided into three categories:

i) spectral matching methods

ii) exploratory analysis, and

iii) supervised techniques

As mentioned, various types of fraudulent activities (formulation approaches to counterfeiting) will generate unique spectral characteristics. The chemometric techniques to be reviewed have been applied for detecting different scenarios anticipated in counterfeiting. Uses of

these chemometric techniques are discussed below, with a description of theory and relevant applications. Criticisms of each method will be provided to give the reader an understanding of their limitations for the application of authentication.

1.3.3.1 Spectral Matching Method

1.3.3.1.1 Theory

Historically, spectral features of known components have been used to accomplish qualitative identification of pharmaceutical samples. This would involve assigning absorbance bands to corresponding functional groups of the expected component. Then, the presence or absence of these spectral bands in the sample spectra could be used to distinguish between genuine and falsified products [12]. However, this method requires recognition of the distinct peaks and may not be suitable for automatic detection by non-specialist analysts in the field. To simplify a field analyst's work, spectral matching (SM) algorithms have been used to compare spectra of unknown test samples to a reference spectrum collected from genuine material. SM algorithm compare the proximity between vectors of a reference (or genuine) sample and an unknown sample to determine sample identity [67].

Proximity is computed by calculating distance and spectral correlation. Distance is also often described as SD, a spectral dissimilarity (i.e., the greater the distance, the less similar the objects are), which is measured based on following relations: the sum of least squares (Equation l), and the sum of absolute value differences (Equation 2) [68].

$$SD_1 = \sqrt{\left(100 * \sum \frac{(Lib_m - Unkn_m)^2}{N}\right)} \quad (1)$$

$$SD_2 = \left(\frac{1}{N}\right) \sum |Lib_m - Unkn_m| \quad (2)$$

Here N is the number of data points, and Lib_m and $Unkn_m$ is the m^{th} absorption value in the library spectrum and the unknown spectrum, respectively. As SD_1 and SD_2 calculate dissimilarity between the spectra, their minimum value is 0 for identical spectra. On the other hand, spectral correlation (SC), which is often mentioned as a similarity, is the equivalent of measuring the cosine of the angle between two spectra.

$$SC = 100 * \sqrt{[(Lib_m \cdot Unkn_m)^2]/[(Lib_m \cdot Lib_m)(Unkn_m \cdot Unkn_m)]} \quad (3)$$

Here, SC measures the similarity between the spectra; and SC values range from 0 (poorest match possible) to 1 (perfect match).

Generally, the SM method can be employed for identification and verification. Before applying the SM method for identification, a reference library is developed using authentic samples. An unknown sample is systematically compared with spectra in the reference library by using equations 1-3. The corresponding reference spectrum, which has minimum distance or maximum correlation with the unknown sample, is declared as the potential target sample (e.g., target product or target manufacturer). This approach is often referred to as a library search. For verification purposes (e.g., to verify whether the claimed component is present in the sample or not, or if the test sample is an authentic product) the SD or SC value is directly calculated using

target reference spectra. A verification test uses empirically defined target threshold values, usually 0.95, to assign a “Pass” or “Fail” determination to the sample under study [69, 70].

1.3.3.1.2 Applications of Spectral Matching Method

The application of a spectral matching methods to the chemical analysis was reviewed nearly two decades ago by Penchev [67]. The author evaluated the performance of SM methods using infrared spectroscopy. Since 1996, the use of this chemometric technique in the pharmaceutical industry has continued, with increased interest in its application using other analytical tools, such as Raman and NIR spectroscopic methods [14, 71, 72].

McCreery [25] in 1998, was one of the first to use Raman spectroscopy with a SM method. His work involved testing the identity of pure pharmaceutical materials. First, a reference library was prepared using 309 United State Pharmacopeia (USP) standard compounds. Then, a total of 26 unlabeled vials were scanned blindly and used as a test set. After that, the developed reference library was used to calculate SM values for each of the test samples. The highest matching value obtained from the reference library was declared the identity of the test sample, and around 96% of the test samples were accurately identified. Authors noted that the use of the right preprocessing method was critical for getting a successful result, as it affected matching values significantly [25]. Although the components were successfully identified in the McCreery study, it is important to understand that the library search method relies on the listed components already presented in library and provided the best probable compound as the possible target sample.

While detecting pure components using spectroscopy, it is also required to study whether the SM method is able to detect contaminants in the sample. As mentioned earlier, to verify

whether the contaminant is present in the sample, the matching value of the test sample to the claimed compound is calculated directly using SM algorithm. This accurate detection of contaminants is of particular importance when dealing with pharmaceutical excipients because they are susceptible to economically motivated adulteration with substances having comparable physical, chemical, and/or spectroscopic properties. The result is not only financial loss for the patient, but these adulterants can also cause severe health risks. For example, several adverse events have been reported due to adulteration of glycerin with diethylene glycol (DEG) [73] and melamine in baby formula [74]. Therefore, when an analyst uses a spectral matching method to identify the presence of active components, the method should also be sensitive to the presence of contaminants.

Several studies using Raman spectroscopy have been conducted to address the SM method sensitivity for distinguishing adulterants while detecting the presence of anticipated raw materials. [72, 75, 76]. Various adulterants (e.g., DEG in glycerin, melamine in lactose, and DEG in polyethylene glycol) were successfully identified using a spectral matching method [11]. However, the limit of detection by the SM method depends on the intrinsic spectral properties of the materials. For example, glycerin and DEG are spectrally very close and the *SC* value of glycerin gradually changes as the amount of DEG in the test set increases (see Figure 1-4A). Rodriguez and colleagues published a method to measure the detection limit of impurities while using SM method [72]. Experiments were conducted for a range of DEG in glycerin compositions; SC was calculated for each of the compositions, and a polynomial line was drawn using SC values. From this line, the authors estimated the exact DEG compositions that would be expected to cause the SC test to deliver a failed result. In Figure 1-4B, it can be observed that while changing DEG composition, SC remained unchanged until the composition reached 10%. Afterwards, the SC value begins to

drop noticeably, crossing the 0.95 threshold when DEG is around 18%. Therefore, the authors note that if glycerin contains DEG below a content of 18%, contaminated samples will be misidentified as the pure sample. Additional studies are required to justify this detection limit, as the threshold value of 0.95 used by this study is an arbitrary value; there is no probabilistic interpretation associated with this. While setting the detection limit, other validation criteria such as sample repositioning analyst to analyst variability, etc., should also be considered. Other factors which may also affect the method quality include intra- and inter-day variability. Setting threshold values based on probability statistics would enhance confidence in the limit of detection.

Another potential solution to detect DEG might be to use unique spectrometric methods. For example, DEG and glycerin may have different spectral features in the NIRS, which will be more effective for detecting DEG in glycerin. Of course, thorough investigations would be required to develop NIRS methods for detecting adulterants.

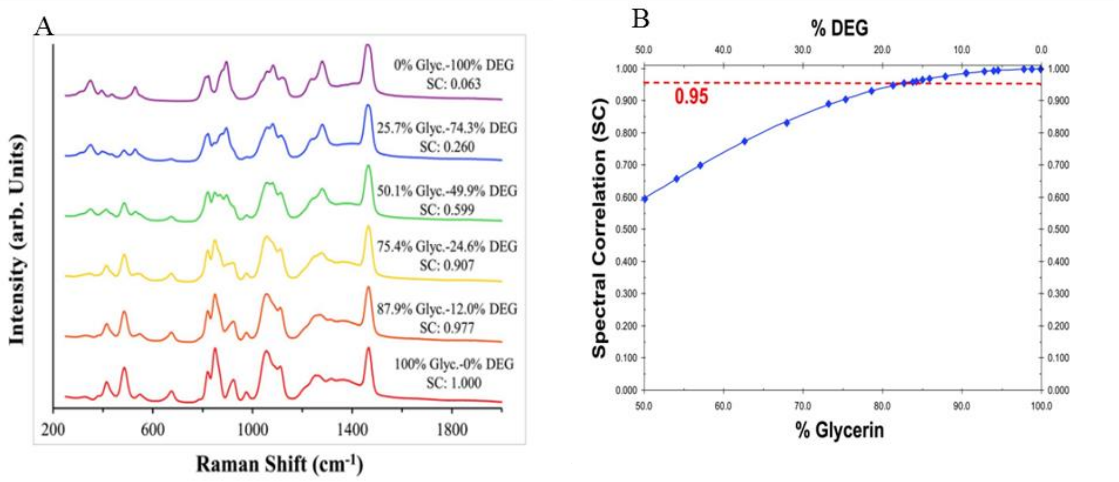

Figure 1-4: (A) The Raman spectra for a series of glycerin-DEG samples. From bottom to top, the spectral correlation value diminishes as the DEG amount increases. (Glyc- glycerin; DEG- diethylene glycol). (B) Quantifying the effect of increasing DEG on Raman spectra for the glycerin–DEG system. The red dotted line is the threshold value (0.95) to pass the test. The spectral correlation value is expected to drop below the threshold when glycerin samples contain 18% DEG or more. Figures obtained from Rodriguez et al [77], Copyright (2014) with permission from American Chemical Society.

The SM method has also been applied to detect falsified tablets. One potential approach is to detect API in tablets using a pure component spectral library. Since 50% of tested falsified products do not have the claimed API, or contain the wrong API [27], such a method can screen this type of falsified product. Loethen et al. [27] attempted to detect falsification in antimicrobial and antimalarial tablets acquired from multiple manufacturers. The spectral library was prepared using the antimicrobial and antimalarial pure components. Results showed that all the samples acquired from different manufacturers had a correlation value higher than 0.95 with the claimed API while lab-based products, which did not contain any API, had low SC values (see Figure 1-5)**.** According to this method, samples manufactured by any company can be authenticated using a pure component library, eliminating the need to collect sample spectra from each manufacturer

while developing a reference library. Therefore, this method would appear promising for detecting the presence of the declared API.

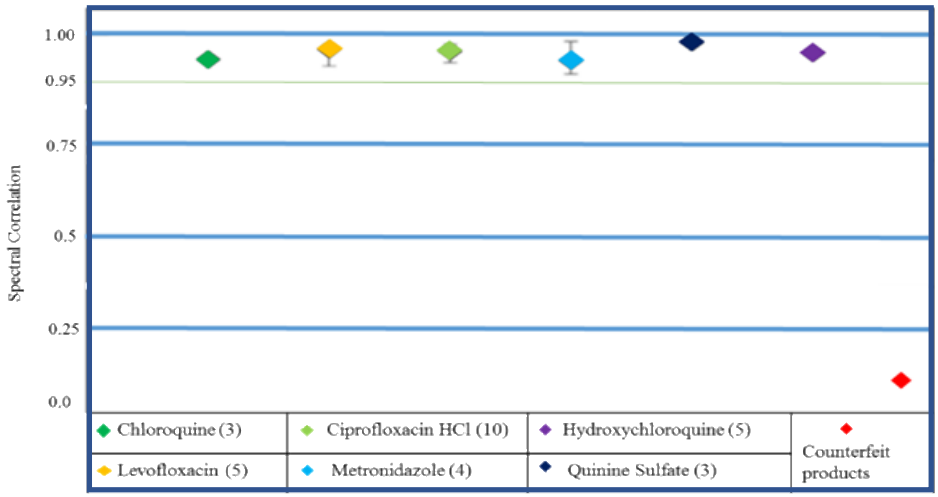

Figure 1-5: SC values were calculated for drug product spectra compared to the API library spectra. The numbers in parenthesis ( ) are the number of manufacturers in the sample set. Adapted from Loethen et al [27], Copyright (2015) with permission from Society of Public Analysts (Great Britain), Chemical Society (Great Britain), Society for Analytical Chemistry, Society of Public Analysts (Great Britain), Royal Society of Chemistry (Great Britain).

Though detecting API in the finished dosage form is an efficient process, this approach has more potential for Raman spectroscopy due to the presence of sharp API features relative to that for excipients. While Raman offers sharper absorbance bands, NIRS has an advantage of more significant excipient signals compared to Raman, due to the presence of C-H and C=O bonds in the excipients. Ultimately, it is assumed that excipient signal will be overlapping with API peaks, making Loethen's method impractical for NIRS. Additionally, samples evaluated by the Loethen group were relatively high-dose formulations. Low-dose drugs with overlapping API and excipient bands would provide difficulty in extracting the API signal using a SM method.

Rather than using the SM method with pure component libraries, some researchers have used the method to compare authentic samples with test samples allowing both NIR and Raman spectroscopy to be used for authentication of various finished dosage forms [14, 35, 78-80]. Because samples spectra would contain the data from each component, this method can be used to authenticate whether a solid dosage form contains the correct formulation. However, using sample spectra also has barriers. One limitation is the sensitivity of the analytical method. Studies have shown that, since different generic samples of a specific therapeutic group will often contain similar formulations (i.e., excipient compositions are often very similar to each other), both NIRS and Raman were unable to differentiate generic products from different manufacturers using the SM method [14, 15]. Therefore, cautions application of this method is recommended for authentication purposes.

1.3.3.1.3 Limitations of Spectral Matching Method

While the SM method has been useful for authentication of pure materials and finished products, the method has many limitations. The biggest drawback is that there is no specific direction established for setting a threshold value while using spectral correlation algorithms. Many studies used a threshold of 0.95 to determine whether two spectra are matched [13, 15, 35, 79, 80]. However, this value does not imply any probability or assurance statistics. Moreover, in different studies, this threshold was determined on a system-by-system basis to suit the desired application and the pass/fail decision was taken based on that unique threshold. Several examples are provided in Table 1-3, where different applications demonstrated the unique threshold values. For example, to differentiate the products produced from different manufacturers, threshold values were set to 0.99 for NIRS and 0.95 for Raman spectroscopy.

Table 1-3: Variation of spectral correlation method in different scenarios

Analytical technique	Applications	Spectral Correlation Threshold	Ref.
NIR	Differentiating batches	0.9999	[80]
NIR	Differentiating manufacturers	0.99	[15]
NIR	Differentiating batches	0.996	[13]
Raman	Differentiating molecules	0.92	[14]
Raman	Differentiating manufacturers	0.95	[27]
Raman	Differentiating expired products	0.996-0.998	[44]
Raman	Differentiating liquid injectable	0.95	[43]

Additionally, the threshold can be affected by many external factors such as spectral noise, environmental temperature, operator variability, etc. Unfortunately, most of the studies which applied the SM method did not validate that the developed method would perform consistently over time, since they did not consider the fluctuation of these external factors [72]. While developing a spectral library, spectra should be collected more rigorously to avoid the effect of this external variability. If an effect is observed, the relative standard deviation of the measurement should be reported.

Another limitation of this method is illustrated when it is used to test high quality falsified medicines. High quality falsified medicines are commonly produced with a recipe that is similar to the genuine product and manufactured with modern equipment [15, 16, 40]. Most often, one or two excipients vary in the high quality fake products, compared to the genuine products. This causes minimal spectral differences between samples, which is insufficient to separate falsified product and genuine samples by the SM method.[14, 15]

Moreover, the effect of excipient variation on the correlation value will vary for different analytical techniques. As Raman spectroscopy offers lower spectral absorbance for excipients compared to NIR spectroscopy, small changes in formulation may be more difficult to detect using Raman spectroscopy [31, 45]. However, a comprehensive comparative study between Raman and NIR spectroscopy has not been conducted to fully understand the effect of formulation changes on the SM method. Therefore, further studies are required to understand the effect of different spectral features of the commonly used excipients on the SM method.

1.3.3.2 Exploratory Methods of Data Analysis

Exploratory methods of data analysis have been used to measure similarity or dissimilarity of samples without any prior information regarding their identity. These types of analyses are often called as unsupervised methods, as the analysis procedure does not have affiliation with the group or the source of the data. Principal component analysis (PCA) and clustering analysis (CA) are two of the most often applied methods for exploratory data analysis.

1.3.3.2.1 Theory

Principal component analysis (PCA): The PCA method projects multivariate spectra into low-dimensional space, highlighting the variabilities present in spectral data, although not specifically identifying the cause of such variability [81, 82]. Spectral variability arising from unique sample characteristics (physical or chemical) can often be visualized by this technique. PCA decomposes the multivariate response arranged in an X matrix into a product of two new matrices as indicated in the following equation:

$$X = T_k P_k^T + E \qquad 4$$

Where T_k is the matrix of scores which represent how samples relate to each other, P_k is the matrix of loadings which contain information about how variables relate to each other, *k* is the number of factors included in the model and *E* is the matrix of residuals, which contains the information not retained by the model. Falsified products often have different chemical profiles or are produced by different manufacturing conditions which are discernable by this data decomposition mechanism [41]. Additionally, PCA is convenient to use for other chemometric methods, such as clustering analysis, SIMCA, support vector machines etc., which will be discussed in subsequent sections. The reader is referred to the works of Wold et al. [81] and Martens & Naes [82] for a more detailed discussion of PCA.

Clustering method (CA): Clustering involves the partitioning of a dataset of 'n' objects in such a way that objects in the same group (cluster) are more homogeneous to each other than to those in other groups. Clustering analysis is accomplished using the entire spectra or using scores of the principal components computed with the previously described PCA models. Grouping of multivariate data is based on a similarity criterion. Many concepts and definitions of how to score the chemical or physical similarity between two samples or variables have been proposed in the literature [83, 84]. Among these, Euclidian distance, Mahalanobis distance, and correlation coefficient are commonly used to calculate similarity indices [84, 85]. These similarity indices are used to cluster the data in two ways: i) partition clustering and ii) hierarchical clustering. The partitioning method uses similarity indices to separate the dataset into user defined groups, whereas hierarchical clustering establishes a data hierarchy. It should be noted that while clustering

methods may identify patterns in the data, but a conclusion about sample identity (whether falsified or genuine) should not be drawn from such method.

1.3.3.2.2 Applications of Exploratory Methods

PCA: PCA has been successfully applied to visualize the difference of genuine and falsified samples. Dégardin et al. [86] presented a large and complicated NIR data set which included 29 different pharmaceutical product families. Some of the product families have similar spectral signatures as they used similar excipients. Moreover, low dosage forms resembled the spectral signatures of placebo samples. However, while PCA was applied to this dataset, the first two PC scores enabled visualization of only two groups, while PC 3 and PC 4 helped to observe at least eight other groups. Consequently, after considering additional PCs, most product families were discernable (See Figure 1-6). Therefore, transforming raw spectra to a lower dimension made these samples statistically different. This is advantageous for falsified drug detection, as falsified products often contain unique formulations in comparison to genuine samples [63].

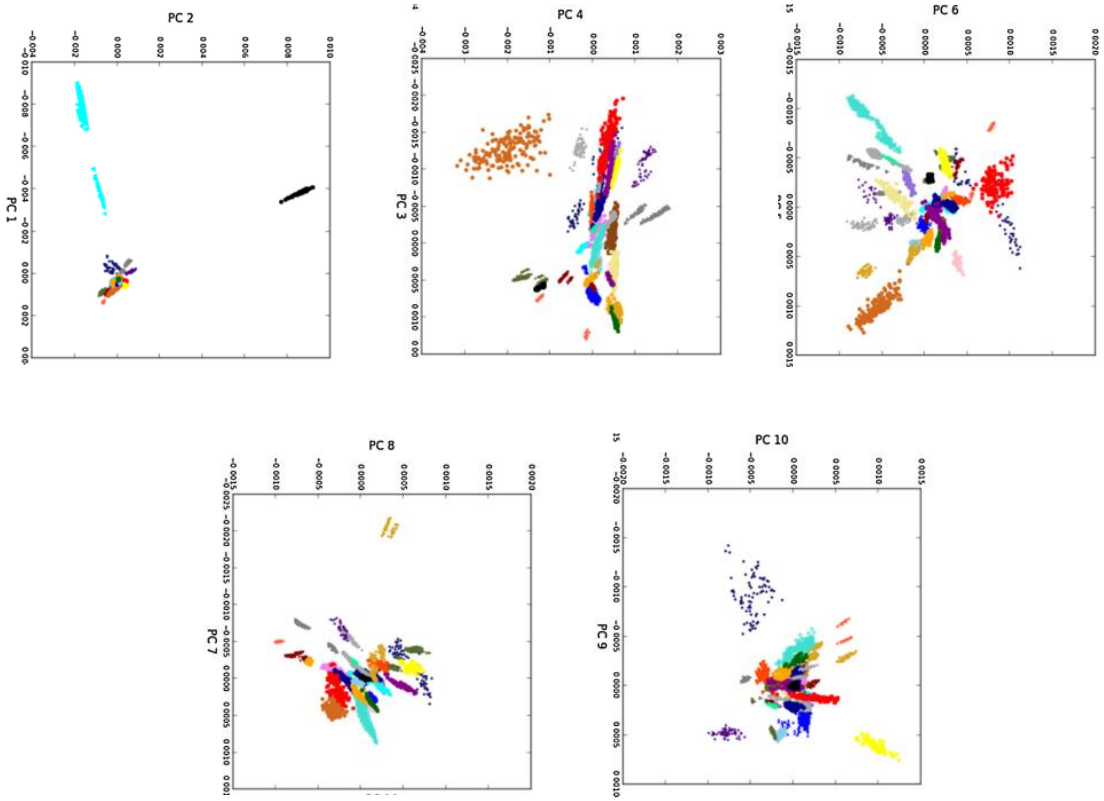

Figure 1-6: Results of the PCA applied to the calibration spectra pretreated with SNV. Each color represents one of the 29 product families. Figure obtained from Dégardin et al. [86], Copyright (2016) with permission from Elsevier.

Since falsified drugs are typically manufactured without the benefit of Current Good Manufacturing Practice (cGMP), the poor quality of these products is typically reflected in higher inter- and intra-tablet variabilities of components. Inter-batch variability will also be more significant than is typical for genuine products [41, 80, 87, 88]. These variabilities can usually be distinguished by NIRS or Raman spectroscopy using the PCA method. Rodionova et al. [41] showed that the spread of scores (generated from spectral data) in falsified products was higher relative to that of the genuine samples (see Figure 1-7A). Here, single point spectrometers were used to visualize these inter-tablet variabilities.

To demonstrate intra-tablet variabilities, a NIR-CI imaging system was used in other studies. Statistical parameters of score distributions (mean, standard deviations, skewness) showed significant differences between genuine and falsified medicines [89, 90]. Figure 1-7B shows a PC image of the falsified (left) and genuine samples(right).

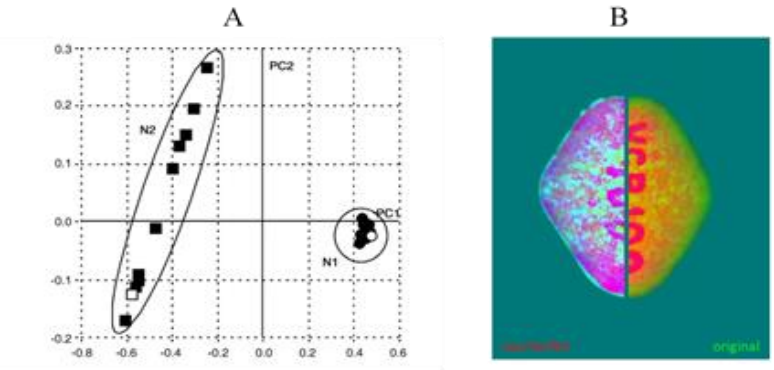

Figure 1-7: (A) PCA scores plot of genuine tablets (dots) and falsified tablet (squares). Tablets were also cut and the internal surface scanned; genuine and falsified samples are displayed in open dots and squares B) NIR Hyperspectral imaging of counterfeit (left) and original tablet (right). Figures obtained from A) Rodionova et al. [41], Copyright (2005) and B) Wilczyński et al. [90], Copyright (2016), with permission from Elsivier.

Compared to NIRS, Raman spectroscopy may demonstrate greater sensitivity towards the variation of API between genuine and falsified products. Neuberger et al. [91] systematically investigated the capability of Raman to differentiate chemically dissimilar samples. Raman spectroscopy distinguished samples with different coating levels, varying amount of drug loading, and different excipients using PCA. Also, Raman spectroscopy successfully detected the degradation of aspirin over time due to changes in storage conditions [91].

Additionally, by analyzing the loadings plot of PCA analysis, it is possible to discern probable reasons for score variations. Ryder et al. [92] showed that the loading plot was correlated

with narcotic components, which might have been attributed to the API variation. The character of a loadings plot may provide information related to the presence of a certain molecule, which is especially critical when samples are seized by law enforcement without any packaging or details regarding sample origin [92].

Along with chemical content, the physical structure of the samples often provides useful information to detect falsified products, since it is difficult for fraudulent manufacturers to follow exact manufacturing steps such as blending, granulation, compression, etc. NIR spectra are sensitive towards the physical characteristics of the sample, and this can make NIR measurement information-rich. For example, samples manufactured at two different sites can be distinguished using NIRS [35]. Vrendenbregt et al [35] demonstrated that similar tablets from two manufacturing sites (Europe and the USA) were statistically separated by PCA. In another study, acetaminophen tablets prepared in the United Kingdom and Malaysia were also identified accurately using PCA [80]. Neuberger et al. [95] aimed that Raman is not adequately sensitive to detect physical differences (e.g., density variability associated with compression force, mixing quality), which ultimately created minimum PCA variations among these samples (see Figure 1-8). However, this study did not consider other physical factors such as particle size variations, tablet size, etc., which might have effects on Raman spectra. Therefore, further studies are required to investigate whether falsified and genuine samples are differentiable based on the physical factors of the samples using Raman spectroscopy.

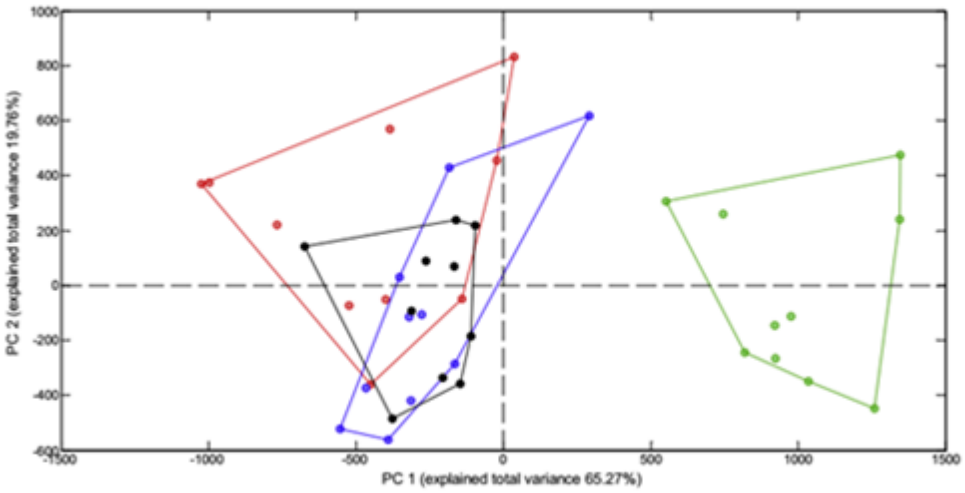

Figure 1-8: Score plot of PC1 and the PC2 of the samples which were prepared using different compression force. (very low = black, low = red, optimal = blue and high = green). Figure obtained from Nuremberg et al. [91], Copyright (2015) with permission from Elsevier.

Cluster Analysis (CA): It is known that the global spread of falsified drugs is most likely funded by organized criminal activity involving manufacturers, wholesalers, distributors and local sellers. Hence, there is significant possibility that some falsified products are manufactured from common sources [33]. Investigating the source of such falsified drugs will be helpful in finding the origin of criminal activities. Various types of cluster analysis facilitate the development of dendrograms, which may provide an opportunity to visualize the clusters of the seized samples ultimately help to separate genuine from falsified drugs.

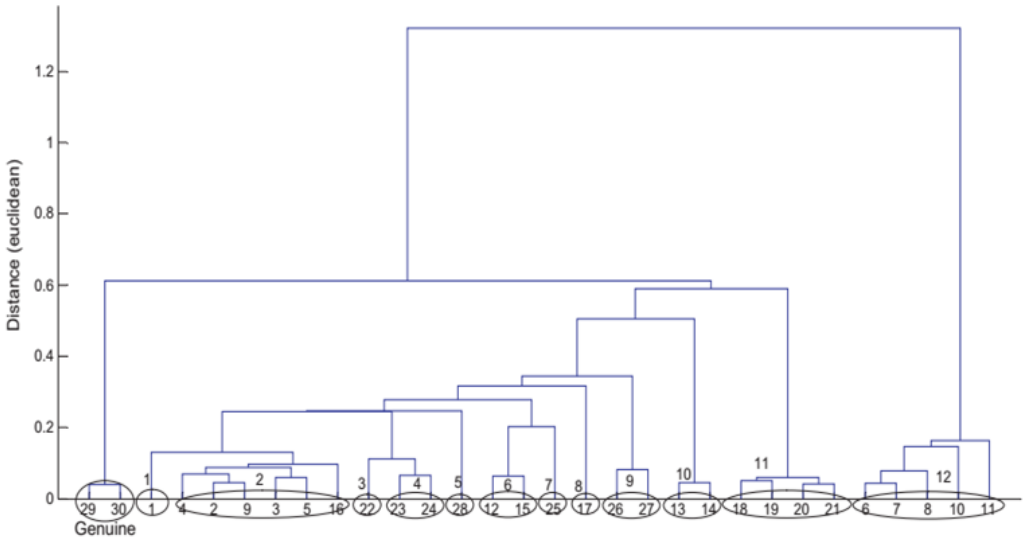

Figure 1-9: Dendrogram computed using Euclidean distance and average linkage method. NIR spectra were collected from capsules and SNV preprocessed. Figure obtained from Been et al. [45], Copyright (2011) with permission from Elsevier.

Been et al. [45] used a large database of samples which were seized from 27 different regions and a hierarchical clustering method was applied to form a dendrogram by computing Euclidean distances to separate the underlying groups (see Figure 1-9). Authors found that 12 types of chemical profiles existed among these seized samples; the unique profiles were later confirmed by the reference method. This cluster formation was beneficial for profiling newly acquired samples. New samples were projected to these 12 groups and the distances between the test sample and different clusters were calculated. The cluster which provided the minimum distance was the suspected source of the seized sample. Therefore, cluster analysis helps to efficiently investigate the sources of different falsified products [42, 45, 53, 56].

1.3.3.2.3 Limitations of Exploratory Methods

Though PCA is one potential approach to identifying falsified samples, certain challenges exist for the application of this algorithm. One of the drawbacks is that a large number of samples

are required to build an effective model. Preparation of a sufficiently large reference library can be difficult for the PCA method. Unfortunately, there is no clear direction as to how many samples should be used for method development and the number of samples needed for PCA analysis varies across studies [88, 93]. Additionally, the boundary design, which is often 95% equal frequency ellipses, varies depending on the nature and quality of samples used in calibration development [31, 40, 89, 91]. As PCA explains the variation between groups, it is challenging to separate sample groups when intra-group variation is higher than inter-group variability. Therefore, representative samples should be collected from the pool of genuine samples for the development of the PCA method.

Cluster analysis is useful to understand the types of seized samples. However, the most significant challenge for the analyst is setting an appropriate threshold value, as the actual number of potential sample groups is unknown to the analyst. Arbitrarily setting a threshold value often results in an over-classification or under-classification problem. This becomes more critical when the same source of sample has high batch-to-batch variability. Therefore, samples from the same source may be classified into two different clusters. Even genuine samples can be clustered into two groups if they are stored under unique conditions [94].

As there is generally no reference information used for the unsupervised method, careful interpretation of PCA or CA results is required. While in typical pharmaceutical applications of NIRS or Raman spectroscopy, it is comparatively straightforward to gain an understanding of the score variability because samples are relatively well characterized, for falsified sample detection the samples are obtained without much detail about the source. To ensure the correct interpretation of the visualized differences of PCA or CA, the data collection should be consistent across the

samples. For example, if repositioning error dominates in the spectral pattern, it is difficult for the analyst to make conclusions about the source of variation in the scores.

1.3.3.3 Supervised Techniques

1.3.3.3.1 Theory

Supervised techniques are the most applicable methods for false product identification since they provide direct decisions about the test samples (whether it is falsified/genuine). Supervised techniques are mainly classified into two categories: class-modeling and discrimination. Class-modeling (also known as the soft classification approach) allows samples to be assigned to one or multiple groups. However, discrimination methods (also known as hard classification methods) always allow a sample to be considered as a member of only one group from the pool of groups being considered. This is illustrated in Figure 1-10, where examples of both the class-modeling and discrimination approaches are shown for a data set where objects are described by two variables and grouped into three classes (blue, green and brown). When a class-modeling technique is applied, each class space is separated by a specific boundary from the rest of the data space (Figure 1-10A). Considering three unknown subjects (T_1, T_2, T_3), T_2 is considered as class 2, whereas here T_3 is considered as an unclassified object, and T_1 falls outside the model boundary, and therefore cannot be considered at all.

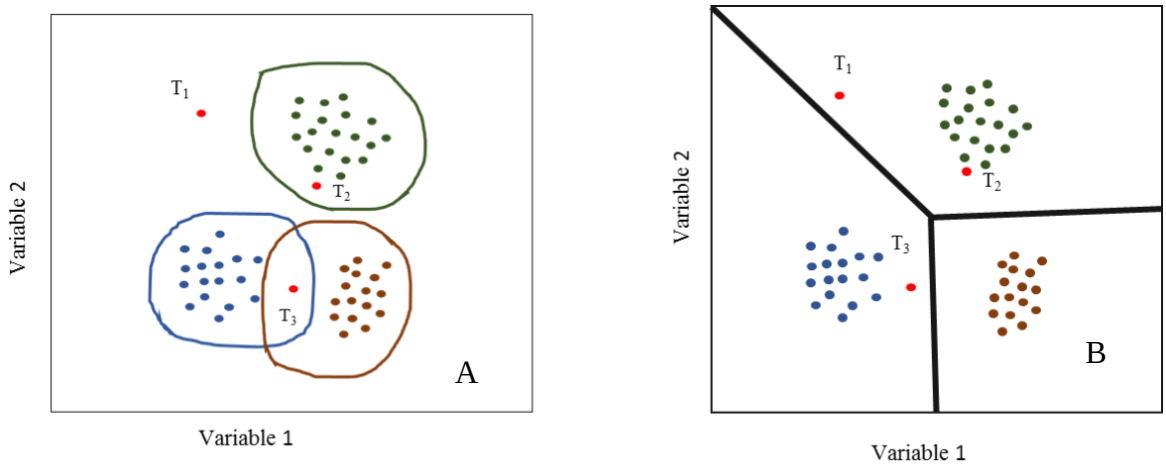

Figure 1-10: Example of both class-modeling (A) and discrimination (B) on a data set including 52 objects described by two variables and grouped into three classes (blue, green, and brown circle). Figures adapted from Ballabio et al. [83], Copyright (2009) with permission from Elsevier.

In the case of discrimination, T_1, T_2 and T_3 must be classified into three classes (see Figure 1-10B). These objects are projected into data space and assigned to the category corresponding to the hyperspace where they are placed. T_1 and T_2 are assigned to class green, even if T_1 is far from the green samples, while T_3 are recognized as blue [83, 95].

The outcome of these two supervised classification methods is assessed by two important figures of merit: sensitivity and specificity [83, 96-98]. Sensitivity is defined as the percentage of samples correctly classified to the class of interest. Authentication methods should be able to identify the genuine samples correctly, reflecting the sensitivity of the model. Specificity is defined as the percentage of samples correctly rejected, since it is also important to recognize different types of falsified products, and reject them [99]. These two parameters are calculated by the following formulas:

Sensitivity $= TP/(TP + FN)$ 5

Specificity$= TN/(TN + FP)$ 6

where TP, TN, FP and FN are true positive, true negative, false positive and false negative, respectively [99]. A visual tool that compares sensitivity with (1-specificity), is the so-called receiver operating characteristic (ROC) curve, which has been applied in spectroscopic classification methods [96, 100]. By calculating the area under the ROC curve, it is possible to derive a summary performance parameter for sensitivity and specificity that may serve as adequate figures of merit for model comparisons.

An assortment of multivariate modeling approaches has been developed to be used both as class-modeling and discriminant methods. Here, some of the most commonly applied techniques are briefly discussed. More detailed information on the considered techniques can be found in the technical literature [18, 84, 96, 97].

1.3.3.3.1.1 Class-Modeling Approach: SIMCA

SIMCA is a PCA based approach where calibration samples are used to develop a PCA model. After decomposing the data and reducing it to lower dimension, a decision boundary is formed. Over the years, different versions of SIMCA models have been developed based on unique approaches to boundary formation around the training set. These different versions are based on two distances: 1) score distance (SD): determined by computing the distance in PC space between an unknown sample and a target group, referred to as Hotelling's T^2, and 2) orthogonal distance (OD): determined by calculating the unknown sample's squared residual distance to the model space, known as the Q residual [17, 18, 82, 101-104].

The Q_i statistic is defined as the sum of squares of the residuals and can be calculated according to Equation 2, where e_i is the residual of sample *i* after applying the SIMCA model.

The Hotelling's T^2 measures the information of each sample within the PCA or SIMCA model and is calculated by means of Equation 1, where t_i is the i-th row of the T_k, the n by k matrix of k score vectors from the PCA model, and matrix of k scores vectors from the PCA model of n number of target class samples and Λ^{-1} is a diagonal matrix containing the inverse of the eigenvalues associated with the k eigenvectors (principal components) retained in the model.

The $Q_i$statistic is defined as the sum of squares of the residuals and can be calculated according to Equation 2 where e_i is the residual of sample *i* after applying the SIMCA model.

$$T_i^2 = \sqrt{t_i \Lambda^{-1} t_i^T} \quad (7)$$

$$Q_i = e_i e_i^T \quad (8)$$

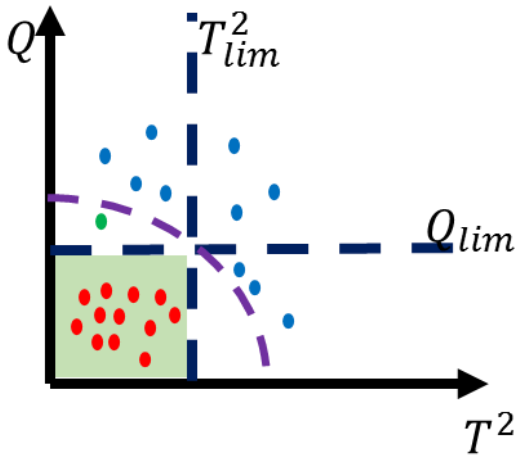

Figure 1-11: Graphical representation of Hotelling's T^2 and Q residual. Threshold boundary based on T^2 versus Q residual. The acceptance area is the squared space in the graph, where samples plotted at any point outside of this area are rejected. According to this threshold, nearly every sample will be accepted, with only the green sample being rejected. A more flexible boundary could be applied as shown by the semi-circular area. Then, both green and red samples will be accepted. Figure is adapted from López et al.[100], Copyright (2014) with permission from Elsevier.

A sample is assigned to a target class if the computed distances are shorter than a predefined threshold value. These threshold values are based on T^2_{lim} and Q_{lim}, which are the confidence interval for the model under consideration. Confidence limits for SD (that is referred to as T^2 in the PLS_Toolbox and related literature) are given from Hotelling's T^2 to obtain T^2_{lim}, i.e. ($T^2_{lim} = F_{k,n-k}k(n^2-1)/(n-k)$) considering k and $n-k$ degrees of freedom, where k is the number of PCs and n is the number of calibration samples for the target class. The $\chi 2$ distribution is used for the squared residuals and confidence limits for the orthogonal distance (OD, that is also referred to as Q in the PLS_Toolbox and related literature) are computed by the Jackson and Mudholkar

(JM) approximation. Wolf et al. developed SIMCA model based on Q residual. Candolfi et al. proposed a SIMCA model which is based on the Mahalanobis distance; details will be found in the relevant literature [68, 105].

A more recent approach is to consider both Hotelling's T^2 and Q residual. According to this approach, boundaries are defined considering the reduced statistics. The reduced Hotelling's T^2 (T_r^2) and the reduced Q statistic (Q_r) values can be calculated from the ratio between the corresponding statistic of the sample i and the corresponding limit at α = 0.05. Here, samples must have values under 1 for both statistics to be considered ''within the model'' which was defined by the square boundary in the Figure 1-11. A newer version used by PLS toolbox takes the distance defined by Equation 9 [17, 18]. In this case, the boundary considered as ''within the model'' forms a semi-circle with a radius of $\sqrt{2}$, which is mentioned as d in the Equation 9.

$$d = \sqrt{\left(\frac{Q}{Q_{lim}}\right)^2 + \left(\frac{T^2}{T_{lim}^2}\right)^2} \qquad 9$$

A variety of methods are proposed to develop an acceptance area are based on different distribution assumptions of OD and SD. Pomerantsev proposed to use the χ2 distribution for both of these parameters. This method is referred to as data-driven SIMCA (DD-SIMCA) [106].

1.3.3.3.1.2 Discrimination Analysis: PLS-DA

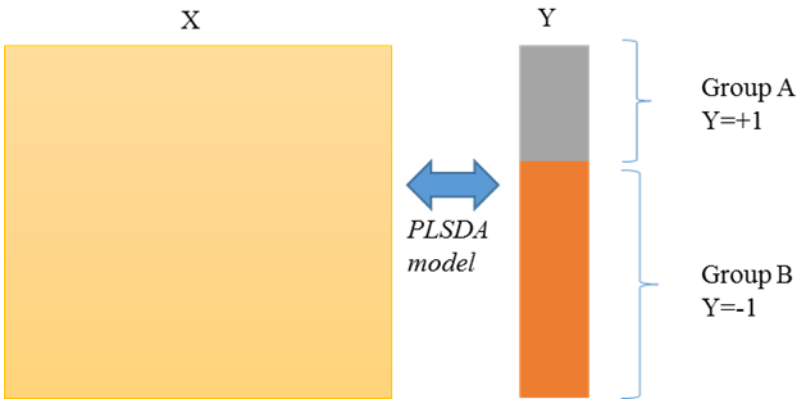

Figure 1-12: Partial least squares discriminant analysis (PLS-DA) model for two classes, where X is a matrix containing spectral data, Y are dummy variables categorized as genuine (Group A) and falsified samples (Group B). Adapted from Brereton et al. [107], Copyright (2014) with permission from John Wiley and Sons.

Partial least-squares discriminant analysis (PLS-DA) is derived from PLS regression to develop a model that predicts the class number for each sample. While developing a PLS-DA calibration model, the number of groups and the samples that belong to each group are defined with dummy variables. For example, if a data set contains just two classes, Y can be set up easily by assigning samples in one of the classes as 1 if the samples are in the class, and 0 if it is not. This membership is paired with a training set (X block), and PLS is implemented in the usual way (Figure 1-12). During the calibration process, the PLS-DA method is trained to compute membership values and assigned a class membership. It is reasonable that the model does not predict perfectly, so a limit must be set, for example, 0.5, above which the sample is estimated as 1 and below which the sample is estimated as 0. For spectroscopic product authentication system development, PLS-DA can give good insight to the underlying reason for discrimination via weight and loadings. Also, it is a popular technique due to the advantages of wavelength selection and noise reduction associated with the PLS algorithm. A more detailed discussion of the PLS-DA algorithm is available elsewhere [107-109].

1.3.3.3.2 Applications of Supervised Classifications:

SIMCA: PCA analysis utilizing both Raman and NIR spectroscopy can separate diverse samples based on physico-chemical differences (e.g., composition differences, API amount differences, etc.). SIMCA, using PCA, is an effective method for detecting falsified drugs. Scafi and colleagues [34] demonstrated the use of SIMCA to detect 12 types of falsified products of different compositions. Scafi used PCA, constructed from NIR spectral data generated from the genuine samples. Then, falsified products were projected onto these PCA models, and distances were calculated for each falsified sample showing clear separation. Here, it is important to mention that this method only rejected samples declared as falsified products. Further reference analysis could provide better understanding of the specific nature of these falsified samples relative to the genuine samples.

In another study, Storme-Paris and co-authors [20] used SIMCA, noting that the SIMCA method distinguished tablets with small differences of composition Raman spectral data. In their study, falsified and genuine products varied by 1.0 - 2.5% API (%w/w), and the SIMCA method was successfully able to identify the falsified products.

SIMCA was used in a later study with NIR and Raman to overcome some of the limitations of the spectral matching method, detecting a small amount of impurities in the raw materials. This study detected a contaminant (DEG) in glycerin up to 5% w/w; three times lower concentration range than using the spectral matching method [11]. It is important to note that although SIMCA provides certain advantages, this method is only providing information about whether the sample is pure or has some adulterants. Additional investigation may provide information about the types of chemicals present in the sample.

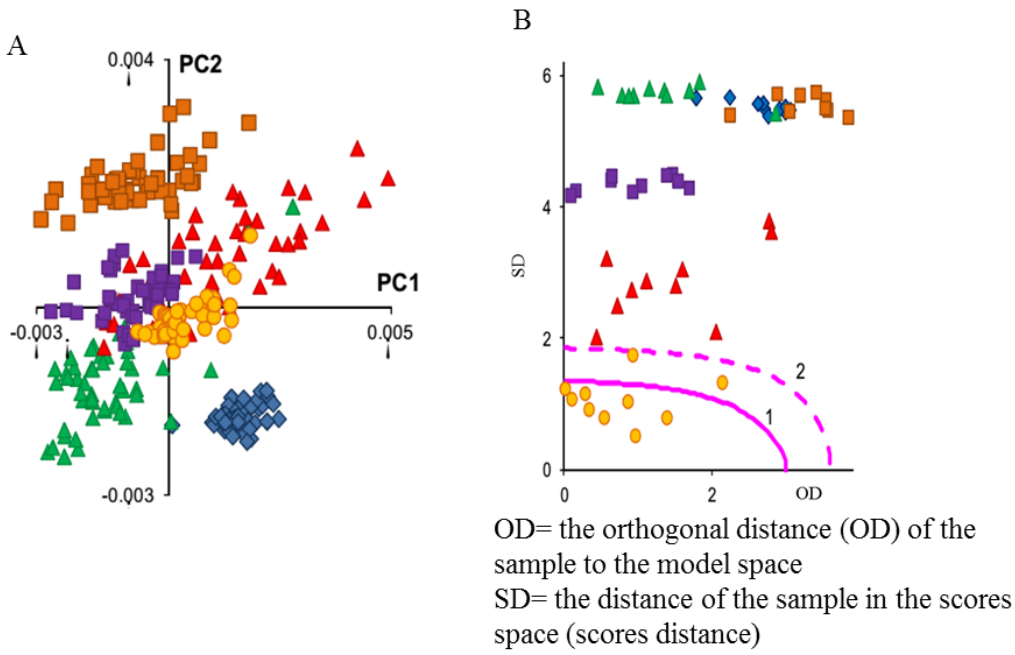

Figure 1-13: (A) Score plots for PCA analysis: (a) PC1 vs. PC2. (Different color and shape represent different groups of samples, (B) Result of the Test sets is displayed. Here, SIMCA model is developed from the target class (yellow-round). Figure adapted from Zontov [15], Copyright (2016) with permission from Elsevier.

Liquid dosage forms have also been authenticated using SIMCA. One example is the authentication of dexamethasone ampules [40]. This study used two genuine batches (G1 and G2) of 4% dexamethasone 21-phosphate, and a batch of falsified product (F2) in 1 mL closed transparent glass ampoules. NIR spectra were collected through the vials. The performance of this approach was evaluated with reference testing by CE-UV, GC-MS, and HPLC-DAD. SIMCA analysis of NIRS data demonstrated comparable performance to the reference techniques.

SIMCA has also been used to detect high quality falsified products. However, to detect this type of product, adjustment of the decision boundary improved the model performance, demonstrated using DD-SIMCA. Figure 1-13A shows, when products contained the same API but have one or two different excipients, PC scores generated from different products were closely

grouped. This tight representation of scores also reflects the similarity of the formulation of the scanned samples. In Figure 1-13B it was observed that, if method developed using one group (yellow-round), and all the other groups (green- triangle, red-triangle, brown-square, blue-diamond) projected onto the developed model, then initially developed model rejected two of its test samples (yellow-round). This decreases the sensitivity of the model by tuning the confidence interval. The authors moved the boundary from 1 to 2, which changed the acceptance area of the model. This change avoided rejection of two genuine samples and improved the sensitivity of the model [15, 16, 110-113]. Despite this successful result, risks of changing boundaries may be high without using an independent validation set to test the consistency of the result. Without an independent validation, it is difficult to predict if the model will be adequately sensitive to accept other batches of genuine samples consistently. Also, enhancing the model with representative genuine samples from different batches would reduce this concern. Above all, this study emphasized the importance of considering a change in the decision boundary to enable detecting high quality falsified products [17, 111].

Though there are advantages of using SIMCA, it is also highly sensitive towards small variation of external factors which can decrease the performance of the method. For example, operator and instrument variabilities caused spectral perturbation, which often projected genuine test samples outside the PCA space, causing degradation of model performance [114, 115]. This introduces new challenges, especially when the analyst needs to transfer the model from one instrument to another instrument [116]. Some of these issues can be resolved by removing unwanted variables, which have small discriminant power [117]. Selection of appropriate preprocessing methods may help to reduce some of this variability. For example, offset or baseline drifts are removed by derivative, standard normal variate (SNV), or multiplicative scatter

correction (MSC) algorithms [18]. Calibration transfer and method algorithms are useful when analysts are required to use multiple instruments. The following studies provide direction for analysts who must transfer spectroscopic methods [116, 118, 119].

Another essential model parameter is selection of the appropriate number of PCs to use for calibration development. Rodionova et al [16] developed two SIMCA models by selecting a different number of PCs. Here, a model developed using three PCs successfully separated samples prepared in the different seasons, whereas the model developed including only two PCs did not [15, 105]. Proper statistical approaches should be followed in selecting PCs. One way to select the appropriate number of PCs is via cross-validation (CV) [82]. Finally, selecting the proper number of PCs avoids unnecessary rejection of genuine samples (false negative) or incorrect authentication of falsified products (false positive). Analysts should be careful about both factors, as rejecting falsified samples are important from a patient's perspective, but, similarly, accepting genuine samples is critical from a manufacturer's perspective. Further discussion about selecting principal components can be found in Bro el al. [120]

PLS-DA: PLS-DA successfully identified falsified tablets containing the wrong API in an example by Piender et al [31]. Lovastatin is occasionally used in falsified products instead of atorvastatin. For discriminating lovastatin from atorvastatin, Piender et al [31] demonstrated PLS-DA as a useful technique for discriminating the two active components. Moreover, investigations of the regression vector of PLS-DA analysis demonstrated the important features which helped to distinguish the differences (Figure 1-14) [31, 45, 121]. Similarly, tadalafil and sildenafil were separated using the PLS-DA method. Another potential application for the PLS-DA method is to detect adulterated products [26]. However, it is important to note that, while developing a

calibration method, samples containing the expected amount of impurities should be added into the model as an alternate class of the pure sample. Otherwise, impure samples may be accepted as pure samples, which will give false positive result.

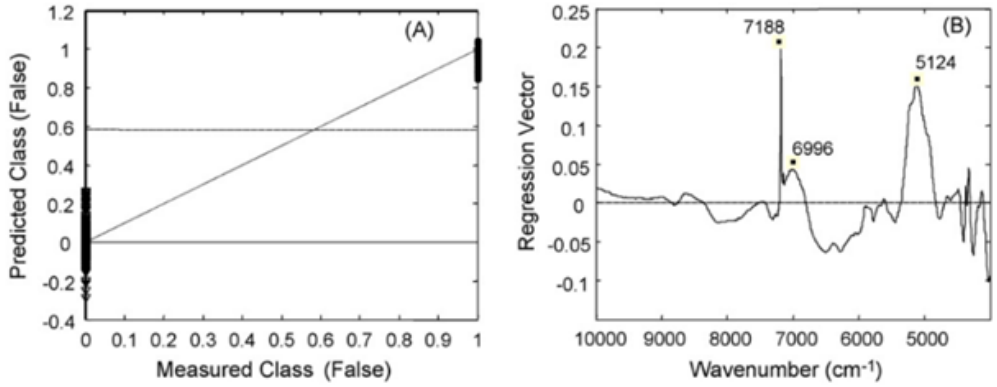

Figure 1-14: Class prediction plot (A) and regression vector(B) of the PLS-DA model of NIR spectra based on three LV's to discriminate counterfeits (•) from genuine tablets (▼). Figure obtained from Peinder [31]. Copyright (2008) with permission from Elsevier.

PLS-DA is also useful for identifying expired products which are often repackaged and resold, resulting in a major public health risk. Qun et al.[44] used both expired and non-expired products to develop the PLS-DA calibration model, where expired products and non-expired products are used as two classes. Then expired products were detected by using an independent test set [20, 36, 44]. The success rate of detecting the expired product in this study was possible due to a change in the expired tablet's matrix. Raman spectroscopy was sensitive to the change of the tablet matrix. However, this might not be true in other cases. Therefore, before implementing the PLS-DA method to detect expired products, analysts should carefully investigate whether the expiration of the product creates any change in the sample spectra. PCA can also be an important tool to understand the variabilities among the expired and non-expired products before developing PLS-DA method. It is also suggested that manufacturers store their expired products and develop

a reference library. This will be helpful to develop an authentication system to detect expired products in the future.

Similar to SIMCA, proper wavelength selection and preprocessing methods also help to improve PLS-DA classification model performance [36]. For example, baseline removal by a derivative method minimizes spectral changes associated with the tablet geometry, physical differences in tablet faces, and sample position relative to the probe beam [34]. Theoretical and experimental evidence showed that elimination of useless predictors (wavelengths which are not carrying important information) increases the anticipated performance of PLS-DA [121, 122]. Li et al [121] showed that classification of five different manufacturers of anisomide tablets was successfully accomplished by appropriate variable selection method. Here, iterative PCA (iPCA) was successfully applied to find the superior spectral regions to predict and classify falsified products. However, wavelength selection is not always necessary. In fact, Fernandes et al [26] demonstrated cases where false sample identification was less effective with wavelength reduction as there is a risk of inadvertently removing an essential wavelength region [44, 121].

1.3.3.3.3 Limitations of Supervised Techniques

It is evident from the literature that SIMCA and PLS-DA are often used for the same application, and their performance has been compared [20, 45]. However, this comparison is not necessarily reasonable, since different models use varying amounts of information. In the case of PLS-DA, the algorithm uses information regarding several classes and develops a decision boundary based on the existing classes; whereas SIMCA develops a decision boundary based on only one (its own class).

Depending on the different scenarios, PLS-DA and SIMCA should be used carefully. For example, SIMCA is one of the best choices when the variabilities of falsified samples are not possible to be sampled sufficiently. By using genuine samples, a target class can be developed, and any new unknown sample which is dissimilar from the genuine samples is projected outside. However, when an analyst develops a PLS-DA model, the model assigns class membership based on the variability modeled from available samples. Then, predicted unknown samples are assigned to any of the classes, even if they have very different compositions. This leads to an incorrect recognition of new samples [123].

On the other hand, when the potential variability of falsified samples has a limit, PLS-DA is applicable. For instance, when the types of impurities found in falsified samples are expected, then the discriminant techniques may perform better than class-modeling. Since data from genuine and impure samples have different directions in the score space, effective boundaries around different groups' scores form easily. For the above reasons, PLS-DA and SIMCA should be selected depending on the target sample.

Supervised classification methods provide only diagnostic results (in class or out of class), but other specific information, such as types of impurities, whether a sample contains any harmful content, or whether a tablet contains any API or not, is not typically identified using this method. Therefore, while developing authentication systems, the analyst should consider a variety of chemometric techniques to enhance the potential for a successful authentication method (see Table 1-4).

Table 1-4: Comparison of different chemometric methods:

Data Analysis Method	Method	Aim	Relevant applications and comments
Spectral matching	Spectral correlations Spectral Distance	Similarity and dissimilarity measurement between spectra	• Prescreening of raw material identification • Impurities/adulterant detection • Detection of API or excipients in the finished dosage form. • Must determine a useful threshold. • For NIRS broad overtones and combination bands reduce the usefulness of this applications.
Exploratory analysis	PCA	Projection and visualization of data in a low- dimensional space	• Physico-chemical differences of the genuine and falsified products captured by spectroscopic techniques. • PCA forms data clusters, which are related to the sample variance. Examples: composition differences between genuine and falsified products, variance observation between genuine and falsified samples.
	Clustering method	Partitioning data into clusters	• Link developed between seized samples from different regions based on differences.
Supervised techniques	Class-Modeling: SIMCA	Genuine samples are used to develop class and unknown sample is classified based on its distance to the class	The class-modeling approach is useful for detecting unknown falsified samples: • Finished falsified dosage forms which are highly similar to genuine products, and difficult to separate by spectral matching method, are easily identifiable. • Drugs containing the wrong active substance and or the correct active substance with wrong dose are detectable. Adulterated raw materials (API and excipients) may be detectable. • Rigorous method development is required.
	Discriminant analysis: PLS-DA	Covariance between data and class membership is stablished to develop classifications	• Classification methods are developed from two or more classes, for example, a) the original drugs with expired date and b) drug developed from different APIs. • Directions in the data space that discriminates the two or more medicine classes can be directly developed from this method.

1.3.3.4 Other Methods

Raman Barcode: Lawson and colleagues developed an interesting method to screen whether seized finished products contain API or not, which they stated as “Raman barcode” method [32, 64]. A barcode is developed from API spectra and finished products by replacing zero intensity to every wavelength shift except the wavelength shift that represented Raman peaks. The identity of API was ensured by comparing the percentage of nonzero overlap between the target API barcode and finished drug product barcode (Figure 1-15). This method was successfully applied to test 18 different original products acquired from the market and nine simulated falsified products. A Raman barcode was applied only for high dose drug products with the assumption that excipients are Raman inactive. However, this conjecture restricted the use of this method only for Raman spectroscopy, as NIRS demonstrates high excipients signal. Additionally, this method was only applied for samples containing a single API and was not tested for the tablets which contained multiple APIs. Overlapping of different API peaks increases the risk of detection of a specific API.

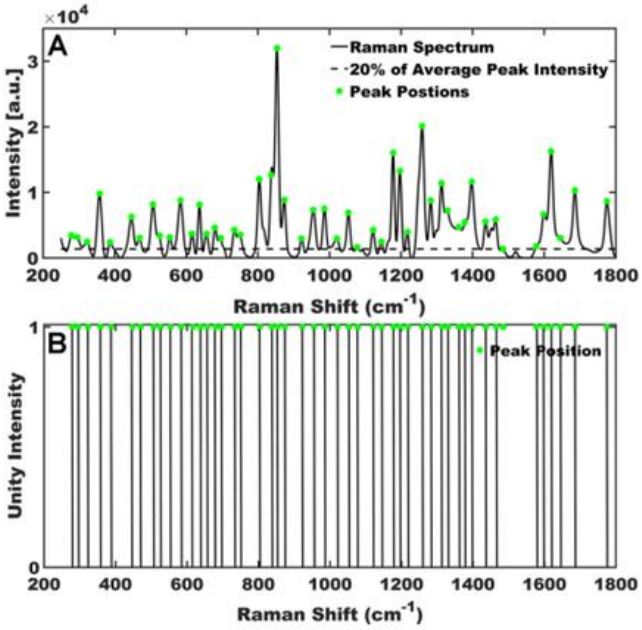

Figure 1-15: Generation of Raman Barcode. All peaks denoted with a green circle are included in the barcode spectrum. Figure obtained from Lawson et al. [32], Copyright (2016) with permission from American Chemical Society.

Machine Learning Method (Support Vector Machine): A Support Vector Machine (SVM) is developed by constructing the best separation hyperplane to maximize the margin between different groups. The widest margin between the two groups is identified using several samples residing in the boundary, which are called support vectors. This margin can be linear or nonlinear depending on the type of kernel function that is applied. Finding the optimal hyperplane requires optimization of the model parameters. Details of the methods are discussed elsewhere [124, 125].

SVM can handle some of the challenges usually related to a) large datasets [86], b) samples which are collected using a limited spectroscopic wavelength range[63], and c) calibration transfer [116]. For example, newly developed pocket size spectrometers span a limited wavelength range

compared to full size spectrometers, creating sensitivity challenges in terms of detecting product identity. However, falsified products can be successfully separated from genuine products using SVM even with limited wavelength range. SVM is also less affected by small spectral perturbation when compared to SIMCA, which makes it a better algorithm for calibration transfer [116, 126]. However, careful optimization of SVM parameters are required before implementation.

Though classical SVM has been applied for falsified drug detection, other forms of the SVM algorithm, such as the support vector data description (SVDD) method, can also be useful for class-modeling. The advantage of SVDD is that it does not require two classes of samples during method development. Therefore, it is more suitable to use class-modeling techniques for analysis of pharmaceutical samples. In this dissertation project, SVDD was explored as a potential class-modeling technique for falsified drug detection.

Multivariate Quantitative Analysis: Hyperspectral chemical imaging systems use different multivariate regression methods to quantify the composition of falsified products. In most cases, compositions of the seized samples are generated without knowing actual formulations. Different algorithms, for example, classical least-squares (CLS) and multivariate curve resolution (MCR) methods, are useful to determine the compositions. Details of such algorithms are found elsewhere [66].

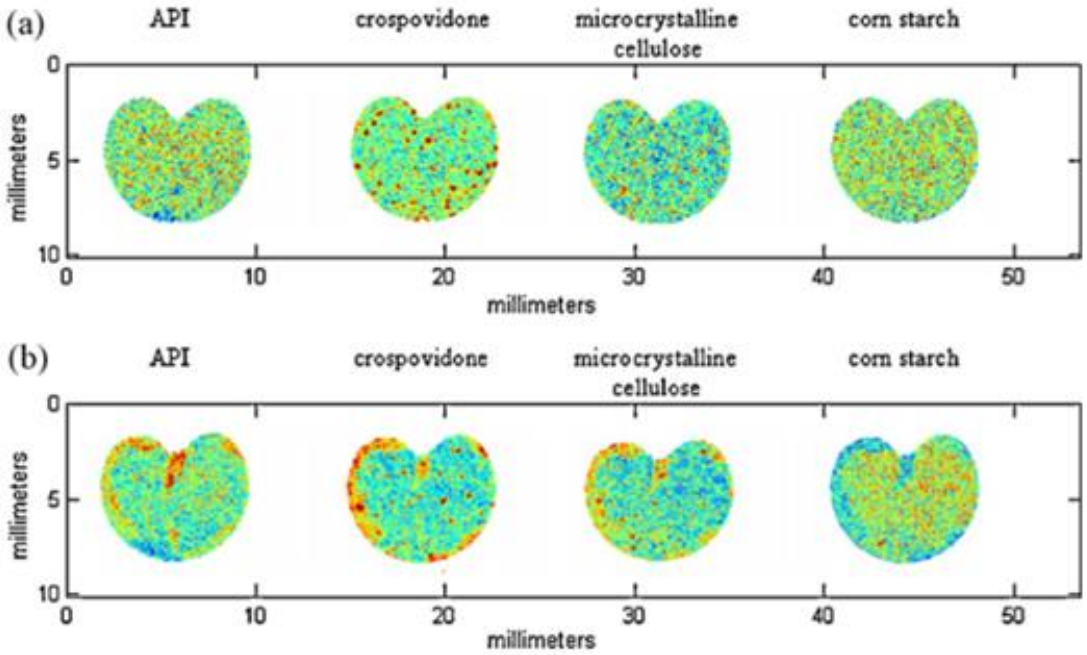

Figure 1-16: PLS predicted images of (a) genuine tablet; (b) falsified tablet– red pixels indicate higher concentration and blue pixels indicate lower concentration of the target component [89], Copyright (2010) with permission from Elsevier.

Lopes and co-authors [89] implemented Classical Least Squares to quantify pure components of falsified and genuine samples. Concentration maps of each pure material, including the API (lamivudine) and the excipients microcrystalline cellulose, sodium starch glycollate, rice starch and talc, were estimated using CLS [89]. Imaging of predicted concentration of the components showed apparent differences in the sample (see Figure 1-16) [127].

1.3.4 Challenges and Considerations of Routine Spectroscopic Authentication Methods

Many sources of variability impacting the spectra of pharmaceutical samples occur during the life-cycle of a spectroscopic technique. Some examples include manufacturing process variability, analytical instrument variability, and environmental fluctuations. Sample variability is introduced through raw material inconsistencies or through the impact of a manufacturing process

on material variability. Lot-to-lot variations of incoming raw materials introduce new physical and chemical variations to which both Raman and NIR spectra have been shown to be sensitive [128, 129]. However, the significance of variabilities on spectral quality depends on the sampling configuration, collection modalities, etc. [130-132]. For Raman spectroscopy, the effect of particle size variation in tablets between backscatter and transmission mode were compared. As the Raman backscatter mode generates most of the signal from the tablet surface, it was relatively less impacted by the variation in particle size relative to the transmission mode [133]. Tablet surface roughness also affected the impact of particle size on the spectra for the backscatter mode. However, in transmission mode, photon propagation characteristics were more influenced by particle size variations due to the scattering coefficient and optical path length [1, 133-135]. A change of size, shape or density of tablets due to the changes in the manufacturing process also generate spectral variabilities [134, 136, 137]. Physical factors are very critical for NIRS, as this method is highly sensitive to physical variations of the samples mentioned above [138-144]. These sources of variability are well known, but their effect on the model is not always well characterized. One way to test the effect of such physical variation is to develop calibration models with and without these variations in the model, and then determine whether including the variabilities improves the model performance.

Another challenging source of variability that analysts often encounter with the spectroscopic method development and deployment is environmental variability; for example, relative humidity often varies from the warehouse, where materials are stored, to the manufacturing facilities where samples are analyzed. The impact of relative humidity and extreme temperatures on model performance is critical to product quality and must be considered during method development [34]. Figure 1-17 demonstrates the spectral variability two samples scanned

using NIRS over the duration of a one year period .The variability was due to moisture variations of the testing period. This highlights the importance of including moisture variability in a NIRS model development [71, 91, 145-147].

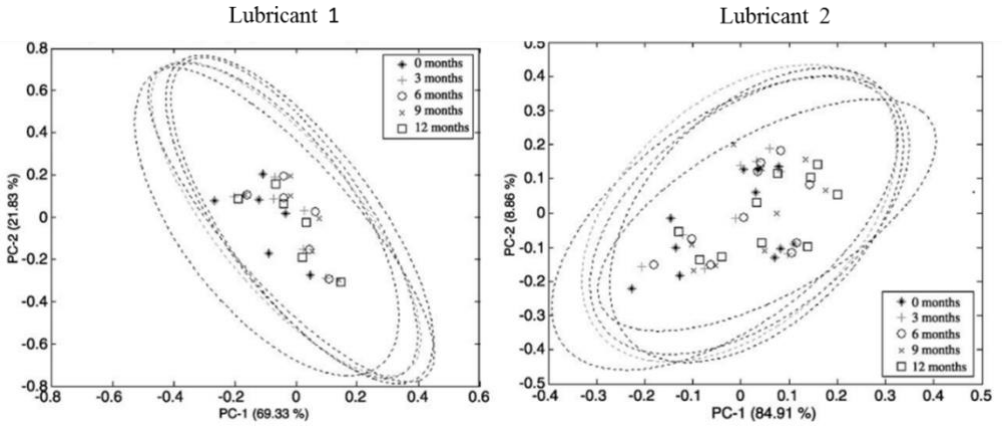

Figure 1-17: PCA plots (PC1/PC2) and the related 95% confidence intervals of two lubricant spectra recorded five times over a 1-year period. Figures obtained from Vredenbregt [148], Copyright (2003) with permission from Elsevier.

For Raman spectroscopy, although water has a weak Raman scattering, it was found that for tablets exposed to high humidity and temperature, the spectral baseline demonstrated variation. As chloroquine has broad fluorescence background, moisture variability caused spectral artifacts in the form of baseline variations, which is associated with fluorescence quenching [146]. This caused failure of the detection method. Fluorescence quenching also happens due to long laser exposure to samples. It was reported that due to the fluorescence background, obtaining reliable Raman spectra was an issue [147]. Using a 1064 nm laser can decrease fluorescence background, but requires longer exposure time to acquire similar S/N compared to 785 nm [149, 150]. McCreery showed that among 308 reference samples, around 8% of compounds showed a fluorescence background, and 3% of compounds were misidentified using the SM method [25]. However, the effect of moisture on different supervised models needs to be investigated more

rigorously for Raman Spectroscopy. Also, the suitability of baseline removal algorithms for removing this unwanted effect should be carefully evaluated.

Two recommendations are proposed to fill the gap in current literature regarding authentication method development. First, before developing a multivariate calibration model, a thorough investigation should be conducted to identify and understand the possible risks that may occur throughout the life-cycle of the method [151, 152]. Introducing systematic risk assessment based on previous experiences can be helpful to achieve this goal. For example, using Ishikawa diagrams and Failure Mode and Effects Analysis (FMEA) can be beneficial for developing a robust authentication model. Such risk assessment techniques were used to develop robust quantitative modeling in past studies [153, 154]. It is recommended that even for qualitative modeling to detect falsified drugs, risk assessment approaches may be quite practical. In Figure 1-18, an Ishikawa diagram showed critical factors for NIR and Raman spectroscopic techniques to detect falsified samples.

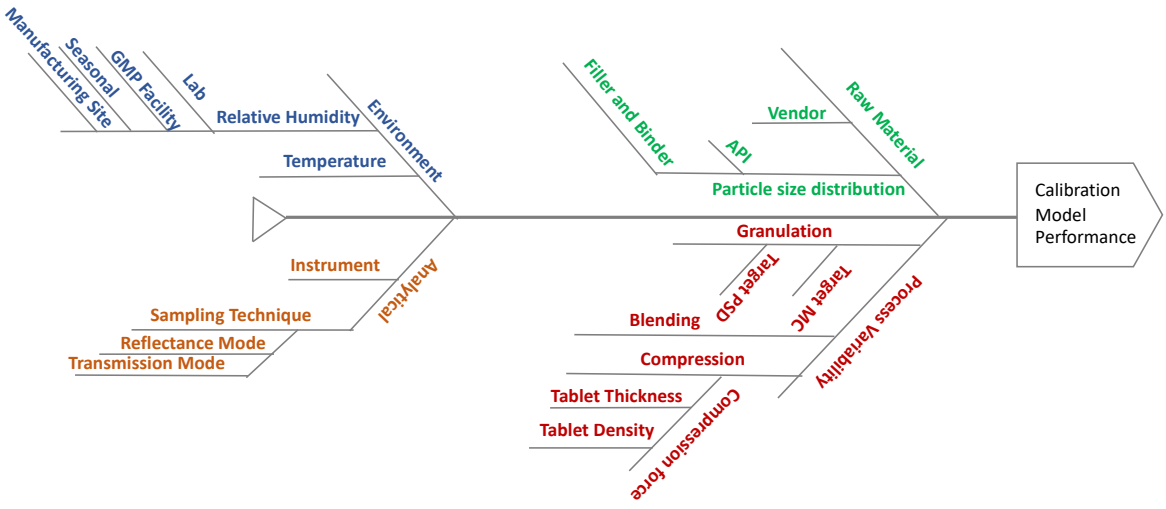

Figure 1-18: Ishikawa diagram for a risk assessment of a NIR spectroscopic techniques of pharmaceutical tablets.

Second, using an independent validation set over time to validate model performance will be helpful. This will also ensure long-term model performance [109, 151, 155].

1.3.5 Project Description

In this dissertation project, detailed investigations were conducted to demonstrate an optimized spectroscopic authentication method using class-modeling techniques for the detection of falsified pharmaceutical samples.

Appropriate prior knowledge of the pharmaceutical product, the manufacturing process, the spectroscopic technique, and the mathematical algorithm for calibration were required to develop and validate a sensitive, selective, and robust method. For a proper spectroscopic authentication system, the method was validated using independent sample sets, and the developed method met two validation criteria: 1) acceptance of genuine products and 2) rejection of falsified products.

The first validation parameter was that the model must accept authentic samples. To ensure long term model performance, proper risk assessment was investigated during method development. This risk assessment explored a variety of critical factors, including the effect of variability in materials, environmental conditions, manufacturing variability, and analytical instrument parameters. To understand the effect of these factors on the multivariate model performance, further studies were conducted. When it was found that certain factors were a risk for the model performance, inclusion of these factors improved the long-term model performance and decreased the burden of updating the model over time. Also, this work demonstrated that the typical current

method, e.g., SIMCA, had certain limitations that may be resolved with more modern algorithms, in particular, a SMV based algorithm.

The research project generated simulated falsified samples to test the capability of the analytical technique and to test the second validation criteria, i.e., rejection of falsified product. A variety of falsified sample characteristics were simulated in the lab. Specifically, the models were tested against falsified samples which contained the appropriate API but different excipient compositions. This was the most difficult condition of falsified samples to detect. To evaluate the ability of the analytical techniques and the developed chemometric model, a systematic variation of excipients was required in the formulations. Statistical method such as design of experiment (DOE) is a valuable tool to explore the spectroscopic capability to identify different falsified products. DOE is also helpful to understand which falsified samples are spectrally similar in comparison to genuine samples, and which pose a risk on the developed method. Carefully developed DOE, accomplished with appropriate prior knowledge, minimized the risk of model failure. Using samples created at small scale, in the laboratory, reduced the burden of sample preparation and made the model development efficient.

A detailed discussion of these strategies is offered in the following chapters.

Chapter 2: Evaluation of SVDD and SIMCA methods as Class-Modeling Techniques using Near-Infrared Calibration Sets of Pharmaceutical Tablets Containing Moisture Variation

2.1 Introduction

Protection of pharmaceutical materials from fraudulent activities is becoming increasingly critical due to the growing distribution of falsified products. The rise of procurement of internet products by American consumers increases the chance of exposure to these falsified products [6]. Currently, 10%-30% of drugs in the world are falsified [156, 157] and pharmaceutical tablets are the most common type of falsified products.

The primary method of pharmaceutical tablet falsification is to vary the chemical composition. This includes, but is not limited to, tablets prepared without active pharmaceutical ingredient (API), tablets manufactured using the wrong API and tablets generated using the correct API but different excipient compositions. Implementation of tools to monitor the chemical composition of pharmaceutical products during distribution from manufacturers to customers can reduce fraudulent activities [3, 4].

Near infrared spectroscopy (NIRS) offers the ability to rapidly determine the chemical content of pharmaceutical tablets. In studies utilizing NIRS, antimalarial, antimicrobial, antispasmodic and other medicines were successfully authenticated [28, 34, 96]. In these studies,

medications were collected from around the world and tested in the laboratory. Further progress in instrumentation technology has led to opportunities for NIRS to be implemented as portable, even handheld spectrometers, for the detection of falsified products in the field. These spectrometers allow screening for the quality of medicines in multiple locations (e.g., in different locations of the supply chain including rural hospitals, clinics, drugstores, etc.) [51].

However, developing authentication methods using NIRS is challenging due to sample constraints and the multivariate nature of the collected data. Only authentic samples are available during method development, as it is impracticable to produce or collect all types of falsified samples. Additionally, rigorous chemometric methods are required to statistically compare an authentic sample's NIR spectrum with an unknown sample's spectrum to determine whether the unknown sample is genuine or falsified.

Two types of chemometric techniques are highlighted in the literature for authentication of pharmaceutical tablets: 1) spectral matching (SM) and 2) class-modeling (CM) techniques [11]. SM compares two spectra, including a reference NIR spectrum from an authentic tablet and an unknown spectrum from a sample. The spectral correlation or spectral distance is calculated between these two spectra and, if these values fall within a target threshold, the unknown sample is declared to be genuine [158]. Research has shown that the SM method is successful when samples have large chemical differences providing sufficient spectral uniqueness [14]. For example, the SM method was used to identify placebo samples and samples containing the wrong API. However, this method struggled to separate samples containing identical APIs and similar excipient compositions or what would be considered high quality falsified products [15]. Moreover, most current portable spectrometers provide limited sensitivity and selectivity relative

to research instruments, and insufficient spectral resolution to distinguish the differences between authentic and falsified samples. Regardless, SM is a popular technique included in most of the current portable spectrometers due to its rapid and relatively simple assessment of authenticity.

Class-modeling (CM) is another chemometric technique that can be applied for the purpose of authentication. Multivariate methods such as SIMCA and its extended versions have been used for spectroscopic class-modeling techniques for authentication. The primary premise of these methods is to develop a target class using representative samples from an authentic source. A calibration model is developed from the target class, comprised of NIR spectral data containing API and excipient information. CM estimates a decision boundary which is formed around the calibration data at a specific significance level. For example, the boundary of different versions of SIMCA is developed based on the distribution assumptions such as normal, χ^2, etc. [17-19]. Several studies have compared the performance of SM and CM, and proposed that CM techniques are more effective than the SM method. In these studies, portable spectrometers successfully separated pharmaceutical tablets containing similar compositions [15, 20].

The CM methods require two critical considerations: suitable target class samples and the establishment of appropriate boundary conditions. A typical target class includes authentic samples; however, it does not necessarily include the variabilities that have a critical impact on NIR spectra. For example, a CM method using NIRS data based on a target class including authentic samples from one batch may consider an authentic sample from a different batch to be falsified because batch-to-batch variability is not considered in the original calibration. Batch-to-batch variability can have a severe impact on the performance of NIR prediction models, potentially due to small physical and/or chemical differences in the samples from unique batches.

Specific sources of small chemical and physical changes between authentic samples include raw material variability and environmental (i.e., temperature, relative humidity) fluctuations. Specifically, environmental variability is of high concern because authentic samples are often produced in different manufacturing sites around the world with varying relative humidity conditions. NIR spectra are highly sensitive to moisture; thus, the relative humidity variation needs to be considered during method development, especially if the NIRS method is to be directly applied at these different sites. To reduce the impact of these potentially important variabilities, several spectral preprocessing techniques are available. However, these pre-processing techniques are not always sufficient; an additional, valuable option is to update the calibration model using new samples comprising these variabilities.

The addition of samples to the target class to create a robust model can be accomplished in two ways. First, the empirical approach where the model is updated over time by adding samples to include newly evolved variabilities. This empirical approach depends on stepwise addition of newly available samples to the calibration set and rebuilding the model over time [159]. Another approach can be taken by implementing risk-assessment concepts during method development. According to ICH-Q9 guidelines, a risk-assessment can be conducted while developing the calibration method, and factors which can be risks for spectroscopic method performance are added into the target class during model development [154].

In addition to sample considerations for development of a suitable target class, the boundary conditions are also important. The boundary around the target class decides if an unknown sample is authentic or falsified. The CM method assumes that the target class forms one cluster, with the boundary formed around this cluster. However, including spectrally different

samples (e.g., samples with different moisture levels) may introduce multiple clusters within the target class. This violates the assumption of the model by forming a binomial or multimodal distribution in the model space. In addition, the boundary formed around the multiple clusters may not include all potential calibrations samples, and the model will be more prone to rejecting authentic samples. Therefore, the caveat of this approach is that without prior knowledge of the shape of the underlying distribution of samples, satisfactory results may not be achieved.

This chapter explores the use of a support vector machine based method to resolve boundary condition issues of a traditional CM method. Support vector machine methods create a spherically shaped boundary around the samples. The boundary is typically described by a few training objects which are mentioned as support vectors. It is possible to replace normal inner products by kernel functions to obtain more flexible data descriptions. This method is often referred to as a support vector data description (SVDD) approach, proposed by Tax et al [21]. This method has been used for the detection of machine faults, outlier detection, etc., and has shown similar results to the one-class support vector machine (OC-SVM) developed by Schölkopf et al [22]. However, the SVDD method has not yet been evaluated for analyzing pharmaceutical samples using spectroscopic data, particularly for authentication purposes.

The objective of this paper is to explore the performance of SVDD as a class-modeling technique relative to that of the widely used SIMCA method in order to authenticate pharmaceutical products. This study emphasized the suitability of these chemometric techniques in the presence of seasonal variations. To demonstrate the capabilities of these methods, tablets were prepared in-house (in the laboratories of the Duquesne University Center for Pharmaceutical Technology) throughout a year's worth of environmental variation. Although these samples were

generated in the laboratory, this study provides direction for further development of an authentication method using spectroscopic data.

2.2 Materials and Methods

2.2.1 Theory

2.2.1.1 SIMCA based Approach

SIMCA is extensively used as a class-modeling technique for authentication purposes. The procedure for SIMCA first involves decomposing calibration samples using a PCA model with the optimal number of principal components. Classification rules are then constructed to create a decision boundary. Different versions of classification rules have been developed over time; this is discussed extensively in existing literature [17, 103, 160]. However, in this study, one of the most immediate and commonly used versions was applied for the SIMCA analysis. In this method, the boundary around a training set of SIMCA is based on two distances: 1) score distance (SD) and 2) orthogonal distance (OD). The SD is determined by computing the distance, in the space of the PCs, between an unknown sample and a target group, commonly referred to as the Hotelling's T^2. The OD is determined by calculating the unknown sample's squared residual distance from the model space, referred as the Q residual [17, 82]. Hotelling's T^2 measures the information of each sample within the PCA, or SIMCA model, and is calculated by Equation 1, where t_i is the i-th row of the T_k, the n by k matrix of k score vectors from the PCA model, and matrix of k scores vectors from the PCA model of n number of target class samples and Λ^{-1} is a diagonal matrix containing the inverse of the eigenvalues associated with the k eigenvectors (principal components) retained in the model.

The Q_i statistic is defined as the sum of squares of the residuals and can be calculated according to Equation 2 where e_i is the residual of sample *i* after applying the SIMCA model.

$$T_i^2 = \sqrt{t_i \Lambda^{-1} t_i^T} \quad (1)$$

$$Q_i = e_i e_i^T \quad (2)$$

A sample is assigned to a target class if the computed distances are shorter than a predefined threshold value. These threshold values are based on T_{lim}^2 and Q_{lim}, which are the confidence intervals for the model under consideration. Confidence limits for SD (referred to as T^2 in the PLS_Toolbox and related literature) are given from Hotelling's T^2 to obtain T_{lim}^2, i.e. ($T_{lim}^2 = F_{k,n-k} k(n^2-1)/(n-k)$ considering k and $(n-k)$ degrees of freedom, where k is the number of PCs and n is the number of calibration samples for the target class.

The $\chi 2$ distribution is used for the squared residuals and confidence limits for the orthogonal distance (OD, also referred to as Q in the PLS_Toolbox and related literature) are computed by the Jackson and Mudholkar (JM) approximation.

The limit of Hotelling's $T^2 (T_{lim}^2)$ and the limit of Q statistic (Q_{lim}) values can be calculated from the ratio between the corresponding statistic of the sample i and the corresponding limit at α = 0.05 [$e.g.$, ($T_{lim}^2 = T_{95\%}^2$ and $Q_{lim} = Q_{95\%}$] [17]. A more flexible boundary is developed by a semi-circle with a radius of $\sqrt{2}$, which is mentioned as d; this d is calculated according Equation 3.

$$d = \sqrt{\left(\frac{Q}{Q_{lim}}\right)^2 + \left(\frac{T^2}{T_{lim}^2}\right)^2} \quad (3)$$

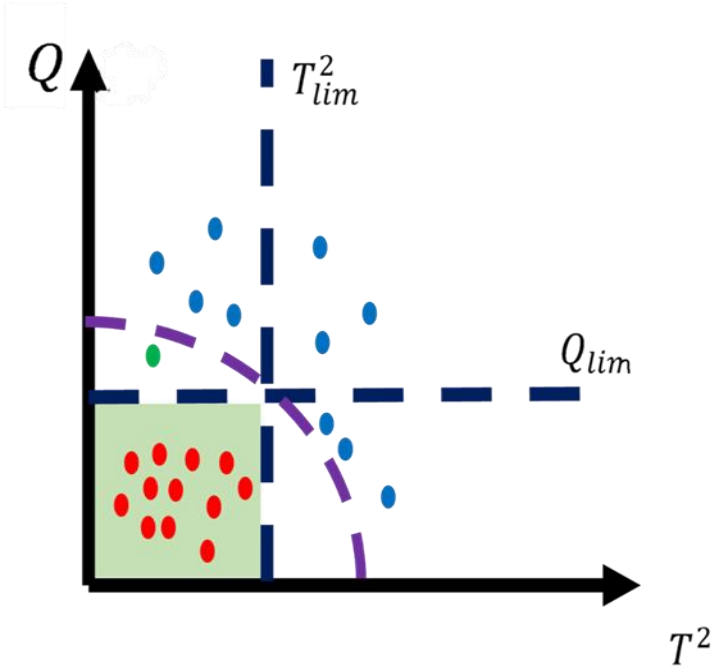

Figure 2-1: Threshold boundary based on the confidence interval of Hotelling's T^2 versus Q residual. The squared acceptance area is the green space in the graph, where samples plotted at any point outside of this area are rejected. According to this threshold, nearly every sample will be accepted, with only the green sample being rejected. A more flexible boundary could be applied as shown by the semi-circular area. Then, both green and red will be accepted. Figure is adapted from López et al.[100] Copyright (2014) with permission from Elsevier.

This distance measure gives equal weighting to distance in the model space, i.e. scores distance (SD or T^2) and residual space, i.e. orthogonal distance (OD or Q). The outcome of this boundary was depicted in Figure 2-1.

2.2.1.2 SVDD based Approach

The theory of SVDD has been extensively described in the literature [21, 161]. Therefore, only a brief description of the concept of SVM in the framework of classification is given here.

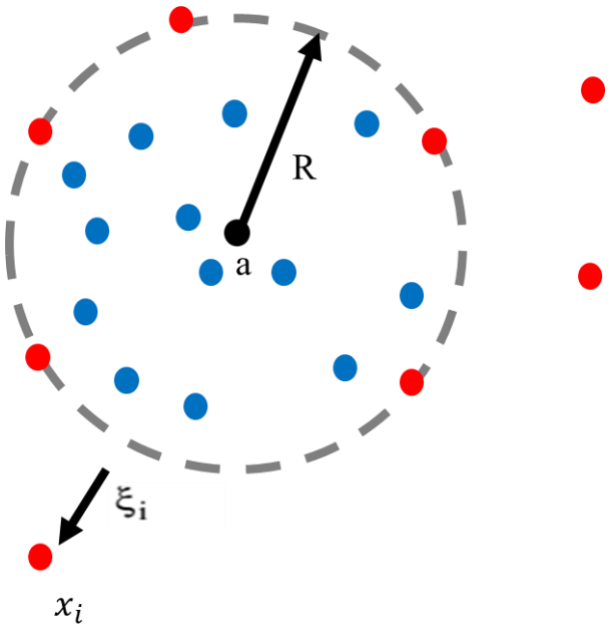

Figure 2-2: The hypersphere containing the target data (blue), described by the center *a* and radius R. Five objects (red) are on the boundary. Three object (red) x_i is outside and has $\xi_i > 0$.

$$\emptyset(R, a, \xi) = R^2 + C\sum \xi \qquad 3$$

$$||x_i - a||^2 \leq R^2 + \xi, \qquad \xi \geq 0 \qquad 4$$

The SVDD algorithm avoids the estimation of a complete probability density; it obtains a data boundary by forming a circle or hyperplane around the data where μ is the data center and R is the distance from the center to the hyperplane that forms the boundary around the samples (Figure 2-2**)**. However, it is not always possible to include all data within the boundary. Therefore, this algorithm has adapted to tolerate errors for some objects that fall outside of the boundary.

Usually, slack variables ξ, allow a probability that some of the training samples will be placed outside the boundary. Samples which reside on the boundary ($\xi = 0$), or outside of the hypersphere ($\xi > 0$), are referred to as support vectors. Development of the hypersphere is based on the optimization of these support vectors, where the distance of each of the samples should be less than or equal to $R^2 + \xi$. Therefore, mathematically, it is possible to define a structure error function ($\emptyset$) for an SVDD model with a constraint.

In Equation 4, C shows the trade-off between the volume of the hypersphere (calculated by R^2) and the number of errors (ξ) and therefore controls the fraction of samples lying outside the boundary. The higher the C value, the more samples are included in the model space. This C can also be expressed as "a fraction of target class samples rejected" by D value which is defined in Equation 5.

$$D = \frac{1}{nC} \qquad 5$$

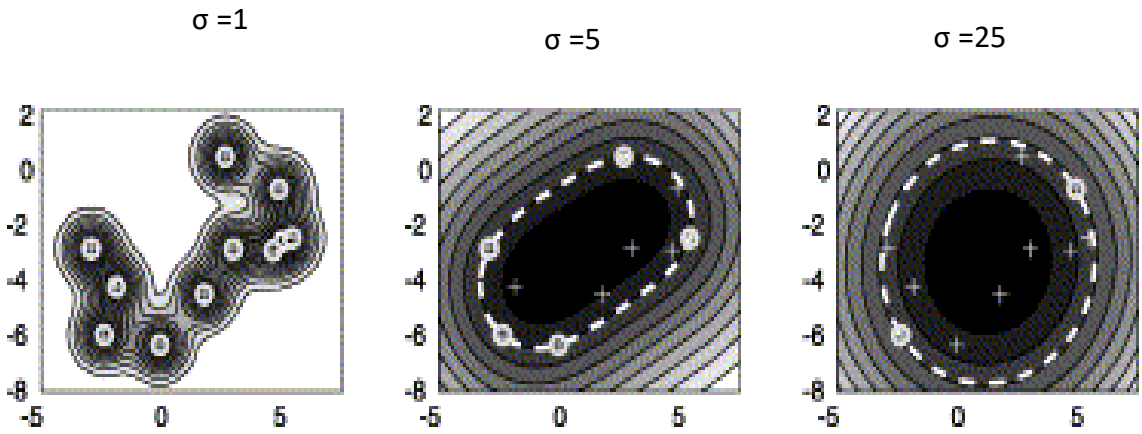

Figure 2-3: Data description trained on a banana-shaped data set. The kernel is a Gaussian kernel with different width sizes σ. Support vectors are indicated by the solid circles; the dashed line is the description boundary (adapted from Tax et al. [160]). Copyright (1999) with permission from Elsevier.

The C and D are related by n which is defined as the number of samples in the calibration set. D has some analogy to confidence levels in distance-based classifiers. When D = 0, no target samples are misclassified, whereas D = 0.05 means 5% of samples will be outside the boundary. However, this number is an approximation. This optimization problem was further modified using the Lagrangian method which simplified the calculation [21].

It is also possible to incorporate kernel functions into the model to create a non-linear boundary (Figure 2-3) [21]. It provides additional dimensions which transform the shape of the data. The shape of the boundary can be optimized using different kernel function, but most popular is the Gaussian radial basis function (RBF),

$$K(x_i, x_j) = exp\frac{-\|x_i - x_j\|}{2\sigma^2} \quad 6$$

The broader the Gaussian, the smoother is the surface; hence, the radius of the RBF (or σ) relates to how 'bumpy' the surface is, and varying this parameter can change the appearance of boundaries between points. Using a small σ results in a sharp Gaussian that effectively forms a boundary around each point (or occasionally neighboring points). Therefore, a small σ value may overfit the model, whereas as σ increases, the model becomes smoother and more circular, resembling a PCA or SIMCA models. It is essential to understand that the number of samples on the boundary decreases as σ increases—this is because fewer points are required to model a smooth boundary and so fewer SVs are required.

2.2.2 Figures of Merit

In the class-modeling approach, two validation parameters are used for performance analysis. The goal of the method is to accept target class samples. This is referred to as the sensitivity of the model. It describes the ability of the model to declare genuine samples. The following formula calculates the sensitivity of the method (accepting genuine samples):

$$Sensitivity=TP/(TP+FN) \qquad 7$$

where TP and FN are true positive and false negative, respectively. If the model accepts falsified samples, it needs further optimization.

The second measure of model performance is rejection of the non-target class samples. This is called specificity. The specificity of the method (rejecting falsified samples) is used as a validation parameter. The following formula calculates this parameter:

$$Specificity=TN/(TN+FP) \qquad 8$$

where TN and FP are true negative and false positive, respectively.

To consider both factors simultaneously, the geometric average of these two parameters were calculated. The average of sensitivity (Equation 7) and specificity (Equation 8) will be indicated as average performance (see Equation 9).

Average performance= (Sensitivity + Specificity)/2 9

2.2.3 Sample Set

2.2.3.1 Sample Preparation

For this study, acetaminophen (APAP) was used as a model drug. The target formulation was APAP (27.30%w/w), microcrystalline cellulose (MCC 200; 34.15% w/w), lactose (34.15% w/w), hydroxypropyl methyl cellulose (HPMC; 3.90% w/w), and magnesium stearate (0.5% w/w). Tablets were generated with a wet-granulation approach. First, granules containing APAP, HPMC, and lactose were manufactured using a fluid bed granulator (model WSG 5, Glatt, Binzen, Germany). Then, granules and extra-granular excipients (MCC 200, lactose, magnesium stearate) were mixed in a 3.5 quartz V-blender for a total blend mass of 1 kg for 45 min. Target blending time for homogeneity was tested using NIRS. The blends were subsequently compacted on a 38-station rotary tablet press (Elizabeth-Hata International, Inc., North Huntingdon, PA, USA). The target tablet weight was 350 mg.

To consider non-target class test samples during model development, another set of samples containing low concentration of API (19% w/w) was manufactured. The shape and size of both sets of tablets were the same.

2.2.4 NIR Scanning

NIR reflectance measurements were acquired for both sides of each tablet over the wavelength range of 925 to 1700 nm at a 6.38 nm increment, averaging 5000 scans (JDSU MicroNIR). Before scanning, the tablets were precisely centered using the positioning iris, standard on this instrument. A period of two weeks elapsed between compression and spectral collection to allow the tablets to undergo viscoelastic relaxation.

All spectral data were analyzed in Matlab (version 8.6, MathWorks, Natick, MA) using PLS_Toolbox (version 8.8, Eigenvector Research, Inc, Manson, WA) [162], and software developed by the Duquesne University Center for Pharmaceutical Technology.

2.2.5 Reference Testing

Acetaminophen reference values for all compacts were determined using high-pressure liquid chromatography (HPLC; Waters Alliance 2790, Milford, MA, USA), followed by ultraviolet detection (Waters 2487). A method, modified from USP29-NF24 (“Acetaminophen Tablets’’), was employed [41]. The mobile phase was water: methanol: acetic acid (80: 17: 3), and the stationary phase was a 15 cm by 4.6 mm C18 column with 3μm packing. The detection wavelength was 243 nm. The error of the reference measurement was estimated at 0. 83%.

2.2.6 Sample Considerations for Calibration, Test and Validation

During the study, a total of six granulations and fourteen tablet batches of the target formulation were manufactured. There was significant variability in the particle-size distribution of the granules and in the moisture content of the excipients and granules. These variabilities were

observed because the environment of the laboratory in which the experiments were performed was not controlled for humidity; during winter the air was dry (20–30% relative humidity (RH)). During the summer months, typical RH was between 60 and 70%.

Samples prepared in the lab were used to investigate these seasonal spectral variabilities and the subsequent effect on the model performance during spectroscopic analysis. Samples were prepared using six different granules (containing different particle size distribution) and in different seasons of the year (in the presence of different relative humidity).

The target class samples were developed from the target concentration, and the non-target class product was prepared using a lower concentration of API, as mentioned previously.

Calibration, test, and validation sets were the sample sets used for the model development process. The model was optimized using the test set which contained both target and non-target class samples, whereas the calibration set contained only target class samples. Non-target class samples were used during the optimization process to enhance the model performance (Figure 2-4) [163].

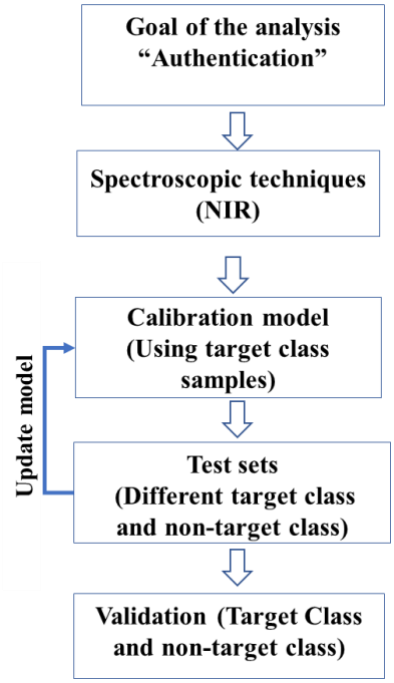

Figure 2-4: Method development flow chart and considered samples.

Three calibration scenarios were created to demonstrate three conditions of calibration sets:

1) Basic: Samples prepared in the summer (lab humidity ~ RH65%) were added to the calibration set. This set will be further mentioned as the "basic calibration set".

2) Updated: The updated data includes the basic calibration set and additional samples created during the winter, representing a real-life scenario in terms of the likely scenario for the model update. This data set will hereafter be called the "updated calibration set."

3) Risk-based: In this approach, samples prepared during the summer were stored in lower humidity condition (~20% RH) to mimic the winter condition, and later added into the calibration

sample set along with the samples of the basic calibration set. This will be henceforth described as the "risk-based calibration set."

Calibration sets for model development: Samples were considered for calibration set from three scenarios mentioned above. Each of these calibration sets were used to generate SIMCA and SVDD model. Test sets were used to optimize calibration model and validation sets were used to measure the final performance. (Table 2-1).

Test sets for model optimization: Cross-validation was conducted using calibration sample sets of target class samples. Samples of similar composition containing a low level of API (19%w/w) were used as non-target class samples to optimize the model parameters.

Validation sets for performance evaluation: The model was challenged with the validation set to test whether it could accommodate seasonal variabilities present in the independent target class samples. Three batches of target class validation sample sets were generated from new granules (that had not been present in the calibration set) and manufactured under summer, spring, and winter conditions.

Table 2-1: Details of the modeling scenarios

	Scenarios		
	Basic	**Updated**	**Risk-Based**
Calibration Set			
Moisture variations	High	High+Low	High+Low
API Concentration	Target	Target	Target
Test Set			
Moisture variations	High+Low	High+Low	High+Low
API Concentration	Target+Low	Target+Low	Target+Low
Validation Set			
Moisture Variation	High+Low	High+Low	High+Low
API Concentration	Target+Low	Target+Low	Target+Low

2.3 Results

2.3.1 Spectral Investigation and Exploratory Analysis

Samples were prepared using granules containing different particle size distributions and created in different seasons of the year (containing different relative humidity conditions). Figure 2-5 shows the second derivative treated spectra of tablets. Figure 2-5A used the same granules manufactured in two different seasons. Different spectral regions of the samples generated in the summer (~60% RH) and in the winter (~25%RH) demonstrated intensity differences [164, 165]. The preprocessing method removed the effects of physical variation by eliminating the baseline differences. However, the water bands around 1470 nm exhibited significant variability compared to other regions of the spectra. This 1470 nm region represents primarily the combination bands of water. This spectral change depicts the influence of moisture on the spectra [164, 165]. Figure 2-5B showed the spectral difference in the 1167 nm region due to APAP concentration differences; here, the target concentration and low concentration tablets represented target class and non-target class product, respectively.

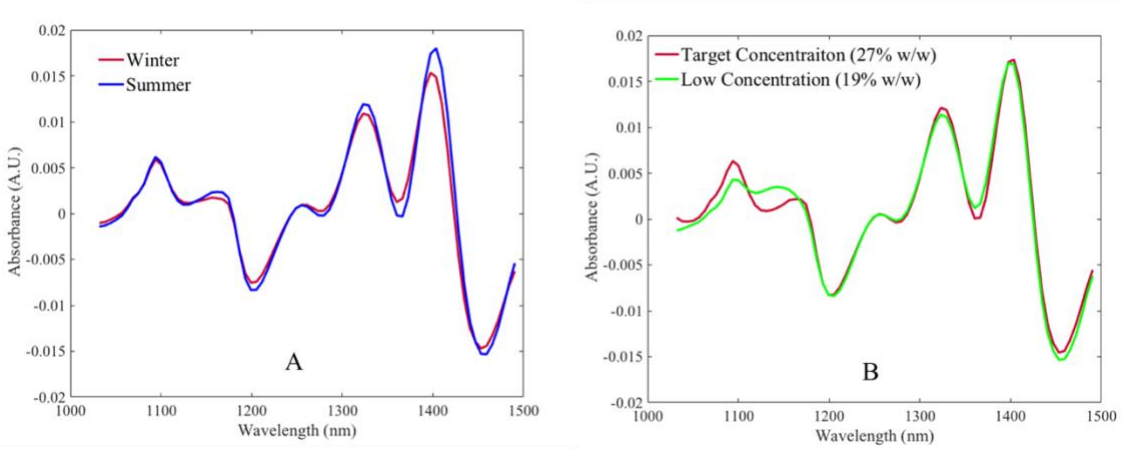

Figure 2-5: A) NIR spectra of different moisture conditions B) Two different concentration levels of API.

A PCA algorithm was used to decompose the calibration spectra after SNV and mean-centering treatment [81]. Figure 2-6A shows that the scores of the first two PCs, generated from the basic-calibration set, are uniformly distributed. However, when the PCA algorithm was applied to the updated and risk-based calibration scenario data (preprocessed), two clusters formed in the PCA space (Figure 2-6B). This clustering indicates that variabilities were present across the calibration set, mostly in the PC2 direction. As most of the samples were prepared and scanned in the summer-season, the largest group contained summer-samples. Whereas, the smaller group contained samples added from the winter-season (low humidity condition). Also, a boundary was developed using a 95% confidence interval of PC1 and PC2 scores. It was observed that the developed confidence interval in the PC space of the updated calibration model mostly excluded samples from the smaller cluster (Figure 2-6B). Therefore, the samples that resided outside the boundary were primarily from the winter season. Nevertheless, increasing the confidence interval includes all samples within the boundary (Figure 2-6C).

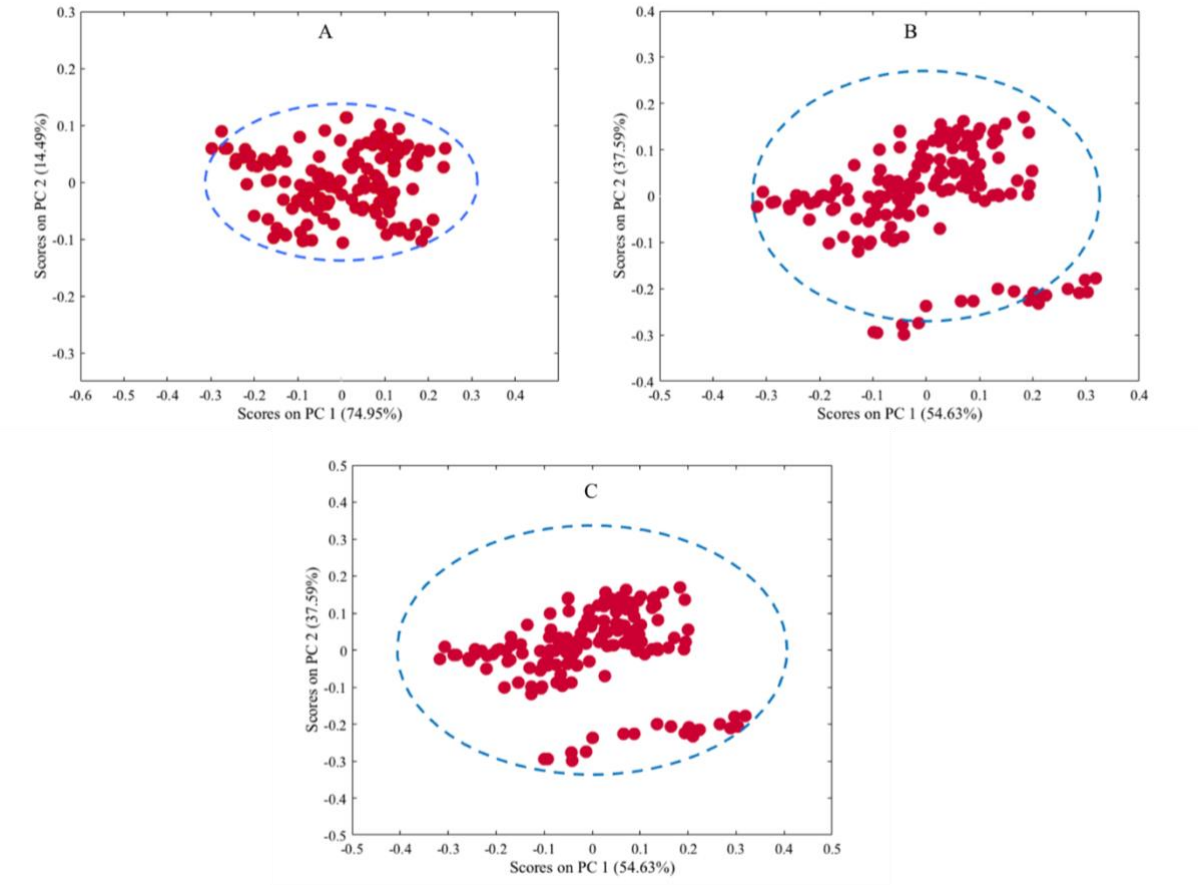

Figure 2-6: A) PCA of the basic calibration model with a 95% confidence interval, B) PCA of the updated calibration model with a 95% confidence interval, and C) PCA of the updated calibration model with a 99% confidence interval. Here the red circles are samples, and the dashed line is the confidence interval.

Table 2-2: Performance of the different modeling approaches

Different Models with predefined threshold	**Calibration scenarios**								
	Basic			Updated			Risk-based		
	Sensitivity	Specificity	Average	Sensitivity	Specificity	Average	Sensitivity	Specificity	Average
SIMCA (T^2 & Q=0.95)	0.5	1	0.75	0.67	1	0.83	0.85	1	0.925
SIMCA (T^2 & Q =0.99)	0.5	1	0.75	1	0.92	0.96	1	0.6	0.80
PCA-SVDD (D=0.05)	0.5	1	0.75	1	1	1	0.93	0.98	0.955
PCA-SVDD (D=0.01)	0.5	1	0.75	1	1	1	0.94	0.94	0.94
Spectral SVDD (D=0.05)	0.5	1	0.75	1	1	1	0.93	1	0.965
Spectral SVDD (D=0.01)	0.5	1	0.75	1	1	1	0.93	1	0.965

2.3.2 Model Performance of SIMCA and SVDD Methods

2.3.2.1 SIMCA Method Performance

While developing the SIMCA calibration model, several parameters were optimized. Spectra were preprocessed and PCs were determined using independent test sets (containing both target and non-target class samples) by maximizing the classification average performance of sensitivity and specificity. The baseline correction method was required as a preprocessing method to minimize batch-to-batch variabilities due to particle size differences. Standard normal variate (SNV) helped to remove these variabilities. The number of selected PCs has a major impact on the classification results. Adding more PCs into the model increases the complexity of the model, which typically helps to reject non-target class samples. However, a more complex model means that a higher amount of variation in the training set is considered; adding more PCs may result in an over fitted model and a potential risk of rejecting target samples during routine analyses. Hence, a model containing a minimum number of PCs to generate adequate specificity is preferable. This approach is often referred to as a parsimonious approach [163].

After establishing a PCA model, an acceptance area is developed based on a threshold value. In this study, the decision threshold is set at $\sqrt{2}$ which creates a semi-circle in Hotelling's-T^2 and Q residual plot. This is based on a priori significance level of Hotelling's T^2 and Q residual. This significance limit for these two statistics are estimated based on the internally cross-validated values of T^2 and Q residual associated with the calibration samples. In this study, two fixed significance levels, 95% and 99%, were used to measure the performance.

In Table 2-2, the performance of SIMCA models is shown. Here, it was observed that, regardless of the significance level, the basic design scenario showed 100% specificity using 1 PC (rejected all the non-target class samples). According to Figure 2-7A, these non-target class samples have higher Q residual and Hotelling's T^2 and resided outside the boundary. Non-target class samples, containing a lower concentration of API, were separated from the target class. However, the other critical parameter, sensitivity of the model, is 50%. The rejected target samples have high Q residuals in the diagnostics plot (Figure 2-7A), which indicates that the target-class samples in the validation set had unmodeled variance. This performance is not unexpected, as 50% of validation target class samples were generated in the winter and had different moisture content. The model accepted target class samples which were manufactured during the summer seasons and had similar features of the basic calibration design set.

The updated calibration scenario (which was developed by adding winter samples to the summer sample set) improved sensitivity compared to the basic set. This result indicated that to improve model performance, winter samples are required in the calibration set. Moreover, changing the threshold value from 0.95 to 0.99 further improved sensitivity. The diagnostic plot in Figure 2-7B, showed that calibration samples prepared in the winter season had higher Q residuals and Hotelling's T^2 relative to the samples prepared in the summer. While developing a decision boundary using 95% CI, most of these winter samples resided near the boundary or outside of the decision boundary. These samples are typically referred to as high-leverage samples. Similar patterns were observed for the risk-based calibration model (Figure 2-7C). Changing the significance level of Hotelling's T^2 and Q residual to 99% placed these high leverage samples into the decision boundary. This change in the significance level improved the sensitivity of the model by accepting validation samples which were rejected in the previous model threshold. However, it

is also important to understand that the specificity of the model decreased due to the change of the significance level. Hence, with this higher significance level (99%), the model began to accept non-target class samples **(**Figure 2-7D).

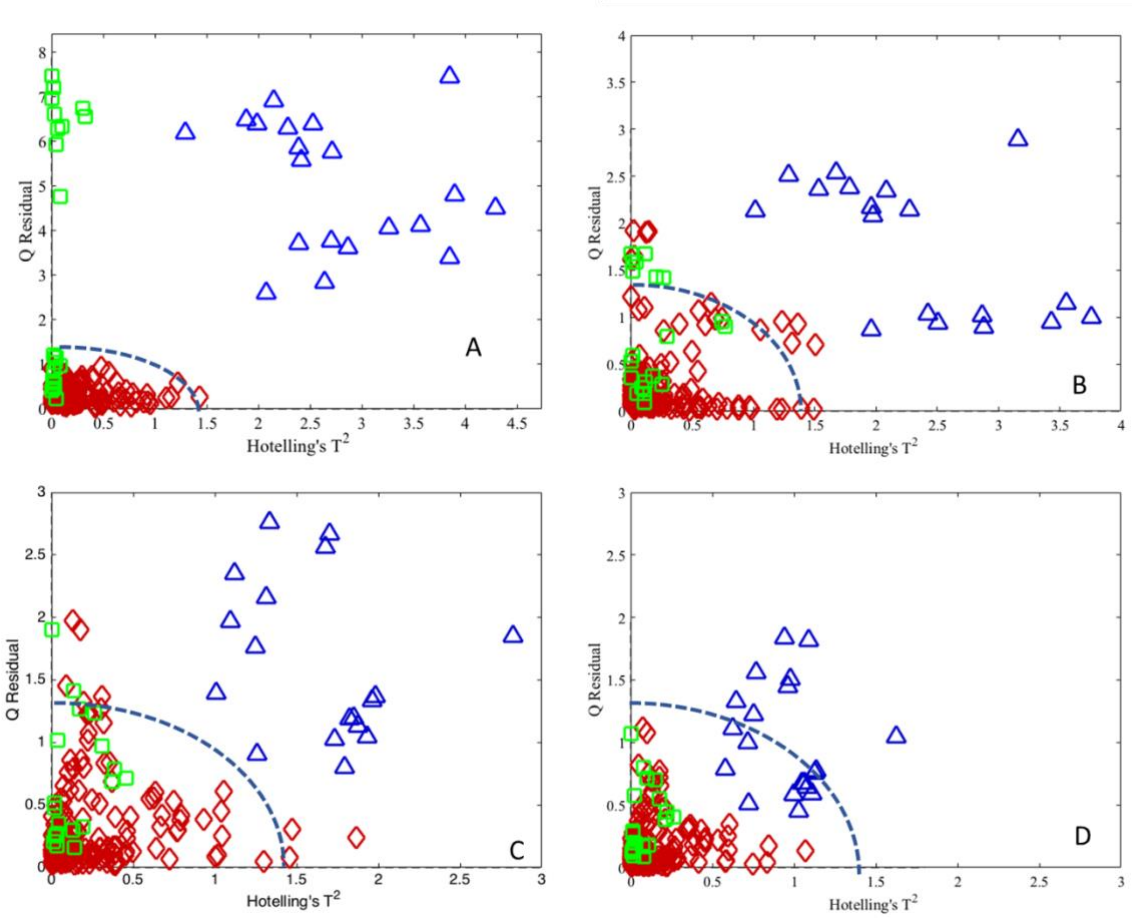

Figure 2-7: Diagnostics plots of SIMCA using 95% threshold value of Hotelling's T^2 and Q residuals of A) Basic calibration set, B) Updated calibration set, C) Risk-based calibration set, and 99% threshold value of Hotelling's T^2 and Q residual of D) Risk based calibration set. Here, red indicates the calibration samples from the target class, green indicates validation samples from the target class, and blue indicates validation samples from the non-target class.

Similar results were observed for the risk-based scenario. By including samples stored in the low humidity condition, the sensitivity of the model improved. As the model also contained samples stored at 11% RH, model performance improved by accepting validation samples

generated in the winter. This was an efficient approach of method development as it included moisture variabilities in the calibration set without considering samples generated during winter seasons. Therefore, analysts were not required to wait to update the model until generating samples, which is often a tedious process. However, this model also had high leverage samples; changing the threshold value from 0.95 to 0.99 improved sensitivity but decreased the specificity of the model by accepting non-target class samples.

2.3.2.2 SVDD Method Performance

In this study, the SVDD algorithm was applied to the PCA decomposed data and preprocessed spectral data; these will be mentioned as PCA-SVDD and Spectral-SVDD subsequently. Both approaches were optimized individually using the test set to obtain the best possible results. During optimization, different factors such as the preprocessing method, the number of PCs, and the parameters of SVDD (i.e., D and σ) were considered. Previous literature suggested to fix the rejection fraction of the calibration model (D) according to a predefined value and then to optimize σ. In this study, two D values: 0.05 and 0.01 were considered. These two values represent the comparative performance of 95% CI and 99% CI of the method [166]. To optimize σ for three calibration scenarios, a search was performed based on the test set. While calculating the σ value, a series of values ranging from 0.1-2.5, with incremental steps of 0.1, was used.

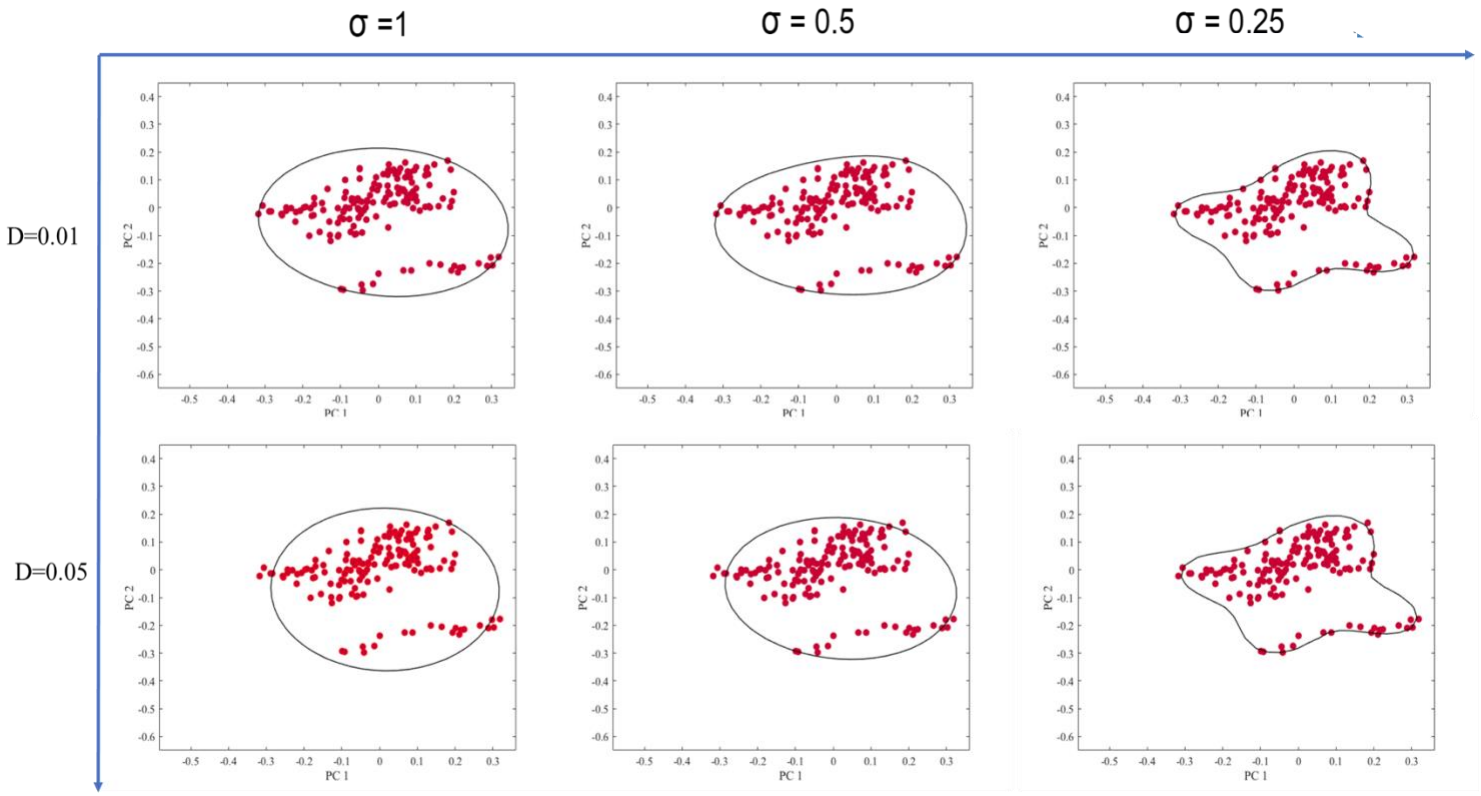

Figure 2-8: A boundary was developed using a support vector machine approach for updated calibration samples. Each row represents different D values whereas each column represents σ values.

While developing the PCA-SVDD method, the first two principal components' scores were selected to develop the model for each calibration scenario. PCA-SVDD models were developed by optimizing σ. The impact of the σ parameter on the boundary development of the updated calibration scenario was visualized in Figure 2-8**.** Decreasing the σ value tightened the non-linear boundary of the updated calibration scenario by exploiting a higher number of support vectors (samples resided on the boundary) [21]. However, analysts should be cautious about the unnecessary tightening of the boundary, which may increase risk of overfitting of the model. Also, changing D values allowed more samples to reside outside the boundary, which is representing a similar approach to the confidence interval of PCA or SIMCA. One crucial difference between the decision boundary of SIMCA (based on the confidence interval) and PCA based SVDD analysis was identified. In the SVDD approach, samples from both summer and winter samples resided inside the boundary. However, while developing a SIMCA model based on the 95% CI, the model excluded most samples from the winter season.

Performance of the different calibration scenarios is presented in Table 2-2. Basic calibration scenarios of PCA-SVDD did not contain moisture variation in the calibration model, and, therefore, failed to accept validation samples from different seasons. This performance is comparable to the SIMCA modeling approach. However, the performance of PCA-SVDD generated from updated and risk-based scenarios improved significantly relative to the SIMCA approach. The developed PCA-SVDD model successfully accepted more target class validation samples, compared to SIMCA, and demonstrated higher sensitivity. Additionally, the model successfully rejected non-target class samples by projecting them outside the boundary. Therefore, the PCA-SVDD algorithm improved the model performance of the NIRS method. The risk-based

scenario also showed a similar trend to the updated approach. D values of both 0.01 and 0.05 showed improved performance compared to SIMCA.

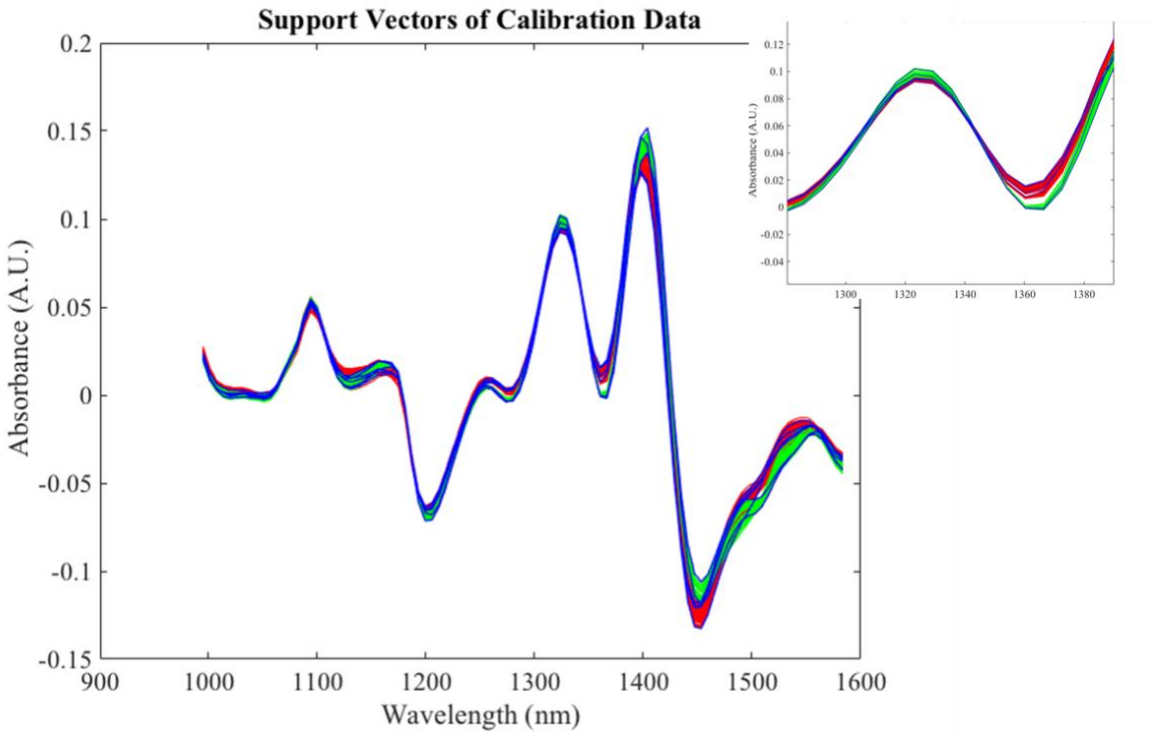

Figure 2-9: Depiction of selected support vectors of updated calibration set where the blue spectra are support vectors, red spectra are summer samples and green spectra are winter samples. Particular section is magnified to visualize the data clearly.

The Spectral-SVDD approach also showed improved prediction results compared to SIMCA. Data is visualized in Figure 2-9. As the boundary was not possible to show for the multivariate spectral data, support vectors were depicted using the preprocessed spectra. According to Figure 2-9**,** the SVDD algorithm selected blue samples as support vectors from the calibration sample set. These support vectors were chosen from both summer (red) and winter (green) samples, indicating that the boundary was selected using both summer and winter sample sets, unlike the SIMCA approach.

2.4 Discussion and Summary

Traditional development of decision boundaries for CM models is based on the assumption that there is a specific distribution that exists in the multivariate space (i.e., F- distribution or χ^2 distribution on the Hotelling's T^2 and Q residual space). Though these assumptions often vary in different versions of SIMCA, analysts develop decision boundaries at a specific significance level α (often set to 0.05) [17]. However, these assumptions are frequently violated as samples containing spectral variabilities may introduce bimodal, multimodal, non-symmetric statistical uncertainties, degrading model performance.

This work proposes the use of SVDD as a class-modeling technique using NIRS. Due to distribution free boundary development, SVDD is a promising technique for use in both the laboratory and field for solving the calibration development challenges described above. The most important advantage of SVDD is that boundary samples are determined without relying on distribution assumptions. Using a well-known example from NIRS (the effect of moisture on NIR spectra), this chapter demonstrates the advantage of SVDD.

Though compared to the traditional SIMCA method, SVDD has not been widely used in pharmaceutical applications of chemometrics. However, it has been proven useful for class-modeling applications. Moreover, the kernel feature allows the development of a non-linear boundary around calibration samples, offering a significant analytical advantage compared to traditional CM methods.

One challenge of the SVDD approach is the visualization of data. While it is impossible to visualize the highly dimensional data, observation of selected samples as support vectors may

provide valuable insights about the developed method. Another risk of using SVDD methods is overfitting. Here in this study, independent samples were used as test and validation sets, decreasing the risk of overfitting. However, analysts may not always have access to independent samples for optimization. In that case, separating the training set into two sets might be an option. To separate samples into two sets, randomization algorithms will ensure homogenous distribution of the available samples.

Many studies have demonstrated the capabilities of different class-modeling techniques for pharmaceutical samples, but the development of methods for validating such models is still in its infancy. However, as regulatory bodies attempt to implement different spectroscopic techniques in the field for routine surveillance, analytical methods must be validated to ensure that these methods perform consistently during routine analyses. This work offers insight on 1) understanding the physical and chemical variability of typical pharmaceutical tablets, required knowledge for development of robust models, and 2) the advantages of SVDD methods for the detection of falsified drugs using spectroscopic techniques.

Chapter 3: Application of Class-Modeling Techniques using Raman spectroscopy in the Presence of Moisture Variation

3.1 Introduction

Raman spectroscopy has emerged as a promising tool for detection of falsified drug products due to sharp peak features offering inherently good chemical specificity, the non-destructive nature of the method, and the flexibility in sampling interfaces.

One of the proposed uses of Raman spectroscopy is to detect active pharmaceutical ingredient (API) in the test sample. A pure component spectrum collected from API and a spectrum from the test sample may be utilized to determine correlation by a spectral matching algorithm. Because 50% of the falsified products detected in a recent study did not have the claimed API or contained the wrong API [27], this method was used to detect such falsified products.

In another approach, instead of using pure component spectra, samples collected from an authentic manufacturer have been used to find the correlation between authentic and test spectra [14, 35, 78-80]. Utilizing authentic sample spectra allows the analyst to verify the correct formulation (including excipient composition) of the test sample. However, relying on the sample spectrum to calculate correlation has drawbacks. One limitation is that pharmaceutical excipients generally have less Raman signal compared to the API. Studies have showed that, since different generic samples of a specific therapeutic group contain similar formulations (i.e., excipient compositions are often very similar to each other), Raman was unable to differentiate generic

products using correlation values because of the inadequate signal intensity from different excipients [14, 15]. This drawback of SM algorithms is also true when an analyst wants to detect highly similar falsified products (samples containing the same API, but unique excipient composition). Therefore, using class-modeling techniques can offer advantages of decreased false positives and false negatives.

As an important step in development of any class-modeling technique, a calibration model development effort is required. While developing Raman calibration methods, it is necessary to ensure that models meet the required performance standards; in particular, the sensitivity and specificity must meet predetermined validation criteria. One of the widely used class-modeling algorithms, soft independent class modeling analogy (SIMCA), has been used to create models for detection of falsified medicines [109, 151, 155]. Though this method allows the analyst to extract relevant chemical and physical information about samples to get qualitative information, numerous sources of spectral variability that occur during the method life-cycle may confound Raman measurements and may ultimately decrease the sensitivity of the model (ability to accept target-class samples). Therefore, to ensure long-term model performance, model sensitivity may be enhanced by including such sources of spectral variability in the target-class. These sources of variability may be identified during a risk assessment. Understanding the impact of such variability on the spectra and the effect of these spectral changes on model performance is a critical part of a sound model development process [151, 152].

Many sources of Raman spectral variability arise during the pharmaceutical manufacturing process, including sampling error, analytical instrument instability, sample property variation and environmental fluctuation. Sample variability may be introduced through raw material or process

variability or as a result of sampling procedure: the time, location and method of sampling is often at fault. Typically, lot-to-lot differences of incoming raw materials introduce new physical and chemical variations [128, 129]. The consequence of these variations on Raman spectra may depend on the sampling configuration, spectral collection modalities, etc. [130-132] As an example, the effect of particle size variation in tablets has been compared for backscatter and transmission Raman spectroscopy [133]. Because backscatter Raman generates most of the signal from very near the tablet surface [167], particle size had a reduced impact relative to the transmission mode. In the case of transmission measurements, photon propagation characteristics were more influenced by particle size variation due to the effect of light scattering on the effective optical path length. When particle size variability was not included in the calibration set, quantitative model accuracy suffered. Spectral processing methods such as derivative, normalization, etc., were applied to remove the baseline effect of particle size variation, thereby improving model performance. Also, by matching particle size variability for both API and excipients in the calibration, adequate quantitative predictions were obtained for independent test sets [1, 133-135]. A change of size, shape or density of tablets due to changes in the manufacturing process can also introduce spectral variability [136, 137]. By adjusting laser power and accumulation time, or enhancing density range in the calibration model, robustness can be enhanced against tablet size and density variations [134, 136].

While the implementation of Raman in pharmaceutical applications has increased dramatically over the past decades due to the improvement of instrumentation [54, 168, 169], one continuing challenge, and a major source of spectral variability causing interference with the Raman spectral signal, is fluorescence. Produced by emission of photons from low-lying excited electronic states, fluorescence often masks the vibrational shift of Raman spectra. This effect

occurs in a sample whenever the frequency of the excitation laser coincides with transition energy from the ground to an electronically excited state. Different experimental strategies and instrument modifications have been developed to overcome this problem [170]. By using excitation sources in the near-infrared region coupled with multichannel detectors, modern dispersive Raman spectrometers decrease the fluorescence background and provide adequate Raman intensity [171]. Different spectral preprocessing methods have been used to reduce the impact of fluorescence signal on prediction results [172-175]. Moreover, model performance should be adequate as long as both calibration and validation sets contain similar fluorescence background without introducing other spectral disturbances [176].

One of the challenging sources of variability that analysts often encounter during spectroscopic model development and deployment is environmental variability; for example, relative humidity will often vary from the warehouses where raw materials are stored to the facilities where products are manufactured. This can cause significant variability in the amounts of water sorbed by pharmaceutical samples [177-179]. Additionally, falsified products are often seized after being exposed to unknown storage conditions. Therefore, the impact of relative humidity on model performance is critical and needs to be tested. Most often, Raman analytical methods ignore the effect of moisture because Raman presents relatively weak water scattering. However, because pharmaceutical samples exhibit fluorescence from active pharmaceutical ingredient (API) [146] , excipient [173, 174], dyes [175], capsule shells [180], etc., the effect of moisture as a fluorescence quencher needs to be considered [181]. This can introduce unwanted spectral inconsistency across calibration and test samples. Nevertheless, there is not enough literature evidence to show the moisture effect on Raman spectra. Therefore, influence of moisture on Raman spectra was investigated, along with the model performance.

The objectives of this chapter are to investigate the effect of moisture and fluorescence on Raman spectroscopic analysis for pharmaceutical solid oral dosage forms. The effect of these changes on Raman spectra and multivariate qualitative model performance was assessed. As SVDD is a potential class-modeling technique, performance of this method was compared with the SIMCA method during this investigation. Finally, strategies for the development of robust qualitative calibration models were discussed.

3.2 Experimental Plans

In this chapter, two datasets were used to provide adequate understanding of the effect of moisture on calibration model performance.

1) Dataset 1: Lab-based acetaminophen tablets- Acetaminophen tablets were manufactured in the Duquesne University Center for Pharmaceutical Technology (DCPT).

2) Dataset 2: Artemether- lumefantrine combinations tablets- Artemether-lumefantrine fixed dose combination tablets were collected from a generic manufacturer.

3.3 Dataset 1: Lab-based acetaminophen Tablets

Tablet were prepared at two scales of manufacturing for this data set, including:

A) Lab-scale tablets, to study the effect of moisture on Raman spectra.

B) Pilot scale tablets, to study the effect of moisture on Raman model performance.

3.3.1 Lab Scale Tablets to Understand the Effect of Moisture on Raman Spectra

This experiment investigated the deleterious effects of water quenching on Raman spectra. To demonstrate this, a formulation composed of acetaminophen, lactose, microcrystalline cellulose (MCC), hydroxypropyl methylcellulose (HPMC) and magnesium stearate was used.

Granules of acetaminophen (APAP; Mallinckrodt Inc., Raleigh, NC, USA), HPMC (Pharmacoat 606, Shin-Etsu Chemical Co. LTD, Tokyo, Japan) and lactose (modified spray-dried; Foremost Farms USA, Rothschild, WI, USA) were manufactured using a fluid bed granulator (model WSG 5, Glatt, Binzen, Germany). The active containing granules were mixed with extra-granular MCC (MCC; Avicel PH 200, FMC Biopolymer, Mechanicsburg, PA, USA), lactose and magnesium stearate (Fisher Scientific, Waltham, MA, USA) in a bin blender. The mixture comprised of the aforementioned components were blended in a 3.5-quart V-blender (total mass of 1 kg) for 45 min. NIRS was used to demonstrate homogeneity at the target blending time.

The tablets were generated on a Carver automatic tablet press (Model 3887. 1SD0A00, Wabash, IN, USA) using a 13 mm die and flat-faced punches. Target tablet weight was 700 mg. A five by three level, two factors [active content (19.11%, 23.21%, 27.30%, 31.40% and 35.49% w/w; and excipient ratio levels 2, 1, 0. 5)] full factorial design was created. The use of a full-factorial experimental design provided orthogonality between the active ingredient and the excipient ratios. While it would have been possible to have all other components vary independently from the active ingredient, the use of excipient ratio helped to reduce the number of design points, as summarized in the design (Table 3-1). After allowing the tablets to undergo viscoelastic relaxation (two weeks), they were placed in environmental chambers at room temperature. The four chambers equilibrated with a relative humidity (RH) of 11% (saturated

lithium chloride), 32% (saturated magnesium chloride), 52% (saturated magnesium nitrate) and 75% (saturated sodium chloride). Tablets were left to equilibrate in each chamber, beginning with the lowest moisture level. Once the mass of tablets had equilibrated in the 11% RH chamber, they were analyzed and moved to the 32% RH chamber. The equilibration and analysis were repeated for each chamber. Tablets were moved from low to high relative humidity to simplify the experimental design and reduce the experimental period.

Table 3-1: Design for lab-scale tablets to vary API and excipients level

Design #	Acetamino-phen	Hypro-mellose	Intra-granular lactose	Micro-crystalline cellulose	Extra-granular lactose	Magnesium Stearate	Excipient ratio
1	19. 11	2. 73	5. 46	51. 77	20. 43	0. 50	2. 0
2	23. 21	3. 32	6. 63	48. 65	17. 70	0. 50	2. 0
3	27. 30	3. 90	7. 80	45. 53	14. 97	0. 50	2. 0
4	31. 40	4. 49	8. 97	42. 41	12. 24	0. 50	2. 0
5	35. 49	5. 07	10. 14	39. 29	9. 51	0. 50	2. 0
6	19. 11	2. 73	5. 46	38. 83	33. 37	0. 50	1. 0
7	23. 21	3. 32	6. 63	36. 49	29. 86	0. 50	1. 0
8	27. 30	3. 90	7. 80	34. 15	26. 35	0. 50	1. 0
9	31. 40	4. 49	8. 97	31. 81	22. 84	0. 50	1. 0
10	35. 49	5. 07	10. 14	29. 47	19. 33	0. 50	1. 0
11	19. 11	2. 73	5. 46	25. 89	46. 31	0. 50	0. 5
12	23. 21	3. 32	6. 63	24. 33	42. 02	0. 50	0. 5
13	27. 30	3. 90	7. 80	22. 77	37. 73	0. 50	0. 5
14	31. 40	4. 49	8. 97	21. 21	33. 44	0. 50	0. 5
15	35. 49	5. 07	10. 14	19. 65	29. 15	0. 50	0. 5

Fluorescence quenching effect

To understand the nature of spectral change due to fluorescence quenching, spectra of pure components were collected in the presence of water and molecular gases, oxygen (O_2) and nitrogen (N_2). To investigate the impact of water, pure component compacts were created by compressing approximately 700 mg of each material in the Carver press. Then, these pure component compacts were stored in the four aforementioned humidity conditions to observe the effect of moisture on Raman spectra. In addition, spectra were collected in the presence of O_2 and N_2 using custom gas chambers.

3.3.2 Pilot scale Tablets to Understand the Effect of Moisture on Raman Model Performance

In this experiment, the blends were compacted on a 38-station rotary tablet press (Elizabeth-Hata International, Inc., North Huntingdon, PA, USA). The stations were tooled using 3/8 in. (9.5 mm) diameter, round biconvex punches and the corresponding dies. Only two stations were tooled to facilitate the collection of the tablets post ejection. Three tablets were collected every minute for 20 min. The turret speed was left constant at 30 rpm, and the target compression force was 8000 kp. The target tablet weight was 350 mg. HPLC was performed on the tablets to ensure uniformity of blend and tablets.

During the course of the study (from June 2014 - March 2015), a total of six granulations and fourteen tablet batches were manufactured using the target formulation. A large variability existed in the in the moisture content of the excipients and granules. These variabilities were observed because the environment of the laboratory in which the experiments were performed was

not controlled; during the winter the air was dry (20–30% relative humidity (RH)), but during the summer months it was typical to observe a RH between 60% and 70%. Based on the seasonal differences, samples are categorized as summer, spring and winter samples. Both calibration and test sets included all these three seasonal samples.

3.3.3 Raman Data Collection

Raman spectra were collected on a TRS 100 (Cobalt Light Systems Ltd., Abington, Oxfordshire, UK) for analysis of compacts. The transmission spectrometer is equipped with a diode laser operating at 830 nm as the radiation source, a long pass spectral filter and a thermoelectrically cooled CCD camera for the detector. All compacts were scanned over the wavenumber range of 38-2400 cm^{-1}. The measurements were conducted at room temperature (approximately 24ºC). Parameters were tuned according to the tablet scale: exposure time for pilot and lab scale tablets were 0.5 seconds and 1.3 seconds, respectively. Five accumulations were collected per spectrum with a laser power of 0. 6W.

The effect of O_2 and N_2 gasses on the spectra of powdered samples was evaluated with a RamanRxn2™ backscattering spectrometer (Kaiser Optical Systems, Inc, Ann Arbor, MI, USA) and iCRaman software (version 4. 1, Mettler Toledo, Columbus, OH, USA). A fiber-coupled PhAT probe (HoloGRAMS version 4. 0, Kaiser Optical Systems Inc., Ann Arbor, MI, USA) was equipped with a 400-mW laser at 785 nm. The diameter of laser spot size was 6 mm. Accumulation time was 3 seconds, and the spectral range was 38-2400 cm^{-1}.

3.3.4 Model Evaluation

In order to evaluate class-model for authentication purpose and to determine the potential impact of moisture variation, both SVDD (see Section 2.2.1.2) and SIMCA (see Section 2.2.1.1.) was applied [109]. The capability of a model developed at one moisture level to predict the target class of compacts stored at other relative humidity levels was tested. The sensitivity **(**see Section 2.2.2) was used to evaluate the effect of moisture variability on model performance. Various diagnostic plots were employed to understand the underlying causes of model performance.

3.3.5 Results and Discussions

3.3.5.1 Effect of Moisture Variability on Raman Spectra using Lab-based Acetaminophen Tablets

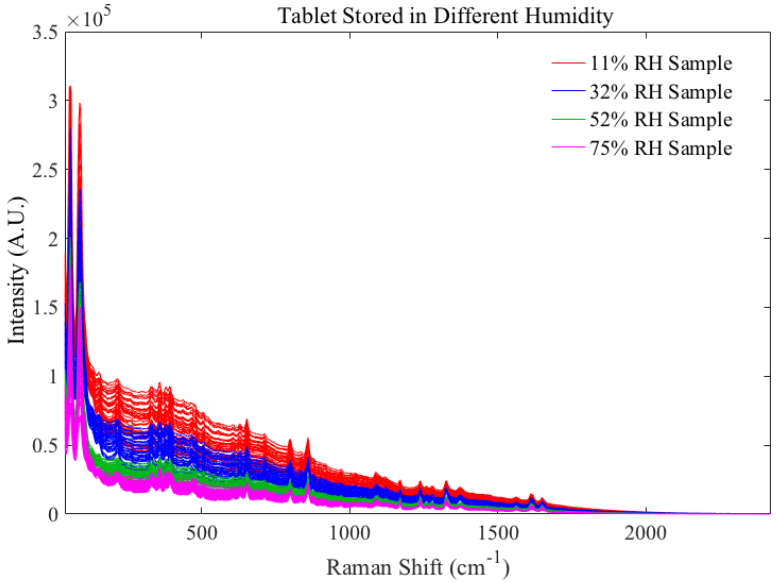

Figure 3-1: Raw spectra of calibration tablets at different moisture conditions: 11% RH (red), 32% RH (blue), 52% RH (green), and 75% RH (magenta).

Figure 3-1 shows spectral baseline changes when tablets were exposed to four different moisture levels (11% (red), 32% (blue), 52% (green) and 75% (magenta) RH). It can be observed that increasing the water content in the tablet leads to a decrease in the fluorescent background.

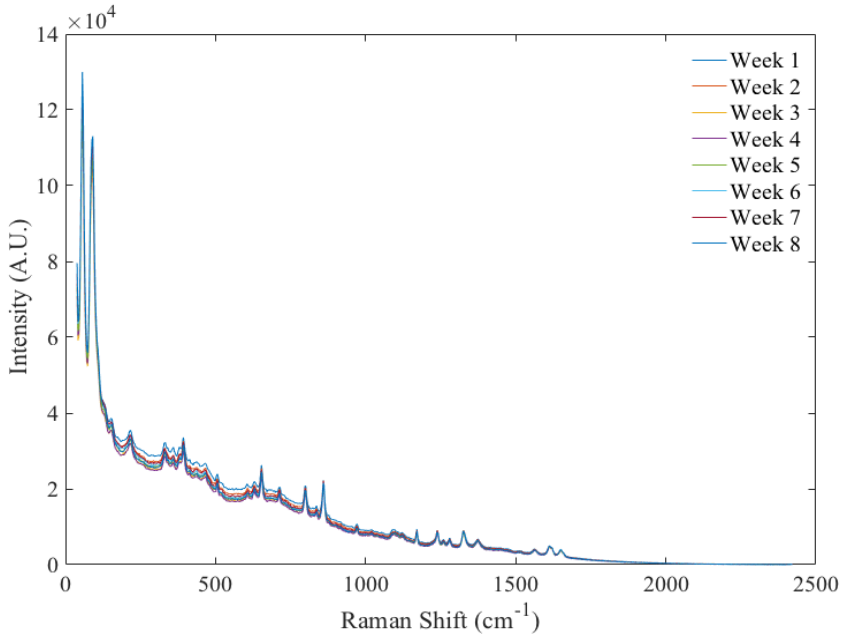

Figure 3-2: Raw spectra of a tablet (target formulation) exposed to repeat scans over eight weeks to test the photobleaching effect.

Mechanistically, the decrease in fluorescence intensity was caused by the deactivation of the excited-state fluorophores in contact with certain molecules (e.g., water in this study) in the sample. These molecules are referred to as quenchers [39]. This spectral change, due to the presence of water, was much more significant than the effect of photobleaching (due to successive exposure of the sample to the laser). The effect of photobleaching is illustrated in Figure 3-2, where a tablet was stored at a relative humidity 52% and scanned repeatedly over eight weeks. With an increasing number of scans and storage time, there was a small decrease in the baseline due to photobleaching.

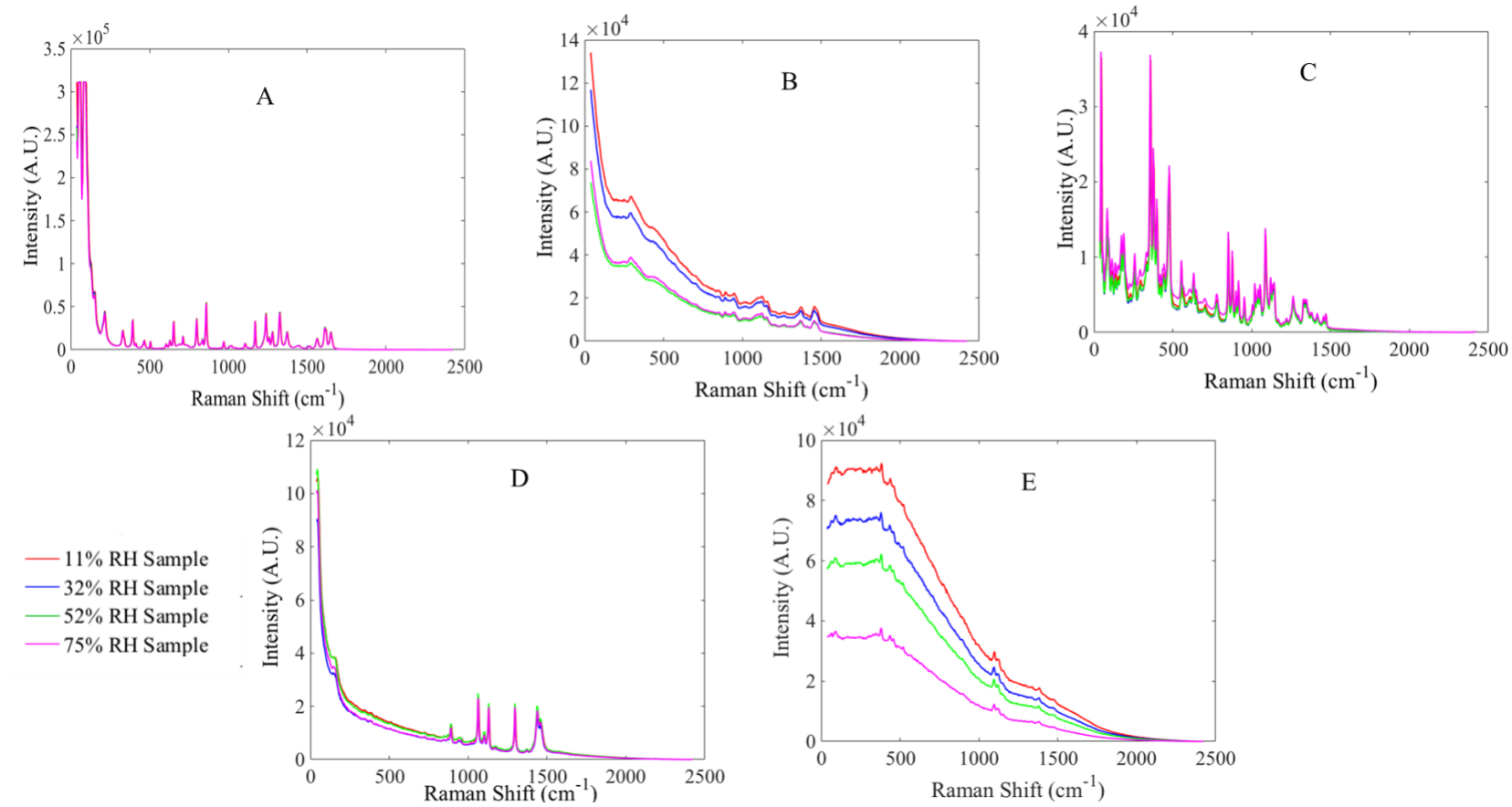

Figure 3-3: Pure component raw spectra of A) acetaminopen, B) hypromellose, C) lactose, D) magnesium stearate, and E) microcrystalline cellulose stored in four different humidity conditions (11% RH, 32% RH, 52% RH and 75% RH in red, blue, green and magenta respectively)

. To understand the source of spectral variation in the presence of moisture, a variety of compacts were prepared using pure components; the compacts were then exposed to different moisture levels. Figure 3-3 reveals that MCC and HPMC compacts demonstrated a significant decrease in the baseline with increasing water adsorption, which may be due to fluorescence quenching. However, APAP, lactose and magnesium stearate spectra demonstrated very small changes in the different conditions. This is likely due to the absence of fluorescence with these three pure components. The results indicate that the primary source of spectral variation in the prepared samples was from MCC and HPMC, with water acting as a quencher. In Figure 3-4, fluorescence quenching for MCC and HPMC was demonstrated in the presence of oxygen, a known quenching agent in cellulosic materials [42]. Previous studies demonstrated that, due to the presence of lignin in the fiber component, a large number of pulp and paper samples exhibit laser induced fluorescence (LIF). However, in the presence of molecular oxygen, lignin caused LIF contributions to Raman spectra were significantly decreased [182]. Figure 3-4 shows that due to the presence of O_2, the spectral baseline of MCC changed over time. But, when spectra were collected in the presence of N_2 or air, quenching was reduced. This result suggests that fluorescence decreases dramatically in the presence of the quenching agent O_2. A small spectral change was observed with MCC in the presence of air due to the continuous laser exposure. This provides another demonstration that the effect of photobleaching was less than that of quenching associated with moisture. Acetaminophen and lactose spectra demonstrated limited spectral change due to the lack of fluorophores.

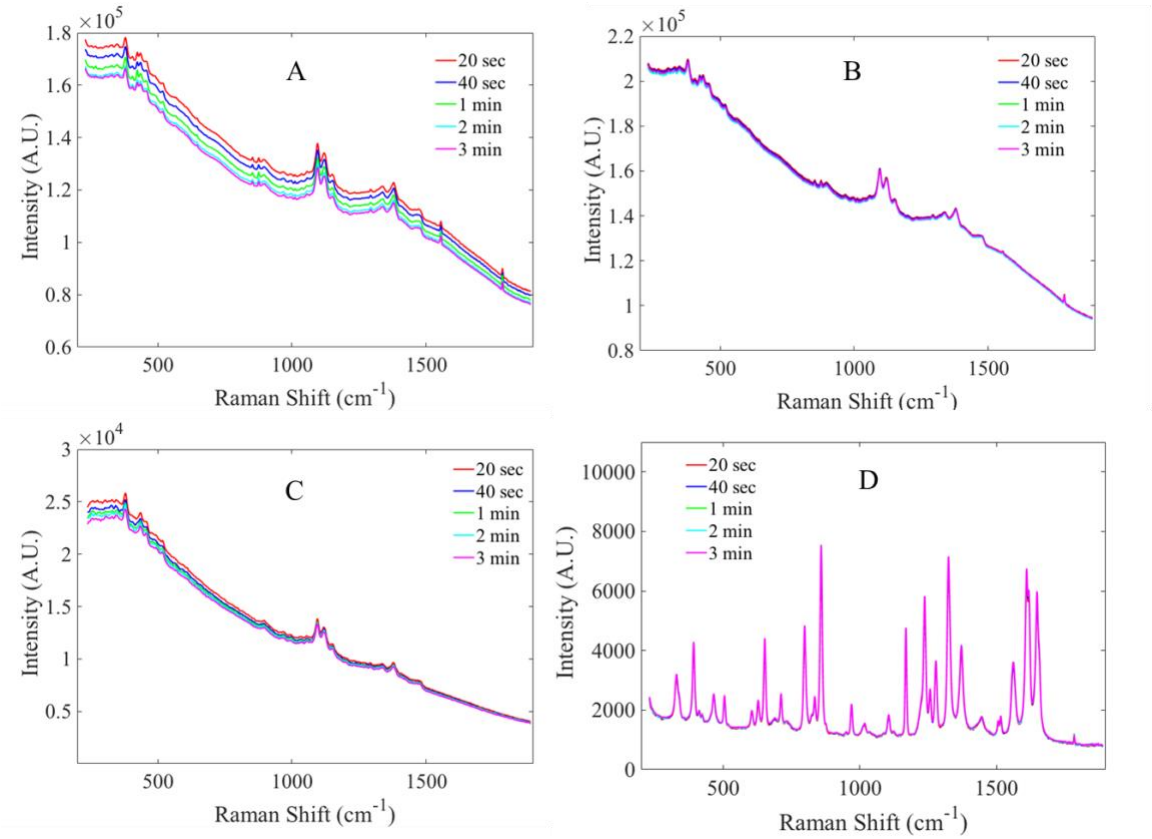

Figure 3-4: Raman spectra collected in the presence of molecular gas A) MCC in presence of O_2, B) MCC in presence of N_2, C) MCC in presence of air, D) Acetaminophen in presence of O_2.

The effect of fluorescence quenching on spectral baseline has been shown to vary with the content of both fluorophores and moisture. To characterize the impact of these two factors, spectral slope and intensity was observed for raw spectra. The slope of the spectra was calculated from a simple least-squares regression between Raman shift and Raman intensity. Three Raman shifts (276, 750, 1404 cm^{-1}) were chosen from the spectra to calculate this slope. The slope values are displayed in Table 3-2, where results from four moisture levels and three excipient ratios (2:1, 1:1 and 0. 5:1 of MCC: lactose) are presented.

First, the amount of fluorescent components affected the baseline intensity, as anticipated. Fluorescence intensity decreased with a decreasing amount of MCC (for a given moisture level). This change was reflected in the slope. Second, the moisture content had a significant impact on the baseline: the Raman intensity decreased with increasing water content (for a given compact composition), causing a dramatically reduced slope with increasing moisture content (Table 3-2). These results emphasize the quenching effect of water on Raman spectra.

Table 3-2: Effect of fluorescent containing material and moisture on Raman spectra

MCC: Lactose Ratio	%RH	RS=276 cm-1	RS=750 cm-1	RS= 1404 cm-1	Slope (Calculated from least square)
		Intensity count	Intensity count	Intensity count	A. U.
2	11	85896	47659	14711	35593
	32	59688	33290	10039	24824
	52	34189	19205	5590	14300
	75	22719	12889	3585	9567
1	11	81946	45242	13930	34008
	32	56868	31702	9737	23565
	52	33534	18615	5531	14001
	75	24557	13951	3982	10287
0. 5	11	61985	34349	11061	25462
	32	42609	23625	7491	17559
	52	27139	15339	4803	11168
	75	22087	12424	3659	9214

RS= Raman Shift.

3.3.5.2 Effect of Sample Moisture Variability on Qualitative Model Performance using Pilot Scale Acetaminophen Tablets

The observed spectral variations due to the presence of water had a significant impact on qualitative model performance using SIMCA and SVDD model. Performance was evaluated by developing three models, prepared in winter, summer and spring, where relative humidity was varied from 15%-75% RH. These models were then used to predict sensitivity of three test sets corresponding to the three seasons.

A number of preprocessing methods such as baseline weighted least squares, normalization, mean centering, derivative, and detrending were evaluated to eliminate the baseline changes of the full spectral range described before. Random block cross-validation (five blocks) was used to determine the most suitable spectral pre-treatments and model complexity (number of principal components for SIMCA and C and σ for SVDD). An optimization was independently conducted based on the minimization of cross-validation error. Savitzky-Golay first derivative (window size-31, polynomial order-2) followed by normalization to unit area and mean-centering was chosen for all models. Derivative methods were helpful to remove baseline variations and normalization decreased the intensity of variations introduced due to the fluorescence quenching or any physical differences between calibration and test sets.

As shown in Table 3-3, both SIMCA and SVDD models offered good sensitivity for samples from the same moisture levels, where the preprocessing method was successful at removing fluorescent baseline variability. However, poor results were achieved for prediction of samples from unique moisture levels; error statistics increased with increasing range between the

moisture levels of calibration and test sets. Figure 3-5 presents Hotelling's T^2 and Q residual plots for spring calibration model. The reconstruction error for summer and winter test sets was higher, indicating that the lack of robustness of the calibration model to moisture variability.

Table 3-3: Effect of sample moisture variability on test set predictions: Lab Scale Tablet

SIMCA					
		Summer	**Spring**	**Winter**	**Global**
Test Set Sensitivity	**Summer**	0.95	0.75	0	1
	Spring	0	0.84	0.75	1
	Winter	0	0	1	1
SVDD					
		Summer	**Spring**	**Winter**	**Global**
Test Set Sensitivity	**Summer**	0.95	0.7	0	1
	Spring	0	0.93	0.8	1
	Winter	0	0	1	1

Global models include all of the expected variability in the calibration set. In this case, calibration sets from three seasons were combined to facilitate the creation of robust model: sensitivity for the test set at the different humidity levels are provided in Table 3-3. The global model demonstrated a lower prediction error compared to models created at unique humidity conditions

3.4 Dataset 2: Artemether- Lumefantrine Combinations Tablets

The World Health Organization (WHO) introduced artemisinin-based combination therapy (ACT) as first-line therapy to decrease the falciparum malaria, which was adapted by most countries [183]. Successful prevention and control of malaria can be achieved by ensuring the

quality of ACTs and other antimalarials. However, one-third of anti-malaria medicines from malaria-endemic countries failed the quality test, which is alarming for the prevention of malaria [184]. Different fast screening processes have been proposed to test pharmaceutical tablets at different stages of the supply chain. Raman spectroscopy has been used to test the quality of artemether-lumefantrine fixed-dose combination products [146].

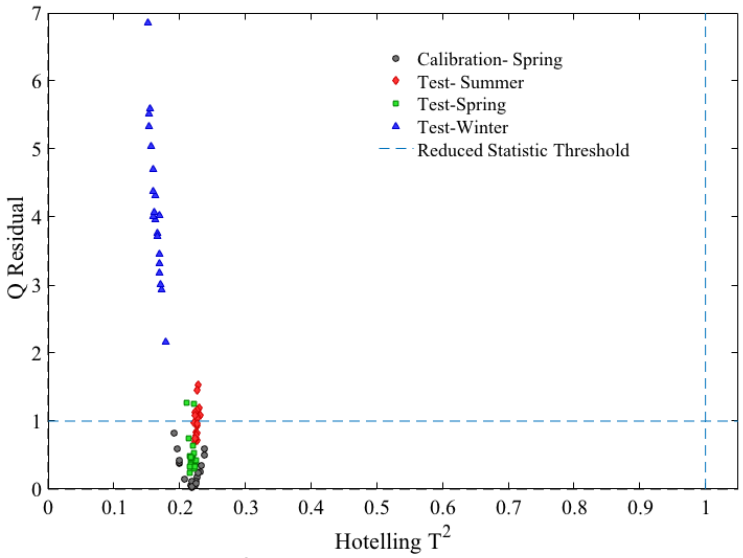

Figure 3-5: Hotelling's T^2 vs. Q residual plot was generated from different seasonal conditions of test tablets (summer (red), spring (green), winter (blue)) , which were projected on the calibration set (spring (black)).

However, as artemether has a high fluorescent background while using Raman spectroscopy, model performance may deteriorate due to the fluorescent quenching in the presence of moisture [146]. Therefore, it is hypothesized that, for artemether-lumefantrine samples, it is essential to consider moisture throughout the method development process. Artemether-lumefantrine tablets produced by generic manufacturers were used as a model drug to evaluate the influence of moisture variation on tablet's spectra and model performance.

3.4.1 Sample Collection

Anti-malarial drugs were obtained from a government registered pharmacy in Dhaka, Bangladesh. A total of 56 artemether-lumefantrine tablets, manufactured by Square pharmaceutical Ltd. (Lumetram®) were collected. Packaging was visually inspected to avoid any fraudulent activities, and the batch numbers were confirmed with the manufacturer for authenticity. Further, to independently verify the active ingredient in the manufacturers' standards, pure components of artemether (J&K Scientific San Jose, CA), and lumefantrine (Combi-block, San Diego, USA) were used.

3.4.2 Samples Scan

Raman data were collected using a RamanRXN2 spectrometer (Kaiser Optical Systems, Inc, Ann Arbor, MI, USA) and iC Raman software (version 4.1, Mettler Toledo, Columbus, OH, USA). The spectrometer was equipped with a 785 nm laser excitation and a fiber-coupled PhAT probe (HoloGRAMS version 4.0, Kaiser Optical Systems, Inc, Ann Arbor, MI, USA) with a 6 mm spot size. One accumulation with 5 s integration times were acquired over the range of 150–1,890 cm^{-1} at 1 cm^{-1} increments. A dark scan was subtracted, and the cosmic ray filter and intensity calibration options were selected. Tablets were positioned at the end of the probe unit using an in-house machined copper sample holder with a 10 mm diameter. The sample holder was threaded into the end of the PhAT probe tube so as to provide a fixed distance from the laser source to each sample. This reduces error related with repositioning and re-focusing. To decrease stray light effects while collecting samples spectra, a black cap was kept over the top of the sampling interface. The average of spectra from both sides of each tablet was used for calibration development and testing, respectively.

3.4.3 Samples Preparation to Investigate the Effect of Moisture

Three chambers were used with target relative humidity (RH) of 15% (saturated solution of lithium chloride), 50% (magnesium nitrate) and 70% (sodium chloride). A total of 15 Tablets were left to equilibrate in each chamber. The equilibration of the mass over storage time at each RH condition was used as an indicator of stability. Tablets were moved from low to high relative humidity to simplify the experimental design and reduce the experimental period. Both sides of the tablets were scanned 5 times using the same parameters described above.

3.4.4 Testing the Effect of Moisture on Model Performance

Individual classification models were constructed from each sample set equilibrated at a single relative humidity. Test samples stored at the alternate relative humidity conditions were predicted. When the moisture level is different between calibration and test sets, method sensitivity should be challenged. Moreover, depending on the performance of sensitivity, the effect of moisture variance should be accounted for during method development.

3.4.5 Results and Discussions

3.4.5.1 Moisture Effect on Artemether-Lumefantrine Tablets

Sample spectra of artemether-lumefantrine collected using Raman spectroscopy showed high fluorescence background (Figure 3-6). These spectral features were similar to the acetaminophen tablet dataset. Raw spectra of two pure components were collected. Here, artemether showed strong fluorescent background and peak features were suppressed. However, lumefantrine had sharp peak features and fluorescence background was absent.

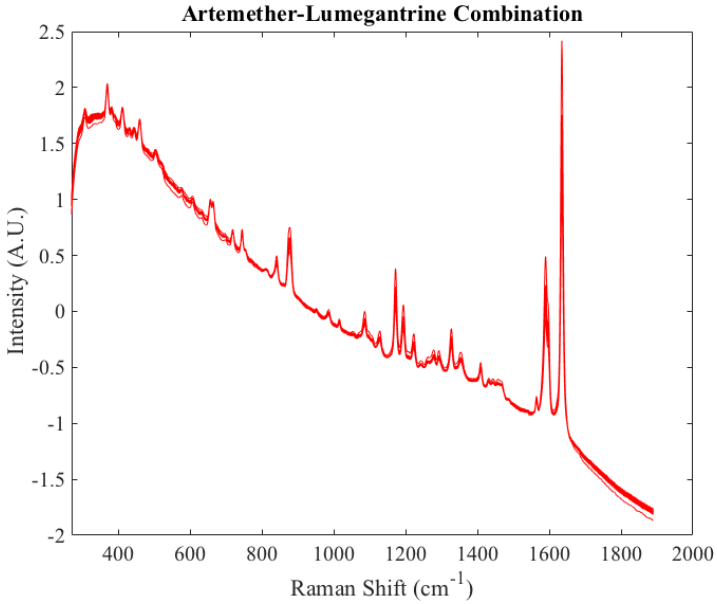

Figure 3-6: Raman spectra of artemther-lumefantrine combination.

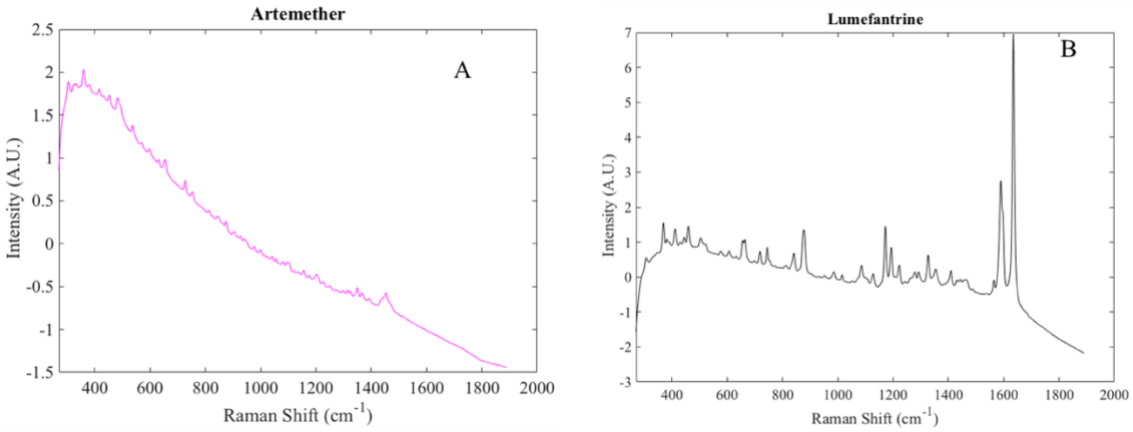

Figure 3-7: Pure component spectra of A) artemether and B) lumefantrine.

Spectral variations were observed due to the presence of water in the tablet. As both samples and pure components were placed in different humidity chambers, fluorescence

quenching was observed due to the presence of water in the samples (Figure 3-8). It was also revealed that this quenching effect was prominent in the artemether (Figure 3-9).

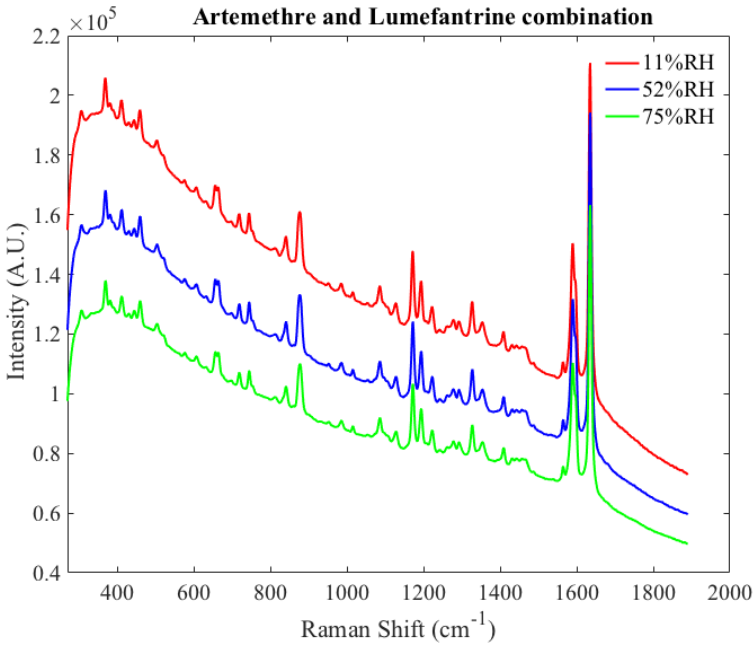

Figure 3-8: Spectra of tablets collected from three humidity conditions

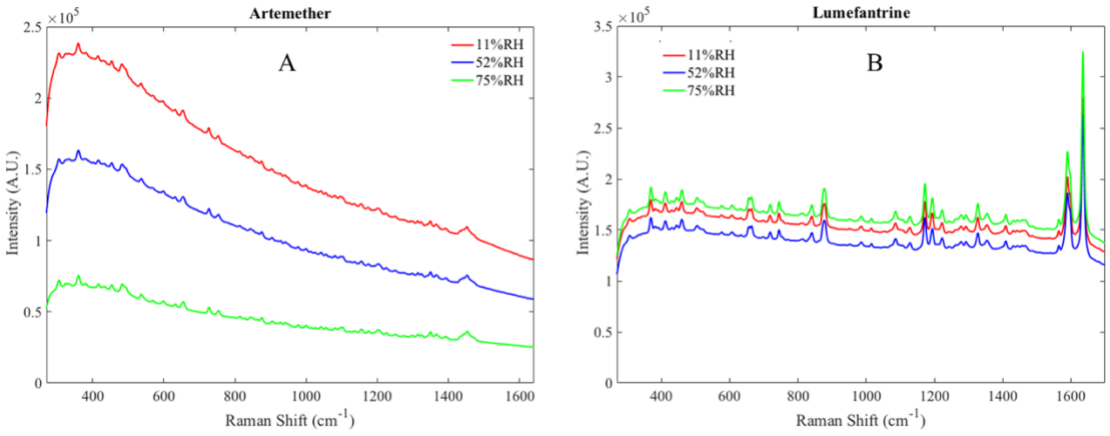

Figure 3-9: Moisture variation of artemether and lumefantrine in different humidity conditions.

3.4.5.2 Model Performance in Presence of Moisture Variations

Models developed at individual moisture levels accepted target class samples stored at similar moisture levels. However, the models failed to predict test sets collected at other moisture levels. This study resembled the previous acetaminophen studies described in this Chapter (using Raman) and Chapter 2 (using NIRS). The error statistics became higher in different humidity conditions, due to the increment of the difference of moisture level between calibration and test sets (Table 3-4). This was largely because of fluorescence quenching and resulted increase of baseline change. Therefore, Raman qualitative model performance decreased due to the lack of robustness.

Table 3-4: Model performance of artemether-lumefantrine tablets in different moisture conditions

SIMCA					
		11%	**52%**	**70%**	**Global**
Test Set Sensitivity	**11%**	1	0.3	0	0.9
	52%	0	0.95	0.4	1
	75%	0	0	1	1
SVDD					
		11%	**52%**	**70%**	**Global**
Test Set Sensitivity	**11%**	1	0.4	0	1
	52%	0	0.925	0.2	1
	75%	0	0	1	1

The effect of these spectral variabilities was observed in multivariate space described by Q residual and Hotelling's T^2 (Figure 3-10). The Q residual values for the low moisture level of calibration set and high moisture level for the test set indicated that this test set has different spectral shape compared to the calibration set (Figure 3-10A). Global models including moisture variability showed improved performance by reducing Q residual (Figure 3-10B). This global model is often considered as a risk-based model. In this case, calibration sets from three relative humidity levels were combined to facilitate the creation of a global model. This global model demonstrated a lower prediction error compared to the models created at unique humidity conditions. Moisture variabilities can cause density changes of tablets which may also have effect on the spectra. Baseline correction and derivative methods were conducted to remove this interference.

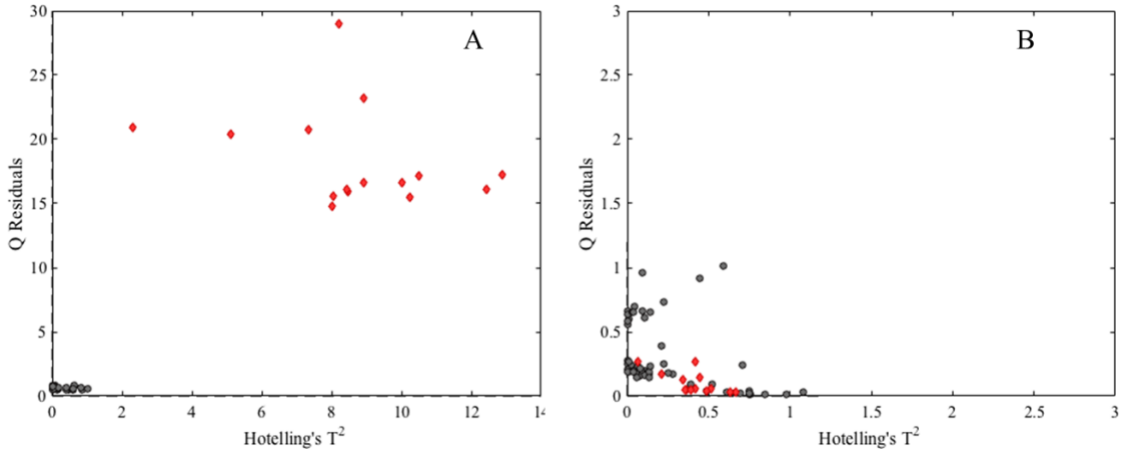

Figure 3-10: Hotelling's T^2 vs. Q residuals plots were generated from calibration plot (A) 11% RH samples (black), 52% RH samples (red) (B) global RH samples (black), 52% RH samples (red).

Changes of relative humidity often cause polymorphic changes in API or excipients. However, this formulation did not demonstrate such a risk. Also, as the drug is stable over the proposed humidity range, stability was not an issue for the considered formulation.

3.5 Summary and Conclusion

It is difficult to preemptively identify all sources of variation that will be encountered during the pharmaceutical life-cycle. The experimental approach in this study provides an example of how a simple phenomenon like moisture variability, arising from such phenomena as inconsistent environmental conditions, can, through fluorescence, significantly affect spectral baseline and model performance. Both SVDD and SIMCA methods were tested in this work using a global modeling approach to demonstrate opportunities for the creation of robust models for laboratory and production scale tablets.

In this study, the presence of components containing 1) fluorophores and 2) moisture, negatively affected model performance. Pharmaceutical raw materials, including excipients and APIs, often contain fluorescent components. In Dataset-1, lignin in the microcrystalline cellulose caused laser induced fluorescence [182, 185]. In Dataset-2, artemether showed a strong fluorescence background. Moreover, variable moisture content also introduced spectral variance for these two datasets. The water content of tablets will often vary between and within different tablet batches, depending on the relative humidity conditions during production, packaging, storage and analysis. Water may be sorbed by samples very quickly depending on the relative humidity of the environment and material attributes [34]. While it is likely that the relative humidity of the laboratory may be controlled, it is very unlikely that the same environmental conditions will be observed in the field analysis. Analysts may need to test the suspected samples

which have been exposed to a different humidity condition. This is particularly true in situations where spectroscopic method development takes place at one geographic and climatic location and routine use of the method occurs elsewhere [177].

It is typically beyond the capacity of an analyst to eliminate sample components or strictly control the sources of variability. Understanding the effect of variabilities such as moisture and fluorescence during multivariate calibration model development will facilitate the generation of models which are robust against these variations. In the present study, the effect of fluorescence background was reduced by preprocessing the spectra. However, when calibration and test sets contained different moisture content, prediction performance was degraded. These findings regarding the effect of moisture on the Raman spectra should be useful information for method development. This is true for both SVDD and SIMCA algorithms.

Though both SVDD and SIMCA algorithms performed satisfactorily after adding moisture variations in the calibration model, SVDD showed promising results. This study highlighted the usefulness of the SVDD algorithm for Raman spectroscopic techniques as a class model for pharmaceutical tablet authentication system. This was the first use of SVDD and Raman spectroscopy for tablet authentication.

Chapter 4: Developing a SVDD Method with Non-Target Class Samples to Detect 'Highly Similar' Acetaminophen Tablets Collected from Global Sources

4.1 Introduction

The development and implementation of class modeling typically occurs in two stages, including 1) building a target class by generating a decision boundary around the target class samples, and 2) evaluating a test samples to determine method sensitivity and specificity, based on whether the sample resides inside or outside of the established multivariate decision boundary.

Typically, development of a decision boundary for a SVDD model does not rely on samples from the non-target class. Method development using only target class samples is known as a 'one-class SVDD' approach. In such a case, the model reaches an optimal condition by achieving the best sensitivity (ability to accept target class samples).

However, samples from the non-target class can be used to optimize the model [21]. Including non-target class samples during modeling improves the description of the target class by defining a tighter boundary around the target class data in the areas where non-target objects are present. In contrast with the target class samples residing within the boundary, the non-target class samples should be outside of the multivariate boundary. This type of method development is feasible when several datasets from extraneous classes are available. These new non-target class samples enable the calculation of an additional figure of merit — specificity (the rejection of

objects from the non-target class). Understanding model specificity reduces the risk of accepting false samples.

While developing a spectroscopic authentication method using a SVDD algorithm, the non-target class samples should be a true representation of falsified drugs.

The pharmaceutical literature reports pharmaceutical products, including pure components and finished dosage forms, could be falsified in various ways. Primary methods of falsification involve altered composition of final dosage forms. This includes, but is not limited to, intentional adulteration of pharmaceutical ingredients, tablets prepared without active pharmaceutical ingredient (e.g., using only excipients), tablets manufactured using the wrong API, and tablets generated with the correct API, but unusual compositions of excipients. In practice, the most difficult samples to detect using spectroscopic methods could be the last category, which are often generated using similar manufacturing techniques. Therefore, during authentication model development, analysts should select non-target class samples which have similar compositions and have similar spectral features to the target class. Spectral matching algorithms would be one appropriate method to evaluate the spectral similarity between target and non-target class samples during development of a SVDD method.

In this chapter, it is proposed that an appropriate non-target class of samples is essential for optimizing a SVDD method. To prove this, challenging samples (which are difficult to distinguish between non-target class and target class) from various producers containing identical API and similar excipient compositions were considered. Highly similar acetaminophen tablets collected from China, India, and Bangladesh were used in the study.

4.2 Materials and methods

4.2.1 Sample collection

Tablet formulations containing acetaminophen were obtained from outlets readily available to tourists or visitors in Bangladesh, India, and China (Figure 4-1). The tablets were uncoated, intact and blister-packed. All tablets contained 500 mg of APAP according to the label. Samples which had similar size and shape were only considered in this study (Figure 4-2). Nine different manufacturers' samples were collected from these three countries. The tablets were collected from different batches, 10 tablets per batch. Details are presented in Table 4-1.

Figure 4-1: Samples were collected from India, Bangladesh, and China.

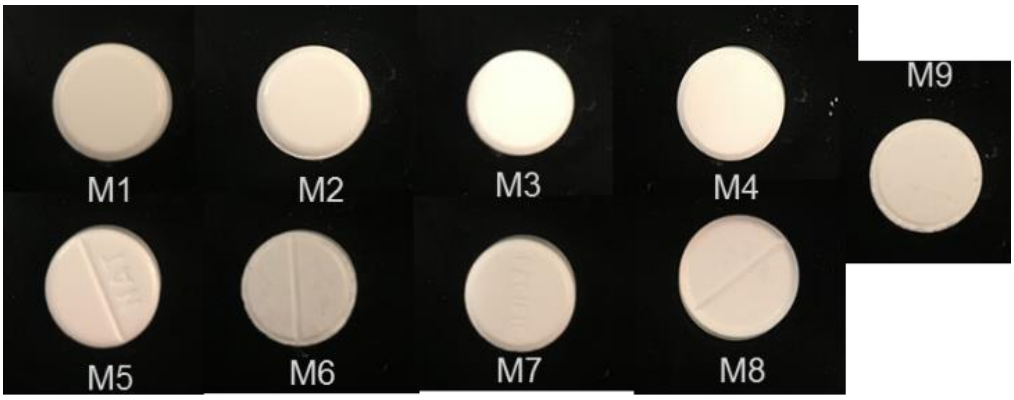

Figure 4-2: Image of the tablets from different manufacturers (M1-M9).

Table 4-1: Characteristics of tablets from different manufacturers (M1-M9).

Manufacturer Code	Tablet Weight	APAP amount	APAP Percentage in the tablet
M1	558.3	500	89.55
M2	599.7	500	83.37
M3	582.7	500	85.81
M4	577.7	500	86.55
M5	557.3	500	89.71
M6	582.3	500	85.86
M7	554.0	500	90.25
M8	590.7	500	84.65
M9	545.7	500	91.63

4.2.2 Confirming the Chemical Similarity of Samples using Raman Spectroscopy:

Raman spectra were collected by following the protocol mentioned in section 3.3.3 .

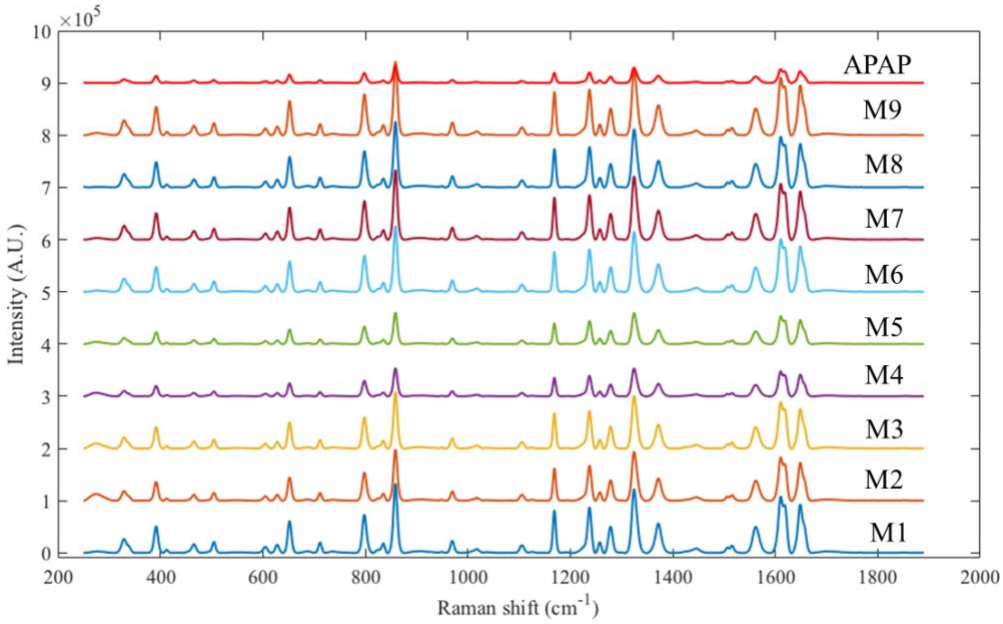

Figure 4-3: Raman spectra of different manufacturers' samples and APAP.

The presence of acetaminophen in each product was confirmed using Raman spectroscopy. The spectra are observed in Figure 4-3. Here, the spectra were stacked to demonstrate the presence of API. Tablet spectra were compared in the fingerprint region (1850–400 cm^{-1}), to verify the presence of API. The spectral correlation was calculated by comparing each of the sample spectra, with the acetaminophen spectrum. All products showed correlation coefficient values greater than 0.95, confirming the presence of acetaminophen (see section 1.3.3.1.2).

4.2.3 NIR Measurement

NIR spectra were acquired in the range of 1550–1950 nm with a 10 nm wavelength increment using a portable NIR ONE Sensor (Spectral Engine, VTT, Finland). Measurements were carried out in diffuse reflectance mode. For analysis, the entire spectral region (1550-1950 nm) is utilized because it is difficult to foresee at which wavelength alien objects will manifest deviations from the genuine sample. Each time, both sides of the tablets were scanned to increase the sample representation. Replicas were averaged before the analysis.

4.3 Figures of Merit

The following formula (Equation 1) calculate sensitivity of the method (accepting genuine samples):

$$Sensitivity=TP/(TP+FN) \qquad 1$$

where TP and FN are true positive and false negative, respectively. If the model accepts falsified samples, the model needs further optimizations.

The Specificity of the method (rejecting falsified samples) is used as validation parameter. The following formula (Equation 2) calculates this parameter:

$$Specificity=TN/(TN+FP) \qquad 2$$

where TN and FP are true negative and false positive, respectively.

4.4 Theory

4.4.1 Unsupervised analysis (PCA)

The Principal Component Analysis (PCA) method projects multivariate spectra into low-dimensional space, which emphasizes the variabilities present in the collected spectral data although they do not precisely aim to identify them [81, 82]. PCA decomposes the multivariate response arranged in an X matrix into a product of two new matrices as indicated in the following equation 3:

$$X = T_k P_k^T + E \qquad 3$$

Where T_k is the matrix of scores which represent how samples relate to each other, P_k is the matrix of loadings which contain information about how variables relate to each other, k is the number of factors included in the model and E is the matrix of residuals, which contains the information not retained by the model. The reader is referred to the works of Wold et al. [81] and Martens & Naes [82] for a more detailed discussion of PCA.

4.4.2 SVDD

See Section 2.2.1.2.

4.4.3 Spectral correlation method

The spectral correlation method compares two spectra under study. This algorithm considers the two spectra as two vectors, and then calculates correlation between these vectors

(Equation 4) [67]. This spectral correlation (SC) method is often mentioned as a similarity and is the equivalent of measuring the cosine of the angle between two spectra.

$$SC = 100 * \sqrt{[(Samle1_m \cdot Sample2_m)^2]/[(Sample1_m \cdot 1)(Sample2_m \cdot Sample2_m)]} \quad 4$$

Here $Sample1_m$ and $Sample2_m$ is the m^{th} absorption value in the spectra. SC measures the similarity between the spectra, and SC values range from 0 (poorest match possible) to 1 (perfect match).

4.5 Experimental Strategy

Acetaminophen tablets manufactured by nine generic manufacturers produced in three countries were used to demonstrate the proposed model development approach. In this study, the calibration model was first developed using M1. After that, the model was optimized and validated with both target and non-target classes (using M2-M9). Figure 4-4 displays a flow diagram of the protocol.

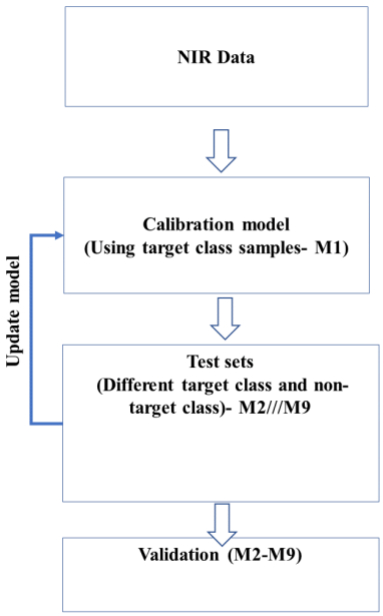

Figure 4-4: Method development flow path. Relative to the contemporary process analytical method development cycle which typically includes target class samples, proposed SVDD method will be optimized using both target class and non-target class samples

4.6 Result

4.6.1 Spectral Investigations and PCA Analysis

Raw spectra failed to reveal significantly unique features of different sample sets. Baseline shifting in the raw spectra was caused due to sample positioning variability. A standard normal variate (SNV) method removed the baseline shifting associated with sample positioning variability. Figure 4-5 shows the preliminary differences where primary variations were observed in 1650-1850 nm and 1900-1950 nm.

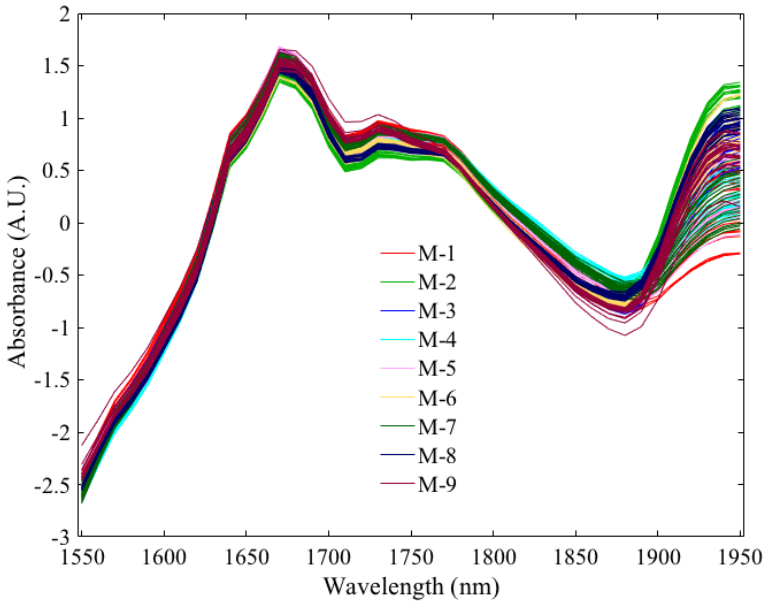

Figure 4-5: SNV treated spectra from nine different manufacturers.

While using the PCA algorithm, different preprocessing methods and their combinations were tested. To distinguish product from different manufacturers, the most efficient preprocessing methods were SNV following the second order Savitzky Golay derivative, using a second-order polynomial with a 5-point window and mean-centering. These combination of different

preprocessing methods further removed baseline shifts and sharpened the spectral peaks. Principal component analysis (PCA) was applied to different manufacturers' samples (M1-M9). The results show that 4 PCs describe 97.46% of data variation. The score plots presented in Figure 4-6 demonstrated that M9, M2, M4, and M5 were well separated from M1 (target class). However, other groups showed substantial overlapping, in the plot of PC1 vs. PC2 scores. When considering the plots generated using subsequent PCs, it is possible to separate other classes from the target class. However, the close location of different groups indicated the high similarity of samples from different manufacturers. In this case, PCA alone would not be adequate to consistently discriminate all tablets from the target class.

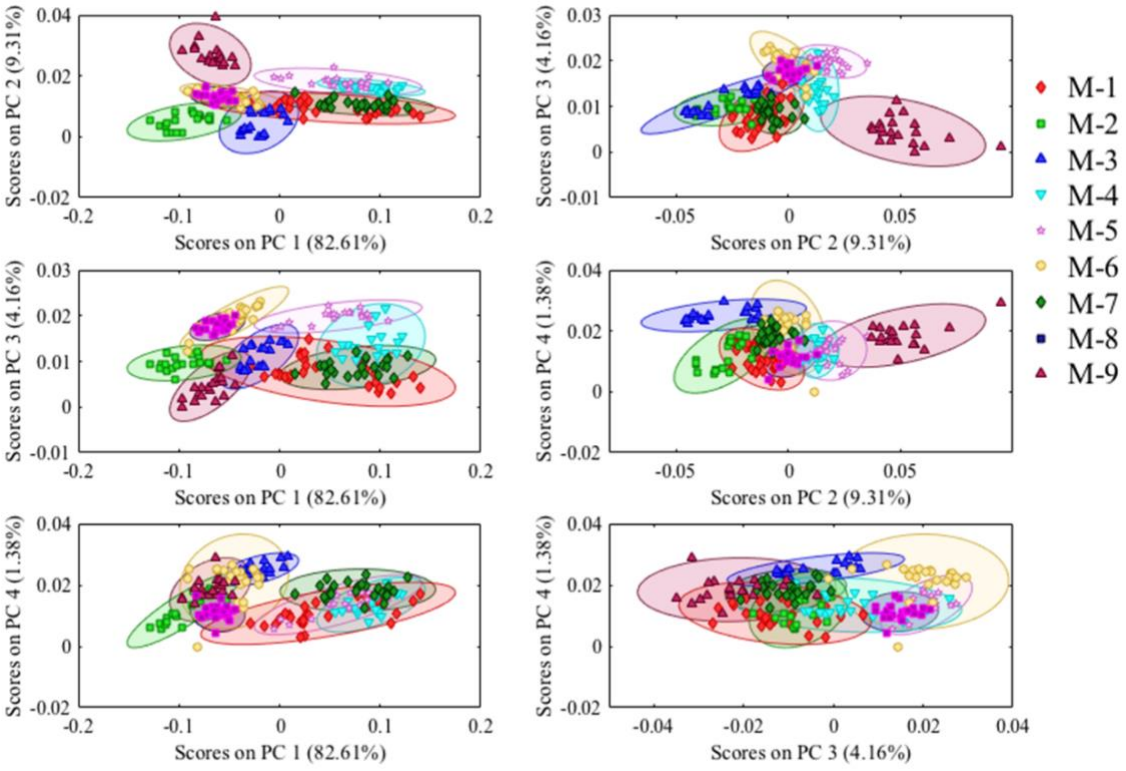

Figure 4-6: A combined PCA model including all the calibration and test manufactures.

4.6.2 SVDD Model Performance:

The spectra of 30 samples from M1 manufacturer were used for the calibration model development. Then, 20 more samples from M1 were used for sensitivity calculation. Additionally, 20 samples from each of the other eight manufacturers (M2-M9) were considered as non-target class samples for optimization and for use as the validation sets. These non-target class samples were used for the assessment of specificity. Among these eight manufacturers (M2-M9), one was used to optimize the model and the other seven were used for validation purposes. Therefore, a total of eight models were developed using optimization sets to calculate specificity. For each non-target class, a total specificity is computed along with seven partial specificities, one for each non-target class. The total specificity is the average of the seven partial specificities (Table 4-2). Column one contains the non-target class names used for optimization. The second and third columns show the number of support vectors and selected σ, respectively. The other eight columns present the partial specificities, calculated separately for each non-target class. Mismatches (total specificity less than 90%) are bold marked in column 9.

Table 4-2: Performance of SVDD using NIR spectroscopy

	Validation specificity										
	D= 0.01		Partial specificity								
Non-target class	No o of SV(s)	σ	**M2**	**M3**	**M4**	**M5**	**M6**	**M7**	**M8**	**M9**	Total specificity
M2	2	0.3		0.65	0.15	0.45	0.91	0	1	1	**0.59**
M3	2	0.23	1		1	1	1	0.63	1	1	0.95
M4	2	0.23	1	1		1	1	0.63	1	1	0.95
M5	2	0.245	1	0.9	0.55		1	0.54	1	1	**0.86**
M6	2	0.27	1	0.7	0.25	0.8		0.5	1	1	**0.75**
M7	3	0.21	1	1	1	1	1		1	1	1.00
M8	2	0.3	1	0.65	0.15	0.45	0.91	0	1	1	**0.74**
M9	2	0.3	1	0.65	0.15	0.45	0.91	0	1		**0.59**

It can be seen that values of total specificity obtained for the models which used M2, M5, M6, M8 and M9 as optimization sets are unsatisfactory. This result means that if these samples are used as the non-target class to optimize the SVDD, the model could run the risk of having higher false positives. This was observed in the Table 4-2. Such models failed to reject the rest of the classes (M3, M4, M7). However, three models which used M3, M4 and M7 to optimize the model reliably distinguished between target and the non-target class samples. Among these, M7 worked best as that model rejected all non-target class samples. Figure 4-7 shows that M2 is spectrally different than the calibration spectra, whereas M7 is highly similar.

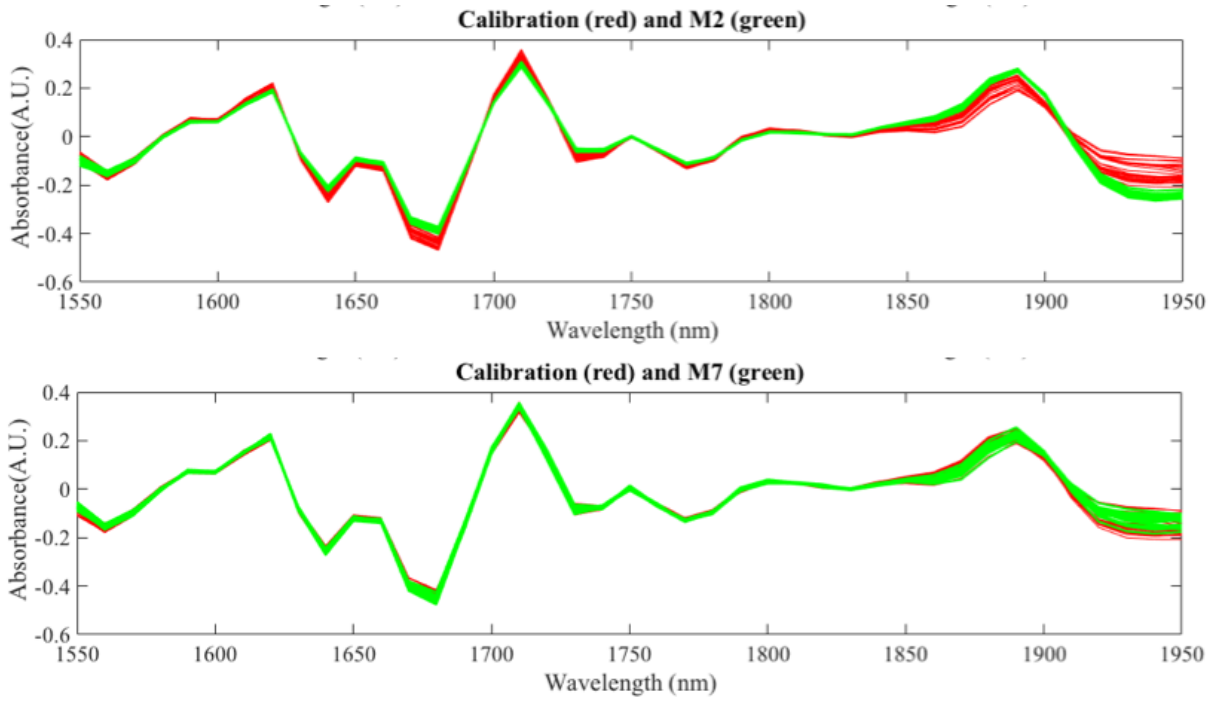

Figure 4-7: Spectral comparison of calibration set (M1), and non-target classes (M2 and M7)

Therefore, it can be concluded that the selection of a pertinent non-target class set for the SVDD can significantly influence the results of classification. This experiment suggests that to

reject “highly similar” samples using the SVDD method, it is essential to use highly similar non-target class samples for model optimization. This creates a model that is sensitive to non-target class test samples that are “highly similar” to target class samples.

4.7 Non-Target Class Sample Selection:

A correlation coefficient was calculated to automatically select a suitable non-target class set for model optimization of falsified drug detection. This effort defined a method for setting quantitative criteria for selection of ideal non-target class samples which would help to optimize the model. Figure 4-8 showed the correlation coefficient values between the calibration set and different non-target class sets. All of the samples exhibited a correlation of more than 0.95. However, among these, non-target class, M7, showed the highest correlation with the target class, M1. This correlation value between M1 and M7 was similar to the correlation values of different batches of M1 (as different batches of M1 were used as calibration and test sets). Because of this, it was difficult to separate M7 from M1, when other sample sets (M2-M6, M8 and M9) were used to optimize the model. Therefore, M7 was the ideal non-target class candidate to be used for optimizing the SVDD model.

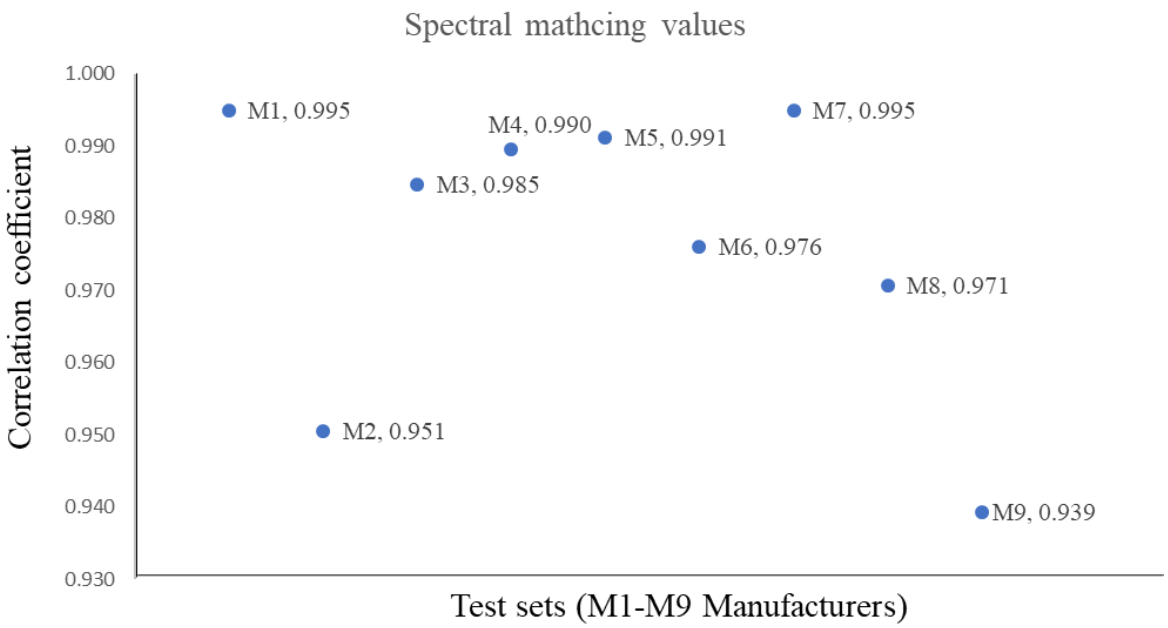

Figure 4-8: Spectral correlation coefficient values between the calibration set and different manufacturers' samples sets (M2-M9) including a unique batch of a calibration set (M1).

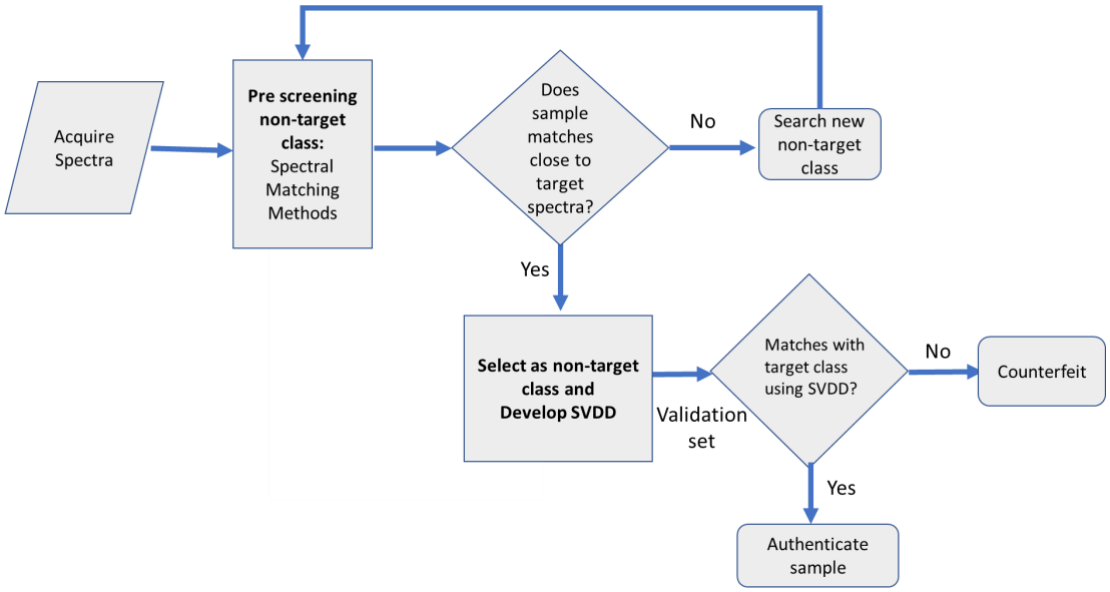

Figure 4-9: Workflow of a method development for a spectroscopic authentication system.

The final workflow for falsified detection is proposed in Figure 4-9. To obtain better performance, a SVDD model will be optimized using a non-target class sample. Before applying the SVDD algorithm, these non-target class samples can be selected using a simple mathematical treatment, such as correlation coefficient, for testing similarity between the target class and non-target class.

4.8 Discussion and Conclusion:

It is understood that a spectroscopic system for authentication of pharmaceutical products will require modern chemometric tools. The SVDD method was used with both target and non-target class samples to demonstrate an approach for development of an authentication method. The proposed SVDD method differs from a conventional two-class classification method because the SVDD defines a closed boundary around target-class samples, whereas traditional two-class support vector machine methods develop a boundary between these two classes. Furthermore, the method does not require a strict representative sample of the target distribution; a calibration set with extreme objects is acceptable, even desirable. However, it is also important to understand that an effort to reduce false positives (accepting falsified samples) can result in an increase in false negatives (rejecting authentic samples). With the presence of non-target class samples used for model optimization, the boundary is developed rationally.

In this chapter, it was observed that exploiting non-target class samples during model development is useful for optimization of SVDD models. Adding non-target class samples in the method development process enabled the investigators to optimize the boundary of the SVDD

model based on both sensitivity and specificity parameters. Selecting appropriate non-target class samples to optimize the model requires a quantitative approach such as spectral correlation calculation.

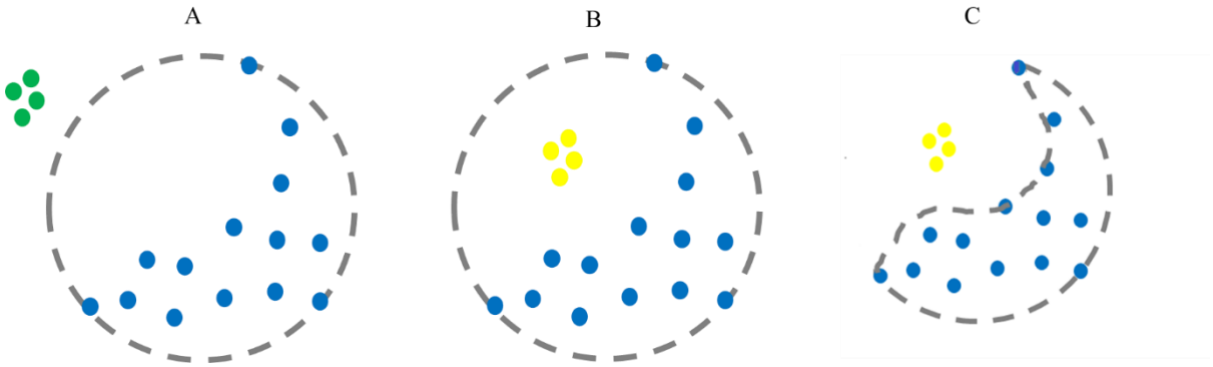

Figure 4-10: Modeling of a banana-shaped data set (blue) using non-target classes: green (A) and yellow (B, C).

Figure 4-10 demonstrates the importance of careful non-target class sample selection. In Figure 4-10A, when green samples are used as the non-target class, the spherical boundary around the banana shaped target class data (blue) is appropriate to reject these green samples. However, if yellow samples (which are closer to the target class blue samples than the non-target class green samples) are used as non-target class samples, the spherical boundary is inadequate to reject these non-target class yellow samples (Figure 4-10B). Therefore, model optimization using ideal non-target class samples is required. After model optimization, an appropriate non-linear boundary could be developed. This tighter boundary is seen in Fig 4-10C, around the target-class data, which allows the model to distinguish non-target class (yellow objects), seen outside the boundary.

The finding from this study emphasized that to develop a spectroscopic method with the help of chemometric methods, analysts should consider a pertinent test set and validation. Without utilization of appropriate samples to optimize the model, the method will not perform adequately. This proved the hypothesis mentioned in section 1.2.

Chapter 5: Application of Experimental Design to Generate Synthetic Non-Target Class Samples and the Effect of Raw Material Variability of the Target Class on the Class- Model Performance

5.1 Introduction

Development of class-modeling methods typically involves two stages. Initially, the model should be developed using a calibration data set containing representative variations of target-class samples; ideally, these samples should contain all possible sources of product variation. In Chapters 2 and 3, the effect of moisture variation on NIR and Raman spectroscopy was discussed. After an initial calibration model development, the model is then optimized using various complex test sets, an approach that is highlighted in Chapter 4. Therefore, for proper model performance, the optimization set (or test set) should include both authentic target class and non-target class samples originating from alternative classes (see Figure 4-4).

One of the challenges of model development that has not been adequately addressed in the literature is to find appropriate falsified samples to consider as an alternate class. Notably, it is crucial to test the ability of the model to recognize samples which have a highly similar composition to the target class. These falsified samples are often referred to as “high quality” falsified products [15]. It is often difficult to find these alternate classes to be used in model development.

Researchers have proposed several strategies to collect alternate classes of samples. Products manufactured by competitors can be a potential source of the non-target class sample. Rodionova et al. used competitors' products as a non-target class to optimize the decision boundary for the SIMCA-DD method and successfully improved model performance by adjusting the boundary area [186]. In the previous chapter of this dissertation, the SVDD method was optimized using legitimate analogs of the target class; this approach demonstrated good performance. However, samples from different manufacturers may not always be available, especially for brand products (which have a high risk of falsification). Another group of researchers proposed the use of samples stored in higher humidity conditions [13]. However, a high-water content may change physico-chemical structures of the samples significantly, which may not be appropriate to be considered as "high quality" falsified products.

One potential strategy to overcome this challenge is to generate synthetic samples in the lab using statistical experimental design, or design of experiments (DOE), which can be a useful statistical tool to explore the capability of spectroscopic identification of falsified products containing unique chemical compositions. DOE is useful to gain understanding about which non-target class samples are spectrally similar to the target class samples.

Synthetic samples, generated in the lab, can provide progress in resolving another challenge of method development; namely to collect a fully representative calibration set accounting for possible future variations in the target class. Using a material sparing approach, potential sources of product variation such as moisture deviations, variabilities from raw material sources, etc., can be added into the calibration model. In Chapters 3 and 4, laboratory generated

samples with significant moisture variation were used to improve model performance. Likewise, the effect of raw material variabilities can be addressed.

It is understood that the change in chemical composition or physical variations due to raw material variability may exhibit a unique inherent response with different analytical techniques. For example, NIR spectra involve a combination of absorbance and scattering properties of light and exhibit response to both chemical and physical changes in pharmaceutical products. Raman spectroscopy, on the other hand, is very sensitive to fluorescence; this is a major source of spectral variability causing interference with the Raman spectra. Fluorescence is produced by the emission of photons from low-lying excited electronic states, and often masks the vibrational shift of Raman spectra [59]. Different pharmaceutical samples exhibit fluorescence arising from various active pharmaceutical ingredients [146] , excipients [173, 174], dyes [175], capsule shells [180], etc. As anticipated, samples generated using different excipient compositions should have a different response for Raman and NIR spectroscopy. Therefore, non-target class samples will be different based on the anticipated chemical response of the analytical method used to detect falsified samples. Likewise, the impact of physical variability will also typically be different for NIR and Raman spectroscopy. This chapter will evaluate such phenomena.

The objectives of this chapter include:

1. To demonstrate the usefulness of DOE during spectroscopic model development with class-modeling techniques such as SIMCA and SVDD.

2. To use raw material variability to demonstrate the importance of creating representative training sets in development of robust models.

3. To explore the effect of DOE and raw material variability on NIR and Raman models for false-sample identification.

5.2 Materials and Methods

5.2.1 Target Class Samples

The model drug product is a 350 mg tablet containing Acetaminophen (APAP; Mallinckrodt Inc.,Raleigh, NC, USA) at 50% w/w active pharmaceutical ingredient (API), microcrystalline cellulose (MCC; Avicel PH 200, FMC Biopolymer, Mechanicsburg, PA, USA) at 15% w/w lactose (modified spray-dried; Foremost Farms USA, Rothschild, WI, USA), Starch at 15% w/w (Pharmacoat 606, Shin-Etsu Chemical Co. LTD, Tokyo, Japan), cross carmellose sodium (Pharmacoat 606, Shin-Etsu Chemical Co. LTD, Tokyo, Japan) at 4% w/w and magnesium stearate (Fisher Scientific, Waltham, MA, USA) at 0.50% w/w as excipients. Colloidal silicon dioxide, at 0.50% w/w, is used to improve APAP flow before combining with the excipients.

Materials were dispensed by weight (Data Range, model no AX504DR, Mettler Toledo, Columbus, OH) and were transferred to a bin blender. In total, 1kg of material was weighed and the nominal weights for all constituents were adjusted to the observed mass data to calculate actual concentration. Blending was performed at the Duquesne University Center for Pharmaceutical Technology with a 5.5-L bin blender (L.B. Bohle LLC, Warminster, PA, USA) with DeltaV (Emerson Process Management, Equipment & Controls, Inc., Lawrence, PA, USA) controls.

Blend Monitoring: Lab scale blends with a total mass of approximately 1 kg were created for NIR data collection. The fill ratio of these blends in the 5.5-L bin blender was less than 60%.

The top sensor was set to collect spectra when inverted to assure that each scan had powder directly in front of the sensor. At 15 rpm, the scans were collected at 4 s intervals. Pure component and granule scans were collected by filling the blender for 45 mins. Diffuse reflectance NIR spectral data was collected using the MicroNIR-W spectrometer (Viavi Inc., USA). It uses a linear variable filter (LVF) technology, with an InGaAs detector (900–1,700 nm), a pair of integrated vacuum tungsten lamps, and provides wireless capability. This spectrometer was attached to the lid of the blender and rotated with the blender while running the process. Spectra were collected with 16 co-additions averaged for a single scan with an integration time of 0.033 s. The dark and light reference scans are internal for the top sensor and were collected once daily. Different blend end point criteria were tested using moving block standard deviations. Mixtures were assumed to be homogeneous when standard deviation reached a minimum value.

5.2.2 Sample Considerations for Non-Target Class using Design of Experiment (DOE):

The goal of this effort was to create non-target class products containing identical API concentration but different excipient composition to the target class. As three diluents (lactose, starch and MCC) are the primary excipient compositions, the ratio of these three components was varied. A fully balanced, three-constituent mixture design composed of MCC, lactose and starch were used to generate the appropriate formulation (excipient ratio) for tablets (Figure 5-1). Total composition of these three excipients were kept at 45% w/w of the target formulation because the target tablet contains 45% w/w diluent. Simplex centroid design was used to change the composition of these three excipients in the formulation. Table 5-1 summarizes the design. Figure 5-1 represents different types of alternate class products [187]. The tablets were generated using

Presster (Model 5869, Norwood, MA) by a 10 mm die and flat-faced punches. The target tablet weight was 350 mg. Thirty replicate tablets per level were created to test the performance.

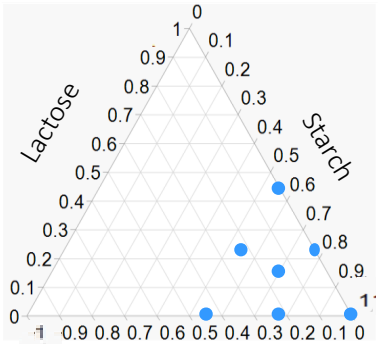

Figure 5-1: Samples generated using different excipients compositions.

Table 5-1: Seven different formulations were generated using a mixture experimental design

	APAP	Lactose	MCC 200	Starch	Croscarmellose sodium	Colloidal Sillicon Dioxide (Aerosil 200)	Magnesium Stearate
Formulation 1	50	0	0	45	4	0.5	0.5
Formulation 2	50	0	22.5	22.5	4	0.5	0.5
Formulation 3	50	22.5	0	22.5	4	0.5	0.5
Formulation 4	50	0	45	0	4	0.5	0.5
Formulation 5	50	15	15	15	4	0.5	0.5
Formulation 6	50	22.5	22.5	0	4	0.5	0.5
Formulation 7	50	45	0	0	4	0.5	0.5

Grey color row: Target class formulation which was used for calibration model development and unique batches of Formulation 5 was used as test set.

5.2.3 Target Class Samples Containing Raw Material Variabilities

Raw material variations were simulated by changing the vendors of starch (Table 5-2). The particle size of these starches was the same according to the vendors' information. Other

components of the target formulation remained unchanged. In total, two batches were prepared. These batches will be further referred as R1 and R2.

Table 5-2: Raw material variations

Design Name	Starch vendor
R 1	EM Solution
R 2	Colorcon

5.2.4 NIR Spectral Collections

NIR reflectance measurements for both sides of each tablet were acquired over the wavelength range of 925 to 1700 nm at a 6.38 nm increment averaging 5000 scans (JDSU MicroNIR). Prior to scanning, the tablets were precisely centered using the positioning iris standard on this instrument.

All spectral data were analyzed in the Matlab environment (version 8.6, MathWorks, Natick, MA) using the PLS_Toolbox (version 8.8, Eigenvector Research, Inc, Manson, WA) and software developed by the Duquesne University Center for Pharmaceutical Technology.

5.2.5 Raman Spectral Collection

Raman spectra were collected by following the protocol mentioned in section 3.3.3 .

5.2.6 Theory

5.2.7 Spectral Investigations

Spectral investigations were conducted using below mentioned methods:

1. *Spectral matching:* See Section 4.4.3
2. *Principal component analysis:* See Section 4.4.1

5.2.8 Class-Model

The chemometric model for this study was developed using SIMCA and SVDD. Details of the methods are reported in earlier section of this document.

1. *SIMCA:* See section 2.2.1.1
2. *SVDD:* See section 2.2.1.2.

5.2.9 Experimental Strategy

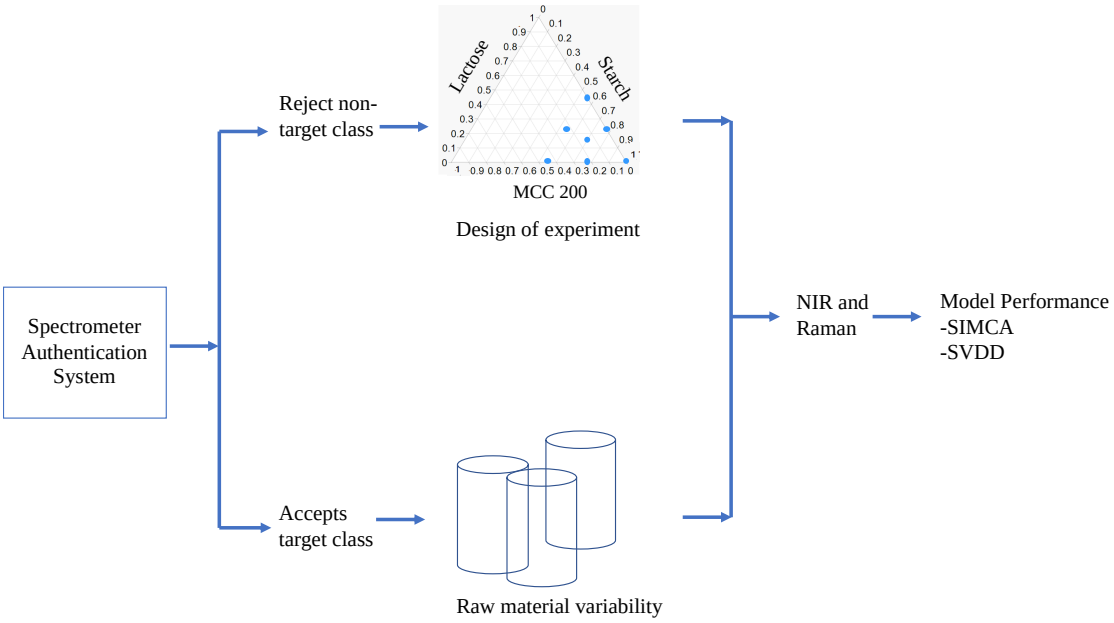

Figure 5-2: Flow chart of experimental plan.

The goal of authentication is to reject non-target class samples and accept target class samples. This study generated sample formulations using DOE to identify suitable compositions for meeting the goals of the experiment. Raw materials from two different vendors were used to generate variations in the target class samples. Both NIR and Raman spectroscopy data were collected, and multivariate models were developed (Figure 5-2).

5.3 Results

5.3.1 Near-Infrared Spectroscopy

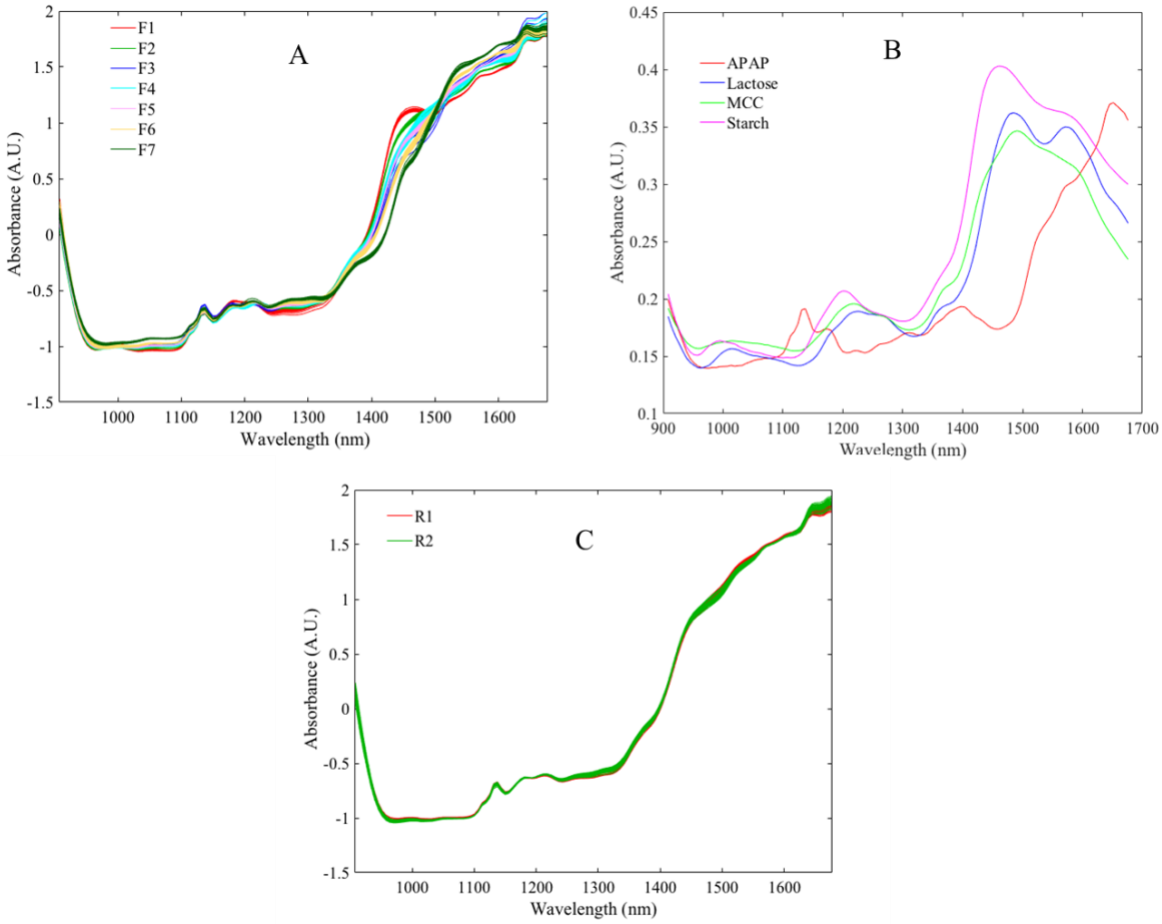

Figure 5-3: Preprocessed NIR spectra of A) samples of different formulation generated using DOE, B) pure component spectra of different components of tablets, and C) samples of target class using two different raw material vendors.

5.3.1.1 Spectral investigations

NIR spectra from the unique formulation design points are shown in Figure 5-3A**.** To understand the source of variation, the spectra of pure components are shown in Figure 5-3B. As lactose, MCC, and starch are cellulosic excipients, spectral similarity is expected for these components; dissimilarity from APAP is noticeable in Figure 5-3B. Moreover, the excipients' peaks dominate the longer wavelength regions. Therefore, spectral variation for the various DOE samples are observed primarily in the excipient dominated regions. Figure 5-3C shows the raw spectra of two different sample sets (R1 and R2, correlating with the formulations created from two unique sources of starch).

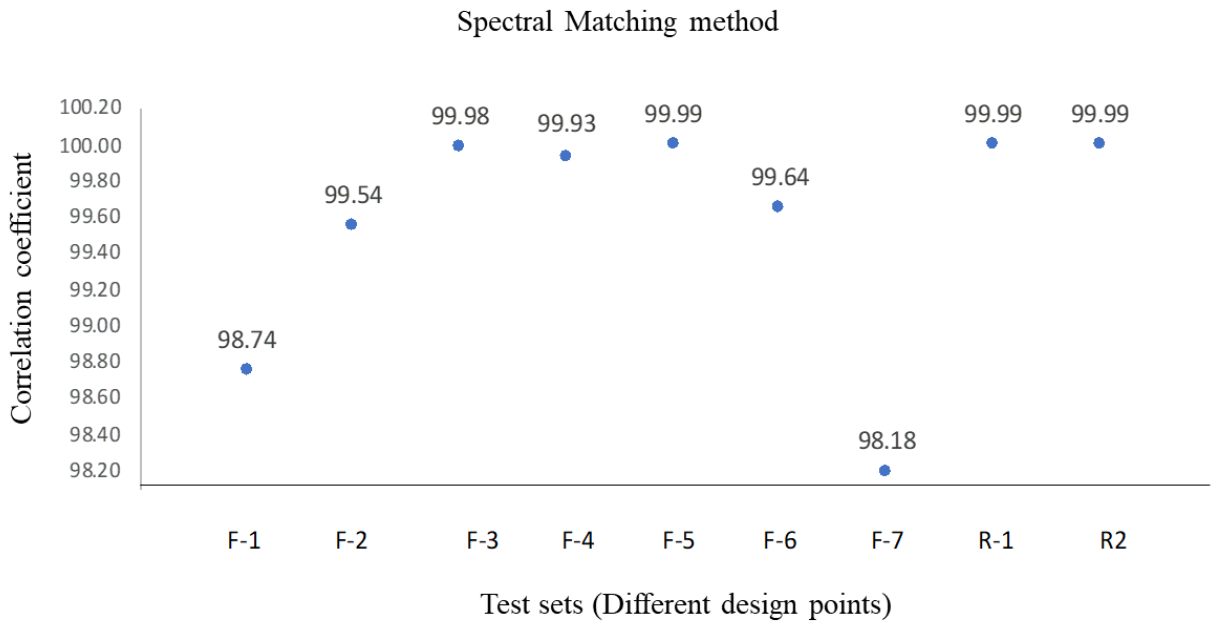

Figure 5-4: Spectral correlation of target class (F-5) with samples containing different chemical and physical variations.

Spectral correlation: Spectral correlations between the calibration set (target class (F5)) and different design points are shown in Figure 5-4. The highest correlation values were observed

for test sets of F5 (different batch), R1, and R2; because there were no chemical differences of these formulations with the target class. However, different chemical design points showed lesser correlations. Other design points, F3 and F4 showed the highest correlation values with the target class, F5.

As described in Chapter 2, spectral correlation is useful for distinguishing different classes of samples. If the spectral correlation value from testing meets a specific threshold value, then the sample is declared as the target class to verify the product empirically. Several studies have suggested using 0.95 as a threshold value to distinguish different classes of samples (see Section 1.3.3.1.2). That means if the matching threshold value is 0.95 between two sample sets, these samples are considered equivalent. However, it is obvious that the threshold may change if samples are highly similar. For example, in this study, the threshold should be higher than 99.98, as the closest non-target class samples have this correlation value.

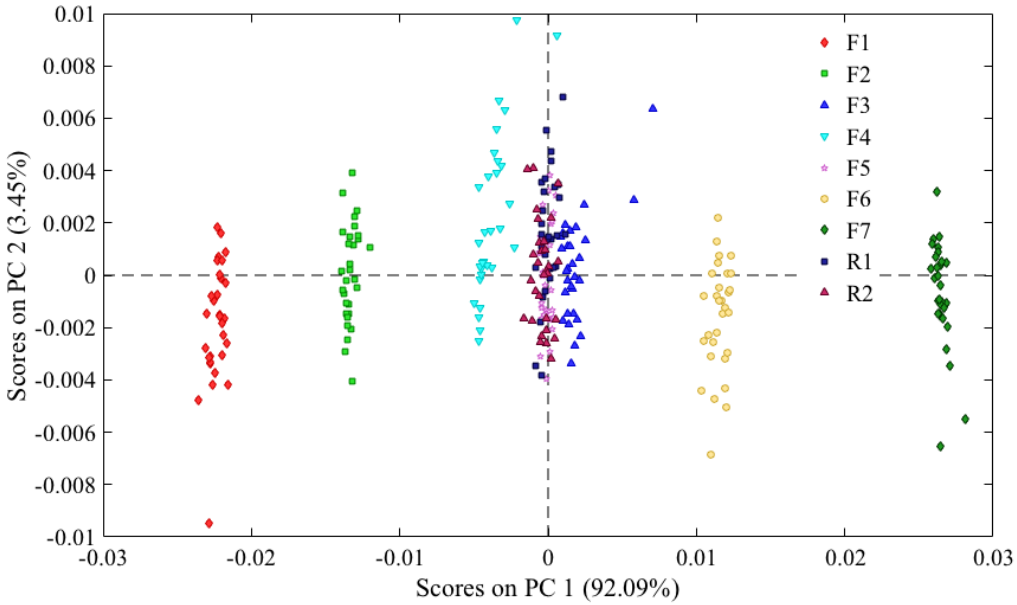

Figure 5-5: The scores plot of a combined PCA model of different design points.

Principal component analysis (PCA): Preliminary PCA was performed on the entire data set. It reveals both similarities and differences in tablets produced by various formulations of DOE and raw material variations. The PCA model with two PCs explains 95.54% of the total variance. The PCA model showed minimal variation for sample spectra derived from R1 and R2 formulations (containing different sources of starch). The preprocessing method removed the spectral deviation arising from variation in physical factors. In the scores plot (Figure 5-5), it was observed that F3 and F5 samples sets were overlapped despite the chemical variations being significantly different between these two sets.

5.3.1.2 Class-Model Performance of NIRS:

SIMCA model performance: As noted, Formulation 5 was considered to be the target class. A total of three batches of this formulation were included into the calibration model to incorporate the batch to batch variabilities. Model performance was observed using DOE and samples having raw material variations.

At first, SIMCA was developed using one PC and a 95% confidence interval threshold of Hotelling's T^2 and Q residual (Figure 5-6A). The model successfully rejected F1, F2, F4, F6, and F7, but failed to reject F3. Hotelling's T^2 and Q residual plots explained the failure of rejecting F3. Low Q residual values showed that this formulation overlapped with the calibration sample set, whereas other formulation design points were located far from the calibration set. The model developed using PC1 successfully accepted test sets R1 and R2, except for two samples from R1. Hotelling's T^2 and Q residual plots showed that genuine samples manufactured using different vendors resided inside the target-class boundary (Figure 5-6(A-B)). After increasing the

confidence interval to 99%, the model accepted only one of these samples (Figure 5-6 (C-D)). However, with the new boundary, the model also started to accept the F4 design point, as F4 is the second nearest design point after F3.

To reject all non-target class design points, a SIMCA model with one PC was not sufficient, even though it accepted samples containing raw material variability. Next, two PCs (explaining 95.54% of total variance) were used to develop a SIMCA model. After adding PC2, the model became more specific and rejected all formulations. Figure 5-7(A-B) revealed that F3 now had higher Hotelling's T^2 and Q residuals compared to the previous PCA model. However, after adding two PCs, the model started to reject samples with raw material variabilities, which were four R1 and seven R2 samples. Nevertheless, increasing the confidence interval from 95% to 99% improved the sensitivity of the model (Figure 5-7 (C-D)). The SIMCA model with 99% CI accepted all samples with raw material variability.

Using cross-validation to select the number of PCs can be another option. Here, cross-validation suggested three PCs for the SIMCA model. However, a SIMCA model developed using three PCs is unnecessary, as the model already rejected all formulations using fewer PCs. Therefore, a model with two PCs showed the best performance (Table 5-3).

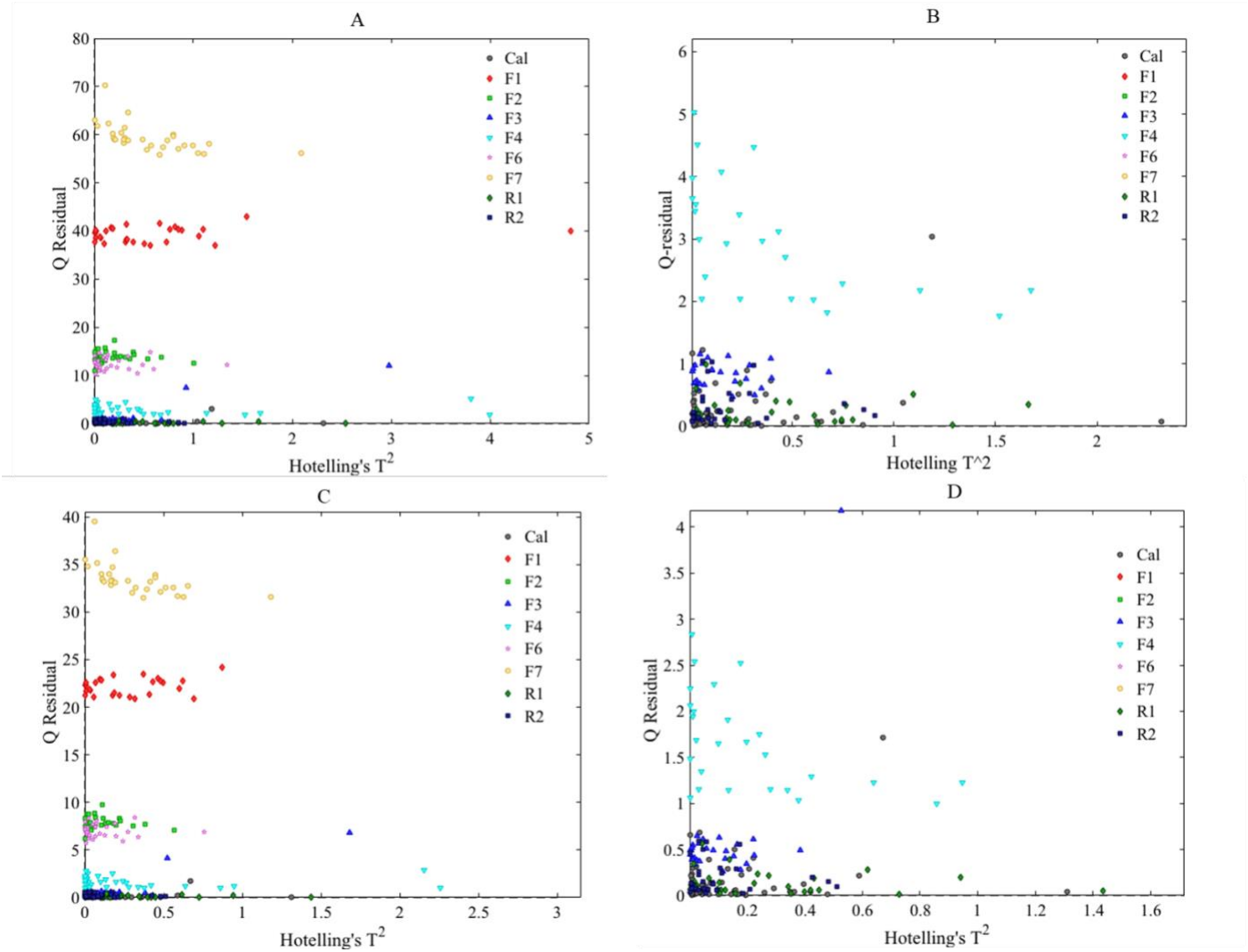

Figure 5-6: Model diagnostics plots of SIMCA model, which was developed using the first PC, (A) Threshold was developed using 95% CI. B) Magnified version of plot A, C) Threshold was developed using 99% CI, D) Magnified version of plot C.

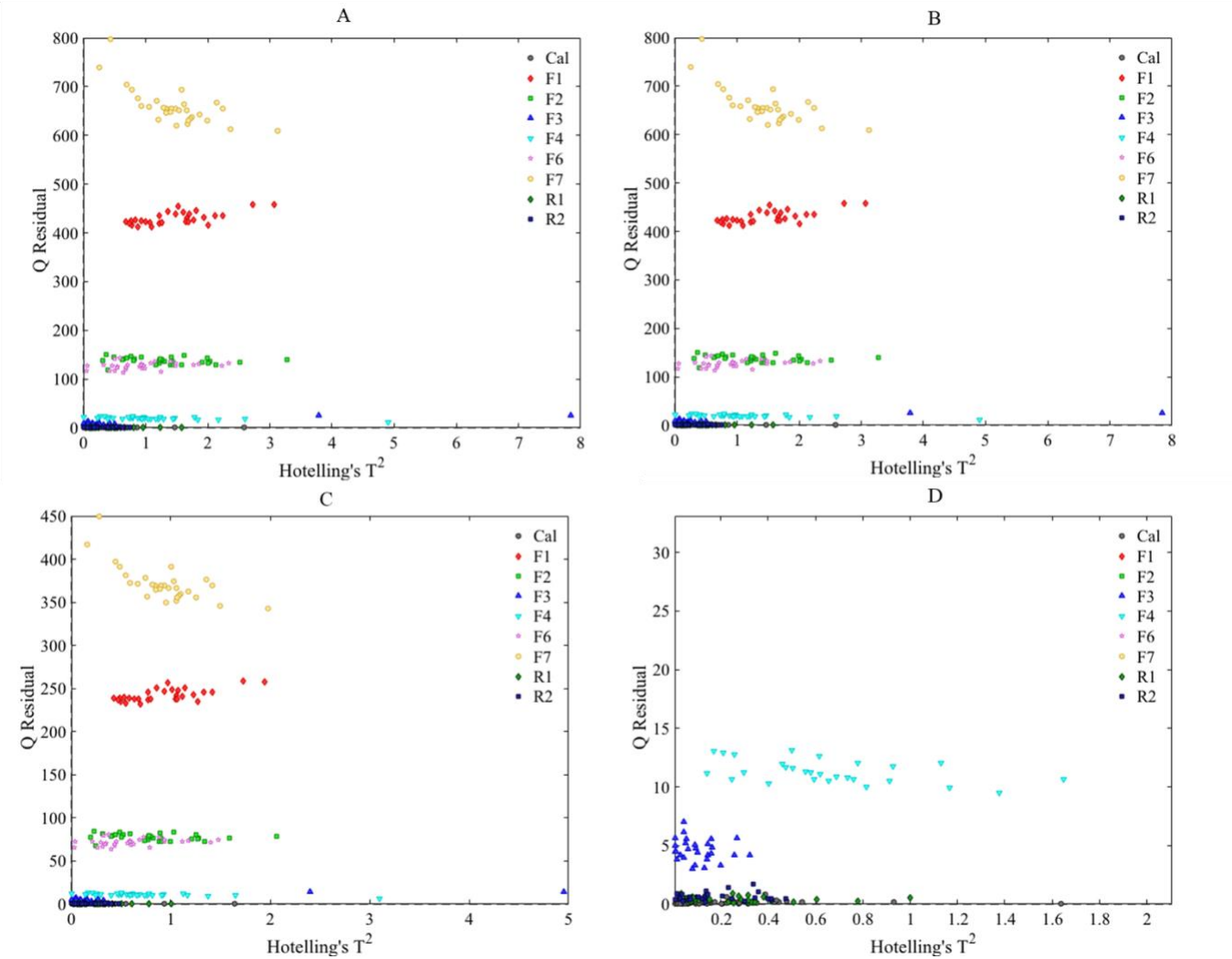

Figure 5-7: Model diagnostics plots of SIMCA model, which was developed using first two PCs, (A) Threshold was developed using 95% CI, (B) Magnified version of plot A, (C)Threshold was developed using 99% CI, D) Magnified version of plot C.

Table 5-3: Performance of SIMCA model using NIRS

Different Models with predefined threshold	Calibration approaches					
	1 PC			2 PCs		
	Sensitivity	Specificity	Average	Sensitivity	Specificity	Average
SIMCA (T^2& Q=0.95)	0.96	0.84	0.9	0.81	1	0.905
SIMCA (T^2 & Q =0.99)	0.98	0.78	0.88	0.97	1	0.985

SVDD model performance: In this study, the SVDD algorithm was applied to the preprocessed spectral data, including Savitzkay-Golay derivative and normalization. Here, two D values, 0.05 and 0.01, were considered. A series of σ values were applied with incremental steps of 0.1. The best performance was obtained from a σ value of 0.9. The performance of the different approaches is summarized in Table 5-4. Both threshold values of D rejected all of the non-target class samples. Support vectors were visualized in Figure 5-8. Formulation 4 was plotted to show the similarity with target class samples.

Table 5-4: Performance of SVDD model using NIRS.

	σ =0.9			
Different models with predefined threshold	Sensitivity	Specificity	Average	No. of SVs
Spectral SVDD (D=0.01)	0.89	1	0.945	6
Spectral SVDD (D=0.05)	0.867	1	0.9335	3

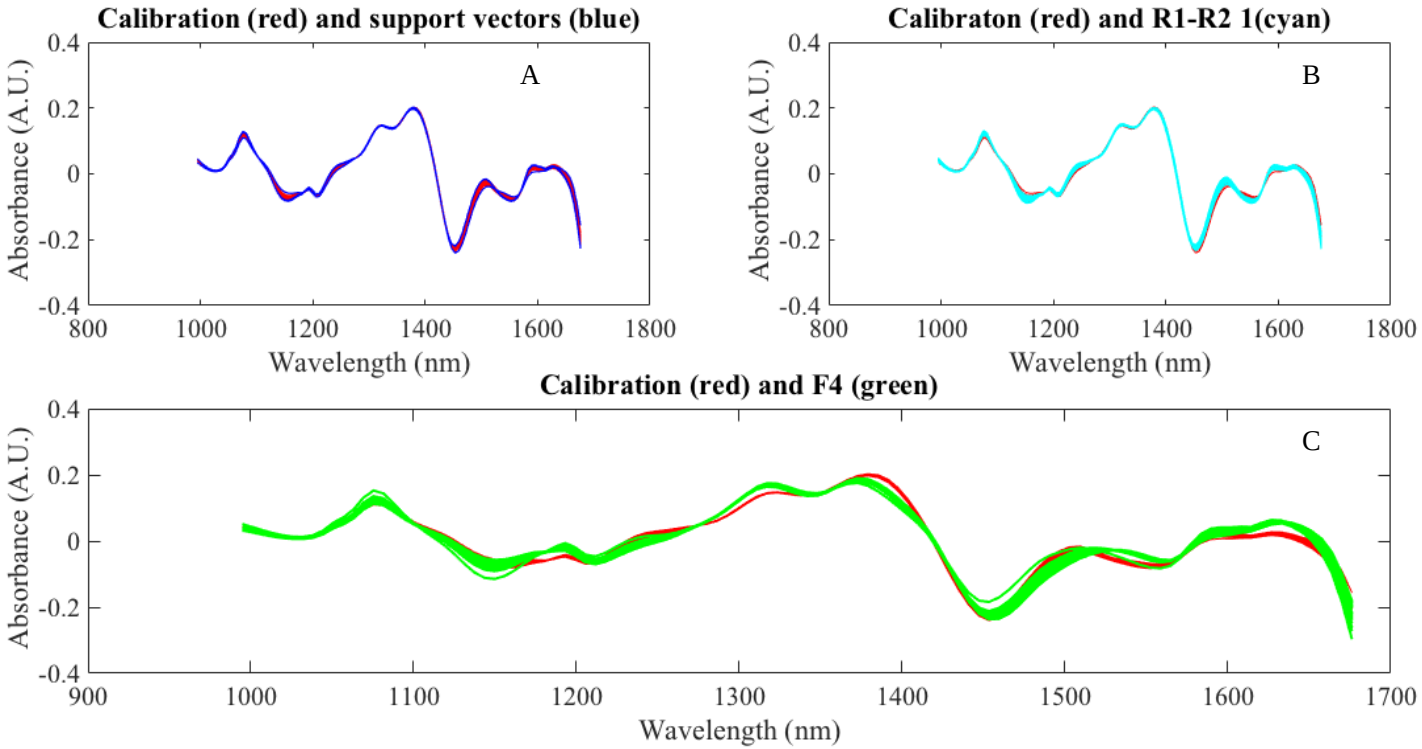

Figure 5-8: A) Depiction of selected support vectors of the calibration set where the blue spectra are support vectors and red spectra are calibration samples B) Calibration set (red), R1 and R2 sample sets (cyan). C) Calibration set (red) and F4 design point (green)

5.4 Raman Spectroscopic Methods

5.4.1 Spectral Investigations

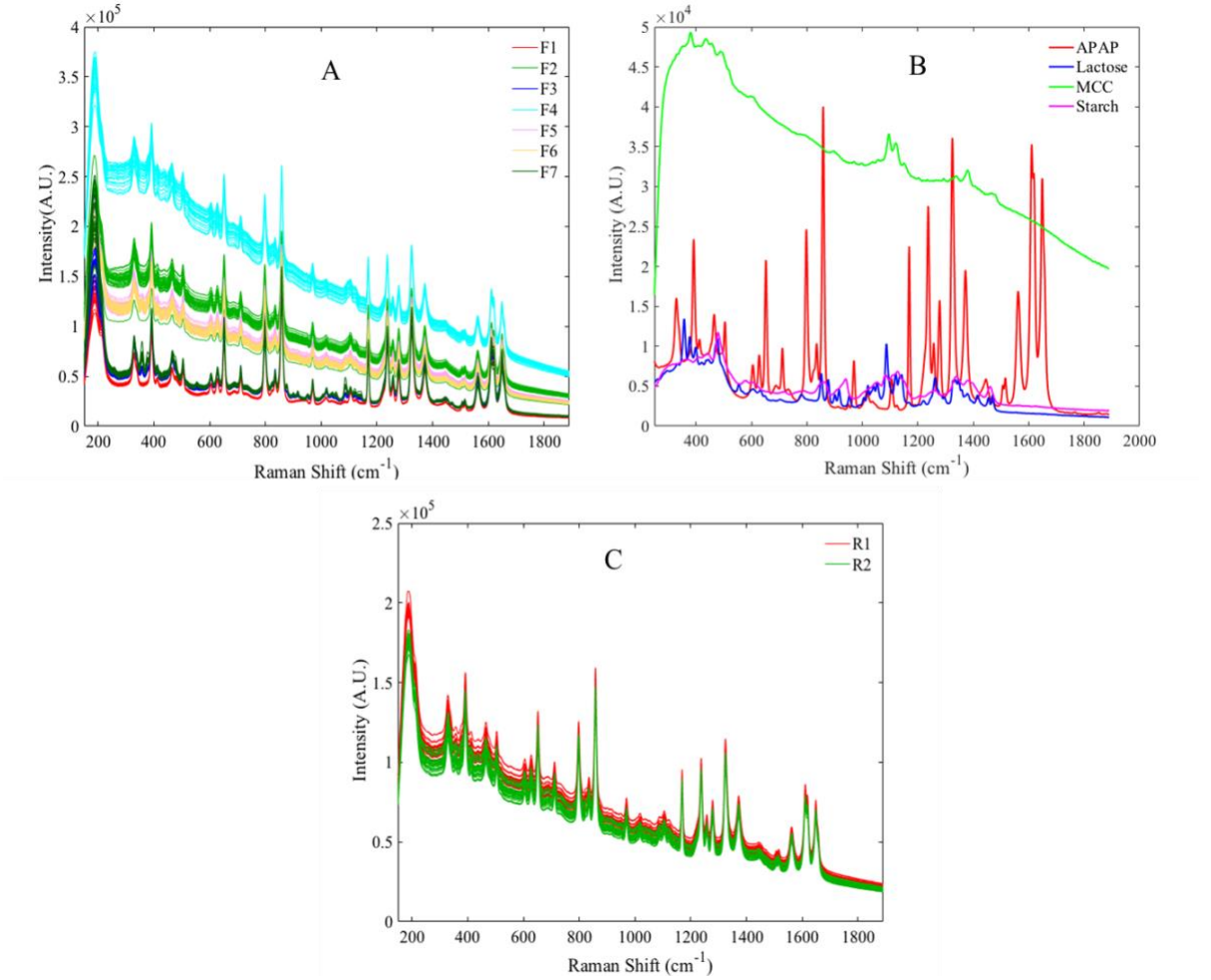

Figure 5-9: A) Spectra of different design points of pharmaceutical formulations, B) Raman spectra of pure components, (C) Spectra of two batches of samples.

In this experiment, the API showed a Raman signature in tested samples. Figure 5-9 shows that Raman spectra of different formulation design points were dominated by the API (acetaminophen or APAP) because the aromatic ring of APAP is a strong Raman scatterer compared to the polar excipients. Therefore, Raman is very useful to identify the API, in this case,

since it exhibits several characteristic bands that are directly correlated with the molecular structure of the substance of interest.

The other dominating spectral source is the fluorescence background of MCC. While this formulation has a high drug load, the APAP is detectable. For products with a low drug load, the Raman spectra of the API may be masked by the fluorescence of the excipients.

Spectral correlation: The spectral correlation value of F5 is displayed in Figure 5-10. It was observed that F2 and F6 showed the highest correlation with the target F5 formulation. Due to the strong fluorescence signal, MCC was the main reason for this similarity. In Figure 5-10, F6 showed the nearest correlation value. The second nearest formulation was F2.

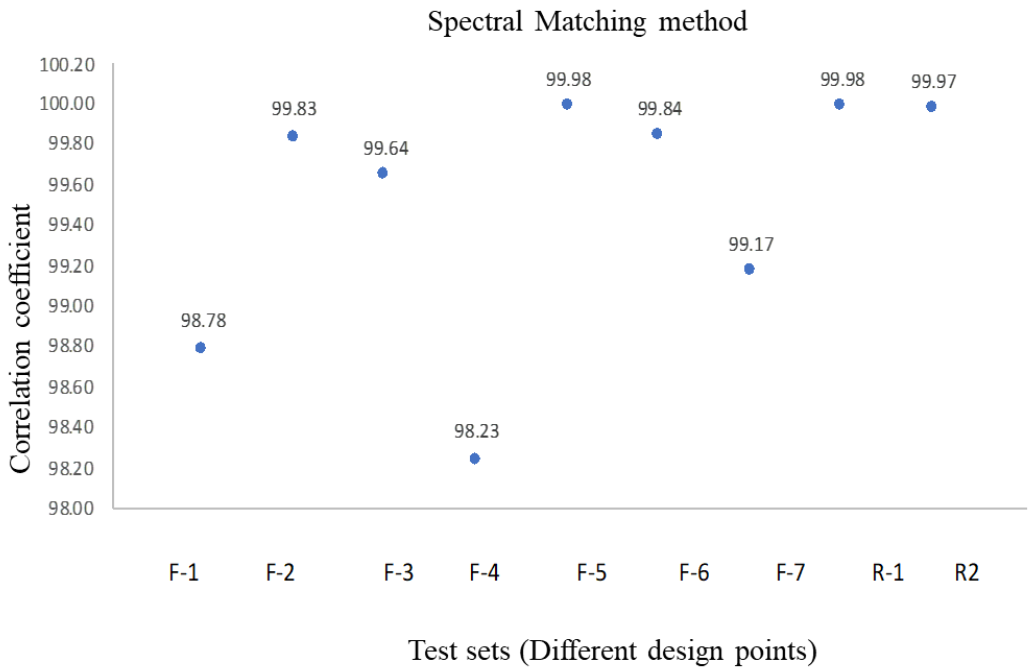

Figure 5-10: Spectral correlation of target class (F-5) with different design points.

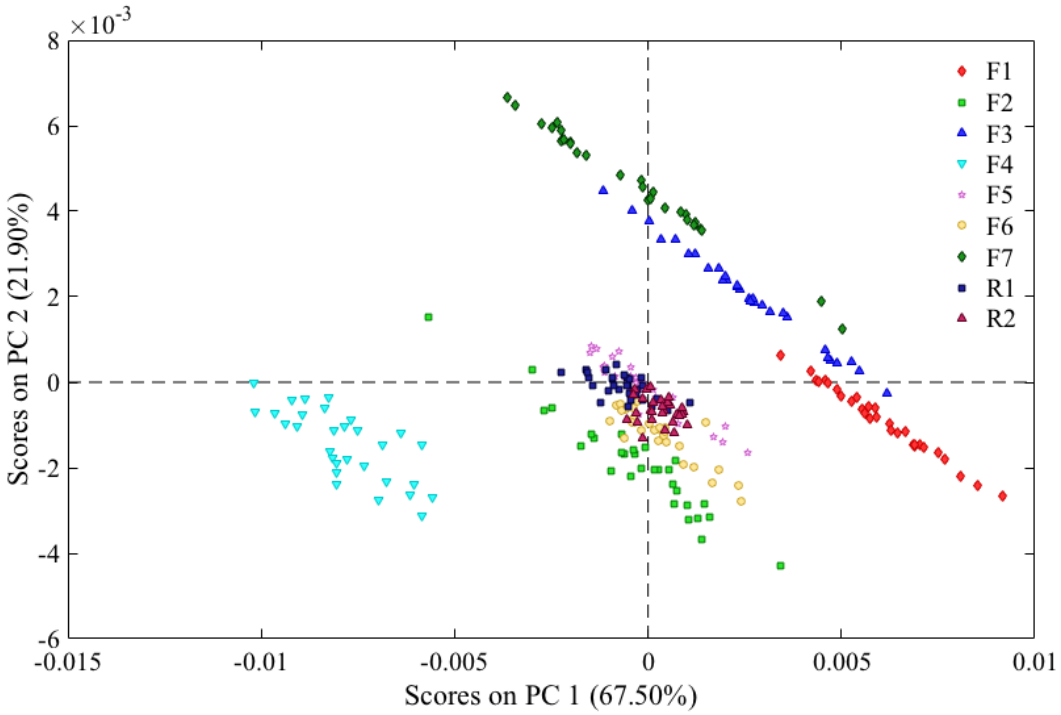

Figure 5-11: The scores plot of a PCA model which was developed combining all formulations.

Principal component analysis (PCA): The total spectral range was used to analyze the data. Data were preprocessed using SNV and mean-centering. The PCA plot (Figure 5-11) shows that the first two PCs explained 89.4% of the total variance. Similar to the spectral correlation value, F2 and F6 resided near the target formulation, F5. From Figure 5-9, it is observed that F2 and F6 have similar spectral features to F5 (target class, F5) due to the presence of fluorescence background. Samples containing raw material variabilities (R1 and R2) overlapped with F5. This indicates that Raman was insensitive to the raw material variability in the present study.

5.4.2 Class-Model Performance

SIMCA: Similar to the NIR model, Formulation 5 was used as the target class. Two batches of Formulation 5 were included in to the calibration model. Sensitivity and specificity were

observed using samples containing raw material variabilities (R1 and R2) and DOE samples (F1, F2, F3, F4, F6 and F7).

Using Raman spectra, the first SIMCA model was generated from one PC and a 95% confidence interval threshold of Hotelling's T^2 and Q residual. In this case, the model appropriately rejected all non-target class formulation design points, except 7 samples from F6. Hotelling's T^2 and Q residual plots explained the failure of rejecting these samples. As Formulation 6 had low Q residual values, these samples resided inside the boundary (Figure 5-12 (A-B)).

While F6 contained MCC which had similar fluorescence background compared to F5 (target class samples), it was observed that the model developed using PC1 successfully accepted the test sets R1 and R2, except 11 samples. After increasing the confidence interval to 99%, the model accepted nine of these eleven samples, improving the sensitivity of the model (Figure 5-12 (C-D)). However, increasing this boundary also influenced the model to begin accepting more samples from the F6 design point, meaning specificity was decreased.

Next, a SIMCA model using two PCs (which explains 89.4% of total variances) was used to develop the SIMCA model. After adding PC2, the model became more specific and rejected all formulations (Figure 5-13 (A-B)). However, after adding two PCs, the model rejected more samples of R1 and R2; as a result, sensitivity decreased significantly. Increasing the confidence interval from 95% to 99% improved the sensitivity of the model. However, the SIMCA model with 99% CI also started to accept non-target class samples of F6 (Figure 5-13 (C-D)).

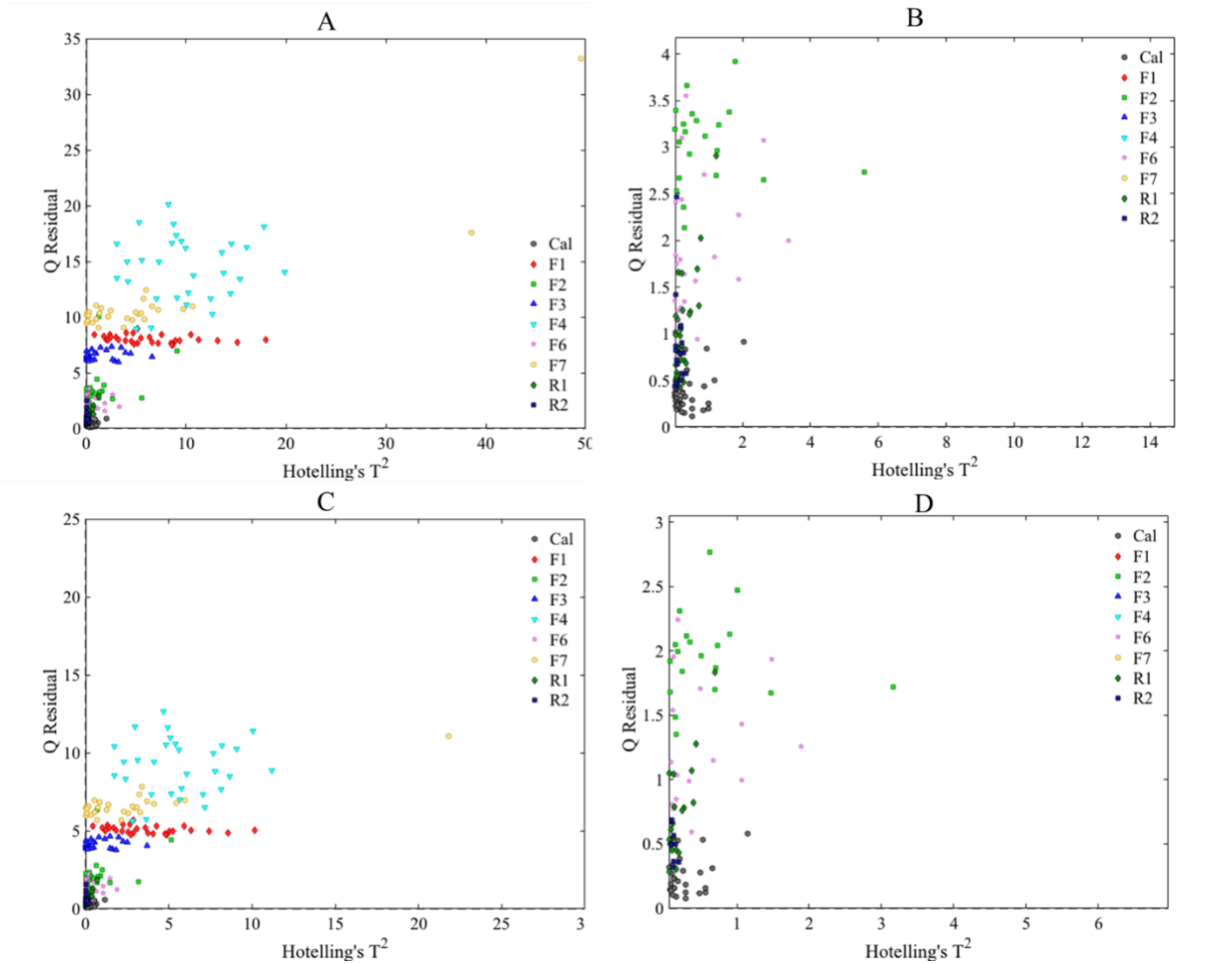

Figure 5-12: Diagnostics plots of SIMCA model, developed using the first PC, (A) Threshold was developed using a 95% CI, (B) Magnified version of plot A, C) Threshold was developed using 99% CI, D) Magnified version of plot D.

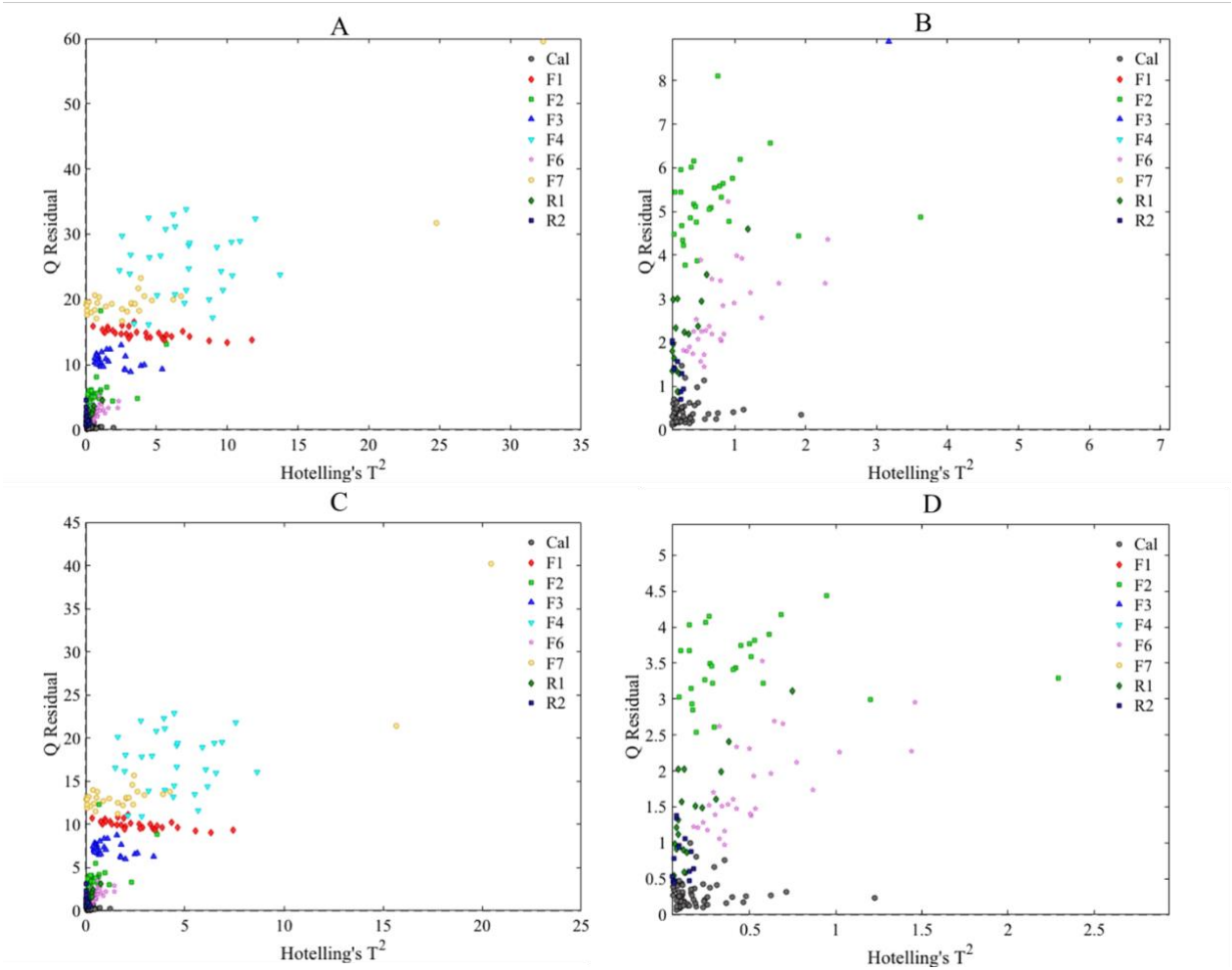

Figure 5-13: Model diagnostics plots of SIMCA model which was developed using first two PCs, (A) Threshold was developed using 95% CI, (B) Magnified version of plot A, C) Threshold was developed using 99% CI, D) Magnified version of plot C.

Raman showed satisfactory performance with the use of one PC. This indicates that Raman spectroscopy does not rely on an extra direction of variations to identify non-target class samples compared to the NIRS. Therefore, Raman model was less complex, and sharp spectral features of Raman may help to identify different non-target class samples. But, this observation may vary depending on the API and excipient signals of different formulations.

Table 5-5: Performance of SIMCA model using Raman spectroscopy.

Different Models with predefined threshold	**Calibration Approaches**					
	1 PC			2 PC		
	Sensitivity	Specificity	Average	Sensitivity	Specificity	Average
SIMCA (T^2 & Q=0.95)	0.972	0.84	0.906	0.4	1	0.7
SIMCA (T^2 & Q =0.99)	0.961	0.905	0.933	0.6	0.95	0.775

SVDD: In this study, the SVDD algorithm was applied to the preprocessed spectral data. A Savitzky-Golay derivative and normalization was applied to the data. Here, two D values, 0.05 and 0.01, were considered. A series of σ values were applied with incremental steps of 0.1.

Performance of the different approaches is described in Table 5-6. Both threshold values of D rejected all non-target class samples. Support vectors were visualized in Figure 5-14A. Raw material did not show variations with the target class samples (Figure 5-14B). Therefore, model was successfully accepted these samples. Formulation 6 was plotted to show the similarity with target class samples (Figure 5-14C). There are slight variations observed between target class and F6 in the lower wavelength regions (around 200 cm^{-1}), which enabled the rejection of this formulation. Therefore, the SVDD model performance was comparable to the SIMCA model.

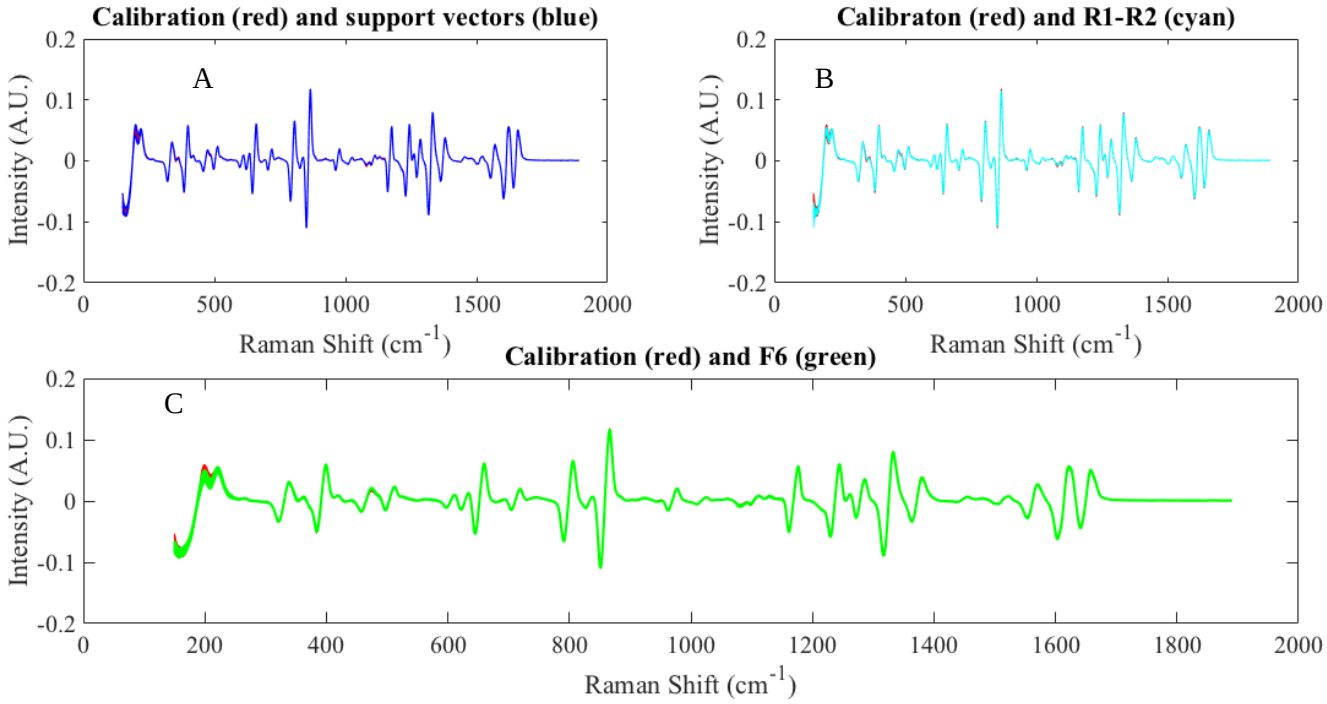

Figure 5-14: A) Depiction of selected support vectors of the calibration set where the blue spectra are support vectors and red spectra are calibration samples, B) Calibration set (red), R1 and R2 samples (cyan), C) Calibration set (red) and F6 design point (green).

Table 5-6: Performance of SVDD model using Raman spectroscopy.

	σ =0.25			
Different Models with predefined threshold	Sensitivity	Specificity	Average	SV
Spectral SVDD (D=0.01)	0.9333	0.9167	0.925	3
Spectral SVDD (D=0.05)	0.8667	0.9778	0.922	4

5.5 Discussion and Conclusion

The proposed DOE approach allows an analyst to test the developed method against various non-target class samples. Given the flexibility of designing samples, analysts should be able to create samples containing the identical API but different excipient composition, as this may be the most challenging condition to detect. Rationally designed samples, defined by DOE, are helpful for identifying which non-target class samples are spectrally similar to the target class samples, and which samples pose a risk in terms of potential method failure.

In this study, CM model using NIRS struggled to separate F3 as non-target class samples, whereas CM model using Raman failed to separate F6 as non-target class samples. NIR spectroscopy is sensitive to the C-OH bond, causing starch, lactose, and MCC to have similar spectral features. F3 showed the highest similarity to F5, and therefore, F3 has a higher risk of increasing the false positives (reduced model specificity). However, for Raman spectroscopy, F6 was a challenging formulation. Both F2 and F6 contained a higher amount of MCC, similar to the target class, F5. Because F6 had lactose in its formulation, it had a more significant peak intensity than the starch. This caused F6 to be the closest non-target class sample. Therefore, using F6 formulation was critical for the development of a successful model.

Moreover, these lab generated non-target class samples have similar solid fraction, size, shape, etc., compared to the target class. Therefore, physical factors demonstrated minimum effect on the spectra in this case.

Although the implementation of DOE requires more samples, this approach offers significant benefit in that it will help to minimize the risk of model failure. Using small scale lab-based samples reduces the burden of sample preparation and makes the model development more efficient.

In this study, changing excipient vendors did not have a significant impact on model performance. However, in general, switching to a different vendor can result in several physico-chemical changes, including moisture variation, particle size variability, etc.

Another source of variation, lot-to-lot variability of excipients, can also be a factor to be modeled. It is expected that the inter-manufacturer variabilities will be more significant than the batch to batch variability of an individual manufacturer (intra-manufacturer variability). However, it is difficult to preemptively identify all sources of variability that might be introduced by different manufacturers during the pharmaceutical life-cycle. The experimental approach of this study provided an example of the effect of manufacturer and lot-to-lot variabilities on sample spectra and model performance.

Having appropriate non-target class samples is critical for model development. These non-target class samples challenged both SIMCA and SVDD. Typically, a model developed using more PCs in the SIMCA model can separate challenging samples which resided near to the target class. However, using samples containing more PCs unnecessarily separates samples containing raw

material variability from different vendors. Nevertheless, the model that is developed using a fewer number of PCs may appropriately accept the samples with variability in raw material supplier. Careful model development will prevent unnecessary rejection of target class samples (false negatives) or incorrect authentication of falsified products (false positives). This model optimization becomes logical in the presence of statistically representative non-target class samples and target class samples containing foreseeable variations in the model.

Chapter 6: Onsite Implementation of Portable Spectrometers to Analyze Commercially Available Pharmaceutical Products

6.1 Introduction

This chapter discusses the use of portable spectrometers to analyze pharmaceutical products in health care settings. Researchers have been using two portable spectrometers to collect data in two different pharmacies over a span of a few months. Theses pharmacies are located in the city of Pittsburgh. Various brand and generic products were selected based on a previous history of falsification. Results from the testing of two products are reported here.

To accomplish this project, a comprehensive data collection protocol was developed. This protocol was used during the feasibility studies to verify the spectral collection methodology and for the collection of data to improve the understanding of factors that influence the product spectra. The effect of sample positioning, lot-to-lot variability, variations from manufacturing site change, and the impact of wavelength range on the performance of two different spectrometers are reported in this chapter.

Different multivariate methods, including, principal component analysis (PCA), Hotelling's T^2 and Q residual statistics were used to develop understanding of the source of spectral variations. Finally, the collected data were used to develop and validate qualitative authentication methods using chemometric models. The model will be included in a cloud-based

data management system to implement a real-time authentication technique. This study will provide direction for the detection of falsified medicines in different locations worldwide.

The objectives of this chapter include:

(1) Evaluate the effect of sample positioning.

(2) Evaluate the possible sources of spectral variation while collecting data from commercial samples.

(3) Compare the effect of spectral wavelength ranges on method performance using two different spectrometers.

(4) Develop NIRS models for the analysis of tablet authenticity.

6.2 Materials and Methods

6.2.1 NIR Instrumentation

Currently, a variety of portable NIR spectrometers are available from different manufacturers. Whereas each technology has its own strengths and weaknesses, micro electro-mechanical systems (MEMS) technology was chosen for this work because of the advantages of fast data acquisition rate, affordability, and lack of moving parts.

The NIR ONE Sensor (Spectral Engine, VTT, Finland) uses the patented Micro Electro Mechanical System (MEMS) Fabry-Perot Interferometer, which is a fully programmable optical

filter with a single-element InGaAs detector. This compact spectrometer has a window made by quartz for a sample surface system.

Two spectral ranges were utilized with two different devices (Figure 6-1).

1) Diffuse reflection spectra were recorded in the wavelength range of 1550–1950 nm. This will be mentioned as **SWL-NIR** (Short Wavelength NIR) in the rest of the chapter.
2) Diffuse reflection spectra were recorded in the wavelength range of 2000–2450 nm. This will be mentioned as **LWL-NIR** (Long Wavelength NIR) in the rest of the chapter.

The spectrometers were connected to a laptop through a USB communication cable and controlled using sensor control software developed by Spectral Engines Oy.

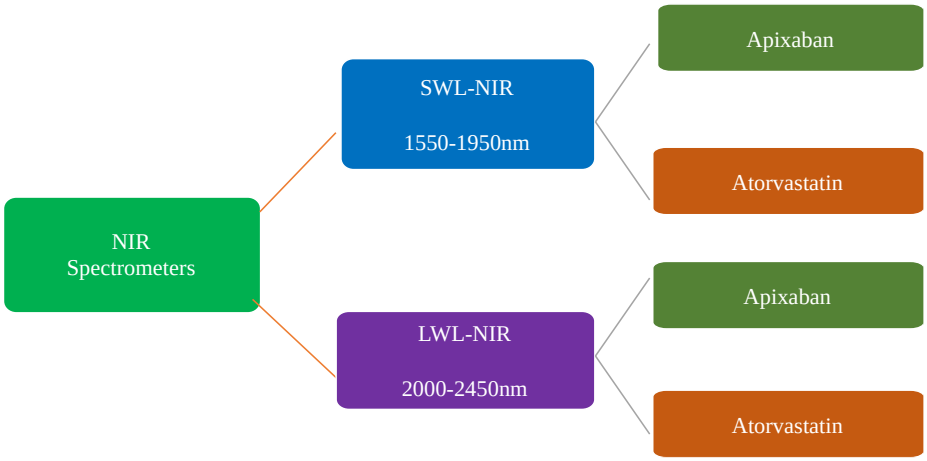

Figure 6-1: Two NIR spectrometers were used to analyze two products, including apixaban and atorvastatin.

6.2.2 Sample Positioning Study

Sample orientation is critical; the instrument has a detector (red circles in Figure 6-2) at the center of the sampling window and two lamps, one located on each side of the detector (yellow circles in Figure 6-2). The spectrometers were marked using a straight line to facilitate sample positioning. The marking is simulated in Figure 6-2. This line was drawn two ways:

A) Passes through the detector but perpendicular to the lamps (Figure 6-2A) and

B) Passes through the detector and lamps (Figure 6-2B).

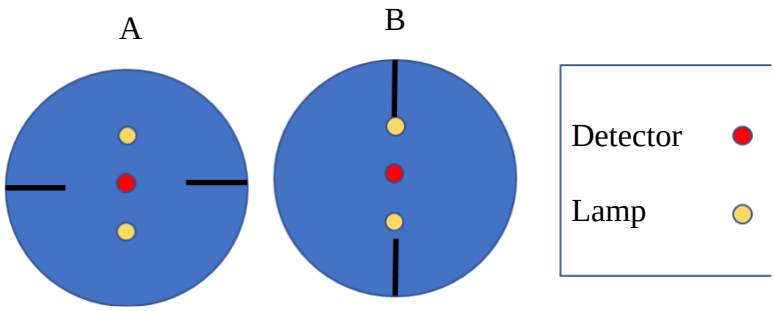

Figure 6-2: Two orientations of the sample based on the drawn line which is, A) Passes through the detector but perpendicular to the lamps, B) Passes through the detector and lamps.

An oval shaped tablet was scanned six times with repositioning. Standard deviation was calculated for these repeated measurements for both the SWL-NIR and LWL-NIR data.

6.2.3 Sample Collection in Pharmacy

Two commercial tablets: apixaban (Eliquis, by Bristol-Myers Squibb) and atorvastatin (Atorvastatin, by Apotex) were scanned at the pharmacies in Pittsburgh. A transportable station was set up containing portable spectrometers and reference standards (Figure 6-3A-B)). Tablets were collected from bottles stored in the pharmacy. From each bottle, 30 tablets were collected and both sides of each tablet were scanned. All tablets were replaced in the bottle after completing the analysis.

All of the calculations were performed using Matlab 8.6 (The Mathworks Inc, Natick, MA), along with the PLS_Toolbox 8.8 (Eigenvector Research Inc, Wenatchee, WA) and other analysis tools written at the Duquesne University Center for Pharmaceutical Technology for this study.

A B

Figure 6-3: Portable stations, A) A briefcase sized transportable system to carry spectrometers and reference standards, B) Spectrometers and laptop controller in use at a pharmacy.

6.2.3.1 Apixaban: Considered Samples

The label claim of apixaban was 5 mg. A total of nine lots of product were analyzed. Among these lots, seven were manufactured in Switzerland and two were manufactured in the USA. Table 6-1 summarizes the lot number, manufacturing site and expected dose of the analyzed tablets.

Table 6-1: Detail of apixaban tablets

Molecule	Product Name and Dose	Lot No	Manufactured Location*
Apixaban	ELIQUIS 5MG	AAY3155	Switzerland
Apixaban	ELIQUIS 5MG	AAY4017	Switzerland
Apixaban	ELIQUIS 5MG	AAK9028	USA
Apixaban	ELIQUIS 5MG	AAT0949	USA
Apixaban	ELIQUIS 5MG	AA22725	Switzerland
Apixaban	ELIQUIS 5MG	AA28472	Switzerland
Apixaban	ELIQUIS 5MG	AA28448	Switzerland
Apixaban	ELIQUIS 5MG	KK2981	Switzerland
Apixaban	ELIQUIS 5MG	KL2418	Switzerland

*It was mentioned in the label that the respective products were from USA and Switzerland.

6.2.3.2 Atorvastatin: Considered Samples

The label claim for atorvastatin tablets tested in the project was 40 mg. A total of fourteen lots of products were scanned. All of these lots were manufactured in Canada. Table 6-2 summarizes the lot number, manufacturing site and expected dose of the analyzed tablets.

Table 6-2: Details of the atorvastatin tablet

Molecule	Product Name and Dose	Lot No	Manufactured Location
Atorvastatin	ATORVASTATIN 40MG	NW6364	Canada
Atorvastatin	ATORVASTATIN 40MG	PJ2815	Canada
Atorvastatin	ATORVASTATIN 40MG	PJ9375	Canada
Atorvastatin	ATORVASTATIN 40MG	NK2915	Canada
Atorvastatin	ATORVASTATIN 40MG	NT7727	Canada
Atorvastatin	ATORVASTATIN 40MG	NT7700	Canada
Atorvastatin	ATORVASTATIN 40MG	3088695	Canada
Atorvastatin	ATORVASTATIN 40MG	3070915	Canada
Atorvastatin	ATORVASTATIN 40MG	PC4481	Canada
Atorvastatin	ATORVASTATIN 40MG	C805309	Canada
Atorvastatin	ATORVASTATIN 40MG	18230211	Canada
Atorvastatin	ATORVASTATIN 40MG	PK0500	Canada
Atorvastatin	ATORVASTATIN 40MG	PT5469	Canada
Atorvastatin	ATORVASTATIN 40MG	PK1767	Canada

6.3 Results and Discussion

6.3.1 Sample Repositioning Study

Spectral variation was observed among different rescans of oval-shaped tablets in both “A” and “B” orientations, whereas round-shaped tablets showed minimum variation, with repositioning as expected. Therefore, the spectral behavior of oval shaped tablets is reported. The bulk of the spectral variations, due to repositioning, took the form of a change in spectral baseline.

For the oval-shaped tablet, the average standard deviation of SWL-NIR absorbance intensity for the orientation “B” was 0.15, whereas for the orientation “A”, it was 0.05. For the LWL-NIR spectrometer, average standard deviations were 0.07 and 0.02 for “B” and “A” orientations respectively. From this study, it was found that orientation “A” produces higher spectral variations

compared to the orientation “B” for oval-shaped tablets. This was true for both SWL-NIR and LWL-NIR spectrometers. Therefore, orientation B was used to analyze all oval shaped tablets in the further research. However, from the data, it was also observed that the SWL-NIR spectrometer was more sensitive for repositioning of tablets relative to the LWL-NIR spectrometer. A number of data preprocessing techniques such as the standard normal variate (SNV) transformation, multiplicative scatter correction (MSC), Savitzky–Golay (SG), etc., can be applied to mitigate this variation.

Exploratory sample analysis

6.3.1.1 Apixaban

Spectral behavior of various batches of apixaban tablets were observed for SWL-NIR and LWL-NIR spectrometers in Figure 6-4A and Figure 6-5A respectively. These spectra were SNV and second derivative Savitzky–Golay treated. From preprocessed spectra, significant spectral variances was observed among different batches. Primarily, the two batches prepared in the USA (blue and green spectra) were different from the batches prepared in Switzerland. Spectral differences were pronounced in SWL-NIR spectra compared to the LWL-NIR spectra. These variations may evolve from different factors such as raw material variabilities, manufacturing variabilities, moisture variabilities, etc. However, a detailed history of sample preparation or manufacturing conditions was not available.

Based on the spectral features of the pure component spectra, it is assumed that the site-to-site variation is likely due to some difference in the excipients (Figure 6-4B, Figure 6-5B). The spectral features were varied around ~1670 nm (Figure 6-4A). Excipients such as lactose

anhydrous, microcrystalline cellulose and sodium lauryl sulfate (SLS) all exhibit peaks in that same region. It is assumed that the contribution from these three components may change between the manufacturing sites. Further analysis might reveal the true source(s) of variation.

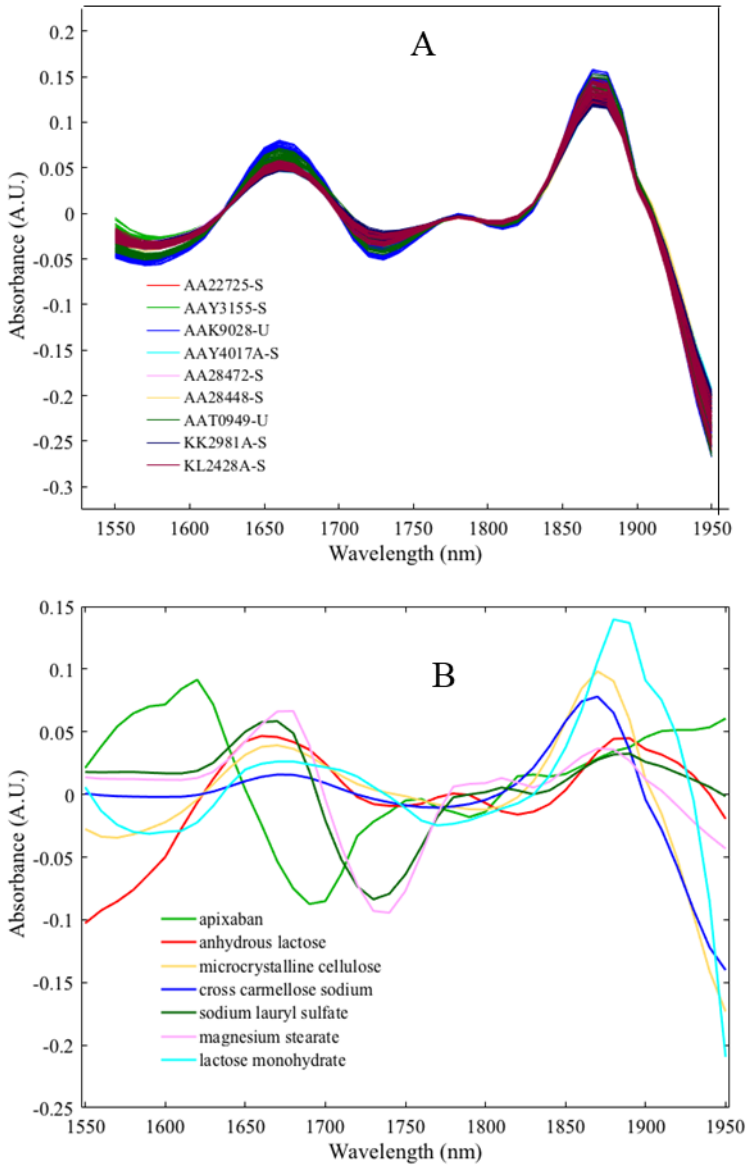

Figure 6-4: A) Preprocessed SWL-NIR spectra of different batches of apixaban, B) SWL-NIR spectra of major components of apixaban tablets.

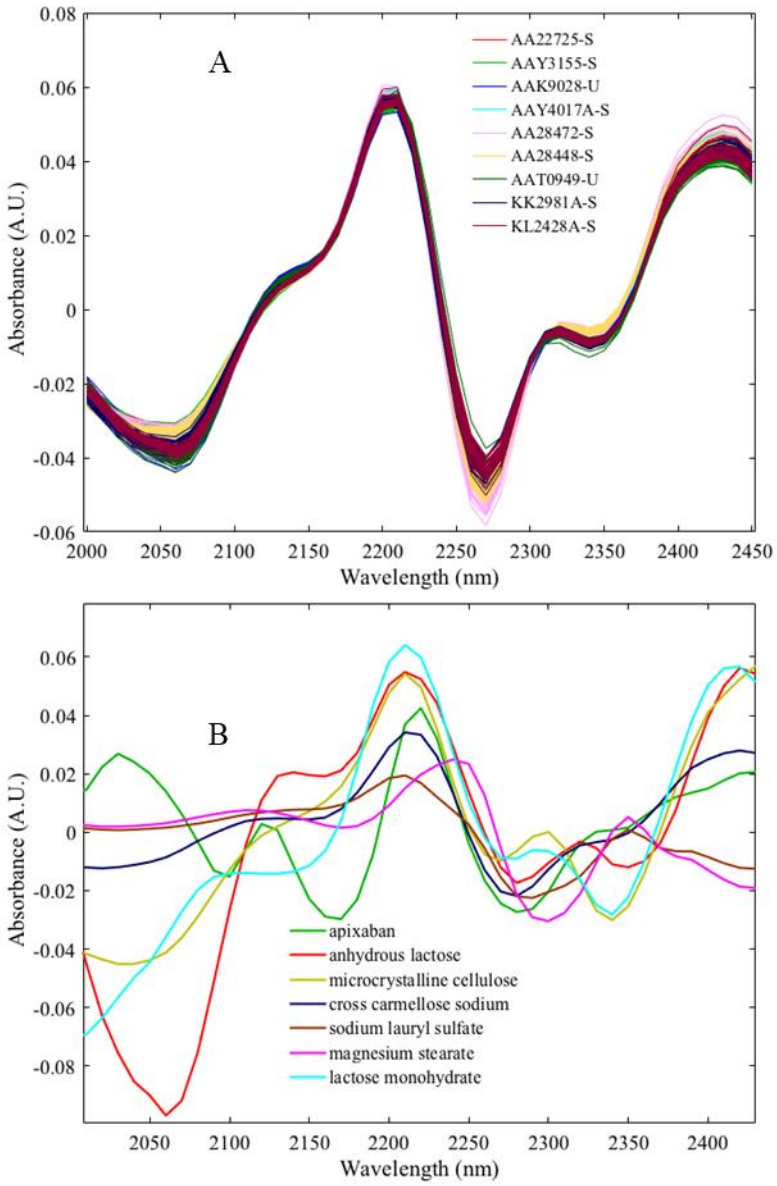

Figure 6-5: A) Preprocessed LWL-NIR spectra of apixaban, B) LWL-NIR spectra of major components of apixaban tablets.

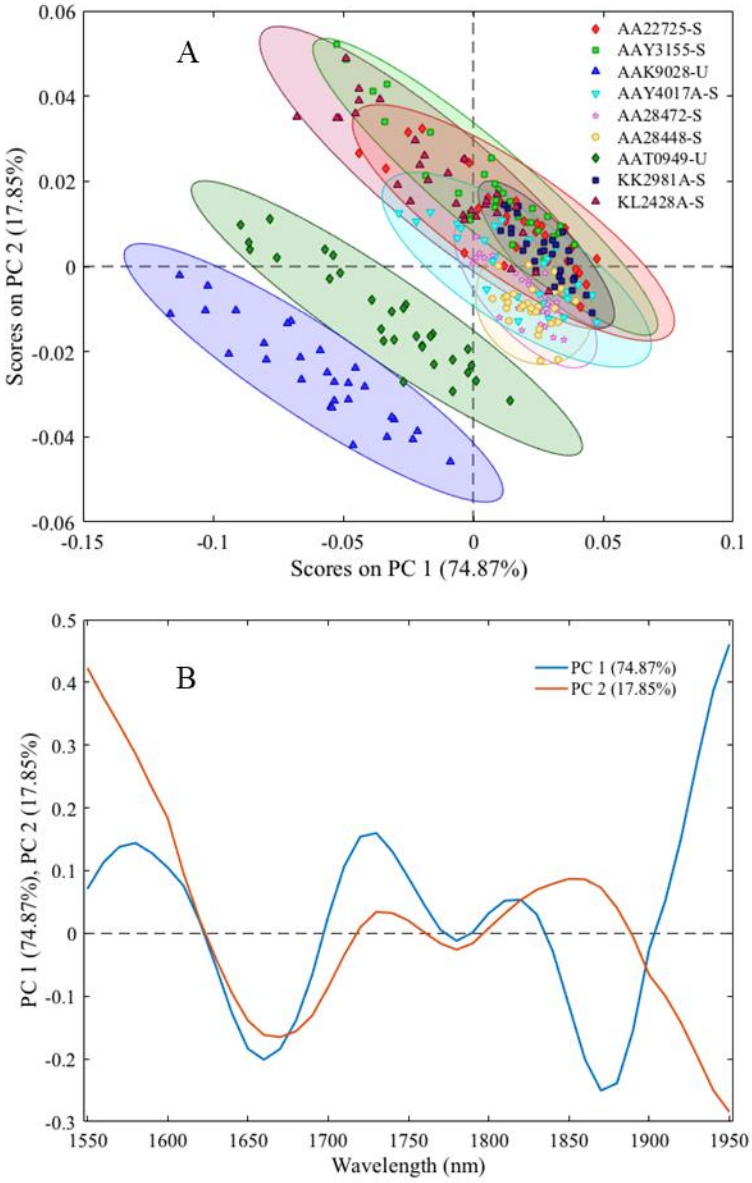

Figure 6-6: A) Scores plot of different batches of apixaban, B) Loadings plot of PCA analysis of apixaban using SWL-NIR spectrometer.

A two component PCA model captured nearly 95.99% of the spectral variation (Figure 6-6). The first PC explained nearly 74.87% of the variance. For SWL-NIR, the PCA analysis revealed cluster formation of PC 1 and PC 2 plot (Figure 6-6A). Though subtle differences were observed in the spectra due to the site differences, the PCA plot highlights the manufacturing site

variation, as displayed in Figure 6-6. As different batches were produced in the USA and Switzerland, the clusters were primarily due to the manufacturing site variations.

Further analysis was conducted by developing a PCA calibration model using only samples manufactured in Switzerland (Figure 6-7). When the USA samples were projected on the PCA model, the nature of the clusters in the manufacture sites were apparent (Figure 6-7B). Also, the diagnostics plots showed the high Hotelling's T^2 and Q residuals. (Figure 6-7C). The Q contribution plot emphasizes the important variables generated by the unmodeled variation in the model. It was apparent from the Q contribution plot that high Q residual was observed around ~1670 nm, which confirmed the previous findings of excipient variations (Figure 6-7D).

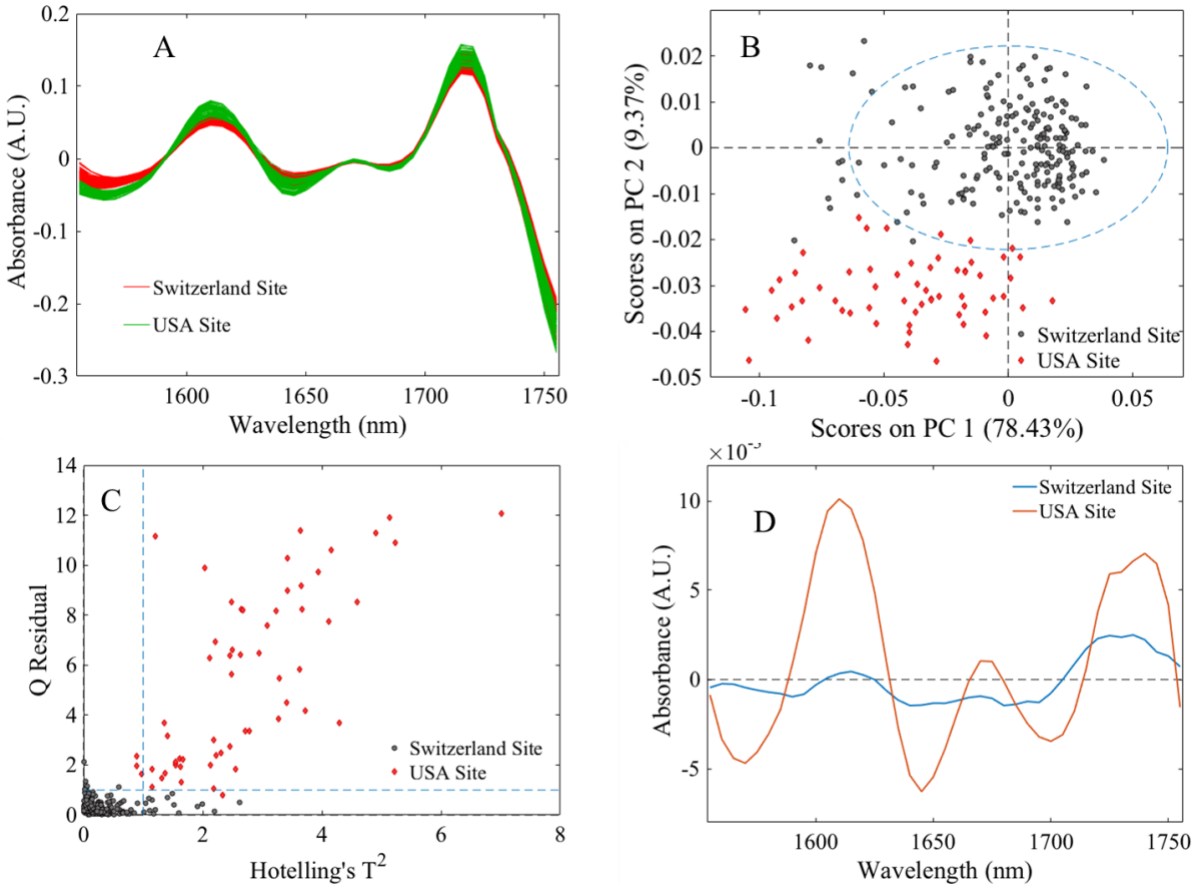

Figure 6-7: SNV treated spectra of product from two manufacturing sites. Using these data, a PCA model was developed where Switzerland lots were used for calibration, and USA manufactured samples were projected. B) Scores plot of PC1-PC2, C) Plots of Hotelling's T^2 and Q residuals, D) Plots of Q contribution. Data were collected using the SWL-NIR instrument.

A two component PCA model explained 81.48% of the LWL-NIR spectral variance. The first PC explained 57.89% of the spectral variance (Figure 6-8). Unlike the SWL-NIR PCA model, the PC scores of the LWL-NIR model appeared to be less related to site differences as the data from two sites were overlapped (Figure 6-8A). However, when the PCA model was developed using samples generated in the Switzerland site, projected USA samples resided outside the calibration space (Figure 6-9). This difference between the two manufacturing sites was also observable using LWL-NIR spectra.

Both the SWL-NIR and LWL-NIR PCA models demonstrated the potential effect of manufacturing site on the prediction model. Samples from two different manufacturing sites should be included in future calibration models as controlled variation. This strategy would cause little effect on the sensitivity (ability to accept target class samples) of the model performance.

In summary, both repositioning studies using the standard deviation data and the exploratory analysis using PCA models suggested that LWL-NIR measurements are less sensitive to sample positioning error and manufacturing site change relative to the SWL-NIR measurements. However, careful data preprocessing method and sample considerations are required while developing model.

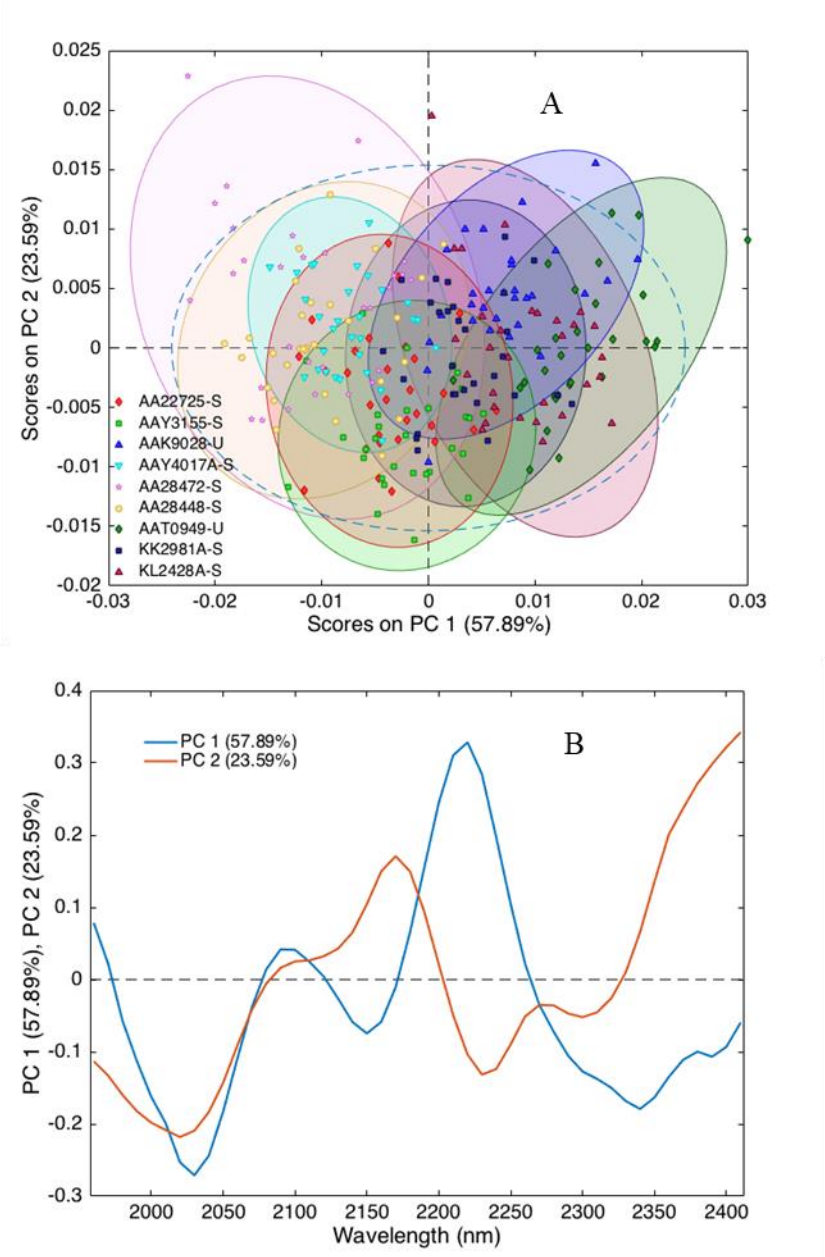

Figure 6-8: A) Scores plot of different lots of apixaban, B) Loadings plot of PCA analysis of apixaban using LWL-NIR spectrometer.

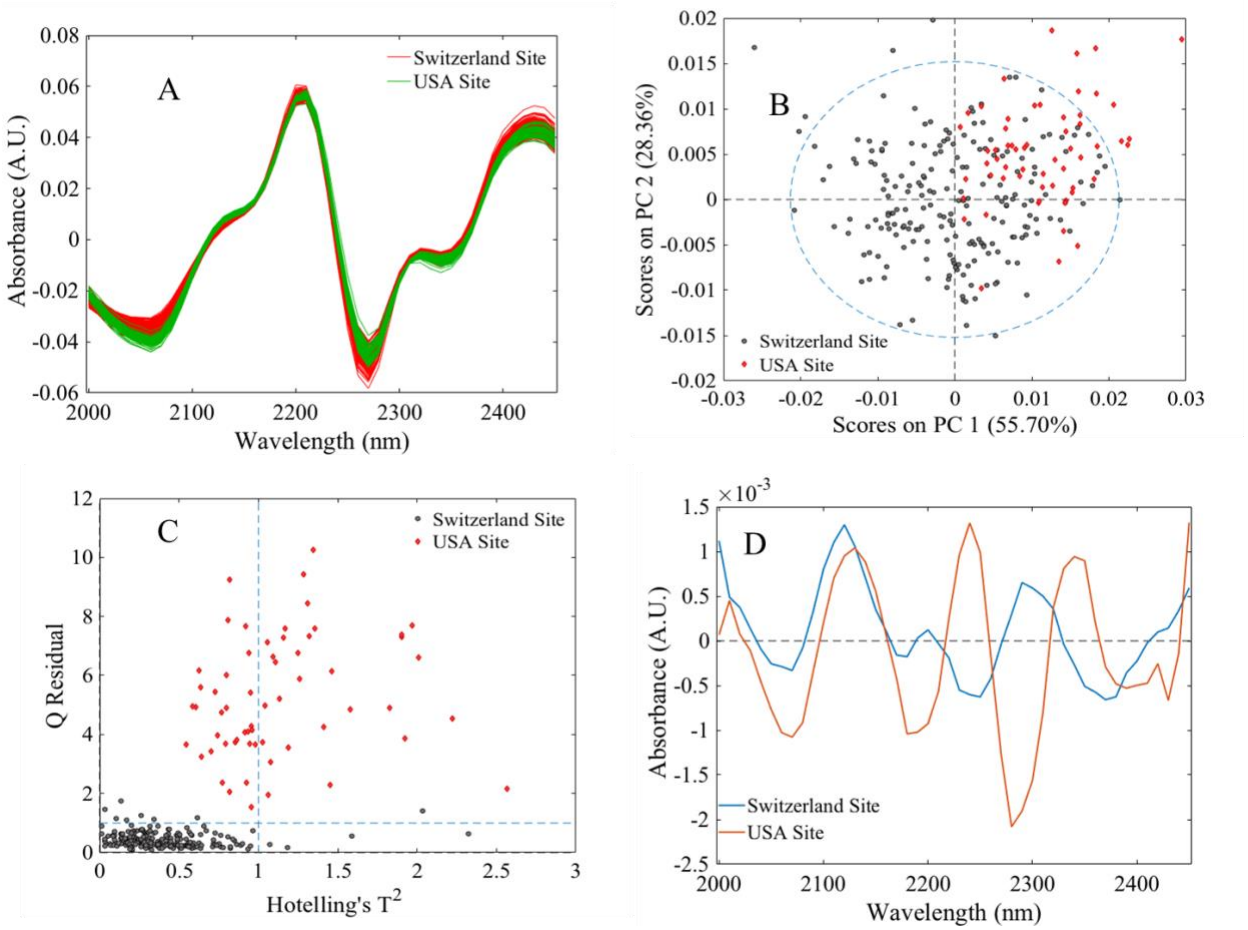

Figure 6-9: A) SNV treated spectra of products from two manufacturing sites. Using these data, a PCA model was developed where Switzerland lots were used for calibration, and USA manufactured samples were projected on PCA model, B) Scores plot of PC1-PC2, C) Plot of Hotelling's T^2 and Q residuals, D) Q contribution plots. Data were collected using the LWL-NIR instrument.

6.3.1.2 Atorvastatin

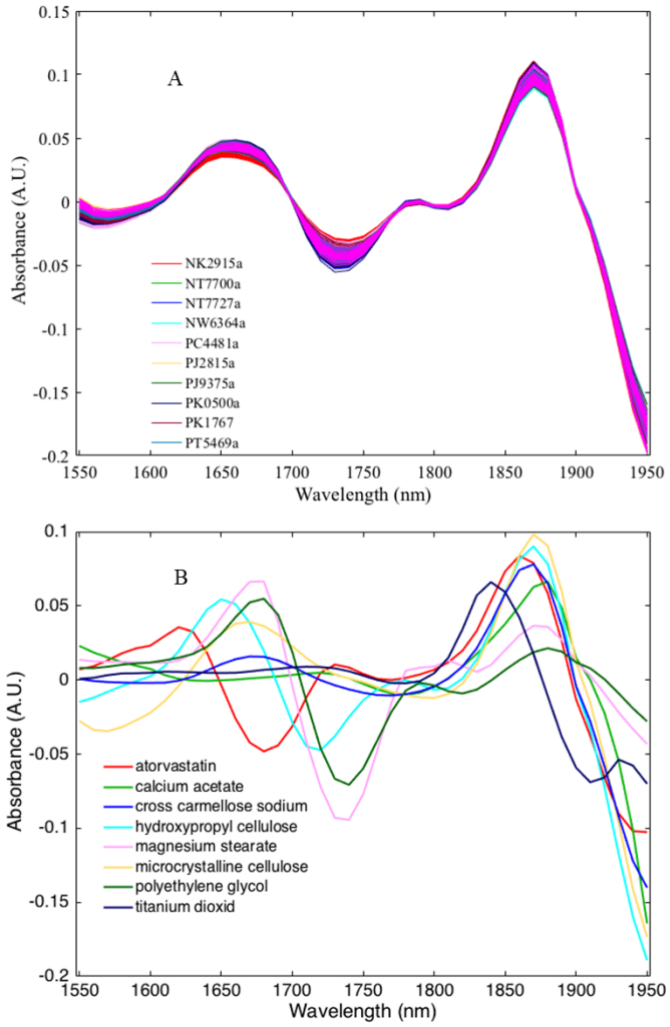

Figure 6-10: A) Preprocessed SWL-NIR spectra of atorvastatin, B) SWL-NIR spectra of major components of atorvastatin tablets.

Different lots of atorvastatin tablets (SNV transformed and second derivative SavGol treated) are shown in Figure 6-10 and 6-11. Unlike apixaban, minimum spectral variations of

different wavelength regions were observed. Major components of these tablets were plotted, as seen in Figure 6-10B and 6-11B.

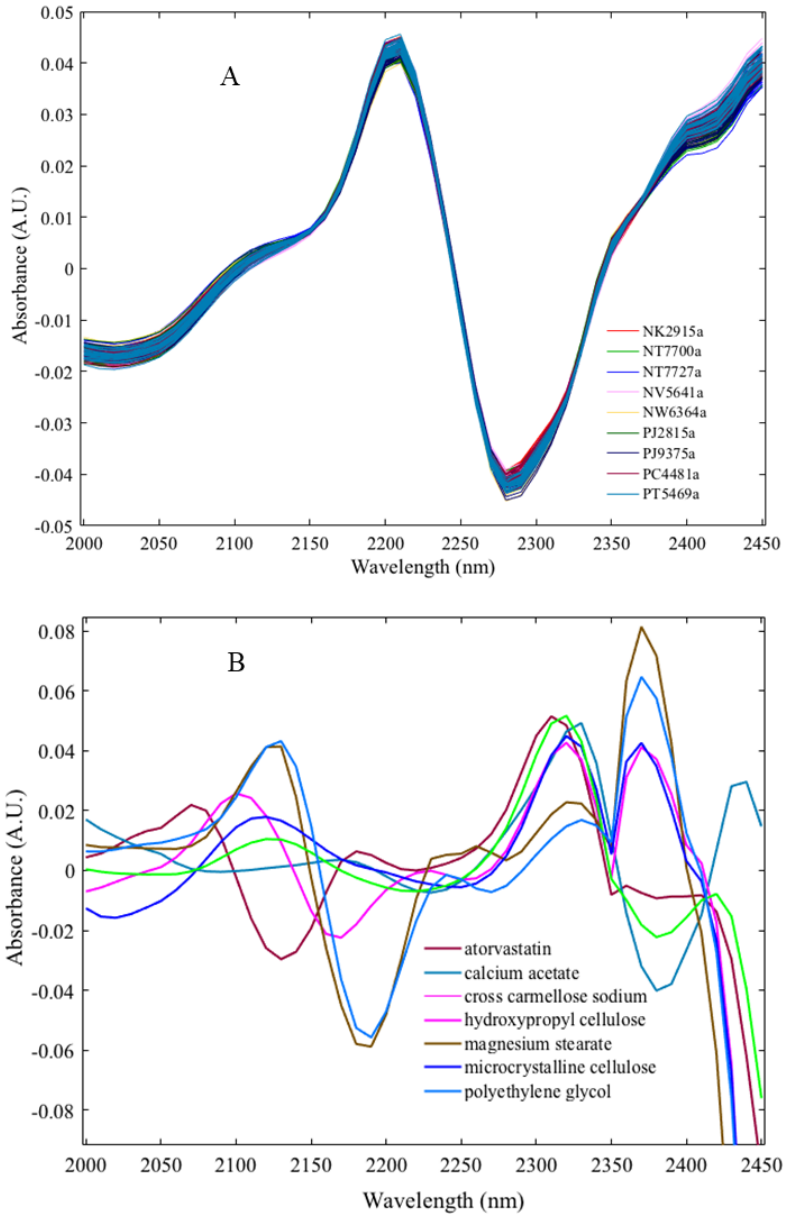

Figure 6-11: A) Preprocessed LWL-NIR spectra of atorvastatin B) LWL-NIR spectra of major components of atorvastatin tablets.

The PCA scores (Figure 6-12A) and loadings (Figure 6-12B) of the SWL-NIR spectra confirmed the minimum variations among different batches, as different groups overlapped. Two PCs explained 92.6% of the spectral variation.

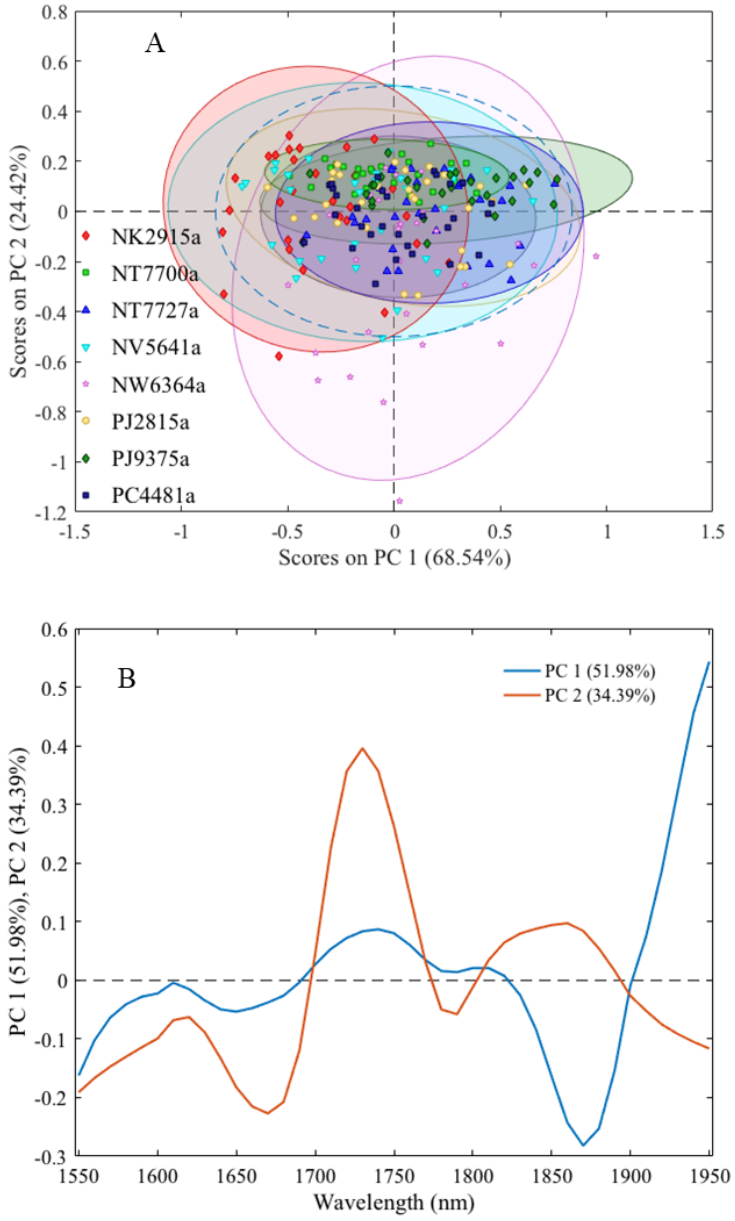

Figure 6-12: A) Scores plot of different lots of atorvastatin, B) Loadings plot of PCA analysis of atorvastatin using SWL

The PCA loadings and scores for the LWL-NIR spectra are shown in Figure 6-13 . The first PC explained nearly 66.85% of the spectral variance, and the second PC explained an additional 19.04% of the spectral variance.

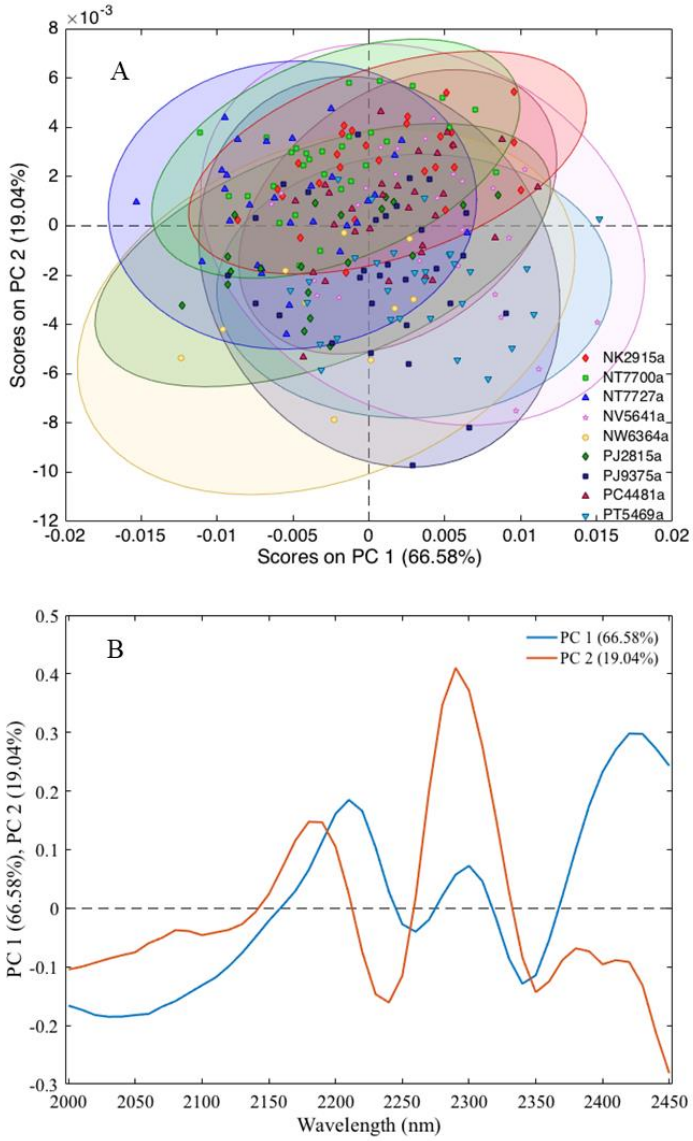

Figure 6-13: A) Scores plot of different lots of atorvastatin, B) Loadings plot of PCA analysis of atorvastatin using LWL spectrometer.

The two-axis plot of the PC scores does not show any significant clustering in the data. The model can be developed using any lots, as no particular attention is required for this product.

6.3.2 Multivariate Model Development: Calibration Set Considerations

Including appropriate samples into the calibration set is an essential element of a multivariate method development process. Section 6.3.3. in this chapter evaluated several important elements of method development while collecting spectra of commercial products. It was observed that spectral variation due to manufacturing site change was prominent. Lot-to-lot variability within sites was less than the spectral variability associated with site differences. Spectral range was also important to consider, as the degree of variation changed based on the wavelength regions. Regardless of the spectrometers used in this study, samples collected from multiple batches and multiple manufacturing sites (if available) were used in the calibration set to provide a sufficiently broad range of variation to develop a robust target class. Also, tablets were scanned with a consistent orientation, as discussed in Section 6.3.2.

The next section focuses on the model performance of the NIRS authentication method.

6.3.3 Method Development and Performance

6.3.3.1 Apixaban

Sample considerations and model development: The calibration model developed for the authentication of apixaban tablets used 150 samples drawn from five production batches including data from both production sites. The calibration datasets are summarized in Table 6-3 and Table 6-4.

Table 6-3: Summary of apixaban calibration and validation sets

SWL-NIR					
	Calibration	**Test**	**Val-1**	**Val-2**	**Val-3**
Samples (n)	150	60	90	30	30
Batches (n)	5	2	3	1	1
Model Type	SVDD, SIMCA on Spectra				
Preprocessing	SNV + Second derivative + Normalize				
Spectral range (nm)	1550-1950				
D	0.01				
σ	0.2				
SV numbers	3				

Table 6-4: Summary of apixaban calibration and validation

LWL-NIR					
	Calibration	**Test**	**Val-1**	**Val-2**	**Val-3**
Samples (n)	150	60	90	30	30
Batches (n)	5	2	3	1	1
Model Type	SVDD, SIMCA on Spectra				
Preprocessing	SNV + Second derivative + Normalize				
Spectral range (nm)	2000-2450				
D	0.2				
σ	0.2				
SV numbers	3				

To optimize the model, independent target (samples from unique batches) and non-target class samples were used to test the model. One new lot of 5 mg apixaban product was used as target class test samples. These tablets were used to ensure the highest specificity of the model. A new batch of samples containing a lower concentration of API (2.5 mg) was used as non-target class samples to ensure the highest sensitivity of the model. The SVDD model parameters, both D and σ were optimized accordingly (Table 6-3 and Table 6-4).

A combination of SNV, second derivative and normalization was chosen based on maximum average performance of sensitivity and specificity. The preprocessed calibration spectra are shown in Figure 6-14A. The calibration model used three samples as support vectors (depicted in Figure 6-14A as blue spectra).

The validation data consisted of three sets of samples.

The first validation set was target-class samples. This validation set (Val-1) consisted of 90 samples of target class samples from three batches containing apixaban (5mg). These batches were manufactured at two different facilities (one in the USA and two in Switzerland).

The second and third validation sets were non-target class samples. The second validation set (Val-2) consisted of 30 commercial samples containing a low dose of apixaban (2.5 mg). The third validation (Val-3) set consisted of 30 laboratory scale samples manufactured at the Duquesne University Center for Pharmaceutical Technology (DCPT) using MCC and apixaban. The purpose of the third validation set is to provide an additional test of the specificity using samples including a similar amount of apixaban (5mg) but different excipient composition.

Validation Method Performance: Method validation (with a validation set) was conducted after the optimization of the model (using a test set). The validation performance was evaluated based on the following two key performance criteria: sensitivity and specificity. The specificity was tested using different batches of target class samples (Val-1), and the sensitivity (ability to reject non-target class samples) was tested using two sets of samples: 1) low dose apixaban tablets (Val-2) and 2) lab based simulated falsified products (Val-3).

Table 6-5: Validation performance of apixaban calibration model

		Sensitivity Val-1	Specificity Val-2	Specificity Val-3
SVDD	SWL- Apixaban	0.9111	0.8667	1
	LWL- Apixaban	0.8667	0.7812	1
SIMCA	SWL- Apixaban	0.76	0.81	1
	LWL- Apixaban	0.8	0.6	1

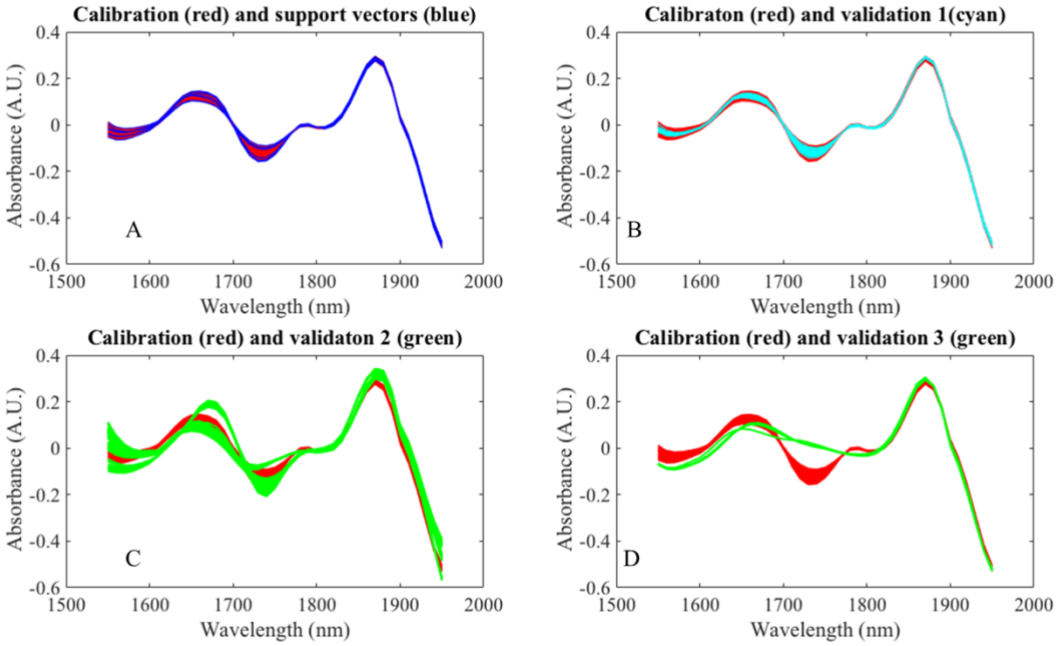

Figure 6-14: SWL-NIR spectra of calibration set with A) support vectors, B) validation set 1, C) validation set 2, and D) validation set 3.

During validation, it was observed that this method successfully rejected all samples from Val-3 set, while rejection of Val-2 was less obvious. The reason for the difference in performance was explained in Figure 6-14 (C and D). It was observed that the Val-3 set (Figure 6-14C) was spectrally significantly different from the target class samples. However, Val-2 is highly similar to the target class which means that the model failed to reject all samples (Figure 6-14D). It is

important to mention that while the Val-2 set was from the same manufacturer, and contained similar compositions, it was challenging for the model to reject all samples from Val-2. This result was confirmed using a diagnostic plot of Hotelling's T^2 and Q residuals. All of the Val-3 (cyan dots) have high Q residuals and Hotelling's T^2 compared to the Val-2 (blue dots) (Figure 6-15). The higher values of these two statistical parameters indicated the successful rejection of Val-3 compared to Val-2.

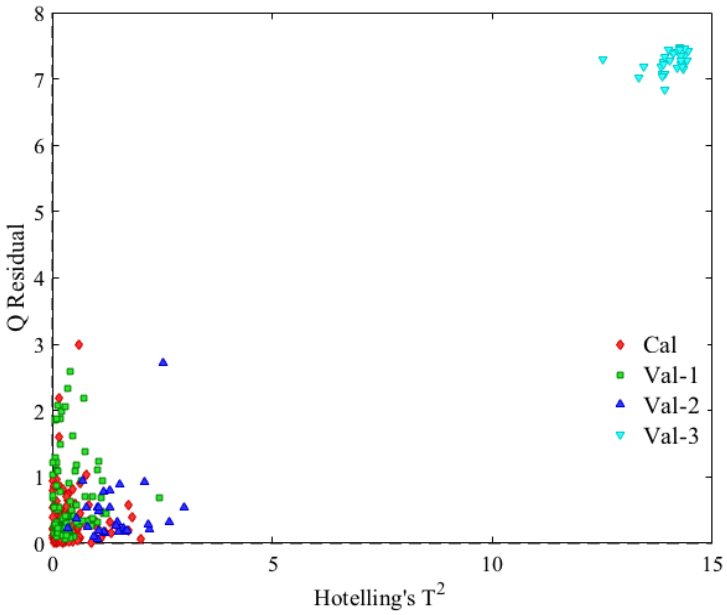

Figure 6-15: A PCA diagnostics plot of validation sets with the calibration set. Spectra were collected using SWL-NIRS.

It was observed that SVDD performed better than SIMCA for authentication of pharmaceutical samples. As, adding different manufacturing sites into the calibration set generated clusters in the calibration space, SIMCA model suffered to provide optimum performance. However, SVDD showed better sensitivity by accepting Val-1 samples, though they were generated in two manufacturing sites. Appropriate preprocessing methods helped to improve

performance. It was observed that combination of SNV, second derivative and normalization showed the best performance compared to other combination of routines. This preprocessing decreased the impact of sources of variability such as sampling variability and correcting for pathlength variation. These overall improved model performances.

Similar performance was observed for LWL-NIR. The results showed comparable patterns because spectral behavior and diagnostic statistics were similar, as shown in Figure 6-16 and Figure 6-17.

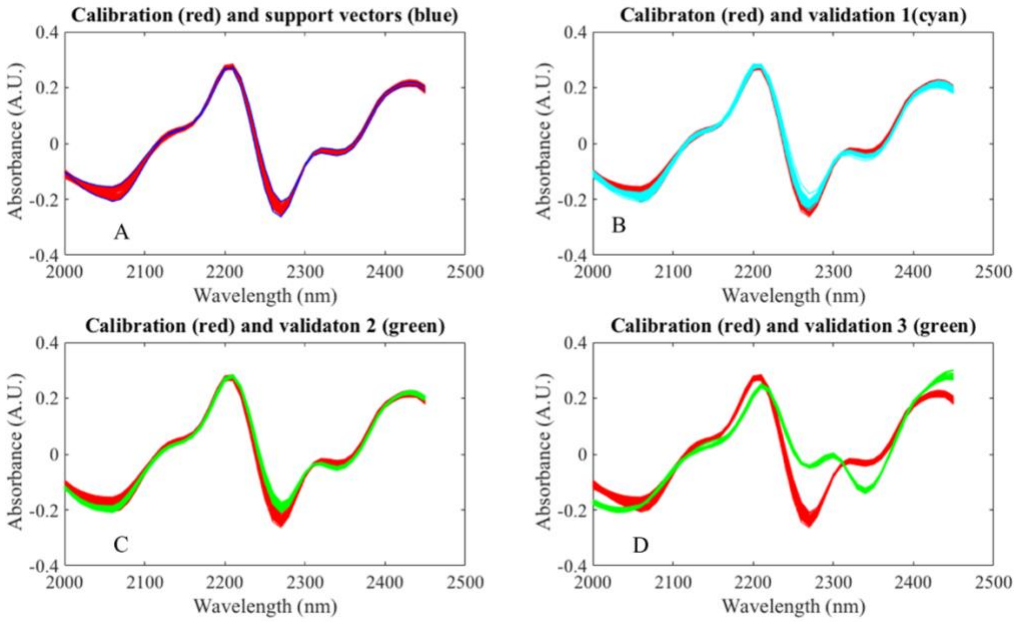

Figure 6-16: LWL spectra of calibration set with A) Support vectors, B) Validation set 1, C) Validation set 2, and D) Validation set 3

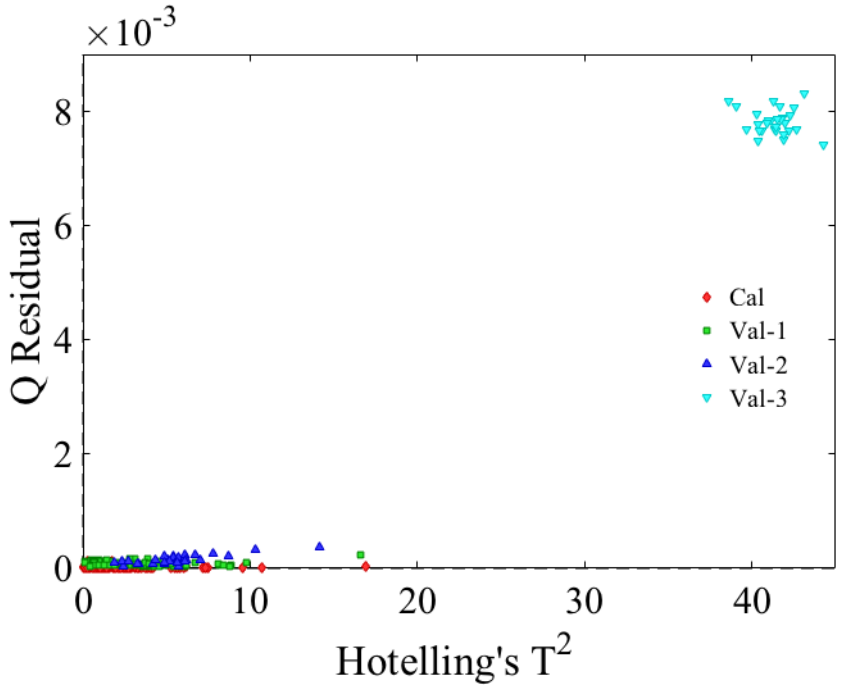

Figure 6-17: A PCA diagnostics plot of validation sets with the calibration set. Spectra were collected using LWL-NIR spectrometer.

6.3.3.2 Atorvastatin

Sample considerations and model development: For atorvastatin, SNV, 2nd Derivative and normalization preprocessing methods were chosen based on the performance. An independent test set (defined below) was used to optimize the model performance. Spectra of the preprocessed calibration set are shown in Figure 6-18A, along with samples which were selected as support vectors (blue spectra).

Model development for authentication of atorvastatin used 150 target class samples drawn from production batches (40 mg). The test set was samples from different batches of product to provide independence. Samples manufactured by three other generic manufacturers were used as the non-target class product to optimize the model. The calibration datasets are summarized in

Table 6-6 and Table 6-7. The validation samples consisted of three subsets of samples selected from production scale and lab scale samples.

Table 6-6: Summary of atorvastatin calibration and validation sets.

SWL-NIR					
	Calibration	**Test**	**Val-1**	**Val-2**	**Val-3**
Samples (n)	150	30	90	90	30
Manufacturers (n)	1	2	1	3	1
Batches (n)	5	1	3	3	1
Model Type	SVDD, SIMCA on Spectra				
Preprocessing	SNV + Second derivative + Normalization				
Spectral range (nm)	1550-1950				
D	0.01				
σ	0.15				
SV numbers	8				

Table 6-7: Summary of atorvastatin calibration and validation sets.

LWL-NIR					
	Calibration	**Test**	**Val-1**	**Val-2**	**Val-3**
Samples (n)	150	30	90	90	30
Manufacturers (n)	1	2	1	3	1
Batches (n)	5	1	3	3	1
Model Type	SVDD, SIMCA on Spectra				
Preprocessing	SNV+ Second derivative + Normalize				
Spectral range (nm)	2000-2450 nm				
D	0.01				
σ	0.2				
SV number	6				

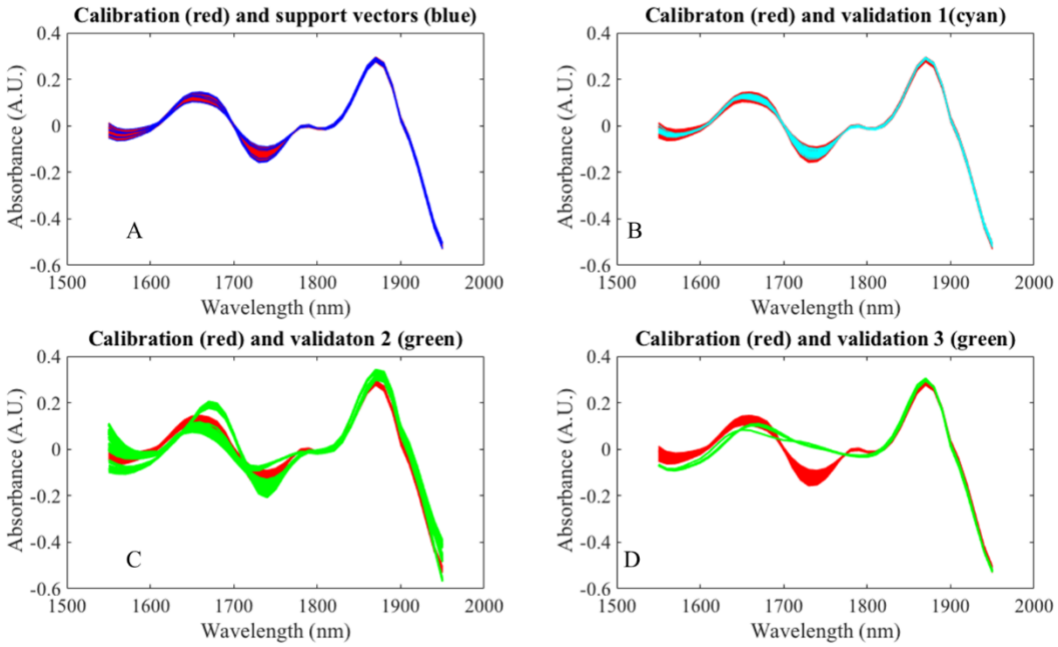

Figure 6-18: SWL-NIR spectra of calibration set with A) support vectors, B) validation set 1, C) Validation set 2, and D) validation set 3.

The first validation set (Val-1) consisted of 30 samples, including one batch of target class samples. As atorvastatin is a generic product, samples available from other manufacturers were used as the validation set. Three different manufacturers products (M1-Atorvastatin 40 mg from Mylan Pharmaceutical, M2-Atorvastatin 40 mg from Lannett Company Inc., M3- Atorvastatin 40 mg from Dr Reddy's Laboratories) were included in the second validation sets (Val-2). The third validation (Val-3) set consisted of one batch of laboratory scale samples manufactured using MCC with atorvastatin. Validation datasets are summarized in Table 6-6 and Table 6-7.

Validation Method Performance: Performance of the atorvastatin model was observed using three validation sets. The SVDD model successfully accepted all samples in the target class

validation set (Val-1). Although Val-3 was significantly different than the Val-2 samples (Figure 18C-D) the model successfully rejected other non-target class validation sets (Val-2 and Val-3). Among the three manufacturers of Val-2, Man-2 was close to the target class samples whereas other alternative class samples (M1 and M3) were demonstrated to reside far from the target class samples (Figure 19). Similar spectral behavior (LWL-NIR) of these samples was observed in Figure 6-20 and Figure 6-21. Samples collected using different spectrometer showed good performance.

Table 6-8: Validation performance of atorvastatin calibration models

		Sensitivity-Val-1	**Specificity Val-2**	**Specificity Val-3**
SVDD	SWL- Atorvastatin	1	1	1
	LWL- Atorvastatin	1	1	1
SIMCA	SWL- Atorvastatin	1	1	1
	LWL- Atorvastatin	1	1	1

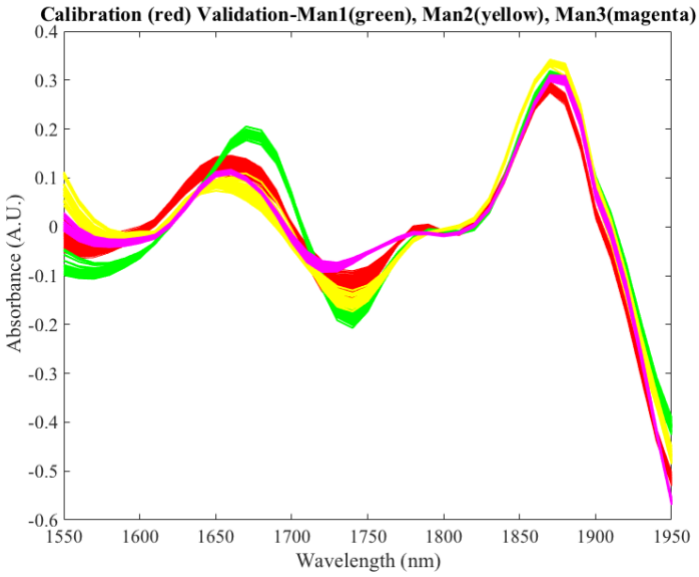

Figure 6-19: SWL-NIR spectra of calibration sets with three manufacturers samples of validation set 2.

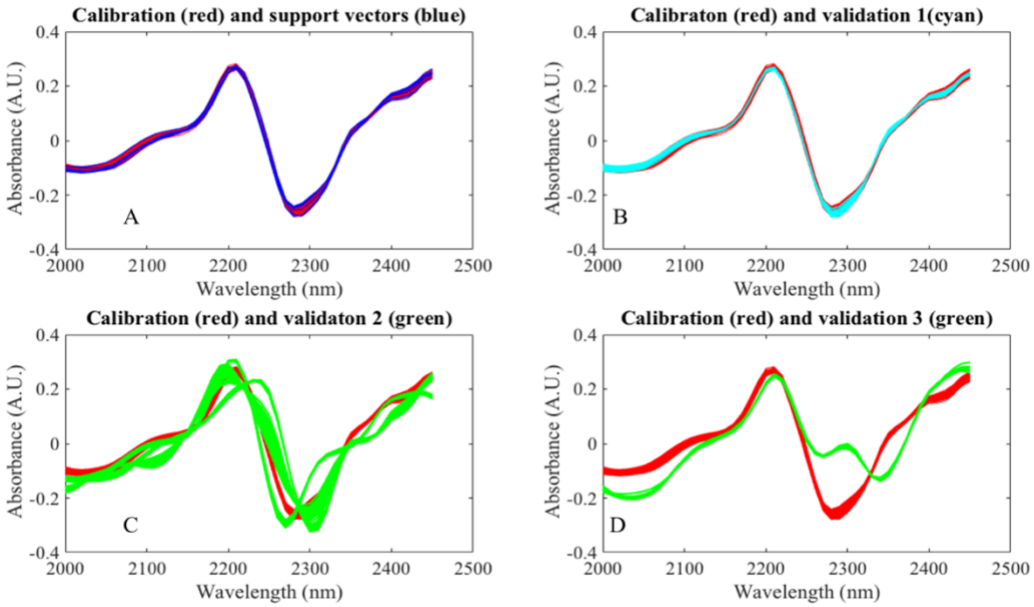

Figure 6-20: LWL-NIR spectra of calibration set with A) support vectors, B) validation set 1, C) validation set 2, and D) validation set 3.

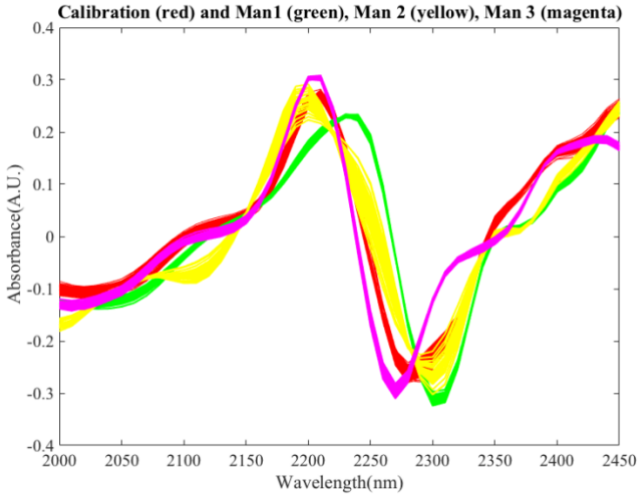

Figure 6-21: LWL-NIR spectra of calibration sets with three manufacturers samples of validation set 2.

6.4 Summary

The goal of an authentication technique is to predict target class samples accurately and to reject non-target class samples. However, many challenges exist in the development of an NIR based classification technique, including the broad spectral features of NIR spectrometers in general, and the unwanted sensitivity to physical variability. In Chapters 2 and 3, it was observed that moisture is a critical factor to consider during multivariate method development. In the current chapter, it was observed that sample manufacturing site change created spectral variation. Spectra acquired from multiple manufacturing sites were pooled for qualitative model development. Including samples from unique manufacturing sites in the calibration sample set created bimodal/ multimodal distribution in the calibration space, violating the assumptions of the traditional parametric distribution-based SIMCA method. Hence, these studies used a non-parametric distribution-based method, the support vector data description (SVDD) algorithm, provided a more robust class. The SVDD method proved to be a useful class-modeling technique for portable NIRS to monitor tablet quality in pharmacies. Additionally, including non-target class samples was critical to the development of robust multivariate models.

This study also explored the impact of positioning error. This was effectively mitigated using a specific sample orientation system and spectral preprocessing techniques. It was also observed that a longer wavelength range spectrum was less sensitive to sample positioning and manufacturing site than a shorter wavelength range spectrum.

This chapter reemphasized the value of using a pertinent calibration model and the SVDD algorithm to develop a robust spectroscopic authentication system, as proposed in the hypothesis.

Chapter 7: Summary

As the spread of falsified drugs is increasing worldwide, it is often difficult for regulatory authorities to surveil falsified products at various locations in the pharmaceutical supply chain. Using portable spectrometers (i.e., Near-Infrared (NIR) and Raman spectrometers) may help to remove this barrier. Rapid screening of pharmaceutical products by these analytical tools is an effective way to enhance consumer safety. However, the use of such techniques is not straightforward due to the multivariate nature of the collected data and the significant variety of potential factors influencing the analytical measurements. To overcome the challenge of current multivariate methods using spectroscopic data, this dissertation compiled three critical elements (see Figure 7-1).

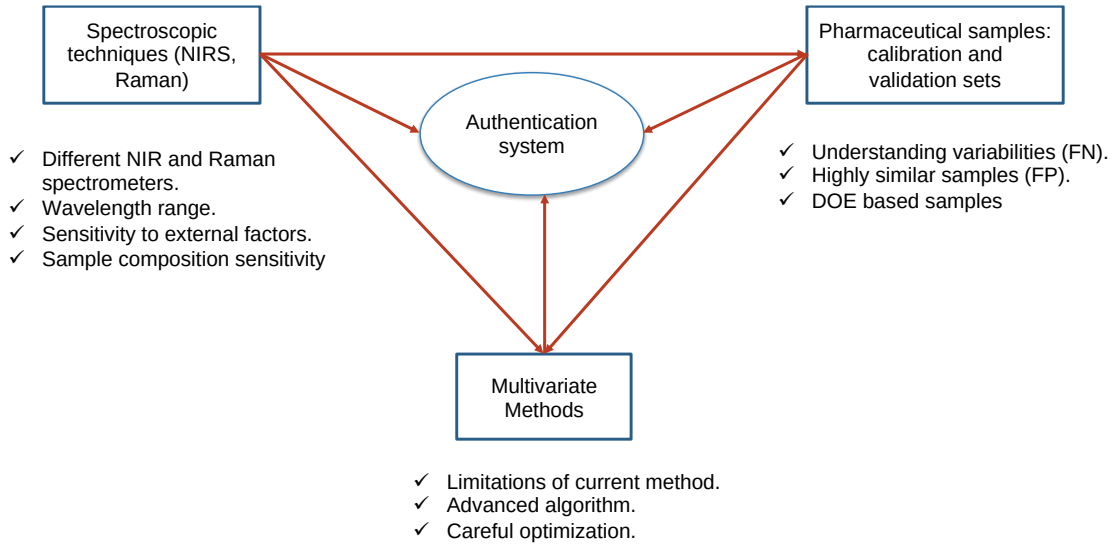

Figure 7-1: Different elements of this dissertation involved with development of a spectroscopic authentication system and accomplished steps (✓). Combination of these three areas enabled development of a successful authentication system. (FN: False Negative, FP: False Positive)

Three elements regarding the project include:

1) While developing a spectroscopic authentication method, the specific advantages and disadvantages of each spectroscopic techniques should be considered by the analyst. A variety of NIR and Raman spectroscopic equipment was explored to understand the sensitivity of these spectrometers to different physico-chemical variations such as moisture and chemical composition.
2) To achieve consistent performance during routine analysis of pharmaceutical samples, calibration and validation sets should include the spectral variation which may arise during routine analysis. Moreover, during model development, the analyst should use highly similar samples to reduce false positives. If these highly similar falsified samples are not readily available, using DOE to generate simulated falsified samples should serve the purpose.
3) Using a support vector machine based calibration method avoids the typical assumptions required with more traditional methods regarding data distributions. Moreover, the SVDD method was demonstrated to offer improved capability for detecting highly similar non-target class samples.

These elements combinedly explored in different experiments of this dissertation.

In Chapter 2**,** a NIR spectroscopic-based class-modeling calibration technique was described. While developing a spectroscopic method for detecting false-samples, several challenges associated with the method development were addressed. One of those challenges is the sensitivity of spectrometers toward unwanted variabilities such as moisture, manufacturing site, instrument parts change, etc. Tablets containing Acetaminophen, MCC, lactose, HPMC, and

magnesium stearate were generated using a pilot-scale manufacturing system over different seasons of the year. Since the lab did not have controlled humidity conditions, samples generated during different seasons were exposed to different humidity levels. Initially, the calibration model was developed in the winter season; the model used to predict validation sets was developed in the summer season. As the season was different between calibration and validation sets, the model failed to accept the target-class samples, indicating a degradation of the model performance when moisture variance was unaccounted for. To resolve this, the model was updated to include summer samples in the calibration set. However, moisture variance in the newly added samples led to significant extrapolation compared to the original experimental domain, defined by the previously collected samples (during the winter). Therefore, adding summer samples to the calibration set created a binomial/multimodal distribution, violating the assumptions of traditional parametric distribution-based SIMCA modeling techniques. Hence, this chapter suggested using a non-parametric distribution-based method, support vector data description (SVDD), to develop a robust NIR class-modeling technique for the detection of falsified samples. Performance of SVDD was evaluated and compared with the traditional SIMCA approach. The SVDD method demonstrated superior performance relative to the SIMCA method for detection of falsified samples. Hence, when a binomial/multimodal distribution exists in the calibration model, SVDD is a useful class-modeling technique for monitoring tablet quality.

In Chapter 3, the influence of moisture variation on the performance of Raman spectroscopy for class modeling was evaluated. Although water is a weak Raman scatterer, moisture variability has an indirect effect on analytical model performance because many pharmaceutical components have artifacts in the form of baseline variation associated with fluorescence quenching. This chapter investigated the deleterious effects of water quenching on

the prediction accuracy of a multivariate calibration algorithm developed using Raman spectroscopy. To demonstrate this phenomenon two sets of tablets were used, 1) lab based acetaminophen tablets containing lactose, MCC, HPMC, and magnesium stearate, and 2) commercially produced artesunate tablets, which is an anti-malarial agent often falsified by fraudulent manufacturers. Tablet moisture variation was introduced by placing samples in a variety of humidity chambers. Significant spectral effects arising from fluorescence were identified in the Raman spectra due to moisture variation and fluorescence related spectral variability. This caused substantial degradation of the prediction performance for target class samples. Thus, the work demonstrated that accounting for moisture variation during method development reduced the prediction error of the SVDD and SIMCA based class-models.

Requirement of appropriate non-target class samples during multivariate authentication system development was highlighted in Chapters 4 and 5. In Chapter 4, it was shown that to enhance spectroscopic performance using the SVDD algorithm, non-target class spectral data are critical for model optimization. This is important for the model which is developed to identify challenging falsified drugs. It was demonstrated that using non-target class data can further tighten the decision boundary around the target class samples, thereby improving model performance. Moreover, if the non-target class samples are highly similar to the target class, the model exhibited the desired performance. For this study, acetaminophen tablets were collected from different parts of the world, which were manufactured by various producers. Tablet size, shape, and weight were analogous, and the products demonstrated similar spectral features. Among the nine manufacturers' tablets, samples from one manufacturer were used to develop a target class, and the eight other data sets were used for model optimization and validation. The model was optimized using one product as a non-target class and demonstrated successful prediction of the

other non-target class samples. Furthermore, optimization of the decision boundary minimizes the false positives.

In Chapter 5, predictions models for highly similar non-target class products were developed using DOE. Both NIR and Raman spectrometers were used to scan the samples. It was demonstrated that the critical non-target class samples were unique for the two different analytical techniques. These DOE based samples were useful to improve the model performance, and they resolved the critical issue of limited accessibility to actual falsified drug products.

The insight gained from Chapters 2 through 5 was used to develop a spectroscopic authentication method for use in the health care setting or other remote testing sites. In Chapter 6, portable spectrometers were used to scan different commercial products in two local pharmacies. A protocol was developed to collect data from available products. This study also highlighted the requirement of careful considerations of calibration samples and the use of an advanced algorithm for the actual modeling. The developed model performed successfully by accepting target class samples and rejecting non-target class samples at the local pharmacies in Pittsburgh.

This dissertation emphasizes the importance of 1) applying critical prior knowledge regarding pharmaceutical products, pharmaceutical manufacturing/processing, analytical methodology, and chemometric techniques, and 2) the application of a specific modern approach to develop a successful spectroscopic authentication system. Combining all these pieces gives a unique insight to direct the analyst during development of an authentication method.

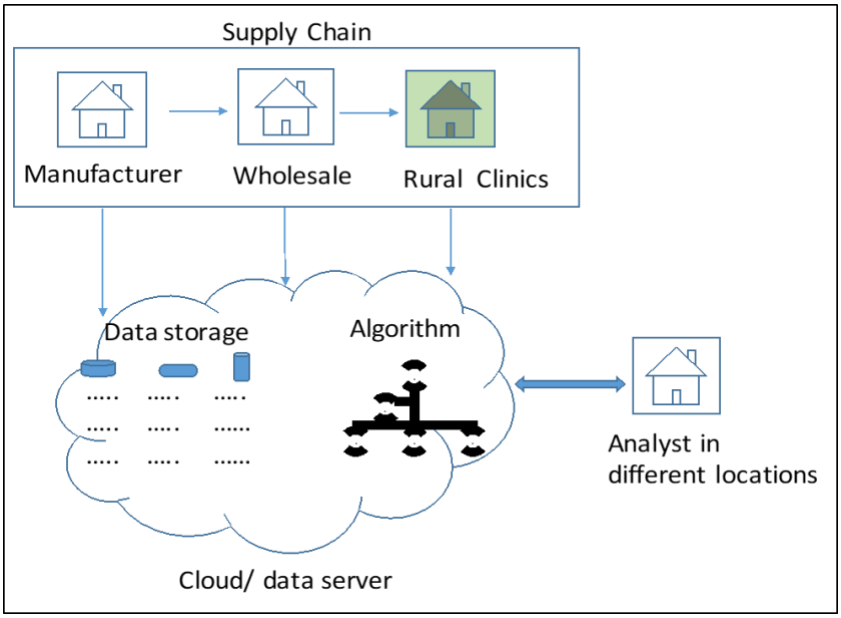

Figure 7-2: A schematic diagram of a possible cloud-based data management and model application of spectroscopic techniques.

Future applications of this project will include developing a cloud-based platform. The developed model will be stored in a cloud-based server, facilitating effective management of models and data for the analyst in the field. It will enable a global product tracking system, from manufacturers to the rural clinics which will address the scourge of falsified drugs. Moreover, a combination of an enhanced modeling approach, utilizing critical prior knowledge, will provide the prescription for the solution to the current crisis of falsified drugs in the developing countries. Also, this can be a potential application for IoT based testing of pharmaceutical products and enhanced supply chain integrity in developed countries.

References

[1] Y. Hu, H. Wikström, S.R. Byrn, L.S. Taylor, Analysis of the effect of particle size on polymorphic quantitation by Raman spectroscopy, Applied spectroscopy, 60 (2006) 977-984.

[2] G.J. Buckley, L.O. Gostin, Countering the problem of falsified and substandard drugs, National Academies Press2013.

[3] M. Shepherd, Beef up international cooperation on counterfeits, Nature medicine, 16 (2010) 366-366.

[4] P.N. Newton, M.D. Green, F.M. Fernández, Impact of poor-quality medicines in the 'developing'world, Trends in pharmacological sciences, 31 (2010) 99-101.

[5] I.o. Medicine, Countering the Problem of Falsified and Substandard Drugs, The National Academies Press, Washington, DC, 2013.

[6] M. Tremblay, Medicines counterfeiting is a complex problem: a review of key challenges across the supply chain, Current drug safety, 8 (2013) 43-55.

[7] D. Custers, P. Courselle, S. Apers, E. Deconinck, Chemometrical analysis of fingerprints for the detection of counterfeit and falsified medicines, Reviews in Analytical Chemistry, 35 (2016) 145-168.

[8] S. Kovacs, S.E. Hawes, S.N. Maley, E. Mosites, L. Wong, A. Stergachis, Technologies for detecting falsified and substandard drugs in low and middle-income countries, PLoS One, 9 (2014) e90601.

[9] D. Desai, G. Wu, M.H. Zaman, Tackling HIV through robust diagnostics in the developing world: current status and future opportunities, Lab on a Chip, 11 (2011) 194-211.

[10] N. Ranieri, P. Tabernero, M.D. Green, L. Verbois, J. Herrington, E. Sampson, R.D. Satzger, C. Phonlavong, K. Thao, P.N. Newton, Evaluation of a new handheld instrument for the detection of counterfeit artesunate by visual fluorescence comparison, The American journal of tropical medicine and hygiene, 91 (2014) 920-924.

[11] C.M. Gryniewicz-Ruzicka, J.D. Rodriguez, S. Arzhantsev, L.F. Buhse, J.F. Kauffman, Libraries, classifiers, and quantifiers: a comparison of chemometric methods for the analysis of Raman spectra of contaminated pharmaceutical materials, Journal of pharmaceutical and biomedical analysis, 61 (2012) 191-198.

[12] H. Luinge, Automated interpretation of vibrational spectra, Vibrational Spectroscopy, 1 (1990) 3-18.

[13] R. Kalyanaraman, G. Dobler, M. Ribick, NIR-Near-Infrared (NIR) Spectral Signature Development and Validation for Counterfeit Drug Detection Using Portable Spectrometer, American Pharmaceutical Review, 14 (2011) 98.

[14] D.E. Bugay, R.C. Brush, Chemical identity testing by remote-based dispersive raman spectroscopy, Applied spectroscopy, 64 (2010) 467-475.

[15] Y. Zontov, K. Balyklova, A. Titova, O.Y. Rodionova, A. Pomerantsev, Chemometric aided NIR portable instrument for rapid assessment of medicine quality, Journal of Pharmaceutical and Biomedical Analysis, 131 (2016) 87-93.

[16] O.Y. Rodionova, K. Balyklova, A. Titova, A. Pomerantsev, Quantitative risk assessment in classification of drugs with identical API content, Journal of pharmaceutical and biomedical analysis, 98 (2014) 186-192.

[17] C. Durante, R. Bro, M. Cocchi, A classification tool for N-way array based on SIMCA methodology, Chemometrics and Intelligent Laboratory Systems, 106 (2011) 73-85.

[18] B.M. Wise, N. Gallagher, R. Bro, J. Shaver, W. Windig, R.S. Koch, PLS Toolbox 4.0, Eigenvector Research Incorporated: Wenatchee, WA, USA, (2007).

[19] A.L.J.J.o.C.A.J.o.t.C.S. Pomerantsev, Acceptance areas for multivariate classification derived by projection methods, 22 (2008) 601-609.

[20] I. Storme-Paris, H. Rebiere, M. Matoga, C. Civade, P.-A. Bonnet, M. Tissier, P. Chaminade, Challenging near infrared spectroscopy discriminating ability for counterfeit pharmaceuticals detection, Analytica chimica acta, 658 (2010) 163-174.

[21] D.M. Tax, R.P. Duin, Support vector data description, Machine learning, 54 (2004) 45-66.

[22] B. Schölkopf, R.C. Williamson, A.J. Smola, J. Shawe-Taylor, J.C. Platt, Support vector method for novelty detection, Advances in neural information processing systems, 2000, pp. 582-588.

[23] J. Weitzel, R.A. Forbes, R.D. Snee, The Use of the Analytical Target Profile in the Lifecycle of an Analytical Procedure: with an example for an HPLC Procedure| IVT, (2015).

[24] E. Rozet, P. Lebrun, P. Hubert, B. Debrus, B. Boulanger, Design spaces for analytical methods, TrAC Trends in Analytical Chemistry, 42 (2013) 157-167.

[25] R.L. Mccreery, A.J. Horn, J. Spencer, E. Jefferson, Noninvasive identification of materials inside USP vials with Raman spectroscopy and a Raman spectral library, Journal of pharmaceutical sciences, 87 (1998) 1-8.

[26] R. da Silva Fernandes, F.S.L. da Costa, P. Valderrama, P.H. Março, K.M.G. de Lima, Non-destructive detection of adulterated tablets of glibenclamide using NIR and solid-phase fluorescence spectroscopy and chemometric methods, Journal of pharmaceutical and biomedical analysis, 66 (2012) 85-90.

[27] Y.L. Loethen, J.F. Kauffman, L.F. Buhse, J.D. Rodriguez, Rapid screening of anti-infective drug products for counterfeits using Raman spectral library-based correlation methods, Analyst, 140 (2015) 7225-7233.

[28] F.E. Dowell, E.B. Maghirang, F.M. Fernandez, P.N. Newton, M.D. Green, Detecting counterfeit antimalarial tablets by near-infrared spectroscopy, Journal of pharmaceutical and biomedical analysis, 48 (2008) 1011-1014.

[29] T.P. Dorlo, T.A. Eggelte, P.J. de Vries, J.H. Beijnen, Characterization and identification of suspected counterfeit miltefosine capsules, Analyst, 137 (2012) 1265-1274.

[30] M. de Veij, P. Vandenabeele, K.A. Hall, F.M. Fernandez, M.D. Green, N.J. White, A.M. Dondorp, P.N. Newton, L. Moens, Fast detection and identification of counterfeit antimalarial tablets by Raman spectroscopy, Journal of Raman Spectroscopy, 38 (2007) 181-187.

[31] P. De Peinder, M. Vredenbregt, T. Visser, D. De Kaste, Detection of Lipitor® counterfeits: A comparison of NIR and Raman spectroscopy in combination with chemometrics, Journal of pharmaceutical and biomedical analysis, 47 (2008) 688-694.

[32] L.S. Lawson, J.D. Rodriguez, Raman Barcode for Counterfeit Drug Product Detection, Analytical chemistry, 88 (2016) 4706-4713.

[33] K. Dégardin, Y. Roggo, P. Margot, Forensic intelligence for medicine anti-counterfeiting, Forensic science international, 248 (2015) 15-32.

[34] S.H.F. Scafi, C. Pasquini, Identification of counterfeit drugs using near-infrared spectroscopy, Analyst, 126 (2001) 2218-2224.

[35] M. Vredenbregt, L. Blok-Tip, R. Hoogerbrugge, D. Barends, D. De Kaste, Screening suspected counterfeit Viagra® and imitations of Viagra® with near-infrared spectroscopy, Journal of pharmaceutical and biomedical analysis, 40 (2006) 840-849.

[36] S.J. Fraser, J. Oughton, W.A. Batten, A.S. Clark, D.M. Schmierer, K.C. Gordon, C.J. Strachan, Simultaneous qualitative and quantitative analysis of counterfeit and unregistered medicines using Raman spectroscopy, Journal of Raman Spectroscopy, 44 (2013) 1172-1180.

[37] S.E. Bell, D.T. Burns, A.C. Dennis, L.J. Matchett, J.S. Speers, Composition profiling of seized ecstasy tablets by Raman spectroscopy, Analyst, 125 (2000) 1811-1815.

[38] P.-Y. Sacré, E. Deconinck, L. Saerens, T. De Beer, P. Courselle, R. Vancauwenberghe, P. Chiap, J. Crommen, J.O. De Beer, Detection of counterfeit Viagra® by Raman microspectroscopy imaging and multivariate analysis, Journal of pharmaceutical and biomedical analysis, 56 (2011) 454-461.

[39] T. Fukami, T. Koide, H. Hisada, M. Inoue, Y. Yamamoto, T. Suzuki, K. Tomono, Pharmaceutical evaluation of atorvastatin calcium tablets available on the Internet: A preliminary investigation of substandard medicines in Japan, Journal of Drug Delivery Science and Technology, 31 (2016) 35-40.

[40] O.Y. Rodionova, A. Pomerantsev, NIR-based approach to counterfeit-drug detection, TrAC Trends in Analytical Chemistry, 29 (2010) 795-803.

[41] O.Y. Rodionova, L.P. Houmøller, A.L. Pomerantsev, P. Geladi, J. Burger, V.L. Dorofeyev, A.P. Arzamastsev, NIR spectrometry for counterfeit drug detection: a feasibility study, Analytica Chimica Acta, 549 (2005) 151-158.

[42] O. Rodionova, A. Pomerantsev, L. Houmøller, A. Shpak, O. Shpigun, Noninvasive detection of counterfeited ampoules of dexamethasone using NIR with confirmation by HPLC-DAD-MS and CE-UV methods, Analytical and bioanalytical chemistry, 397 (2010) 1927-1935.

[43] Y. Zhao, N. Ji, L. Yin, J. Wang, A Non-invasive Method for the Determination of Liquid Injectables by Raman Spectroscopy, AAPS PharmSciTech, 16 (2015) 914-921.

[44] Q. Gao, Y. Liu, H. Li, H. Chen, Y. Chai, F. Lu, Comparison of several chemometric methods of libraries and classifiers for the analysis of expired drugs based on Raman spectra, Journal of pharmaceutical and biomedical analysis, 94 (2014) 58-64.

[45] F. Been, Y. Roggo, K. Degardin, P. Esseiva, P. Margot, Profiling of counterfeit medicines by vibrational spectroscopy, Forensic Science International, 211 (2011) 83-100.

[46] Food, D. Administration, Guidance for industry: PAT—A framework for innovative pharmaceutical development, manufacturing, and quality assurance, DHHS, Rockville, MD, (2004).

[47] T. De Beer, A. Burggraeve, M. Fonteyne, L. Saerens, J.P. Remon, C. Vervaet, Near infrared and Raman spectroscopy for the in-process monitoring of pharmaceutical production processes, International Journal of Pharmaceutics, 417 (2011) 32-47.

[48] P. Esseiva, L. Dujourdy, F. Anglada, F. Taroni, P. Margot, A methodology for illicit heroin seizures comparison in a drug intelligence perspective using large databases, Forensic Science International, 132 (2003) 139-152.

[49] J.S. Jin, Roles and functions of Chinese Pharmacopoeia and Reference Standard in China drug administration, Paper, Conference,New Frontiers in the Quality of Medicines, France, 2008, pp. 44–462008.

[50] R. Bate, R. Tren, K. Hess, L. Mooney, K. Porter, Pilot study comparing technologies to test for substandard drugs in field settings, (2009).

[51] R.A. Crocombe, Portable spectroscopy, Applied spectroscopy, 72 (2018) 1701-1751.

[52] J. Dubois, J.-C. Wolff, J.K. Warrack, J. Schoppelrei, E.N. Lewis, NIR chemical imaging for counterfeit pharmaceutical products analysis, SPECTROSCOPY-SPRINGFIELD THEN EUGENE THEN DULUTH-, 22 (2007) 40.

[53] B.J. Westenberger, C.D. Ellison, A.S. Fussner, S. Jenney, R.E. Kolinski, T.G. Lipe, R.C. Lyon, T.W. Moore, L.K. Revelle, A.P. Smith, Quality assessment of internet pharmaceutical products using traditional and non-traditional analytical techniques, International journal of pharmaceutics, 306 (2005) 56-70.

[54] R.L. McCreery, Raman spectroscopy for chemical analysis, John Wiley & Sons2005.

[55] T. Vankeirsbilck, A. Vercauteren, W. Baeyens, G. Van der Weken, F. Verpoort, G. Vergote, J.P. Remon, Applications of Raman spectroscopy in pharmaceutical analysis, TrAC trends in analytical chemistry, 21 (2002) 869-877.

[56] M. de Veij, A. Deneckere, P. Vandenabeele, D. de Kaste, L. Moens, Detection of counterfeit Viagra® with Raman spectroscopy, Journal of pharmaceutical and biomedical analysis, 46 (2008) 303-309.

[57] K.A. Hall, P.N. Newton, M.D. Green, M. De Veij, P. Vandenabeele, D. Pizzanelli, M. Mayxay, A. Dondorp, F.M. Fernandez, Characterization of counterfeit artesunate antimalarial tablets from southeast Asia, The American journal of tropical medicine and hygiene, 75 (2006) 804-811.

[58] S. Trefi, C. Routaboul, S. Hamieh, V. Gilard, M. Malet-Martino, R. Martino, Analysis of illegally manufactured formulations of tadalafil (Cialis®) by 1 H NMR, 2D DOSY 1 H NMR and Raman spectroscopy, Journal of pharmaceutical and biomedical analysis, 47 (2008) 103-113.

[59] C. Eliasson, P. Matousek, Noninvasive authentication of pharmaceutical products through packaging using spatially offset Raman spectroscopy, Analytical Chemistry, 79 (2007) 1696-1701.

[60] K. Kwok, L.S. Taylor, Analysis of the packaging enclosing a counterfeit pharmaceutical tablet using Raman microscopy and two-dimensional correlation spectroscopy, Vibrational Spectroscopy, 61 (2012) 176-182.

[61] F. Adar, P. Leary, T. Kubic, Raman Microscopy for Detecting Counterfeit Drugs—A Study of the Tablets Versus the Packaging, Spectroscopy, 29 (2014) 10-+.

[62] B.J. Visser, S.G. Vries, E.B. Bache, J. Meerveld-Gerrits, D. Kroon, J. Boersma, S.T. Agnandji, M. Vugt, M.P. Grobusch, The diagnostic accuracy of the hand-held Raman spectrometer for the identification of anti-malarial drugs, Malaria journal, 15 (2016) 160.

[63] K. Dégardin, A. Guillemain, Y. Roggo, Comprehensive Study of a Handheld Raman Spectrometer for the Analysis of Counterfeits of Solid-Dosage Form Medicines, Journal of Spectroscopy, 2017 (2017).

[64] C. Tondepu, R. Toth, C.V. Navin, L.S. Lawson, J.D. Rodriguez, Screening of unapproved drugs using portable Raman spectroscopy, Analytica Chimica Acta, 973 (2017) 75-81.

[65] B. Vajna, A. Farkas, H. Pataki, Z. Zsigmond, T. Igricz, G. Marosi, Testing the performance of pure spectrum resolution from Raman hyperspectral images of differently manufactured pharmaceutical tablets, Analytica chimica acta, 712 (2012) 45-55.

[66] K. Kwok, L.S. Taylor, Analysis of counterfeit Cialis® tablets using Raman microscopy and multivariate curve resolution, Journal of pharmaceutical and biomedical analysis, 66 (2012) 126-135.

[67] P. Penchev, A. Sohou, G. Andreev, Description and performance analysis of an infrared library search system, Spectroscopy letters, 29 (1996) 1513-1522.

[68] R. De Maesschalck, D. Jouan-Rimbaud, D.L. Massart, The mahalanobis distance, Chemometrics and intelligent laboratory systems, 50 (2000) 1-18.

[69] J. Li, D.B. Hibbert, S. Fuller, G. Vaughn, A comparative study of point-to-point algorithms for matching spectra, Chemometrics and intelligent laboratory systems, 82 (2006) 50-58.

[70] A. Kwiatkowski, M. Gnyba, J. Smulko, P. Wierzba, Algorithms of chemicals detection using Raman spectra, Metrology and Measurement Systems, 17 (2010) 549-559.

[71] S. Assi, Raw material identification using dual laser handheld Raman spectroscopy, European Pharmaceutical Review, 18 (2013) 25-31.

[72] J.D. Rodriguez, B.J. Westenberger, L.F. Buhse, J.F. Kauffman, Quantitative evaluation of the sensitivity of library-based Raman spectral correlation methods, Analytical chemistry, 83 (2011) 4061-4067.

[73] M.S. Islam, A review on the policy and practices of therapeutic drug uses in Bangladesh, Calicut Med J, 4 (2006) e2.

[74] C. Xiu, K. Klein, Melamine in milk products in China: examining the factors that led to deliberate use of the contaminant, Food Policy, 35 (2010) 463-470.

[75] J.D. Rodriguez, B.J. Westenberger, L.F. Buhse, J.F. Kauffman, Standardization of Raman spectra for transfer of spectral libraries across different instruments, Analyst, 136 (2011) 4232-4240.

[76] C.M. Gryniewicz-Ruzicka, S. Arzhantsev, L.N. Pelster, B.J. Westenberger, L.F. Buhse, J.F. Kauffman, Multivariate calibration and instrument standardization for the rapid detection of diethylene glycol in glycerin by Raman spectroscopy, Applied spectroscopy, 65 (2011) 334-341.

[77] J.D. Rodriguez, C.M. Gryniewicz-Ruzicka, S. Arzhantsev, J.F. Kauffman, L.F. Buhse, Rapid screening methods for pharmaceutical surveillance, Science and the Law: Analytical Data in Support of Regulation in Health, Food, and the Environment, ACS Publications2014, pp. 149-168.

[78] T. Sakamoto, Y. Fujimaki, Y. Hiyama, NIR spectroscopic investigation of two fluoroquinolones, levofloxacin and ofloxacin, and their tablets for qualitative identification of commercial products on the market, Die Pharmazie-An International Journal of Pharmaceutical Sciences, 63 (2008) 628-632.

[79] J.E. Polli, S.W. Hoag, S. Flank, Comparison of authentic and suspect pharmaceuticals, Pharmaceutical Technology, 33 (2009) 46-52.

[80] M.M. Said, S. Gibbons, A.C. Moffat, M. Zloh, Near-infrared spectroscopy (NIRS) and chemometric analysis of Malaysian and UK paracetamol tablets: A spectral database study, International journal of pharmaceutics, 415 (2011) 102-109.

[81] S. Wold, K. Esbensen, P. Geladi, Principal component analysis, Chemometrics and intelligent laboratory systems, 2 (1987) 37-52.

[82] H. Martens, T. Naes, Multivariate calibration, John Wiley & Sons1992.

[83] D. Ballabio, R. Todeschini, Multivariate classification for qualitative analysis, (2009).

[84] T. Næs, T. Isaksson, T. Fearn, T. Davies, A user friendly guide to multivariate calibration and classification, NIR publications2002.

[85] D.L. Massart, D.L. Massart, L. Kaufman, The interpretation of analytical chemical data by the use of cluster analysis, 1983.

[86] K. Dégardin, A. Guillemain, N.V. Guerreiro, Y. Roggo, Near infrared spectroscopy for counterfeit detection using a large database of pharmaceutical tablets, Journal of pharmaceutical and biomedical analysis, 128 (2016) 89-97.

[87] S. Assi, R.A. Watt, A.C. Moffat, Identification of counterfeit medicines from the Internet and the World market using near-infrared spectroscopy, Analytical Methods, 3 (2011) 2231-2236.

[88] S. Assi, Evaluating handheld spectroscopic techniques for identifying counterfeit branded and generic medicines worldwide, American Pharmaceutical Review, 19 (2016).

[89] M.B. Lopes, J.-C. Wolff, J.M. Bioucas-Dias, M.A. Figueiredo, Determination of the composition of counterfeit Heptodin™ tablets by near infrared chemical imaging and classical least squares estimation, Analytica chimica acta, 641 (2009) 46-51.

[90] S. Wilczyński, R. Koprowski, M. Marmion, P. Duda, B. Błońska-Fajfrowska, The use of hyperspectral imaging in the VNIR (400–1000nm) and SWIR range (1000–2500nm) for detecting counterfeit drugs with identical API composition, Talanta, 160 (2016) 1-8.

[91] S. Neuberger, C. Neusüß, Determination of counterfeit medicines by Raman spectroscopy: systematic study based on a large set of model tablets, Journal of pharmaceutical and biomedical analysis, 112 (2015) 70-78.

[92] A.G. Ryder, G.M. O'Connor, T.J. Glynn, Identifications and quantitative measurements of narcotics in solid mixtures using near-IR Raman spectroscopy and multivariate analysis, Journal of Forensic Science, 44 (1999) 1013-1019.

[93] X.-M. Chong, C.-Q. Hu, Y.-C. Feng, H.-H. Pang, Construction of a universal model for non-invasive identification of cephalosporins for injection using near-infrared diffuse reflectance spectroscopy, Vibrational Spectroscopy, 49 (2009) 196-203.

[94] M.B. Lopes, J.-C. Wolff, Investigation into classification/sourcing of suspect counterfeit Heptodin™ tablets by near infrared chemical imaging, Analytica chimica acta, 633 (2009) 149-155.

[95] D. Ballabio, R. Todeschini, Multivariate classification for qualitative analysis, Infrared spectroscopy for food quality analysis and control, (2009) 83-104.

[96] B. Krakowska, D. Custers, E. Deconinck, M. Daszykowski, Chemometrics and the identification of counterfeit medicines—A review, Journal of pharmaceutical and biomedical analysis, 127 (2016) 112-122.

[97] E. Szymańska, J. Gerretzen, J. Engel, B. Geurts, L. Blanchet, L.M. Buydens, Chemometrics and qualitative analysis have a vibrant relationship, TrAC Trends in Analytical Chemistry, 69 (2015) 34-51.

[98] J. Riedl, S. Esslinger, C. Fauhl-Hassek, Review of validation and reporting of non-targeted fingerprinting approaches for food authentication, Analytica chimica acta, 885 (2015) 17-32.

[99] P. Oliveri, G. Downey, Multivariate class modeling for the verification of food-authenticity claims, TrAC Trends in Analytical Chemistry, 35 (2012) 74-86.

[100] M.I. López, E. Trullols, M.P. Callao, I. Ruisánchez, Multivariate screening in food adulteration: Untargeted versus targeted modelling, Food chemistry, 147 (2014) 177-181.

[101] O.M. Kvalheim, K. Øygard, O. Grahl-Nielsen, SIMCA multivariate data analysis of blue mussel components in environmental pollution studies, Analytica Chimica Acta, 150 (1983) 145-152.

[102] S. Wold, M. Sjöström, Letters to the editor. Comments on a recent evaluation of the SIMCA method, Journal of Chemometrics, 2 (1987) 243-245.

[103] C. Albano, G. Blomqvist, D. Coomans, W. Dunn III, U. Edlund, B. Eliasson, S. Hellberg, E. Johansson, B. Nordén, M. Sjöström, Pattern recognition by means of disjoint principal components models (SIMCA). Philosophy and methods, Proceedings of the Symposium on Applied Statistics, Copenhagen, 1981, pp. 183-203.

[104] P.J. Gemperline, L.D. Webber, F.O. Cox, Raw materials testing using soft independent modeling of class analogy analysis of near-infrared reflectance spectra, Analytical Chemistry, 61 (1989) 138-144.

[105] A. Candolfi, R. De Maesschalck, D. Massart, P. Hailey, A. Harrington, Identification of pharmaceutical excipients using NIR spectroscopy and SIMCA, Journal of pharmaceutical and biomedical analysis, 19 (1999) 923-935.

[106] A.L. Pomerantsev, Acceptance areas for multivariate classification derived by projection methods, Journal of Chemometrics, 22 (2008) 601-609.

[107] R.G. Brereton, G.R. Lloyd, Partial least squares discriminant analysis: taking the magic away, Journal of Chemometrics, 28 (2014) 213-225.

[108] P. Geladi, B.R. Kowalski, Partial least-squares regression: a tutorial, Analytica chimica acta, 185 (1986) 1-17.

[109] S. Wold, M. Sjöström, L. Eriksson, PLS-regression: a basic tool of chemometrics, Chemometrics and intelligent laboratory systems, 58 (2001) 109-130.

[110] O.Y. Rodionova, Y.V. Sokovikov, A. Pomerantsev, Quality control of packed raw materials in pharmaceutical industry, analytica chimica acta, 642 (2009) 222-227.

[111] A.L. Pomerantsev, O.Y. Rodionova, Concept and role of extreme objects in PCA/SIMCA, Journal of Chemometrics, 28 (2014) 429-438.

[112] A.L. Pomerantsev, O.Y. Rodionova, On the type II error in SIMCA method, Journal of Chemometrics, 28 (2014) 518-522.

[113] O.Y. Rodionova, P. Oliveri, A.L. Pomerantsev, Rigorous and compliant approaches to one-class classification, Chemometrics and Intelligent Laboratory Systems, 159 (2016) 89-96.

[114] E.F. Van ZyL, M. Louw, The Differentiation of Illicit Methaqualone Tablet Formulations Using Principal Component and Soft Independent Modeling of Class Analogy Analysis of Their Near-Infrared Reflectance Spectra, Journal of Forensic Science, 40 (1995) 1072-1076.

[115] P. Aldridge, C. Evans, H. Ward, S. Colgan, N. Boyer, P. Gemperline, Near-IR detection of polymorphism and process-related substances, Analytical Chemistry, 68 (1996) 997-1002.

[116] L. Sun, C. Hsiung, C.G. Pederson, P. Zou, V. Smith, M. von Gunten, N.A. O'Brien, Pharmaceutical raw material identification using miniature near-infrared (MicroNIR) spectroscopy and supervised pattern recognition using support vector machine, Applied spectroscopy, 70 (2016) 816-825.

[117] M. Forina, P. Oliveri, S. Lanteri, M. Casale, Class-modeling techniques, classic and new, for old and new problems, Chemometrics and Intelligent Laboratory Systems, 93 (2008) 132-148.

[118] A.J. Myles, T.A. Zimmerman, S.D. Brown, Transfer of multivariate classification models between laboratory and process near-infrared spectrometers for the discrimination of green Arabica and Robusta coffee beans, Applied spectroscopy, 60 (2006) 1198-1203.

[119] J. Workman, EXPRESS: A Review of Calibration Transfer Practices and Instrument Differences in Spectroscopy, Applied Spectroscopy, (2017) 0003702817736064.

[120] R. Bro, A.K. Smilde, Principal component analysis, Analytical Methods, 6 (2014) 2812-2831.

[121] L. Li, H. Zang, J. Li, D. Chen, T. Li, F. Wang, Identification of anisodamine tablets by Raman and near-infrared spectroscopy with chemometrics, Spectrochimica Acta Part A: Molecular and Biomolecular Spectroscopy, 127 (2014) 91-97.

[122] M. Forina, S. Lanteri, M. Casale, M.C.C. Oliveros, Stepwise orthogonalization of predictors in classification and regression techniques: An "old" technique revisited, Chemometrics and Intelligent Laboratory Systems, 87 (2007) 252-261.

[123] O.Y. Rodionova, A.V. Titova, A.L. Pomerantsev, Discriminant analysis is an inappropriate method of authentication, TrAC Trends in Analytical Chemistry, 78 (2016) 17-22.

[124] O. Devos, C. Ruckebusch, A. Durand, L. Duponchel, J.-P. Huvenne, Support vector machines (SVM) in near infrared (NIR) spectroscopy: Focus on parameters optimization and model interpretation, Chemometrics and Intelligent Laboratory Systems, 96 (2009) 27-33.

[125] J. Luts, F. Ojeda, R. Van de Plas, B. De Moor, S. Van Huffel, J.A. Suykens, A tutorial on support vector machine-based methods for classification problems in chemometrics, Analytica Chimica Acta, 665 (2010) 129-145.

[126] F. Chauchard, R. Cogdill, S. Roussel, J. Roger, V. Bellon-Maurel, Application of LS-SVM to non-linear phenomena in NIR spectroscopy: development of a robust and portable sensor for acidity prediction in grapes, Chemometrics and Intelligent Laboratory Systems, 71 (2004) 141-150.

[127] T. Puchert, D. Lochmann, J. Menezes, G. Reich, Near-infrared chemical imaging (NIR-CI) for counterfeit drug identification—a four-stage concept with a novel approach of data processing (Linear Image Signature), Journal of pharmaceutical and biomedical analysis, 51 (2010) 138-145.

[128] B. Igne, Z. Shi, J.K. Drennen, C.A. Anderson, Effects and Detection of Raw Material Variability on the Performance of Near-Infrared Calibration Models for Pharmaceutical Products, Journal of pharmaceutical sciences, 103 (2014) 545-556.

[129] V.S. Dave, S.D. Saoji, N.A. Raut, R.V. Haware, Excipient variability and its impact on dosage form functionality, Journal of pharmaceutical sciences, 104 (2015) 906-915.

[130] M.V. Pellow-Jarman, P.J. Hendra, R.J. Lehnert, The dependence of Raman signal intensity on particle size for crystal powders, Vibrational Spectroscopy, 12 (1996) 257-261.

[131] H. Wang, C.K. Mann, T.J. Vickers, Effect of powder properties on the intensity of Raman scattering by crystalline solids, Applied spectroscopy, 56 (2002) 1538-1544.

[132] T. De Beer, W. Baeyens, Y. Vander Heyden, J.P. Remon, C. Vervaet, F. Verpoort, Influence of particle size on the quantitative determination of salicylic acid in a pharmaceutical ointment using FT-Raman spectroscopy, European journal of pharmaceutical sciences, 30 (2007) 229-235.

[133] N. Townshend, A. Nordon, D. Littlejohn, M. Myrick, J. Andrews, P. Dallin, Comparison of the determination of a low-concentration active ingredient in pharmaceutical tablets by backscatter and transmission Raman spectrometry, Analytical chemistry, 84 (2012) 4671-4676.

[134] A. Sparén, M. Hartman, M. Fransson, J. Johansson, O. Svensson, Matrix effects in quantitative assessment of pharmaceutical tablets using transmission Raman and near-infrared (NIR) spectroscopy, Applied spectroscopy, 69 (2015) 580-589.

[135] D. Oelkrug, E. Ostertag, R.W. Kessler, Quantitative Raman spectroscopy in turbid matter: reflection or transmission mode?, Anal Bioanal Chem, 405 (2013) 3367-3379.

[136] H. Wikström, S. Romero-Torres, S. Wongweragiat, J.A.S. Williams, E.R. Grant, L.S. Taylor, On-line content uniformity determination of tablets using low-resolution Raman spectroscopy, Applied spectroscopy, 60 (2006) 672-681.

[137] B. Igne, J.K. Drennen, C.A. Anderson, Improving Near-Infrared Prediction Model Robustness with Support Vector Machine Regression: A Pharmaceutical Tablet Assay Example, Applied spectroscopy, 68 (2014) 1348-1356.

[138] M. Blanco, M. Alcalá, Content uniformity and tablet hardness testing of intact pharmaceutical tablets by near infrared spectroscopy: a contribution to process analytical technologies, Analytica chimica acta, 557 (2006) 353-359.

[139] M. Blanco, M. Bautista, M. Alcala, Preparing calibration sets for use in pharmaceutical analysis by NIR spectroscopy, Journal of pharmaceutical sciences, 97 (2008) 1236-1245.

[140] M. Blanco, J. Coello, A. Eustaquio, H. Iturriaga, S. Maspoch, Analytical control of pharmaceutical production steps by near infrared reflectance spectroscopy, Analytica Chimica Acta, 392 (1999) 237-246.

[141] M. Blanco, R. Cueva-Mestanza, A. Peguero, Controlling individual steps in the production process of paracetamol tablets by use of NIR spectroscopy, Journal of pharmaceutical and biomedical analysis, 51 (2010) 797-804.

[142] M. Blanco, R. Cueva-Mestanza, A. Peguero, NIR analysis of pharmaceutical samples without reference data: improving the calibration, Talanta, 85 (2011) 2218-2225.

[143] M. Blanco, A. Peguero, Influence of physical factors on the accuracy of calibration models for NIR spectroscopy, Journal of pharmaceutical and biomedical analysis, 52 (2010) 59-65.

[144] M. Blanco, M. Romero, M. Alcala, Strategies for constructing the calibration set for a near infrared spectroscopic quantitation method, Talanta, 64 (2004) 597-602.

[145] M.D. Hargreaves, K. Page, T. Munshi, R. Tomsett, G. Lynch, H.G. Edwards, Analysis of seized drugs using por`Raman spectroscopy in an airport environment—a proof of principle study, Journal of Raman Spectroscopy, 39 (2008) 873-880.

[146] M. Hajjou, Y. Qin, S. Bradby, D. Bempong, P. Lukulay, Assessment of the performance of a handheld Raman device for potential use as a screening tool in evaluating medicines quality, Journal of pharmaceutical and biomedical analysis, 74 (2013) 47-55.

[147] C. Ricci, L. Nyadong, F. Yang, F.M. Fernandez, C.D. Brown, P.N. Newton, S.G. Kazarian, Assessment of hand-held Raman instrumentation for in situ screening for potentially counterfeit artesunate antimalarial tablets by FT-Raman spectroscopy and direct ionization mass spectrometry, Analytica chimica acta, 623 (2008) 178-186.

[148] M. Vredenbregt, P. Caspers, R. Hoogerbrugge, D. Barends, Choice and validation of a near infrared spectroscopic application for the identity control of starting materials.: Practical experience with the EU draft Note for Guidance on the use of near infrared spectroscopy by the pharmaceutical industry and the data to be forwarded in part II of the dossier for a marketing authorization, European journal of pharmaceutics and biopharmaceutics, 56 (2003) 489-499.

[149] S. Assi, A. Guirguis, S. Halsey, S. Fergus, J. Stair, Analysis of 'legal high'substances and common adulterants using handheld spectroscopic techniques, Analytical Methods, 7 (2015) 736-746.

[150] M.D. Hargreaves, R.L. Green, W. Jalenak, C.D. Brown, C. Gardner, Handheld Raman and FT-IR Spectrometers, Infrared and Raman Spectroscopy in Forensic Science, (2012) 275-287.

[151] T. Naes, T. Isaksson, T. Fearn, T. Davies, A user friendly guide to multivariate calibration and classification, NIR publications2002.

[152] P.C. Williams, Implementation of near-infrared technology, Near-infrared technology in the agricultural and food industries, 2 (2001) 143-167.

[153] D.M. Koller, A. Posch, G. Hörl, C. Voura, S. Radl, N. Urbanetz, S.D. Fraser, W. Tritthart, F. Reiter, M. Schlingmann, Continuous quantitative monitoring of powder mixing dynamics by near-infrared spectroscopy, Powder technology, 205 (2011) 87-96.

[154] C.C. Corredor, R. Lozano, X. Bu, R. McCann, J. Dougherty, T. Stevens, D. Both, P. Shah, Analytical method quality by design for an on-line near-infrared method to monitor blend potency and uniformity, Journal of Pharmaceutical Innovation, 10 (2015) 47-55.

[155] D.M. Haaland, E.V. Thomas, Partial least-squares methods for spectral analyses. 1. Relation to other quantitative calibration methods and the extraction of qualitative information, Analytical Chemistry, 60 (1988) 1193-1202.

[156] WHO, Definitions of Substandard and Falsified (SF) Medical Products (Access at 05/01/2018), http://www.who.int/medicines/regulation/ssffc/definitions/en/.

[157] WHO, A study on the public health and socioeconomic impact of substandard and falsified medical products, https://www.who.int/medicines/regulation/ssffc/publications/se-study-sf/en/ (Access at 04/13/2019), (2017).

[158] G.o.t.u.o.n.-i.s.b.t.p.i.a.t.d.r.f.n.s.a.v. EMEA, European Medicines Agency, London, 16 (2012)

[159] B.M. Wise, R.T. Roginski, A calibration model maintenance roadmap, IFAC-PapersOnLine, 48 (2015) 260-265.

[160] R. Vitale, F. Marini, C. Ruckebusch, SIMCA Modeling for Overlapping Classes: Fixed or Optimized Decision Threshold?, Anal Chem, 90 (2018) 10738-10747.

[161] D.M. Tax, R.P.J.P.r.l. Duin, Support vector domain description, 20 (1999) 1191-1199.

[162] D. Tax, Ddtools, the data description toolbox for matlab, Delft University of Technology ed, (2005).

[163] O.Y. Rodionova, P. Oliveri, A.L.J.C. Pomerantsev, I.L. Systems, Rigorous and compliant approaches to one-class classification, 159 (2016) 89-96.

[164] B. Igne, M.N. Hossain, J.K. Drennen III, C.A. Anderson, Robustness considerations and effects of moisture variations on near infrared method performance for solid dosage form assay, Journal of Near Infrared Spectroscopy, 22 (2014) 179-188.

[165] B. Igne, J.K. Drennen III, C.A. Anderson, Improving Near-Infrared Prediction Model Robustness with Support Vector Machine Regression: A Pharmaceutical Tablet Assay Example, Applied spectroscopy, 68 (2014) 1348-1356.

[166] R.G. Brereton, One-class classifiers, Journal of Chemometrics, 25 (2011) 225-246.

[167] N. Townshend, A. Nordon, D. Littlejohn, J. Andrews, P. Dallin, Effect of particle properties of powders on the generation and transmission of Raman scattering, Analytical chemistry, 84 (2012) 4665-4670.

[168] H. Swierenga, A. De Weijer, R. Van Wijk, L. Buydens, Strategy for constructing robust multivariate calibration models, Chemometrics and Intelligent Laboratory Systems, 49 (1999) 1-17.

[169] J. Johansson, A. Sparén, O. Svensson, S. Folestad, M. Claybourn, Quantitative transmission Raman spectroscopy of pharmaceutical tablets and capsules, Applied spectroscopy, 61 (2007) 1211-1218.

[170] W.R. Browne, J.J. McGarvey, The Raman effect and its application to electronic spectroscopies in metal-centered species: Techniques and investigations in ground and excited states, Coordination Chemistry Reviews, 251 (2007) 454-473.

[171] J.M. Chalmers, H.G. Edwards, M.D. Hargreaves, Infrared and Raman spectroscopy in forensic science, John Wiley & Sons2012.

[172] J.F. Kauffman, M. Dellibovi, C.R. Cunningham, Raman spectroscopy of coated pharmaceutical tablets and physical models for multivariate calibration to tablet coating thickness, Journal of pharmaceutical and biomedical analysis, 43 (2007) 39-48.

[173] Y. Li, B. Igne, J.K. Drennen, C.A. Anderson, Method development and validation for pharmaceutical tablets analysis using transmission Raman spectroscopy, International journal of pharmaceutics, 498 (2016) 318-325.

[174] R.N. Palermo, S.M. Short, C.A. Anderson, H. Tian, J.K. Drennen III, Determination of figures of merit for near-infrared, Raman and powder X-ray diffraction by net analyte signal analysis for a compacted amorphous dispersion with spiked crystallinity, Journal of Pharmaceutical Innovation, 7 (2012) 56-68.

[175] S. Romero-Torres, J.D. Pérez-Ramos, K.R. Morris, E.R. Grant, Raman spectroscopy for tablet coating thickness quantification and coating characterization in the presence of strong fluorescent interference, Journal of pharmaceutical and biomedical analysis, 41 (2006) 811-819.

[176] I. Barman, C.-R. Kong, G.P. Singh, R.R. Dasari, Effect of photobleaching on calibration model development in biological Raman spectroscopy, Journal of biomedical optics, 16 (2011) 011004-011004-011010.

[177] B. Igne, N. Hossain, J.K. Drennen III, C.A. Anderson, Robustness considerations and effects of moisture variations on near infrared method performance for solid dosage form assay, Journal of Near Infrared Spectroscopy, 22 (2014) 179-188.

[178] S. Pieters, W. Saeys, T. Van den Kerkhof, M. Goodarzi, M. Hellings, T. De Beer, Y. Vander Heyden, Robust calibrations on reduced sample sets for API content prediction in tablets: Definition of a cost-effective NIR model development strategy, Analytica chimica acta, 761 (2013) 62-70.

[179] T. Van den Kerkhof, R. De Maesschalck, K. Vanhoutte, M. Coene, Augmentation of near infrared diffuse reflectance and transmittance spectral data for the development of robust PLSBC models for classifying double blind clinical trial tablets, Journal of pharmaceutical and biomedical analysis, 42 (2006) 517-522.

[180] M.D. Hargreaves, N.A. Macleod, M.R. Smith, D. Andrews, S.V. Hammond, P. Matousek, Characterisation of transmission Raman spectroscopy for rapid quantitative analysis of intact

multi-component pharmaceutical capsules, Journal of pharmaceutical and biomedical analysis, 54 (2011) 463-468.

[181] S. Tobita, K. Ida, S. Shiobara, Water-induced fluorescence quenching of aniline and its derivatives in aqueous solution, Research on Chemical Intermediates, 27 (2001) 205-218.

[182] U.P. Agarwal, An overview of Raman spectroscopy as applied to lignocellulosic materials, Advances in lignocellulosics characterization, (1999) 201-225.

[183] F. Nosten, N.J. White, Artemisinin-based combination treatment of falciparum malaria, The American journal of tropical medicine and hygiene, 77 (2007) 181-192.

[184] M. Lalani, F.E. Kitutu, S.E. Clarke, H. Kaur, Anti-malarial medicine quality field studies and surveys: a systematic review of screening technologies used and reporting of findings, Malaria journal, 16 (2017) 197.

[185] G. Thoorens, F. Krier, B. Leclercq, B. Carlin, B. Evrard, Microcrystalline cellulose, a direct compression binder in a quality by design environment—A review, International journal of pharmaceutics, 473 (2014) 64-72.

[186] O.Y. Rodionova, K.S. Balyklova, A.V. Titova, A.L. Pomerantsev, Quantitative risk assessment in classification of drugs with identical API content, J Pharm Biomed Anal, 98 (2014) 186-192.

[187] A.S. El-Hagrasy, M. Delgado-Lopez, J.K. Drennen, A Process Analytical Technology approach to near-infrared process control of pharmaceutical powder blending: Part II: Qualitative near-infrared models for prediction of blend homogeneity, Journal of pharmaceutical sciences, 95 (2006) 407-421.